

**A THERMAL/THERMO-MECHANICAL  
AND IMAGING STUDY OF COMPONENT  
DISTRIBUTION AND INTERACTION IN  
PHARMACEUTICAL FILM COATS**



**Jin Meng, BscPharm**

Thesis submitted for the degree of Doctor of Philosophy

University of East Anglia

School of Pharmacy

March 2012

© This copy of the thesis has been supplied on condition that anyone who consults it is understood to recognize that its copyright rests with the author and that no quotation from the thesis, nor any information derived therefrom, may be published without the author's prior, written consent.

## **Acknowledgements**

I would like to take this opportunity to express my gratitude to my supervisors, Prof. Duncan Q.M. Craig and Dr. Sheng Qi, my previous supervisor, Prof. Mike Reading, for their excellent supervision, consideration, continuous encouragement and assistance throughout my PhD study. This work cannot be completed without the support and advice from my industrial supervisors, Dr. Ali Rajabi-Siahboomi and Dr. Marina Levina, and the financial support from Colorcon Limited. Many thanks to product development manager Mr. Charles Vesey, application technologists Miss Hue Vuong and Miss Dasha Palmer from Colorcon for their kind help and advice, Dr. Simon Gaisford from the School of Pharmacy at the University of London for his kind assistance with the hyper-DSC studies, and Dr. Xuan Dai, Dr. Jonathan Moffat and Dr. Andrew Round from the University of East Anglia for their technical support and advice with AFM work.

I would also like to thank all my fantastic friends in the drug delivery group who have been a very important part during my PhD life. In addition, I will not forget to mention the kindness of the staff and technicians from University of East Anglia for all their help and assistance throughout my study.

Last but not least, I would not be able to complete this endeavour task without the continuous support, understanding and encouragement from my loving husband, Charles William Heppell, my dear parents, Suling Luo and Zhaoguo Meng, brother in-law James and parents in-law, Madeleine and Paul Heppell.

*For Charles, my parents, and parents in-law*

## Abstract

*Ethyl cellulose (EC) is one of the most important coating materials for controlled release formulations. To achieve the desirable drug release, the physical properties of EC films incorporated with various functional additives need to be fully understood. Therefore, the aim of this project is to characterize the physical properties of EC films incorporated with various plasticizers and pore forming agents, hence to understand the drug release mechanisms in relation to the physical characteristics of EC films. The thermal properties of EC powder and EC films were initially characterized by means of thermogravimetric analysis (TGA), differential scanning calorimetry (DSC), modulated temperature DSC (MTDSC) and dynamic mechanical analysis (DMA). Subsequently, oleic acid (OA), dibutyl sebacate (DBS) and medium chain triglycerides (MCT) were incorporated as plasticizers while hydroxypropyl methylcellulose (HPMC) was utilized as the pore forming agent. The thermal, thermo-mechanical and phase distribution of EC films incorporated with plasticizers and/or HPMC were investigated using MTDSC, DMA and localized thermal analysis (LTA). These results were compared with the thermal properties and scanning electron microscopy (SEM) images of the free films after immersion into water, pH 1.2 and 6.8 buffers. Dissolution of metoprolol succinate and paracetamol from SureSpheres® pellets coated by these films were then carried out. OA and DBS were more efficient than MCT for EC films. OA and DBS showed good compatibility with EC, whereas at 20% plasticizer level and beyond, EC/MCT films presented two EC phases with 8% and 24% MCT respectively. The addition of HPMC to EC films did not show a significant effect on their thermal properties. However, the phase distribution of HPMC domains was affected by the HPMC levels. After immersion into the release media, HPMC generated water filled pores quickly in the first two hours. The shape and sizes of these pores were corresponding to the phase distribution of HPMC domains. The release from these films appeared to follow zero-order kinetics, except for metoprolol succinate from pellets coated by EC/plasticizer/HPMC films, which followed the Higuchi model. It is suggested that the dissolution rate of HPMC, film properties and solubility of the model drugs is the rate-determining step.*

## **Table of Content**

Acknowledgements .....	2
Abstract .....	4
Table of Content.....	5
List of Figures .....	14
List of Tables.....	22
Abbreviations .....	26
CHAPTER 1 INTRODUCTION .....	28
1.1 General Introduction .....	28
1.2 Film Coating Materials .....	29
1.2.1 Chemical Structure of EC .....	30
1.2.2 Properties of EC .....	32
1.2.2.1 Degree of Substitution .....	34
1.2.2.2 Molecular Weight .....	35
1.2.2.3 Viscosity Grade.....	38
1.2.2.4 Glass Transition Temperature .....	39
1.2.2.5 Liquid Crystalline Nature.....	40
1.3 Plasticizers.....	41
1.3.1 Effects of Plasticizers.....	41
1.3.2 Plasticizers Used for Film Coating .....	43
1.3.2.1 Hydrophilic Plasticizers .....	45

1.3.2.2 Hydrophobic Plasticizers .....	46
1.4 Pore formers .....	49
1.4.1 Pores .....	49
1.4.2 Pore Former – Hydroxypropyl Methylcellulose (HPMC) .....	51
1.4.2.1 Chemical Structure of HPMC .....	51
1.4.2.2 Effect of HPMC on Film Coating .....	52
1.5 Film Formation .....	55
1.5.1 Organic Solvent Systems .....	55
1.5.2 Aqueous Polymeric Dispersions .....	56
1.6 Application of EC Film Coatings for Controlled Release Dosage Forms .....	57
1.7 Aims and Objectives .....	59
<b>CHAPTER 2 MATERIALS AND METHODS.....</b>	<b>61</b>
2.1 Materials.....	62
2.1.1 Ethyl Cellulose .....	62
2.1.2 Plasticizers.....	63
2.1.2.1 Oleic Acid .....	63
2.1.2.2 Dibutyl Sebacate .....	63
2.1.2.3 Medium-chain Triglycerides .....	64
2.1.3 Hydroxypropyl Methylcellulose .....	64
2.1.4 Model Drugs .....	65
2.1.4.1 Paracetamol .....	65

2.1.4.2 Metoprolol Succinate .....	65
2.2 Preparation of EC Cast Films.....	67
2.3 Thermal Analysis .....	71
2.3.1 Introduction .....	71
2.3.2 Differential Scanning Calorimetry .....	71
2.3.2.1 Calibration.....	73
2.3.2.2 Experimental Parameters .....	74
2.3.3.1 Calibration.....	78
2.3.3.2 Experimental Parameters .....	78
2.3.4 Dynamic Mechanical Analysis .....	79
2.3.4.1 Calibration.....	81
2.3.4.2 Experimental Parameters .....	82
2.3.5 Thermogravimetric Analysis.....	84
2.4 Atomic Force Microscopy-Thermal Analysis.....	86
2.4.1 Atomic Force Microscopy.....	86
2.4.2 Hot Stage AFM .....	88
2.4.3 Micro and Nano-Thermal Analysis.....	89
2.5 Scanning Electron Microscopy .....	92
2.6 Dissolution Studies .....	92
2.6.1 Simulated Dissolution Studies on the Cast Films .....	92
2.6.2 Pellets Coating Process .....	94

2.6.3 Dissolution of Coated Pellets .....	98
<b>CHAPTER 3 THERMAL CHARACTERIZATION OF ETHYL CELLULOSE AND</b>	
<b>ETHYL CELLULOSE FILMS .....</b>	<b>101</b>
3.1 Introduction to Ethyl Cellulose Powder and Films .....	101
3.2 Methodology .....	102
3.2.1 Sample Preparation .....	102
3.2.2 TGA .....	103
3.2.3 DSC and MTDSC .....	103
3.2.4 DMA .....	104
3.3 Results .....	104
3.3.1 General Properties of EC Powders.....	104
3.3.1.1 TGA Studies.....	105
3.3.1.2 General Thermal Properties .....	106
3.3.1.3 Glass Transition Temperatures .....	108
3.3.2 Thermal Properties of EC Films .....	112
3.3.2.1 Visual Observation.....	112
3.3.2.2 Residual Solvents .....	113
3.3.2.3 DSC .....	114
3.3.2.4 DMA Studies.....	117
3.4 Discussion .....	122
3.4.1 Thermal Properties of EC.....	122

3.4.2 Thermal Properties of EC Films .....	123
3.5 Conclusion .....	125
<b>CHAPTER 4 THE EFFECTS OF PLASTICIZERS ON ETHYL CELLULOSE FILMS</b>	<b>127</b>
4.1 Introduction .....	127
4.2 Methodology .....	128
4.2.1 Preparation of EC/Plasticizers Films .....	128
4.2.2 Thermogravimetric Analysis.....	130
4.2.4 DMA Studies.....	131
4.2.5 AFM Studies .....	131
4.3 Results .....	132
4.3.1 Visual Observations .....	132
4.3.2 Thermogravimetric Analysis.....	135
4.3.3 DSC Studies .....	138
4.3.4 DMA Studies.....	143
4.3.4.1 Thermal Properties .....	143
4.3.4.2 Mechanical Properties .....	148
4.3.5 AFM Studies .....	149
4.3.5.1 AFM – Thermal Analysis .....	149
4.3.5.2 Hot Stage AFM Studies .....	155
4.4 Discussion .....	157
4.4.1 Visual observations .....	157

4.4.2 The Study of Residual Solvents and Degradation.....	158
4.4.3 Plasticizing Efficiency .....	159
4.4.4 Miscibility Studies of EC/plasticizer Films .....	163
4.4.5 Mechanical Properties.....	166
4.5 Conclusion .....	168
 CHAPTER 5 THE EFFECTS OF PORE FORMER INCLUSION ON ETHYL CELLULOSE FILMS .....	 170
5.1 Introduction.....	170
5.2 Methodology .....	172
5.2.1 Preparation of EC/Pore Former Films .....	172
5.2.2 TGA Studies.....	172
5.2.3 DSC Studies .....	173
5.2.4 DMA Studies.....	173
5.2.5 AFM Thermal Studies.....	173
5.3 Results.....	174
5.3.1 Visual Observations .....	174
5.3.2 TGA Studies.....	175
5.3.3 DSC Studies .....	178
5.3.4 Thermo-mechanical Properties .....	180
5.3.5 Localized Thermal Analysis (LTA) .....	183
5.4 Discussion .....	187

5.4.1 The Study of Residual Solvents .....	187
5.4.2 Miscibility between EC and HPMC.....	187
5.5 Conclusion .....	192
CHAPTER 6 THERMAL AND THERMO-MECHANICAL PROPERTIES OF ETHYL CELLULOSE FILMS INCORPORATING VARIOUS PLASTICIZERS AND HYDROXYPROPYL METHYLCELLULOSE.....	
6.1 Introduction .....	193
6.2 Methodology .....	194
6.2.1 Preparation of EC/Plasticizers/Pore Former Films .....	194
6.2.2 Residual Solvents .....	195
6.2.3 DSC Studies .....	196
6.2.4 DMA Studies.....	196
6.2.5 AFM Studies .....	196
6.3 Results .....	197
6.3.1 MTDSC Studies .....	197
6.3.2 DMA Studies.....	203
6.3.2.1 Thermal Properties .....	203
6.3.2.2 Mechanical Properties .....	207
6.3.3 Localized Thermal Analysis (LTA) Studies .....	208
6.4 Discussion .....	213
6.4.1 Miscibility Studies-MTDSC .....	213

6.4.2 Miscibility Studies-DMA.....	214
6.4.3 Miscibility Studies-LTA .....	216
6.5 Conclusion .....	217
CHAPTER 7 DRUG RELEASE MECHANISMS AND MORPHOLOGY OF EC/PLASTICIZER FILMS INCOPORATING A PORE FORMING AGENT.....	219
7.1 Introduction.....	219
7.2 Methodology .....	222
7.2.1 Simulated Dissolution Studies on the Cast Films .....	222
7.2.2 MTDSC Studies .....	223
7.2.3 Morphology Studies.....	223
7.2.4 Pellet Coating Process.....	223
7.2.5 Dissolution Studies .....	224
7.3 Results.....	224
7.3.1 Simulated Dissolution Studies on the Cast Films .....	224
7.3.1.1 MTDSC Studies .....	225
7.3.1.2 Morphology of Cast Films .....	230
7.3.2 Morphology of Coated Pellets .....	236
7.3.3 Drug Release from Coated Pellets .....	238
7.3.3.1 Metoprolol Succinate as the Model Drug .....	238
7.3.3.2 Paracetamol as the Model Drug.....	241
7.4 Discussion .....	243

7.6 Conclusion .....	246
CHAPTER 8 CONCLUSIONS.....	248
8.1 Thermal Properties of EC and EC Organic Solvent Films .....	248
8.2 Plasticizing Efficiency of OA, DBS and MCT .....	249
8.3 Miscibility of EC and Selected Plasticizers .....	250
8.4 Phase Distribution of EC/Plasticizer/HPMC Films .....	250
8.5 Mechanical Properties of EC films with Additives.....	252
8.6 Dissolution Studies .....	253
8.7 Overall Conclusions .....	255
8.8 Future Work .....	256
References .....	257
Appendix .....	278

## List of Figures

<i>Figure 1-1 Chemical structure of cellulose.....</i>	<i>32</i>
<i>Figure 1-2 Chemical structure of ethyl cellulose.....</i>	<i>32</i>
<i>Figure 1-3 The effect of the molecular weight of ethyl cellulose on the release of the model drug substance: ▼ Grade N7; ■ Grade N10; ★Grade N14; ▲ Grade N20; ●Grade N50... </i>	<i>36</i>
<i>Figure 1-4 The interrelationships between the molecular weight of ethyl cellulose, the amount of the model drug substance release after 2h (▼) and 5h (▲), the tensile strength of free films (●) and the elongation to break of free films (■).....</i>	<i>37</i>
<i>Figure 1-5 Scheme of the plasticizer-water-polymer system.....</i>	<i>47</i>
<i>Figure 1-6 Chemical structure of HPMC.....</i>	<i>51</i>
<i>Figure 1-7 Effect of the pore former HPMC on the MFT of the plasticized ethyl cellulose dispersions (mean ± S.D.;n=6). ○ 12.5% DBS; □ 12.5% DBP; ● 11.0%DEP; ■ 11.0% TEC.....</i>	<i>54</i>
<i>Figure 2-1 REF 1117 film applicator (Sheen Instruments Ltd., England).....</i>	<i>69</i>
<i>Figure 2-2 Tension film mode of DMA.....</i>	<i>83</i>
<i>Figure 2-3 Cantilever clamp of DMA.....</i>	<i>83</i>
<i>Figure 2-4 Basic principle of AFM.....</i>	<i>87</i>
<i>Figure 2-5 Scanning electron micrograph of the μTA probe.....</i>	<i>90</i>
<i>Figure 2-6 Scanning electron micrograph of the nTA probe.....</i>	<i>91</i>

<i>Figure 2-7 A bench-top fluid-bed tablet and spheroid (Pellet) coater/drier for small scale.....</i>	<i>95</i>
<i>Figure 2-8 Calibration curve for paracetamol.....</i>	<i>99</i>
<i>Figure 2-9 Calibration curve for metoprolol succinate.....</i>	<i>100</i>
<i>Figure 3-1 Degradation of EC 20 in TGA and D-TGA at heating rates of 2°C, 5°C and 10°C/min under nitrogen conditions (solid line-weight loss signals, dash line-derivative weight loss signals).....</i>	<i>106</i>
<i>Figure 3-2 DSC heat flow curve showing the heating, cooling and reheating signals of EC 20 powder in hermetically sealed pans at 10 °C/min to 200 °C.....</i>	<i>107</i>
<i>Figure 3-3 Glass transition of EC 7 at 2°C, 5°C and 10°C/min during heating analyzed by conventional DSC.....</i>	<i>108</i>
<i>Figure 3-4 Glass transition of EC 20 powder at 2°C, 5°C and 10°C/min during heating analyzed by conventional DSC.....</i>	<i>109</i>
<i>Figure 3-5 MTDSC reversing signal showing the heating, cooling and reheating of EC 20 in hermetically sealed pans at 2°C/min with a modulated amplitude of ±0.5°C/40s.....</i>	<i>112</i>
<i>Figure 3-6 10% (w/w) EC film prepared from 20 mL ethanol/acetone (40:60 v/v) organic solvent using 9 cm diameter petri dishes.....</i>	<i>113</i>
<i>Figure 3-7 TGA curve of EC 20 organic solvent films on heating from room temperature to 150°C.....</i>	<i>114</i>

<i>Figure 3-8 DSC curve of EC 20 organic solvent films on heating, cooling and reheating signals.....</i>	<i>115</i>
<i>Figure 3-9 Storage modulus, loss modulus and tan <math>\delta</math> of 2.5% EC 20 films with a heating rate of 3°C/min and a frequency of 1 Hz.....</i>	<i>118</i>
<i>Figure 3-10 Storage modulus, loss modulus and tan <math>\delta</math> of 5% EC 20 films with a heating rate of 3°C/min and a frequency of 1 Hz.....</i>	<i>119</i>
<i>Figure 3-11 Storage modulus, loss modulus and tan <math>\delta</math> of 7.5% EC 20 films with a heating rate of 3°C/min and a frequency of 1 Hz.....</i>	<i>119</i>
<i>Figure 3-12 Storage modulus, loss modulus and tan <math>\delta</math> of 10% EC 20 films with a heating rate of 3°C/min and a frequency of 1 Hz.....</i>	<i>120</i>
<i>Figure 4-1 Visual observation of EC cast films incorporated various types of plasticizers with different concentrations dried at room temperature or 45°C in the oven.....</i>	<i>134</i>
<i>Figure 4-2 EC cast films with 8.8% OA-16% DBS and 8.8% OA-16% MCT as the plasticizers, dried under room condition.....</i>	<i>135</i>
<i>Figure 4-3 Thermogram showing the degradation of EC/MCT dry films and pure MCT in weight loss and derivative weight loss signals at a heating rate of 10 °C/min under nitrogen conditions.....</i>	<i>137</i>
<i>Figure 4-4 Decomposition of EC/OA-DBS and EC/OA-MCT films in TGA and D-TGA at a heating rate of 10 °C/min.....</i>	<i>138</i>
<i>Figure 4-5 Derivative reversing heat capacity signals of MTDSC scans of EC/OA films by heating from 20°C to 220°C at a heating rate of 2 °C/min.....</i>	<i>140</i>

<i>Figure 4-6 Derivative reversing heat capacity signals of MTDSC scans of EC/DBS films by heating from 20 °C to 220 °C at a heating rate of 2 °C/min.....</i>	<i>140</i>
<i>Figure 4-7 Derivative Reversing heat capacity signals of MTDSC scans of EC/MCT films by heating from 20 °C to 220 °C at a heating rate of 2 °C/min.....</i>	<i>141</i>
<i>Figure 4-8 Reversing heat flow signals of EC/OA-DBS films and EC/OA-MCT films by heating from 20°C to 220°C at a heating rate of 2°C/min.....</i>	<i>143</i>
<i>Figure 4-9 Tan <math>\delta</math> of DMA scans of EC/OA films by heating from 30°C to 160°C at a heating rate of 3°C/min.....</i>	<i>145</i>
<i>Figure 4-10 Tan <math>\delta</math> of DMA scans of EC/DBS films by heating from 30°C to 160°C at a heating rate of 3°C/min.....</i>	<i>145</i>
<i>Figure 4-11 Tan <math>\delta</math> of DMA scans of EC/MCT films by heating from 30 °C to 160 °C at a heating rate of 3 °C/min.....</i>	<i>146</i>
<i>Figure 4-12 Tan <math>\delta</math> of EC/OA-DBS films and EC/OA-MCT films in tensile clamp.....</i>	<i>147</i>
<i>Figure 4-13 Tan <math>\delta</math> of EC/OA-DBS films and EC/OA-MCT films in single cantilever clamp.....</i>	<i>148</i>
<i>Figure 4-14 Storage moduli, determined at dynamic force of 50 mN and frequency of 1 Hz, of the films from different formulations.....</i>	<i>149</i>
<i>Figure 4-15 Topography, adhesion images and localized thermal analysis of pure EC, EC/30%OA, EC/30%DBS and EC/30%MCT films and their scales. For adhesion images, × marks the site of thermal analysis for data shown in the LTA figures.....</i>	<i>152</i>

*Figure 4-16 Topography, adhesion images and localized thermal analysis of EC/OA-DBS and EC/OA-MCT films and their scales. For adhesion images, × marks the site of thermal analysis for data shown in the LTA figures.....154*

*Figure 4-17 Adhesion images and histograms of EC films incorporated with 0%, 5%, 10%, 15%, 20%, 25% and 30% MCT, scanned at 25°C and 45°C, respectively.....156*

*Figure 5-1 Visual observation of EC/HPMC films.....175*

*Figure 5-2 TGA scans of HPMC powder (weight loss and derivative weight loss signals).....176*

*Figure 5-3 Comparison of the weight loss signals of EC film, EC/HPMC films and pure HPMC powder.....177*

*Figure 5-4 Comparison of the glass transitions of EC film, EC/HPMC films and pure HPMC powder by using the reversing heat flow signals.....179*

*Figure 5-5 DMA scans EC films with different concentrations of HPMC in the tensile clamp at 3°C/min.....180*

*Figure 5-6 Tan  $\delta$  of EC films with 0%, 10%, 20% and 30% HPMC.....181*

*Figure 5-7 Topography, adhesion images and LTA nano-thermal data of EC/HPMC films (5 $\mu$ m $\times$ 5 $\mu$ m).....185*

*Figure 6-1 Reversing heat flow signals of EC/OA free films incorporated with 0%, 10%, 20% and 30% HPMC, obtained from MTDSC at 2°C/min in the standard aluminium pans....199*

<i>Figure 6-2 Reversing heat flow signals of EC/DBS free films incorporated with 0%, 10%, 20% and 30% HPMC, obtained from MTDSC at 2°C/min in the standard aluminium pans.....</i>	<i>199</i>
<i>Figure 6-3 Reversing heat flow signals of EC/FCO free films incorporated with 0%, 10%, 20% and 30% HPMC, obtained from MTDSC at 2°C/min in the standard aluminium pans.....</i>	<i>200</i>
<i>Figure 6-4 Reversing heat flow signals of EC/OA-DBS films with different concentrations of HPMC, obtained from MTDSC at 2°C/min in the standard aluminium pans.....</i>	<i>202</i>
<i>Figure 6-5 Reversing heat flow signals of EC/OA-MCT films with different concentrations of HPMC, obtained from MTDSC at 2°C/min in the standard aluminium pans.....</i>	<i>202</i>
<i>Figure 6-6 Loss modulus and tan <math>\delta</math> signals of EC/OA films with 0%, 10%, 20% and 30% HPMC, obtained from DMA.....</i>	<i>204</i>
<i>Figure 6-7 Loss modulus and tan <math>\delta</math> signals of EC/OA films with 0%, 10%, 20% and 30% HPMC, obtained from DMA.....</i>	<i>205</i>
<i>Figure 6-8 Loss modulus and tan <math>\delta</math> signals of EC/MCT films with 0%, 10%, 20% and 30% HPMC from DMA.....</i>	<i>205</i>
<i>Figure 6-9 Loss modulus and tan <math>\delta</math> signals of EC/OA-DBS films with 0%, 10%, 20% and 30% HPMC from DMA.....</i>	<i>206</i>
<i>Figure 6-10 Loss modulus and tan <math>\delta</math> signals of EC/OA-MCT films with 0%, 10%, 20% and 30% HPMC from DMA.....</i>	<i>206</i>
<i>Figure 6-11 Storage moduli of EC/plasticizer films with 0%, 10%, 20% and 30% HPMC at 30°C, obtained from DMA.....</i>	<i>208</i>

<i>Figure 6-12 Topography, adhesion images (5<math>\mu</math>m<math>\times</math>5<math>\mu</math>m) and corresponding LTA data of EC/OA/30%HPMC, EC/DBS/30%HPMC and EC/MCT/30%HPMC films observed by using pulsed force mode AFM and LTA technique.....</i>	<i>210</i>
<i>Figure 6-13 Topography, adhesion and corresponding LTA data of EC/OA-DBS/30%HPMC and EC/OA-MCT/30%HPMC films observed by using pulsed force mode AFM and LTA technique.....</i>	<i>212</i>
<i>Figure 7-1 Reversing heat flow signals of EC films with 10%, 20% and 30%HPMC before and after immersion into DI water for 24 hours.....</i>	<i>225</i>
<i>Figure 7-2 Reversing heat flow signals of EC films with 10%, 20% and 30%HPMC after immersion into pH1.2 and pH6.8 buffers for 24 hours.....</i>	<i>226</i>
<i>Figure 7-3 Reversing heat flow signals of EC/OA films with 10%, 20% and 30%HPMC before and after immersion into DI water for 24 hours.....</i>	<i>227</i>
<i>Figure 7-4 Reversing heat flow signals of EC/OA films with 10%, 20% and 30%HPMC after immersion into pH 1.2 and pH 6.8 buffers for 24 hours.....</i>	<i>228</i>
<i>Figure 7-5 Reversing heat flow signals of EC/DBS films with 10%, 20% and 30%HPMC before and after immersion into DI water for 24 hours.....</i>	<i>228</i>
<i>Figure 7-6 Reversing heat flow signals of EC/DBS films with 10%, 20% and 30%HPMC after immersion to pH 1.2 and pH 6.8 buffers for 24 hours.....</i>	<i>229</i>
<i>Figure 7-7 Reversing heat flow signals of EC/MCT films with 10%, 20% and 30%HPMC before and after immersion into DI water for 24 hours.....</i>	<i>229</i>

<i>Figure 7-8 Reversing heat flow signals of EC/MCT films with 10%, 20% and 30%HPMC after immersion to pH 1.2 and pH 6.8 buffers for 24 hours.....</i>	<i>230</i>
<i>Figure 7-9 SEM images of EC films with 10%, 20% and 30% HPMC removed from DI water at time=0, 2, 8 and 24 hours.....</i>	<i>232</i>
<i>Figure 7-10 SEM images of EC/OA films with 10%, 20% and 30% HPMC removed from DI water at time=0, 2, 8 and 24 hours.....</i>	<i>233</i>
<i>Figure 7-11 SEM images of EC/DBS films with 10%, 20% and 30% HPMC removed from DI water at time=0, 2, 8 and 24 hours.....</i>	<i>234</i>
<i>Figure 7-12 SEM images of EC/MCT films with 10%, 20% and 30% HPMC removed from DI water at time=0, 2, 8 and 24 hours.....</i>	<i>235</i>
<i>Figure 7-13 Morphology of API pellets coated by EC/10% plasticizer and EC/10% plasticizer/20% HPMC films.....</i>	<i>237</i>
<i>Figure 7-14 The percentage cumulative release profiles of metoprolol succinate from pellets coated with EC/OA, EC/DBS, EC/MCT, EC/OA/HPMC, EC/DBS/HPMC and EC/MCT/HPMC films up to 24 hours.....</i>	<i>239</i>
<i>Figure 7-15 The percentage cumulative release profiles release profile of paracetamol from pellets coated with EC/OA, EC/DBS, EC/MCT, EC/OA/HPMC, EC/DBS/HPMC and EC/MCT/HPMC films up to 24 hours.....</i>	<i>241</i>

## List of Tables

<i>Table 1-1 The permeability, diffusion and solubility coefficients for ethyl cellulose at 35.0°C and at 10 atm (1,013kPa); Units: Permeability coefficient, <math>P \times 10^9</math> [<math>\text{cm}(\text{STP})\text{cm}^{-1}\text{cm}^{-2}(\text{cmHg})^{-1}</math>]; diffusion coefficient, <math>D \times 10^8(\text{cm}^2\text{s}^{-1})</math>; and solubility coefficient, <math>S \times 10^3[\text{cm}^3(\text{STP})(\text{cm}^3\text{polymer})^{-1}(\text{cmHg})^{-1}]</math>.....</i>	<i>35</i>
<i>Table 1-2 Ethyl Cellulose samples used in the study of effect of the molecular weight of EC on the drug release properties.....</i>	<i>36</i>
<i>Table 1-3 Different EC Grades (Aqualon®) and their relative ethoxyl content and viscosity.....</i>	<i>39</i>
<i>Table 1-4 Properties of plasticizers for film coatings for oral drug delivery.....</i>	<i>44</i>
<i>Table 2-1 Summary of the properties of EC, OA, DBS, MCT, HPMC and the model drugs used in this project.....</i>	<i>66</i>
<i>Table 2-2 Formulations of pure EC films.....</i>	<i>68</i>
<i>Table 2-3 Formulations of EC cast films with different additives (plasticizers used were OA, DBS and MCT).....</i>	<i>70</i>
<i>Table 2-4 Paracetamol drug layering formulation.....</i>	<i>96</i>
<i>Table 2-5 Metoprolol succinate drug layering formulation.....</i>	<i>96</i>
<i>Table 2-6 Formulation of the film coatings applied on APIs.....</i>	<i>97</i>
<i>Table 2-7 Parameters used for drug laying, seal coating and film coating process using a Mini Coater/Drier instrument.....</i>	<i>97</i>

<i>Table 3-1 Glass transition temperatures of EC 7 powder on heating, cooling and reheating at 2°C, 5°C and 10°C/min (n=3).....</i>	<i>109</i>
<i>Table 3-2 Glass transition temperatures of EC 20 powder on heating, cooling and reheating at 2°C, 5°C and 10°C/min (n=3).....</i>	<i>110</i>
<i>Table 3-3 Glass transition temperatures of EC 7 and 20 powder during heating, cooling and reheating at 2°C/min in MTDSC (n=3).....</i>	<i>112</i>
<i>Table 3-4 Glass transition temperatures of films prepared by EC 7 with different concentrations in ethanol/acetone (40:60) organic solvent system, obtained from MTDSC (n=3).....</i>	<i>115</i>
<i>Table 3-5 Glass transition temperatures of films prepared by EC 20 with different concentrations in ethanol/acetone (40:60) organic solvent system, obtained from MTDSC (n=3).....</i>	<i>116</i>
<i>Table 3-6 Comparison of T<sub>g</sub> values of EC 20 films produced from MTDSC and DMA (n=3).....</i>	<i>120</i>
<i>Table 3-7 The storage modulus and loss modulus of EC 20 films at room temperature... </i>	<i>121</i>
<i>Table 4-1 Components of EC/plasticizer films.....</i>	<i>129</i>
<i>Table 4-2 Weight loss of EC films with various formulations at 120°C.....</i>	<i>136</i>
<i>Table 4-3 Glass transition temperatures of EC/plasticizer films with different concentrations from MTDSC (n=3).....</i>	<i>142</i>
<i>Table 4-4 Glass transition temperatures of EC/plasticizer films with different concentrations from DMA (n=3).....</i>	<i>146</i>

<i>Table 4-5 Comparison of measured (<math>\Delta T_{gexp}</math>) and calculated plasticizing efficiencies (<math>\Delta T_{gcal}</math>) of EC films with different levels of plasticizers.....</i>	<i>161</i>
<i>Table 5-1 Film formula of EC/HPMC films.....</i>	<i>172</i>
<i>Table 5-2 Amounts of residual solvents of EC films incorporated with 0%, 10%, 20% and 30% HPMC and pure HPMC, data analyzed from TGA results at 120°C (n=3).....</i>	<i>177</i>
<i>Table 5-3 Glass transition temperatures of EC films with 0%, 10%, 20%, 30% HPMC and pure HPMC, obtained from the reversing heat flow signals of MTDSC (n=3).....</i>	<i>179</i>
<i>Table 5-4 Peak temperatures of Loss modulus and <math>\tan \delta</math> of EC films with 0%, 10%, 20% and 30% HPMC, obtained from DMA (n=3).....</i>	<i>181</i>
<i>Table 5-5 Predicted glass transition temperatures of EC films with 10%, 20% and 30% HPMC, using the Gordon Taylor/Simha Boyer equations, providing EC and HPMC are miscible.....</i>	<i>189</i>
<i>Table 6-1 Film formulations of EC/plasticizers/HPMC films.....</i>	<i>195</i>
<i>Table 6-2 Glass transition temperatures of EC/plasticizer films on adding different concentrations of HPMC, obtained from the reversing signals of MTDSC (n=3).....</i>	<i>201</i>
<i>Table 6-3 Glass transition temperatures of EC/plasticizer mixture films on adding different concentrations of HPMC, obtained from the reversing signals of MTDSC (n=3).....</i>	<i>203</i>
<i>Table 6-4 Glass transition temperatures of EC/plasticizer films on adding different concentrations of HPMC, obtained from <math>\tan \delta</math> peaks of DMA (n=3).....</i>	<i>207</i>
<i>Table 7-1 The values of <math>R^2</math> and K (drug release constant) of drug release profiles of metoprolol succinate from pellets coated by EC/OA, EC/DBS, EC/MCT, EC/OA/HPMC, EC/DBS/HPMC, and EC/MCT/HPMC films, obtained from dissolution model fitting,</i>	

*including zero-order, first-order, Hixson-Crowell and Higuchi models, according to Eq 7-1, 7-2, 7-3 and 7-4.....240*

*Table 7-2 The values of  $R^2$  and K (drug release constant) of drug release profiles of paracetamol from pellets coated by EC/OA, EC/DBS, EC/MCT, EC/OA/HPMC, EC/DBS/HPMC, and EC/MCT/HPMC films, obtained from dissolution model fitting, including zero-order, first-order, Hixson-Crowell and Higuchi models, according to Eq 7-1, 7-2, 7-3 and 7-4.....242*

## Abbreviations

AFM	Atomic Force Microscopy
API	Active Pharmaceutical Ingredient
DBS	Dibutyl Sebacate
DMA	Dynamic Mechanical Analysis
DP	Degree of Polymerization
DS	Degree of Substitution
DSC	Differential Scanning Calorimetry
EC	Ethyl Cellulose
FT-IR	Fourier Transform Inferred Spectroscopy
HPMC	Hydroxypropyl Methylcellulose
LTA	Localized Thermal Analysis
MCT	Medium Chain Triglycerides
MFT	Minimum Film Formation Temperature
MTDSC	Modulated Temperature Differential Scanning Calorimetry
nTA	Nano-thermal analysis
OA	Oleic Acid
PEG	Polyethylene Glycol
RCS	Refrigerated Cooling System
RH	Relative Humidity
SEM	Scanning Electronic Microscopy
SPM	Scanning Probe Microscopy
STM	Scanning Tunnelling Microscopy
TEC	Triethyl Citrate
$T_g$	Glass Transition Temperature

TGA

Thermogravimetric Analysis

$\mu$ TA

Micro-thermal Analysis

## **CHAPTER 1 INTRODUCTION**

### **1.1 General Introduction**

Controlled release drug delivery systems have been established in order to deliver a drug to the site of action at a specific rate, as well as to maintain the optimal concentration levels of drugs in plasma within the therapeutically effective range for an extended period of time (Yie and Senshang, 2006). The basic controlled release formulation consists of an active agent and a carrier. In addition, a popular dosage form for controlled release involves film coating for the prolonged and precise release of the drug with good reproducibility (Sousa et al., 2002; Vaithiyalingam and Khan, 2002). The basic elements for a coated drug system are a core matrix and the coating film. The active agents, which can be liquid or solid, are initially loaded into the core matrix, while the coating film is a layer or multiple layers of materials.

Polymeric film coatings have often been used for achieving controlled release of an active substance from a pharmaceutical preparation which primarily regulates the release rate and through which the drug is released. Films mainly consist of film forming materials and plasticizers; pore forming agents may also be included and will be described in more detail in a later section. Every component of the film coatings plays an important role in the process of sustained release. Water-insoluble film forming materials may produce a film coat with adequate mechanical strength to ensure the prolonged release of drug, while pore formers help with the regulation of the rate of drug release. However, plain films which have film coating materials only, such as ethyl cellulose (EC) films, are brittle, hence the

---

addition of a plasticizer is necessary to enhance film forming feasibility and serviceability (Bonacucina et al., 2006).

The main mechanisms for drug release are the following: I diffusion, II erosion or chemical reactions, III swelling and IV osmosis. Diffusion is the most important mechanism for the controlled release of the drug, and will be discussed later in more detail.

The use of pore forming materials as a means of controlling the barrier properties of polymeric films has been of great interest in recent years (Lippold et al., 1999; Ohara et al., 2005; Siepmann et al., 2006). By incorporating a water-miscible polymer as a minor component in water-immiscible films, it is possible to generate pores in that film on contact with water as the water-miscible component dissolves or disperses. A number of relationships between composition, processing parameters and drug release have been described, with issues such as plasticizer types and levels, coating levels, curing conditions and mechanical properties having been studied (Siepmann et al., 2006). However, the link between film structure and drug release is not fully understood. Some issues for describing their relationship are addressed as follows:

- a) Miscibility of the film materials and pore formers
- b) Spatial distribution of the pore formers
- c) Mechanical properties of the films
- d) Link between the above properties and dissolution

## **1.2 Film Coating Materials**

Water-insoluble coating materials play an important role in the controlled release system.

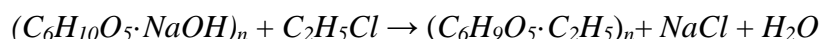
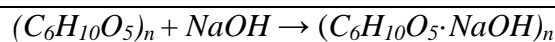
EC is a broadly studied film forming polymer used in coated controlled release solid

---

dosage forms (Krögel and Bodmeier, 1999). EC is a type of thermoplastic cellulose ether, meaning that it can be shaped by pressure when heated, and can form a brittle, glassy state when cooled sufficiently. It is soluble in many solvents and compatible with a number of plasticizers and pore formers (Frohoff-Hülsmann et al., 1999a; Frohoff-Hülsmann et al., 1999b). Its thermo-plasticity makes it widely used in food, cosmetics and pharmaceutical industry (Pearce, 1997). EC may be used on lacquers, and also be used as a vehicle in microscopic circuit printing. It is also used in pigments, inks and vitamin preparations as an ingredient. Within the food and pharmaceutical industries, EC is broadly used as a taste-masking agent, film coating material for controlled release as well as other applications (McConnell et al., 2007; Muschert et al., 2009b).

### 1.2.1 Chemical Structure of EC

EC, which is an ethyl ether of cellulose, is prepared from wood pulp or cotton by treatment with alkali and etherification of the alkali cellulose with ethyl chloride. Cellulose is a biopolymer made up of anhydroglucose units linked in a linear chain formation. For each anhydroglucose unit there are three hydroxyl groups ( $-OH$  groups) that provide reactive centres at which the reactions can take place. Unmodified cellulose is insoluble in water or in conventional solvents. By etherifying hydroxyl groups it is possible to use the substituents to convert it into organo-soluble derivatives. Cellulose is an inert material; therefore a solvating agent and a swelling agent are required for the etherification of cellulose in order to obtain an appreciable reaction. Water and sodium hydroxide are the solvating agent and swelling agent respectively, which are most used. The preparation of EC is an etherification process of the alkali cellulose with ethyl chloride, which is described by as the follow reactions:



The selection of various molar ratios of sodium hydroxide and ethyl chloride may result in varying degrees of substitution (DS) and also the distribution of substitution. The Degree of Substitution (DS) is defined as the average number of substituted hydroxyl groups per glucose. After these reactions, the product must be filtered, washed, neutralized and dried to obtain the finished product.

EC is used within the pharmaceutical industry due to its water-insoluble and viscoelastic properties that are associated with the structure, molecular weight and degree of substitution (DS). All of this information is therefore needed to understand the properties of EC. Cellulose is an organic compound with the formula  $(C_6H_{10}O_5)_n$ . It is a structural polysaccharide comprising of beta-glucose. Cellulose is a straight chain polymer composed of individual anhydroglucose units linked at the 1- and 4- positions with beta configuration. The multiple hydroxyl groups on the glucose residues hydrogen bonds with each other, holding the chains firmly together and contributing to their high tensile strength. The polymer backbone is shown in *Figure 1-1*. Each repeating unit exposes three replaceable hydroxyl groups.

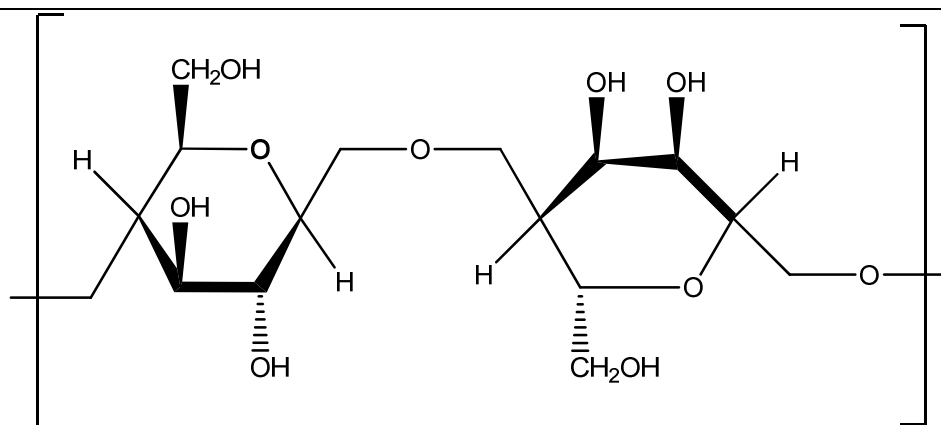


Figure 1-1 Chemical structure of cellulose

Chemically, EC is an ethyl ether of cellulose, arising from substituting the hydrogen atoms of some of the cellulose's hydroxyl groups  $-OH$  with ethyl groups  $-C_2H_5$ , forming  $-OC_2H_5$  groups. Different kinds of EC can be prepared depending on the number of hydroxyl groups substituted. Figure 1-2 shows an EC with a DS of 3.0, which means a complete substitution of all of the three hydroxyl groups of cellulose. The ethoxyl content is approximately 54.88%. However, EC with a DS of 3.0 is not easy to obtain.

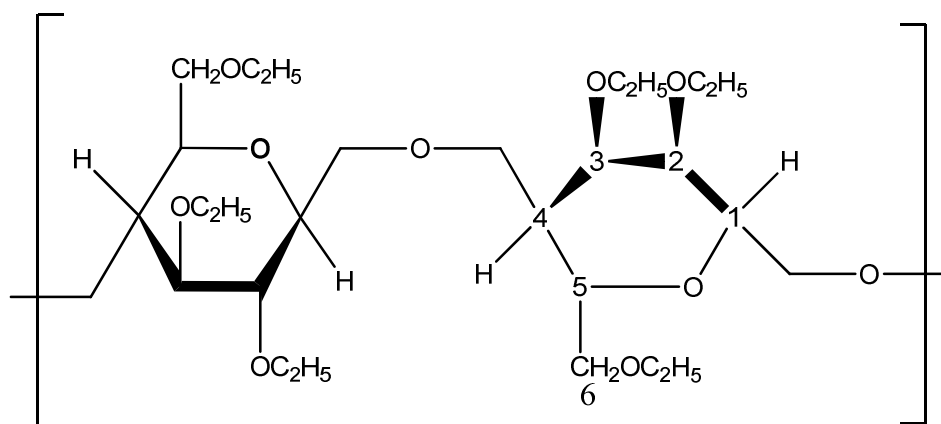


Figure 1-2 Chemical structure of ethyl cellulose

### 1.2.2 Properties of EC

Ethyl cellulose (EC) is a tasteless, non-toxic, thermoplastic, white to light tan-coloured powder, which offers good light and thermal stability but little fire hazard and moisture

absorption. The films and plastics made by EC have a high mechanical strength and flexibility within a wide range of temperatures (Roberts and Rowe, 1987). EC is practically insoluble in water, in glycerol, and in propane-1, 2-diol, but soluble in various proportions in certain organic solvents, depending upon the ethoxyl content. EC that contains less than 46%-48% of ethoxyl groups is freely soluble in tetrahydrofuran, methyl acetate, chloroform and aromatic hydrocarbon ethanol mixtures (Masilungan and Lordi, 1984). EC that contains 46%-48% or more of ethoxyl groups is freely soluble in ethanol, methanol, toluene, chloroform, and ethyl acetate.

EC is compatible with many kinds of resins and plasticizers (such as dialkyl phthalates, polyethylene glycols and dibutyl sebacate, etc.) (Gunder et al., 1995; Rowe et al., 1984; Sakellariou et al., 1986a). The miscibility between EC and plasticizers give the operator flexibility in selecting a suitable EC based film, which makes it popularly used as a water-insoluble material in film coating for pharmaceutical applications. EC can exhibit thermotropic liquid crystalline behaviour which is described in section 1.2.2.5.

The functional properties of EC depend upon the degree of polymerization (DP), the degree of substitution (DS) as well as the distribution pattern of the substituent groups on the C(2),C(3) and C(6) positions of polysaccharide (Yu and Gray, 1998). Therefore, DS, molecular weight, DP and the crystalline nature of EC are of significant importance for its properties, such as elongation, tensile strength, flexibility, glass transition temperature ( $T_g$ ), solubility and water absorption.

---

### 1.2.2.1 Degree of Substitution

The degree of substitution (DS) indicates the average number of etherified hydroxyl groups per anhydroglucose unit (Wu et al., 2002). In the case of EC, it is related to the ethoxyl content of the polymer. The DS (with respect to ester groups) for the polymers prepared can be determined by Fourier transformer inferred spectroscopy (FT-IR) or gas chromatography. Higher DS values result in a lower water-solubility because the polar hydroxyl groups are masked. Therefore, completely substituted tri-ethyl cellulose has no significant application because of its poor strength and flexibility. On the other hand, EC with a DS between 0.8-1.7 (ethoxyl content 19%-35%) is water-soluble; this material has no commercial significance either. The most commonly used EC has a DS range of 2.15-2.50 (ethoxyl content 43%-50%) (Wu et al., 2002).

The solubility and diffusivity of light gases such as  $He$ ,  $O_2$ ,  $N_2$ ,  $CH_4$  and  $CO_2$  is affected by the ethoxyl content of EC (Houde and Stern, 1997). The study showed that the solubility tended to increase when increasing the ethoxyl content of EC, possibly because of an increase in the free volume of the polymer, as reflected in increases in both the specific free volume (SFV) and fractional free volume (FFV). The permeability of EC films also increases when increasing the ethoxyl content of EC. *Table 1-1* presents the permeability, diffusion and solubility coefficients for ethyl cellulose at 35.0°C and at 10 atm (1,013kPa)

Ethoxy content (%)	Property	He	O <sub>2</sub>	N <sub>2</sub>	CH <sub>4</sub>	CO <sub>2</sub>
47.2		4.93	1.46	0.411	0.878	8.90
47.9	<i>P</i>	6.58	1.94	0.579	1.24	11.6
49.6		7.94	2.33	0.655	1.41	14.7
47.2		1.742	94.8	32.1	20.4	48.1
47.9	<i>D</i>	2.056	120.5	45.2	28.1	65.5
49.6		3.031	129.4	43.4	27.7	67.7
47.2		0.283	1.54	1.28	4.30	18.5
47.9	<i>S</i>	0.320	1.61	1.28	4.41	17.7
49.6		0.262	1.80	1.51	5.09	21.7

*Table 1-1 The permeability, diffusion and solubility coefficients for ethyl cellulose at 35.0°C and at 10 atm (1,013kPa); Units: Permeability coefficient,  $P \times 10^9 [cm(STP)cms^{-1}cm^{-2}(cmHg)^{-1}]$ ; diffusion coefficient,  $D \times 10^8 (cm^2s^{-1})$ ; and solubility coefficient,  $S \times 10^3 [cm^3(STP)(cm^3 polymer)^{-1}(cmHg)^{-1}]$  (Houde and Stern, 1997)*

### 1.2.2.2 Molecular Weight

A background knowledge of the molecular weight of the polymer is of importance to the film coating formulation since it has an important effect on the mechanical properties of the films, which are important in governing viscosity of EC films and the incidence of film cracking (Rowe, 1982). *Table 1-2* shows the molecular weight of EC used in the study of the effect of the molecular weight of EC on the drug release properties (Rowe, 1986). These viscosity values were detected at 25°C in a 5% w/w solution of a solvent mixture of toluene and ethanol (80:20). *Figure 1-3* shows the drug release of EC with various molecular weights. It is shown that the drug release decreases with increasing the

molecular weight, but at molecular weights in excess of 35,000, which is equivalent to the N22 Grade, there was no further decrease. The data indicated a change of the mechanism of release at short times leading to a steady-state condition after approximately two hours. At a molecular weight of EC of over 35,000, the drug release does not decrease, probably because the films are coherent at such a high molecular weight.

Sample	Ethoxyl content (% w/w)	Apparent viscosity (cP)	Molecular weight
N7	48.8	6	18,260
N10	48.4	9	22,920
N14	48.6	13	28,160
N22	48.7	20	35,860
N50	48.5	50	59,870

Table 1-2 Ethyl Cellulose samples used in the study of effect of the molecular weight of EC on the drug release properties (Rowe, 1986)

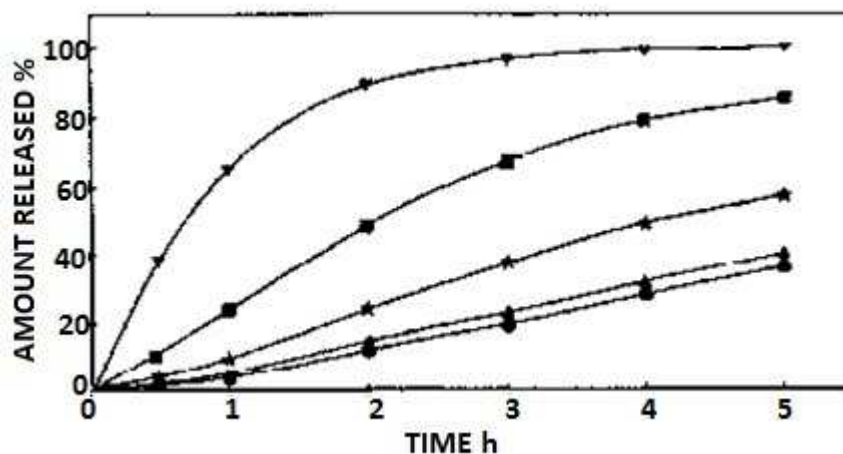
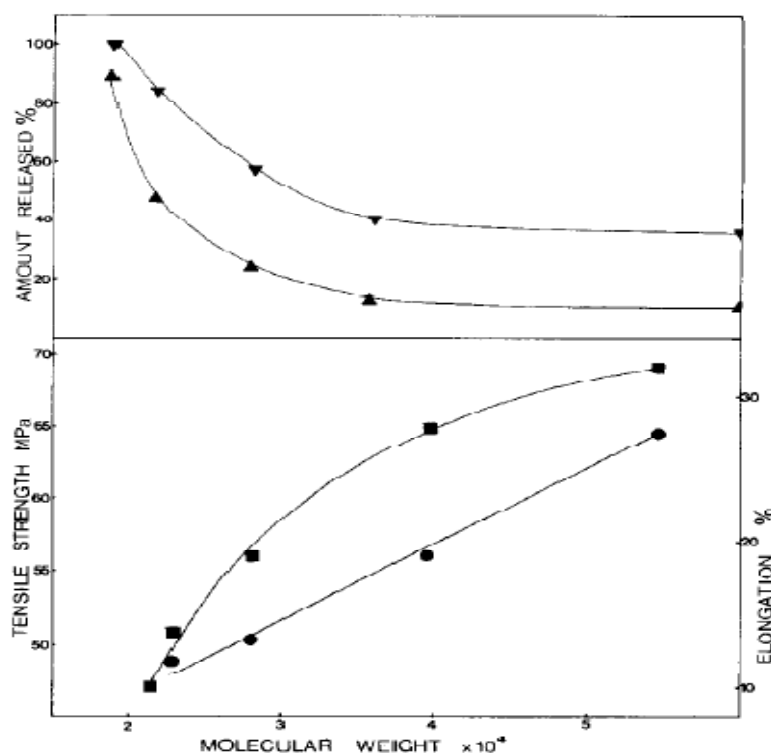


Figure 1-3 The effect of the molecular weight of ethyl cellulose on the release of the model drug substance: ▼ Grade N7; ■ Grade N10; ★ Grade N14; ▲ Grade N20; ● Grade N50.

(Rowe, 1986)

Rowe (1982) suggested that the origins and causes of flaws and cracks in the film coating were created by the shrinkage of the film on evaporation of the solvent and by differences in the thermal expansion of the coating and substrate. If these stresses exceeded the cohesive strength of the film, cracking will occur and film integrity will be lost. Films that are prepared from a low molecular weight with short chains are relatively weak, which would lead to flaws, cracks and imperfections. *Figure 1-4* shows the interrelationships between the dissolution of the model drug substance, the mechanical properties (tensile strength and elongation to break) of EC and the molecular weight of EC (Rowe, 1986). The data supports the idea that the cracks only occur with low molecular weight of EC, which results in a rapid release of the model drug. The frequency of this defect decreases with increasing the molecular weight.



*Figure 1-4* The interrelationships between the molecular weight of ethyl cellulose, the amount of the model drug substance release after 2h (▼) and 5h (▲), the tensile strength of free films (●) and the elongation to break of free films (■). (Rowe, 1986)

---

The relationship between mechanical properties of a polymer and its molecular weight is described by the Flory equation (Rowe, 1992):

$$P = A + \frac{B}{M} \quad \text{Eq1-1}$$

where  $P$  is the mechanical properties (tensile strength and elongation to break),  $M$  is the number average of the molecular weight and  $A$  and  $B$  are constants. The  $B$  values for mechanical properties are negative, which means that the mechanical strength increase with molecular weight.

### 1.2.2.3 Viscosity Grade

Viscosity is a measurement of the resistance of a fluid to deform under a shear stress. Within the application of polymer science, it is an expression of a solvent's ability to swell the polymer. Intrinsic viscosity has been proved to be a useful tool for solvent selection for EC. A solvent system consisting of toluene and ethanol in the ratio of 80:20 (% w/w) or methylene chloride and ethanol in the ratio of 60:40 (%w/w) has been suggested as favourable for EC (Arwidsson and Johansson, 1991). Viscosity is usually measured at 25°C of a 5% w/w solution in a mixture of toluene and ethanol in the ratio of 80:20 (% w/w). The addition of water up to 10% is thermodynamically favourable for an ethyl cellulose solution, however, at this concentration, films are less stress resistant, less ductile and less stiff (Arwidsson and Johansson, 1991). *Table 1-3* provides information on different grades of EC.

EC Grade	Ethoxyl content, %	Viscosity, cP
K50	45.0 – 47.2	40 – 52
N7	48.0 – 49.5	6 – 8
N14	48.0 – 49.5	12 – 16
N22	48.0 – 49.5	18 – 24
N50	48.0 – 49.5	40 – 52
N100	48.0 – 49.5	80 – 105
T10	49.6 – 51.0	8 – 11
T50	49.6 – 51.5	40 – 52
T100	49.6 – 51.5	80 – 105

*Table 1-3 Different EC Grades (Aqualon®) and their relative ethoxyl content and viscosity*

It is necessary to select a suitable viscosity grade for the polymer film so as to balance the film strength with the drug release properties. Polymer films prepared from a solvent system that has a high viscosity value are typically mechanically strong due to the tight intertwining between polymer molecules. Nevertheless, increasing the molecular weight and viscosity grade can result in a lower mobility of the polymer chain and also a reduction of the free volume available for diffusion. Therefore, it will decrease the diffusion rate of drug molecules between the polymer molecules.

#### *1.2.2.4 Glass Transition Temperature*

The glass transition temperature ( $T_g$ ) is the temperature below which molecules of the polymer have little relative mobility. Many thermoplastic polymers form super-cooled

liquids when rapidly cooled down from melt. Electrostatic repulsive forces that exist between segments of a polymer can be ‘frozen’ into the structure. These forces are relieved by the energy supplied to the sample through heating, and the polymer becomes able to flow. Hence, the  $T_g$  can be defined as a temperature range at which an amorphous material becomes less viscous and changes from a glassy phase to a rubbery phase upon heating, or vice versa if cooling. The  $T_g$  is the overall glass transition temperature as a consequence of the mobility of all these motions within the polymer molecule and an increase in heat capacity (Coleman and Craig, 1996).

$T_g$  is very important in polymeric characterization, as the properties of the material are highly dependent on its glass transition. The  $T_g$  of EC determines its behaviour in film coating formulation during the film coating process and the subsequent storage.  $T_g$  can also be a specific measurement of the effect of plasticizers on a polymer since it is a function of chain mobility and the purpose of a plasticizer is to increase chain mobility (Sakellariou et al., 1986a). It can also be applied to assess the miscibility between two or more polymers in a system. A polymer blend could be considered compatible if only one  $T_g$  is observed. If the polymer consists of an immiscible binary blend, then two  $T_g$ s will be recorded.

#### *1.2.2.5 Liquid Crystalline Nature*

Liquid crystals are substances that exhibit properties between those of a conventional liquid and those of a solid crystal. They may flow as a liquid, but contain molecules in a liquid arranged and/or oriented in a crystal-like manner. Liquid crystals can be divided into thermotropic and lyotropic liquid crystals. A liquid crystal is thermotropic if the order of its components is determined or changed by changing temperature. Thermotropic liquid crystals materials are generally rod-like molecules with rigidity in the central region and

---

flexible substituent. They can be converted into a conventional isotropic liquid phase when the temperature is raised resulting in the removal of the cooperative order of the liquid crystal phase. A lyotropic crystal usually consists of two or more components which can form liquid crystals in certain concentration ranges of solvent. In the lyotropic phases, solvent molecules fill the space around the compounds to provide fluidity to the system. In contrast to thermotropic liquid crystals, these lyotropics have another degree of freedom of concentration that enables them to induce a variety of different phases.

EC with an ethoxyl content over 45% has been shown to exhibit thermotropic liquid crystalline behaviour (Wu et al., 2002). Also, EC are semi-rigid chain polymers, which can form lyotropic liquid crystals in appropriate solvents (Dai and Huang, 1998). As a result of the chirality of the cellulose backbone, EC may form chiral nematic structures (Shimamoto and Gray, 1998).

### **1.3 Plasticizers**

One commonly used method to modify the properties of polymers and enhance their film forming properties is the addition of plasticizers. Plasticizers may be defined as low molecular weight substances, ideally of low volatility, which increase the flexibility of the polymer chains, hence producing films that are flexible, more pliable and often tougher with a subsequent improvement in their resistance to mechanical stress.

#### **1.3.1 Effects of Plasticizers**

Plasticizers are additives that increase the plasticity of the material to which they are added. It is usually necessary to include plasticizers in coating films in order to obtain the polymeric films with the appropriate properties. They may reduce the brittleness of the

---

polymeric films, alter the permeability of the drug and promote film formation in the case of aqueous dispersions.

EC films without plasticizers are brittle and will result in a very slow drug release. Plasticizers may increase the flexibility of the macromolecules which may give the desired flexibility and durability to the film. The high glass transition temperature of EC shows that it softens and flows at a high temperature. It does not form flexible films under normal coating conditions. In order to obtain good thermo-plasticity, plasticizers are added, and thus the glass transition is reduced to a lower temperature.

The use of plasticizers is essential for the improvement of the mechanical properties of EC films. Plasticizers work by embedding themselves between the chains of polymers, spacing them apart. In polymeric solutions, plasticizers increase the free volume between the polymer chains (Mauritz et al., 1990). Thus they will significantly lower the glass transition temperature for the polymer and make it softer. They could also reduce the minimum film formation temperature (MFT) below that of the coating temperature (Tarvainen et al., 2003). Plasticizers can penetrate into the polymeric chains of EC more rapidly and completely to take its action between the EC chains once MFT is exceeded, and hence, increasing the flexibility of the polymer chain.

The addition of plasticizers may also decrease the surface free energy of polymeric films, which is important in determining the adhesion between films and the dosage form surfaces (Oh and Luner, 1999). Both the structure and the composition of the film surface could be affected by plasticizers due to the polymer-plasticizer interaction. Plasticizers can moderate hydrogen bonding based on their solubility (Sakellariou and Rowe, 1995a).

---

Interactions between plasticizers and polymers will reduce polymer-polymer reaction, which results in the greater polymer chain mobility.

### 1.3.2 Plasticizers Used for Film Coating

The main requirements for plasticizers used in film coatings are the permanence and the efficiency of plasticization. The compatibility of plasticizers and the other dosage form components also needs to be considered. There are a wide range of plasticizers that are compatible with EC. The most common used plasticizers for oral drug delivery are listed below in *Table 1-4*. Other novel plasticizers have been studied to enhance the film forming properties of EC, such as *n*-alkenyl succinic anhydrides (Tarvainen et al., 2003). Drug release depends strongly on the type of plasticizers. The chemical nature of plasticizers plays an important role in the drug release mechanism (Lecomte et al., 2004).

Plasticizer	Molecular Weight	Density (gcm <sup>-3</sup> ) (20°C)	Refractive Index at 25°C	Tb (°C) (760 mmHg)	Flash Point (°C)
Glycerol	92	1.260	1.473	290	177
Propylene glycol	76	1.035	1.431	188	99
Polyethylene glycol 400	400	1.128	1.455 (70°C)	>300	245
Polyethylene glycol 4000	4000	1.20 (solid)	1.517	Solid at 25°C	262
Dimethylphthalate	194	1.189	1.501	282	163
Diethylphthalate	222	1.123	1.490	296	168
Dibutylphthalate	278	1.051	1.443	340	171
Dibutyl sebacate	314	0.932	1.440	345	185
Triethyl citrate	276	1.136	1.446	127	155
Tributyl citrate	360	1.045	1.438	170	185
Triethyl acetyl citrate	318	1.135	1.441	132	188
Tributyl acetyl citrate	402	1.048	1.431	173	204
Triacetin	218	1.156	1.480	258	132
Castor oil	-	0.960	-	>150	-

*Table 1-4 Properties of plasticizers for film coatings for oral drug delivery*

*(Sakellariou and Rowe, 1995a)*

---

### 1.3.2.1 Hydrophilic Plasticizers

The permeability of the film to the drug is an important factor in determining the suitability of a film for the development of a controlled release preparation. It is also an important factor that governs the rate of release through a polymer which is insoluble in the digestive system, such as EC. EC is a very hydrophobic material and thus the incorporation of hydrophilic plasticizers can increase the permeability for hydrophilic drugs in the EC films.

The interaction between EC and a hydrophilic plasticizer polyethylene glycol (PEG) has been studied by DSC (Sakellariou et al., 1986b). The system consisted of an amorphous polymer (EC) and a crystalline polymer (PEG 6000). Three relatively sharp transitions were recorded at  $-40^{\circ}\text{C}$  to  $-47^{\circ}\text{C}$ ,  $60^{\circ}\text{C}$  and  $118 - 126^{\circ}\text{C}$ , respectively. The first transition is thought to be the amorphous part of the PEG that gives rise to a glass transition. In this case, the transition height will increase with increasing the PEG content. It is thought that increasing the concentration of the amorphous polymer EC results in an increased restriction in movement of the PEG chains. Furthermore, this behaviour is associated with the depression of the degree of crystallinity of the PEG. The second transition of  $60^{\circ}\text{C}$  is associated with the melting of PEG crystallites and the subsequent increase in mobility of this polymer within a rigid matrix of EC.

Triethyl citrate (TEC) is a hydrophilic plasticizer permitted in the fields of food additives, medical and pharmaceutical industry. It has been confirmed that TEC is a suitable plasticizer for an EC aqueous dispersion Aquacoat<sup>®</sup> (Obara and McGinity, 1995). Plasticization time is the time between the addition of the plasticizer to the polymer dispersion and the coating step. It has been demonstrated that the plasticization time had no effect on the distribution behaviour of water-soluble plasticizers (Bodmeier and Paeratakul,

1997). When TEC was added to the aqueous colloidal dispersion, a large amount of the plasticizer was dissolved in the aqueous phase and these plasticizers were not taken up by the colloidal polymer phase prior to the coating. The plasticizer partitioned into the polymer phase during the drying process and resulted in an homogeneous film.

#### 1.3.2.2 Hydrophobic Plasticizers

The disadvantage of using a hydrophilic plasticizer is that it will leak out from the polymer coating after contact with dissolution or physiological fluid. Then the release kinetics will vary due to the change of the film composition, and hence the system is difficult to control accurately. According to the literature, hydrophobic plasticizers can be applied with hydrophilic plasticizers in aqueous dispersions on film coating (Felton and McGinity, 1997).

The process of water-insoluble plasticizer uptake in aqueous dispersion was divided into three steps:

- (1) emulsification: oily plasticizer droplets emulsify in the solvent phase;
- (2) convection and diffusion: emulsified plasticizer molecules are transferred through the well-stirred water phase to the polymer surface;
- (3) diffusion: plasticizer molecules are taken up by the polymer and diffuse with the polymer surface (Siepmann et al., 1998);

In the system consisting of water-insoluble plasticizer, water and suspended polymer particles (shown in *Figure 1-5*), at the beginning, immediately after mixing the plasticizer and aqueous dispersion, emulsification of the plasticizers is the rate-limiting process

(emulsification rate < diffusion rate) and diffusion controls the transfer kinetics at the end (emulsification rate > diffusion rate). This can be explained according to Fick's first law.

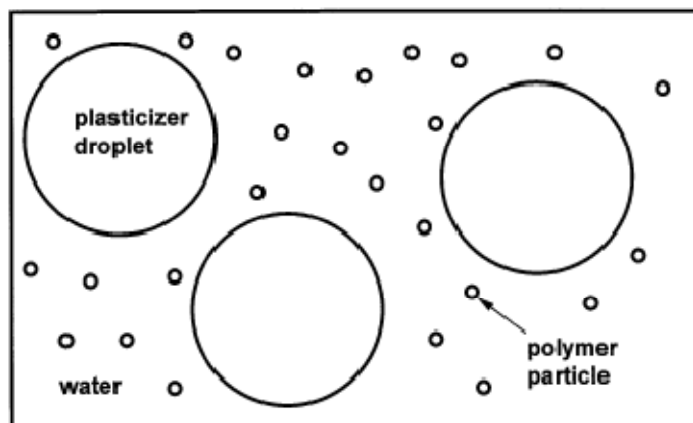


Figure 1-5 Scheme of the plasticizer-water-polymer system (Siepmann et al., 1998)

Plasticization time is the period from the addition of the plasticizers to the EC solutions until the coating dispersions are applied to the formula. The effect of plasticization time on the uptake of water-insoluble plasticizers have been investigated (Bodmeier and Paeratakul, 1997). Water-insoluble plasticizers have to be emulsified in the aqueous phase of the polymer dispersions, and then diffuse from the emulsified droplets into the aqueous phase and partition from the aqueous phase to the polymer phase. The emulsified plasticizers have to be taken up completely by the colloidal polymer particles before the coating process, otherwise both the plasticized polymer and remaining emulsified plasticizer will be sprayed onto the solid dosage forms which will cause inhomogeneous films. Therefore, sufficient plasticization time is necessary when water-insoluble plasticizers are applied. Higher plasticizer levels will lead to a higher absolute amount of plasticizer taken up by the polymer, which also need more time for plasticizer uptake. Dibutyl sebacate, diethyl phthalate, dibutyl phthalate, acetyltriethyl citrate and tributyl citrate are most commonly

---

used hydrophobic plasticizers for EC. Three hydrophobic plasticizers were focused on in this project. The phase behaviour and distribution of EC films with oleic acid or medium chain triglycerides have not been fully understood while dibutyl sebacate has attracted relatively more attention (Frohoff-Hülsmann et al., 1999b; Gunder et al., 1995; Kangarlou et al., 2008; Lippold et al., 1999; Lippold et al., 1989). Therefore, these three hydrophobic plasticizers were chosen to prepare the EC films and study their phase behaviour, distribution and dissolution profiles.

Oleic acid (OA) is pale yellow oily liquid with lard-like odour. It is an 18-C acid with molecular mass of 282.4614 g/mol. It is insoluble in water, but soluble in methanol. Films prepared by using casein as a film forming agent and OA as a plasticizer agent were capable of producing a continuous, acceptable coat (Abu Diak et al., 2007). OA, as a fatty acid, was used to improve the water barrier properties of films (Vargas et al., 2008). The higher the OA content, the lower the water vapour permeability and the moisture sorption capacity of the chitosan/OA dry films. It has been shown that the addition of OA into a chitosan matrix led to a significant increase in the gloss, translucency and a decrease in the tensile strength, elongation at break and elastic modulus of the films (Vargas et al., 2008). This plasticizer has also been reported to have a plasticizing effect in the sodium caseinate films (Fabra et al., 2008). Therefore, OA is an interesting plasticizer candidate to prepare EC films.

The plasticizer referred to as medium chain triglycerides (MCT) is a colourless to light yellow odourless liquid, produced from coconut acid oil by an enzymatic esterification with glycerol (Sumit et al., 2004). MCT has been utilized in the commercial product Surelease® as a plasticizer for EC aqueous dispersions. It was suggested that the

---

hydrophobic EC interacts preferentially with hydrophobic MCT in the EC films (McConnell et al., 2007).

Dibutyl sebacate (DBS) is an organic molecule and is a dibutyl ester of sebacic acid. At room temperature, this material is an oily colourless liquid with a melting point of  $-10^{\circ}\text{C}$  and boiling point of  $344\text{-}345^{\circ}\text{C}$ , insoluble in water, but soluble in ethanol, acetone, toluene and diethyl ether. It provides excellent compatibility with a range of plastic materials. DBS has been used as a plasticizing agent in EC films (Frohoff-Hülsmann et al., 1999b; Gunder et al., 1995; Kangarlou et al., 2008; Lippold et al., 1999; Lippold et al., 1989). It can not only reduce the glass transition temperature, but also improve the flexibility of the EC films. When the hydrophobic plasticizer DBS was used, the drug release mechanism of the EC films was controlled mainly by the diffusion of the drugs through the polymeric films (Frohoff-Hülsmann et al., 1999b).

## **1.4 Pore formers**

### **1.4.1 Pores**

Pores in controlled release films are formed due to the hydration and dissolution of water-soluble pore formers. Using pore formers have been an effective means to control drug release from polymer film coated preparations. The dosage form is coated by inert polymers; therefore, the release rate depends on the properties, thickness and the surface area of the polymer films (Strübing et al., 2007). Several mechanisms to release the drug are described as follows

(1) Diffusion via films with big pores: polymers with pores diameters between  $0.05\ \mu\text{m}$  and  $1.0\ \mu\text{m}$  could be penetrated by most drug molecules;

---

(2) Diffusion via films with micropores: most biomacromolecules could penetrate the micropores whose diameters are between 0.01  $\mu\text{m}$  and 0.05  $\mu\text{m}$ . But the diffusion of drug is affected by the structure of the film pores.

(3) Diffusion via continuous films: if the polymeric films are continuous and uniform, plasticizers and other additives will disperse uniformly inside the coating films. There exist molecular pores between the intertwining polymeric chains. Digestive juice permeates the films into the system to dissolve the drug. Drug molecules are dissolved, diffused and dispersed in the polymeric films, and released into the digestive juice finally. Osmotic pressure differences between the inner core and the release medium has an effect on the drug release rate. The drug release rate is also related to the properties of the model drug and the release medium.

Three different release mechanisms of pellets coated with aqueous EC dispersions with pore formers have been demonstrated (Frohoff-Hülsmann et al., 1999b). The drug release is dependent on the physical state of the swollen EC and on the migration of the water soluble pore former respectively. If the pore former mostly migrates from the coating, the type and amount of plasticizer in the swollen coating and the temperature of the release medium influences the release rate to a large extent. If the film forming polymer is present in the glassy state as it is after the migration of the water soluble plasticizer and pore former at temperatures below  $T_g$ , the drug diffuses through water filled pores (first mechanism). But if the EC is in the rubbery state as it is the case with the water-insoluble plasticizer at temperatures above  $T_g$ , the drug release rate is characterized by a two-phase release profile as a result of pore shrinking (second mechanism). If the migration of the pore former is incomplete, the drug diffuses through a swollen heterogeneous membrane of EC (third mechanism).

### 1.4.2 Pore Former – Hydroxypropyl Methylcellulose (HPMC)

Ethyl cellulose is a water-insoluble polymer. Therefore it requires the addition of a water-miscible polymer, such as hydroxypropyl methylcellulose (HPMC), to produce a film-coat with a desirable permeability for controlled release.

#### 1.4.2.1 Chemical Structure of HPMC

Hydroxypropyl methylcellulose (HPMC) is a semisynthetic, inert polymer that is widely used as an ophthalmic lubricant, as well as a water-soluble pore former in the coating industry for controlled-release. *Figure 1-6* shows the chemical structure of HPMC.

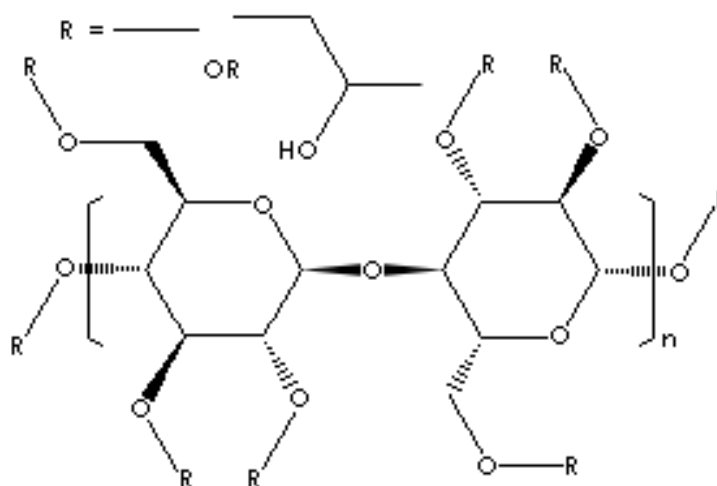


*Figure 1-6* Chemical structure of HPMC

HPMC is white to off-white fibrous powder or granules. It swells in water to produce a viscous colloidal and non-toxic solution. HPMC powder can dissolve slowly in cold water, but is insoluble in hot water. It is soluble in most polar solvents but insoluble in anhydrous alcohol, ether and chloroform. HPMC aqueous solutions are surface active. They can form films upon drying and undergo reversible transformation from solution to gel upon heating and cooling (Ong et al., 2006).

---

HMPC is manufactured by a reaction of purified cellulose with alkylating reagents (methyl chloride) in the presence of a base, typically sodium hydroxide and an inert diluent. The addition of the base in combination with water activates the cellulose matrix by disrupting the crystalline structure and increasing the access for alkylating agent and promotes the etherification reaction. During the manufacture of HPMC alkali cellulose reacts with methyl chloride to produce methyl cellulose and sodium chloride. The methyl cellulose is then further reacted with the staged addition of propylene oxide. After the reaction, HPMC is purified in hot water where it is insoluble. Drying and grinding completes the process of the manufacture of HPMC.

HPMC is widely used in the food industry as an emulsifier, thickening agent, stabilizer, film former, protective colloid, fat barrier and a suspending agent (Lindstedt et al., 1989; Mitchell et al., 1990; Okhamafe and York, 1984). HPMC also has many pharmaceutical uses, as a drug carrier, a coating agent, a tableting agent and an emulsifier in ointments. It is also used in ophthalmic solutions and as a pore forming agent in the film coating industry.

#### *1.4.2.2 Effect of HPMC on Film Coating*

As a pore forming agent, HPMC contributes to the formation of pores in the film to permit transport. Firstly, the hydration and dissolution of HPMC will leave pores in the film, and then the hydrated HPMC may be retained in the film as a barrier. The drug release from polymeric film that consisted of EC, HPMC and dibutyl sebacate (DBS) may take place in two phases (Gunder et al., 1995). During the first phase, water-filled pores were formed through which the drug, depending on its solubility, was able to diffuse in its ionized or unionized form. However, the increase in water content was not maintained. It was

---

assumed that the pores were closed as film continued to form. In the second phase, drug release can only take place as a result of distribution and diffusion of the dissociated form. Both the concentration of HPMC and the pH of environment have a great effect on the release rate of the model drug. The release rate increased markedly in the concentration range (25% - 30%) of HPMC. In the case of 40% HPMC content, the release was no longer membrane-controlled, and the coats disintegrated. HPMC is very sensitive to electrolytes (Mitchell et al., 1990). At a pH value of 9, with the carboxylic groups contained in the EC fully dissociated, the two-phase nature of the release mechanism was only just detectible with 10% w/w HPMC. Higher HPMC contents resulted in single-phase release behaviour. The coat loses more and more of its release-controlling function as the HPMC content increases. Cracks were observed macroscopically in the case of 40% w/w HPMC.

In the film coating process, heat will evaporate the water and soften the colloidal particles so as to make them accumulate. The minimum film forming temperature (MFT) is a temperature at which the aqueous dispersion could form a continuous film without cracks being formed under dry conditions. The coating temperature has to be higher than the MFT to obtain a continuous film. Otherwise, cracks on the coating are formed, hence resulting in a burst release (Lippold et al., 1989). The MFT may be affected by the glass transition temperature ( $T_g$ ) of the polymer and the plasticizers (Leong et al., 2002) and also the concentration of HPMC. The effect of HPMC on the MFT of the plasticized EC dispersions are shown in *Figure 1-7* (Frohoff-Hülsmann et al., 1999a).

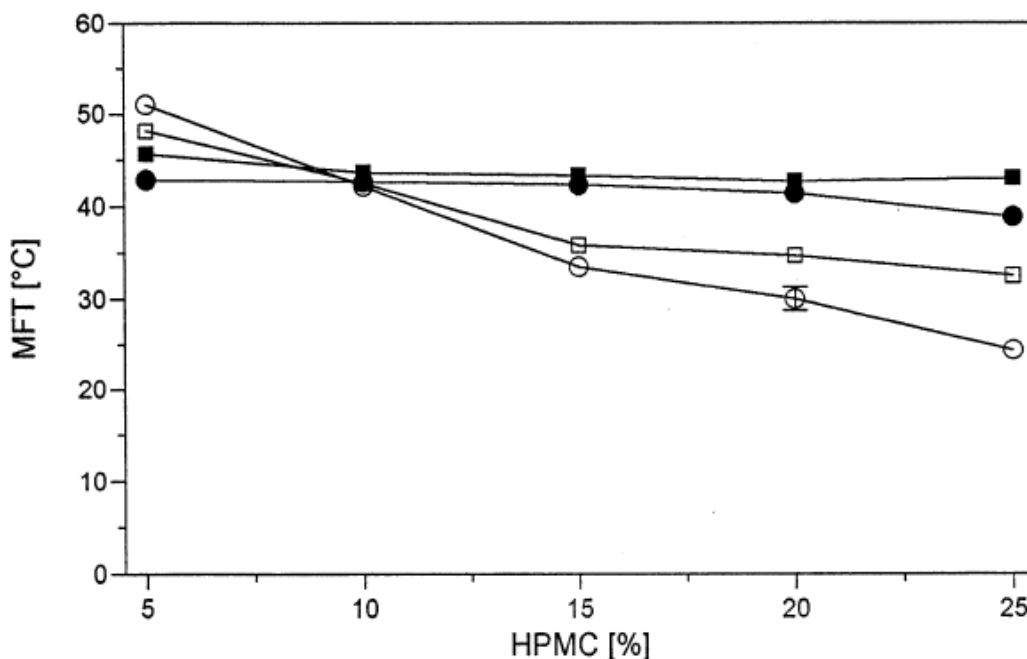


Figure 1-7 Effect of the pore former HPMC on the MFT of the plasticized ethyl cellulose dispersions (mean  $\pm$  S.D.; n=6).  $\circ$  12.5% DBS;  $\square$  12.5% DBP;  $\bullet$  11.0% DEP;  $\blacksquare$  11.0% TEC (Frohoff-Hülsmann et al., 1999a)

The MFT values of the EC dispersion containing the water-insoluble plasticizers DBS (debutyl sebacate) and DBP (diethyl phthalate) decreased with increasing amounts of HPMC. In contrast, the effect of HPMC on the aqueous polymer dispersion containing water-soluble plasticizers, including DEP and TEC was negligible. The MFT varied between 46°C and 43°C.

The phase separation behaviour in the blends of EC/HPMC with different ratios was also studied (Sakellariou and Rowe, 1995a). Both systems with 60% and 80% EC respectively exhibited morphologies typical to nucleation and growth mechanism of phase separation. The authors also confirmed that the observed polymer incompatibility was not due to the effect of the solvent system but due to thermodynamic incompatibility of EC and HPMC.

---

This incompatibility was attributed to the absence of intermolecular interaction between the polymers. The phase separation process occurs during the solvent evaporation process. Once the system concentration has crossed the bimodal and exceeded a critical value, nucleation and growth leads to formation of two phases.

## 1.5 Film Formation

There are several processes to produce films, such as the flat film, film blowing, gel spinning processes, the zone drawing zone annealing method, film casting and calendaring (Pearce, 1997). However, two techniques are particularly important for pharmaceutical systems: organic solvent coating and aqueous polymer dispersions.

### 1.5.1 Organic Solvent Systems

As the solvent system has a great impact on the properties of polymer films, the development of means to predict the effect is of great interest. Intrinsic viscosity,  $[\eta]$ , and an interaction constant,  $k'$ , have been examined as tools for solvent selection for ethyl cellulose (Arwidsson and Johansson, 1991). Intrinsic viscosity,  $[\eta]$ , is an expression of the solvent's ability to swell the polymer and a measure of a solute's contribution to the viscosity of a solution. A polymer solution with a high intrinsic viscosity contains the polymer existing as tight coils, whereas a low value of intrinsic viscosity is a result of the polymer being present as loose coils. Polymer films prepared from a solvent that gives a high intrinsic viscosity value may, therefore, be expected to be mechanically strong due to the tight intertwining between neighbouring polymer molecules. A low interaction constant,  $k'$ , would lead to the polymer solution having a sharp viscosity increase during the organic solvent evaporation. The ability of the polymer molecules to move freely in a good solvent results in less internal stresses in the film (Rowe, 1981). Therefore, a low interaction

---

constant is favourable for better mechanical properties of polymeric films. By using the combination of these two parameters, Arwidsson and Johnsson (1991) studied the mechanical properties in order to choose a favourable solvent system for EC coating, e.g. methylene chloride and ethanol in the ratio of 60:40 (% w/w) or toluene and ethanol in the ratio of 80:20 (% w/w).

Organic solvent systems are used for film coating due to their favourable film formation properties. A number of investigators have shown the influence of solvents system on the properties of the coating (Lindholm et al., 1984). However the method still has its obstacles such as safety and environment problems. Generally, film formation from organic solvents takes place by the evaporation of the organic solvent which increases the concentration of polymer until a gel-like stage is achieved. Through further evaporation, a solvent-free polymeric film is obtained. The intermolecular forces between the film forming polymer molecules and those between the film and substrate control these processes. The residue levels of various organic solvents in the coating films depends on the solvent, quality of the drug cores and conditions used of coating and drying (Lindholm et al., 1984).

### 1.5.2 Aqueous Polymeric Dispersions

The mechanism of film formation by aqueous polymeric dispersion is more complicated than in organic solvent systems. Film formation of aqueous dispersion may involve three processes: (1) aqueous dispersion droplets load and spread on the surface of drug cores; (2) with the water evaporated, polymeric molecules associate tightly; (3) curing, chains of the neighbouring polymeric molecules intertwine with each other; hence a continuous film is formed. Optimal mechanical properties and film formability may be obtained by proper

---

selection of the type and concentration of plasticizers. EC films with different plasticizers were prepared and the drug release was investigated under different curing conditions in the release medium and with different pH values (Siepmann et al., 2007). The addition of the small amount of PVA-PEG to EC-based film coatings allowed effective modulation of the film properties, such as water uptake behaviour, dry weight loss kinetics and drug permeability.

### **1.6 Application of EC Film Coatings for Controlled Release Dosage Forms**

Recently, EC has been widely used as a controlled release coating agent due to its hydrophobic nature and low water permeability. It can form strong films with good adhesion, which provides a diffusion barrier whose properties can be modified by film thickness, level of plasticizers or by modifying the solvent(s) used during the coating process. Arwidsson and Johansson (1991) have studied the mechanical properties and structure of the films casted from different organic solvent systems. The polymeric films prepared by the organic solvent system and the aqueous polymer dispersion in different release media have been compared (Wesseling and Bodmeier, 1999). Strong curing and media effects were seen with beads coated with aqueous polymer dispersion.

Surelease<sup>®</sup> is a commercial plasticized aqueous dispersion of ethyl cellulose (EC) with approximately 25% of solid content. It contains EC (20cP), 28% ammonium hydroxide, oleic acid (OA) and dibutyl sebacate (DBS) as a plasticizer. The average diameter for EC in Surelease<sup>®</sup> is 0.2  $\mu\text{m}$ . The molten EC is emulsified in ammoniated water under high pressure. The formation of ammonium oleate stabilized the formulation and converted to oleic acid, which then plasticized ethyl cellulose during the drying process. Purified water is added at the end of the process in order to achieve the desired solid content.

---

In coated pellets, the core pellets containing the model drug, the lubricant, the binder and the other additives are initially manufactured and the EC solutions/dispersions are then sprayed onto the surface of these pellets forming a controlled/modified release coating. The influence of film coating of the pellets on the *in vitro* drug release profile has been studied (Sousa et al., 2002). The results showed that in this specific case drug release from uncoated pellets was mainly influenced by the solubility of the drug. Pellets coated with aqueous EC dispersion at a 5% weight gain showed an influence of the coat membrane on the drug release. Generally, the drug release is dependent on the drug solubility. However, some physical characteristics of the core of the pellet such as porosity and specific surface area also contribute to the release behaviour. The knowledge of the pellet structure, such as pore diameter and volume is of great importance as a porous structure can decrease the film adhesiveness. Mechanical properties such as tensile strength and elasticity are usually assessed on so-called 'free' or 'cast films'. In addition, the mechanical properties of EC film coatings when applied to the surface of pellets have been studied as well (Podczeck and Almeida, 2002). The parameters of the mechanical properties of the coated pellets were significantly different from the values of the uncoated pellets, which represented the visco-elastic behaviour of the film coatings.

As a water insoluble excipient, EC can effectively control the release of an active ingredient by modifying the size and length of the diffusion path. Typically, EC is used in combination with water-soluble drugs and/or water-soluble excipients in order to achieve the desirable release profiles. EC solid dispersions are usually prepared by the solvent evaporation method. By dissolving or dispersing the drug and EC in an organic solvent, such as ethanol, after evaporation of the organic solvent, solid dispersions are obtained through the drying process. The release mechanism of poorly water-soluble drug

---

indomethacin from the extended release solid dispersion systems with EC and water-soluble hydroxypropyl methylcellulose (HPMC) has been investigated (Ohara et al., 2005). The mechanism of drug release was affected by the internal structure of EC-HPMC matrix that is governed by the preparation method and the medium pH values. If the solid dispersion contained finely and uniformly dispersed HPMC within its internal structure, release of the model drug followed a diffusion mechanism whose dissolution rate constant ( $k$ ) depended on the medium pH values. However, if the solid dispersion contains a mass of HPMC with few tens of micrometer diameters, the drug release mechanism could be divided into two phases, namely release with HPMC erosion and diffusion from the insoluble EC matrix.

### **1.7 Aims and Objectives**

Ethyl cellulose films used for controlled release oral formulations have been one of the most important coating systems in the pharmaceutical industry. Ethyl cellulose films incorporated with water-soluble plasticizers have been used extensively to prepare film coatings for controlled release formulations. However, hydrophobic plasticizers may not dissolve and leak out from the film coatings, hence the film coatings may maintain their mechanical properties during the dissolution process. OA, DBS and MCT are three very promising hydrophobic plasticizers for ethyl cellulose films. Therefore, the plasticizing efficiency of these plasticizers and plasticizer mixtures, and their miscibility and interaction with EC in organic films are investigated. Pore forming materials have been used as a major means of controlling the drug release from polymeric film coating preparations for many years, and HPMC remains one of the most important hydrophilic pore forming agents in the film coating industry. However, the specific relationship between the components of polymer films is not well known. Hence, the principle goal of

---

this project is to investigate the miscibility of the film coating material (EC), plasticizers (OA, DBS and MCT) and the pore former (HPMC) and establish a link between the film structure and release properties of coated dosage forms to predict the release profile of drugs. To achieve this goal, the miscibility of the components of polymeric films and the film structure will be investigated by means of differential scanning calorimetry (DSC), modulated temperature DSC (MTDSC), thermogravimetry analysis (TGA), dynamic mechanical analysis (DMA) and atomic force microscopy (AFM), and localized thermal analysis (LTA). Dissolution studies of water soluble drugs from pellets coated by these films will be performed to understand the release behaviour in relation to the film structure.

---

## CHAPTER 2 MATERIALS AND METHODS

Pure EC films and those with different additives were produced to investigate the effect of the additives on the film properties and the miscibility of the components within the films. All of the films were prepared by the organic solvent casting method instead of using the complex aqueous colloidal dispersions or commercial products due to the simplicity of the organic solvent system approach. Plasticizers and pore former were added to the EC films to investigate their interactions within the cast films.

Several thermo-mechanical and imaging techniques can be used for pharmaceutical material characterization. Typically, multi-approaches are required since no single technique is capable of characterizing the materials thoroughly. Conventional differential scanning calorimetry (Conventional DSC), modulated temperature differential scanning calorimetry (MTDSC) and thermogravimetric analysis (TGA) were utilized to characterize the thermal properties of the raw materials and the produced films. Dynamic mechanical analysis (DMA) was utilized to investigate the thermo-mechanical properties of the films. Scanning electronic microscopy (SEM) and various applications of atomic force microscopy (AFM), such as heated stage AFM, micro-thermal analysis ( $\mu$ TA) and nano-thermal analysis (nTA), provided imaging information related to the thermal properties and miscibility of the films.

Finally, multiparticulate pellets were produced using a drug layering technique, and coated by EC/additive films with desired formulations. These film formulations were tested for

---

their controlled release characteristics. This chapter will give a summary of the principles of these techniques, calibration procedures and experimental parameters.

## 2.1 Materials

### 2.1.1 Ethyl Cellulose

Ethyl cellulose (EC) is prepared from wood pulp or cotton by treatment with alkali and etherification of the alkali cellulose with ethyl chloride. As it is physically and chemically inert, non-ionic and water-insoluble, EC offers good light and thermal stability and can be used in various applications, such as binders, fillers, granulation aids, protective and controlled release coatings, taste masks and flavour fixatives. EC appears as a tasteless, odourless, and white to light tan-coloured free flowing powder which is generally considered non-toxic. EC is practically insoluble in water, glycerine and propylene glycol; EC that contains less than 46.5% of ethoxyl groups is freely soluble in chloroform, methyl acetate and mixtures of aromatic hydrocarbons with ethanol (95%); EC that contains more than 46.5% of ethoxyl groups is freely soluble in chloroform, ethanol (95%), methanol and toluene.

The EC used in this project were ETHOCEL<sup>TM</sup> 7 and ETHOCEL<sup>TM</sup> 20, supplied by Colorcon Ltd. (USA) and were originally from the Dow Chemical Company (USA). It was used as received without further purification or modification and stored in a dry and cool place. These two polymers are white particles with ethoxyl content of 48.0 – 49.5% and viscosity of 6 – 8 cP and 18 – 22 cP, respectively. The viscosity is usually measured at 25°C of a 5% w/w solution in a mixture of toluene and ethanol in the ratio of 80:20 (% w/w) (Rowe, 1986).

Several plasticizers and pore formers were added to the cast films in this project: oleic acid, dibutyl sebacate, medium-chain triglycerides and hydroxypropyl methylcellulose. The following sections give an overview of these materials. A summary of all materials, including the chemical structure and physical properties, is shown in *Table 2-1*.

## 2.1.2 Plasticizers

### 2.1.2.1 Oleic Acid

Oleic acid (OA) is colourless to pale yellow oily liquid with a lard-like odour and taste. It is stored in a closed container in a cool, dry place. It is an 18-C acid with a molar mass of 282.4614 g/mol. It is insoluble in water, but miscible with ethanol (95%), benzene and chloroform. OA, as a fatty acid, was used to improve water barrier properties of films (Vargas et al., 2008), and it has been reported to have a plasticizing effect in the films (Fabra et al., 2008). 25% (w/w) OA can reduce the  $T_g$  of EC in toluene/ethanol (80:20 w/w) organic solvent systems to 45.2°C (Vesey et al., 2005). OA used in this project was supplied by Colorcon Ltd. (USA).

### 2.1.2.2 Dibutyl Sebacate

Dibutyl sebacate (DBS) is an organic chemical, a dibutyl ester of sebacic acid. It is a colourless oily liquid with a melting point of -10 °C and boiling point of 344 – 345 °C. It is insoluble in water and glycerin, but soluble in ethanol and acetone. As a plasticizer, it provides excellent compatibility with a range of plastic materials. 25% (w/w) DBS can reduce the glass transition temperature ( $T_g$ ) of EC ( $T_g = 130$  °C) in toluene/ethanol (80:20 w/w) organic solvent system to 49.6 °C (Vesey et al., 2005). DBS in this project was supplied by Colorcon Ltd. (USA), and was used as received.

---

### 2.1.2.3 Medium-chain Triglycerides

Medium-chain triglycerides (MCT, Captex<sup>®</sup> 300), with the chemical name of triglyceride of caprylic/capric acid, was supplied by Colorcon Ltd. (USA), originally from Abitec Corporation (USA). MCT is a medium chain (6 – 12 carbons) of fatty acid of glycerol. It is a colourless to light yellow odourless and tasteless liquid, practically insoluble in water, miscible with ethanol and fatty oils. MCT has a wide range of applications as a plasticizer, emulsifying agent and suspending agent.

### 2.1.3 Hydroxypropyl Methylcellulose

Hydroxypropyl Methylcellulose (HPMC), with the chemical name of 2-hydroxypropyl cellulose methyl ether, is a partly O-methylated and O-(2-hydroxypropylater) cellulose. It is widely used in pharmaceutical products as a film coating material for controlled release, a binding agent for tablet and pellet coatings, and in the liquid preparations as a stabilizing agent or suspending agent. HPMC is an odourless white powder, practically soluble in cold water, but insoluble in hot water, ethanol, acetone and ether. It swells in water and produces a clear to opalescent viscous, colloidal mixture. HPMC used in this work were METHOCEL<sup>™</sup> E5 (Dow Chemical Company, USA) as the pore former in the film coatings and METHOCEL<sup>™</sup> E6 (Dow Chemical Company, USA) as the binding agent for the drug laying process of the pellets preparation. Both of them have a methoxyl content of 28 – 30% and a hydroxypropyl content of 7 – 12%. METHOCEL<sup>™</sup> E5 has a viscosity (2% solution in water) of 4 – 6 cP, which is 5 – 7 cP for METHOCEL<sup>™</sup> E6. They were all used as received.

---

## 2.1.4 Model Drugs

### 2.1.4.1 Paracetamol

Paracetamol or acetaminophen is a widely used over-the-counter pain reliever and fever reducer. The raw material is an odourless white crystalline powder with a melting point at 168°C. It is very slightly soluble in water (14 mg/mL at 25°C). The half-life of paracetamol is 1 – 4 hours which makes it ascendant to produce a controlled release dosage form, since if the half-life of the active compound is over 6 hours, and its release is sustained on its own. The UV absorption wavelength is 243 nm in water. Paracetamol (4-Acetamidophenol) was purchased from Alfa Aesar, UK and was used as received.

### 2.1.4.2 Metoprolol Succinate

Metoprolol, presented as metoprolol succinate, is used for the treatment of hypertension and angina. It is an odourless white crystalline powder, freely soluble (100 mg/mL at 25°C) in water. 2% solution has a pH of 7.0 – 7.6. The UV absorption wavelength is 274 nm in water. Metoprolol succinate (Toprol XL®, AstraZeneca LP, UK) was stored in a tight and closed container in a cool, dry place, and used as received without further purification.

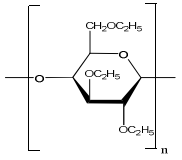
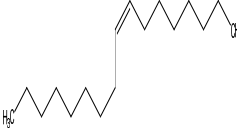
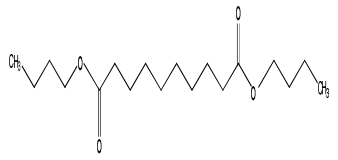
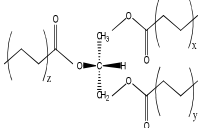
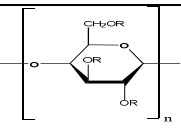
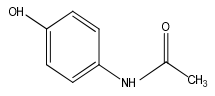
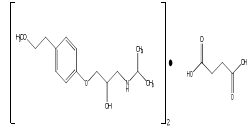
Name	Ethyl cellulose (EC)	Oleic acid (OA)	Dibutyl sebacate (DBS)	Medium-chain Triglycerides (MCT)	Hydroxypropyl methylcellulose (HPMC)	Paracetamol	Metoprolol Succinate
Structural Formula					 R is H, CH <sub>3</sub> or CH <sub>3</sub> (OH)CH <sub>2</sub>		
Material Used	ETHOCEL™7 ETHOCEL™20	Oleic Acid	Dibutyl sebacate, N.F.	Captex®300	METHOCEL™ E5 METHOCEL™ E6	4-Acetamidophenol	Toprol XL®
Description	Tasteless, free-flowing, white to light tan powder	Colourless to pale yellow, oily liquid of characteristic, lard-like odor and taste	Colourless, oily liquid of very mild odor	Odourless, tasteless and colorless to slightly yellowish oily liquid	White to slightly off-white powder.	Odourless white crystalline powder	Odourless white crystalline powder
Moisture Content	≤3.0%	NA	NA	NA	≤5.0% (USP 28) ≤10% (PhEur2005)	≤0.5%	≤0.5%
Solubility	Insoluble in glycerin, propylene glycol, and water; freely soluble in chloroform, ethanol (95%), ethyl acetate, methanol and toluene	Miscible with benzene, chloroform, ethanol (95%), ether, hexane, and volatile oils; insoluble in water	Soluble in alcohol, isopropyl alcohol and mineral oil; insoluble in water and glycerin	Insoluble in water; miscible with alcohol, methylene chloride, hexane, and fatty oils.	Soluble in cold water; insoluble in ethanol (95%), but soluble in mixtures water and alcohol	14 mg/mL in water (25°C)	100mg/mL in water (25°C)

Table 2-1 Summary of the properties of EC, OA, DBS, MCT, HPMC and the model drugs used in this project

---

## 2.2 Preparation of EC Cast Films

All cast films were made from EC ETHOCEL™ 7 or ETHOCEL™ 20 (Dow Chemical Company, USA) with ethoxyl content of 48.0 – 49.5% and viscosity of 6 – 8 cP and 18–22 cP, respectively. All the solvents used in the film preparation were of pharmaceutical grade.

The solvent system may have a great influence on the properties of the produced films. Therefore, it is important to select an optimum solvent system for EC films. It has been suggested that the binary solvent mixtures of a poorly hydrogen bonding and an alcohol, such as methylene chloride/ethanol (80:20 w/w) and toluene/ethanol (80:20 w/w), maybe a suitable solvent system for EC films (Arwidsson and Nicklasson, 1990). However, methylene chloride and toluene are not recommended for use in pharmaceutical products due to their high toxicity. The combination of ethanol/acetone (40:60 v/v) was shown to give the best film appearance in the previous study (Lai, 2005). Therefore this solvent system was applied for EC films in the present study. When water-soluble HPMC is involved, ethanol/acetone is not a desired solvent system. EC and the plasticizers can be dissolved in water and in an alcohol mixture. Theoretically, the addition of water to a good solvent system for the water-insoluble EC is expected to show a low solvent power. However, by using intrinsic viscosity and interaction constant to assess the solvent power, addition up to 10% of water to the favourable solvent system was advantageous (Arwidsson and Nicklasson, 1989). The polymer may precipitate at approximately 13% water content in the solvent mixture. This may result in a relatively weak stress resistance of the films. Therefore, ethanol/water (90:10 v/v) was used for HPMC films and all the films were dried in the oven to speed up the evaporation of water.

2.5%, 5%, 7.5% and 10% (w/v) EC solutions were prepared by dissolving EC with relative weight mass (shown in *Table 2-2*) into 20 mL of ethanol/acetone (40:60 v/v). The EC solutions were heated to 45°C on a hot plate and magnetically stirred until EC was fully dissolved. Parafilm was used to limit the evaporation of solvents during the stirring process. After stirring, the solution was rested on a hot plate for another 5 minutes which allowed the escape of air bubbles. The EC solutions were then cast onto the glass Petri dishes (9 cm diameter). Films from organic solutions were obtained by drying the polymeric solutions at room temperature for 24 hours in a fume cupboard.

Formulation (w/v)	EC (g)	Solvent (mL)	Solvent System (v/v)
2.5%	0.5	20	ethanol/acetone 40:60
5%	1	20	ethanol/acetone 40:60
7.5%	1.5	20	ethanol/acetone 40:60
10%	2	20	ethanol/acetone 40:60

*Table 2-2 Formulations of pure EC films*

As EC is a water-insoluble material, the drug release from EC coated dosage forms is slow and the film coats may be brittle. A number of additives can be added to EC films to produce desired mechanical properties of the films and to improve the permeability to aqueous medium. OA, DBS and MCT were chosen as the plasticizers while HPMC was added as a pore former to modify the release rate of EC films. EC/additive films were prepared (formulations seen in *Table 2-3*) in the same way as in the pure EC films, but used a REF 1117 film applicator to draw the film solutions onto a glass plate instead of the Petri dishes. The REF 1117 film applicator was purchased from Sheen Instruments Ltd.

(England). This is a wet film applicator (shown as *Figure 2-1*) with two built-in metric micrometer heads for adjusting the knife blade so that the wet film thickness can be accurately set from 0 – 8 mm in 10  $\mu\text{m}$  increments.



*Figure 2-1 REF 1117 film applicator (Sheen Instruments Ltd., England)*

EC/OA and EC/DBS films were dried in a cupboard at room temperature whereas EC/MCT films were dried at 45°C in the oven for 3 hours due to their cloudiness on drying at room temperature. EC/HPMC films and EC/plasticizer/HPMC films were all dried at 45°C in the oven for 3 hours so as to allow the evaporation of water. All the films were equilibrated at room temperature for 24 hours before testing.

Formulation (w/w)	Plasticizers (g)	HPMC (g)	EC (g)	Solvent (g)
0% plasticizers	0	0	2.0	2.0
5% plasticizers	0.1	0	1.9	2.0
10% plasticizers	0.2	0	1.8	2.0
15% plasticizers	0.3	0	1.7	2.0
20% plasticizers	0.4	0	1.6	2.0
25% plasticizers	0.5	0	1.5	2.0
30% plasticizers	0.6	0	1.4	2.0
8.8% OA + 16% DBS	0.2 OA + 0.3 DBS	0	1.5	2.0
8.8% OA + 16% MCT	0.2 OA + 0.3 MCT	0	1.5	2.0
10% HPMC	0	0.2	1.8	2.0
20% HPMC	0	0.4	1.6	2.0
30% HPMC	0	0.6	1.4	2.0
10% HPMC + 10% plasticizers	0.2	0.2	1.6	2.0
20% HPMC + 10% plasticizers	0.4	0.2	1.4	2.0
30% HPMC + 10% plasticizers	0.6	0.2	1.2	2.0

*Table 2-3 Formulations of EC cast films with different additives (plasticizers used were OA, DBS, MCT)*

---

## 2.3 Thermal Analysis

### 2.3.1 Introduction

Thermal analysis provides information on the thermal and/or thermo-mechanical properties of materials, such as glass transition, melting, oxidization, crystallization, degradation, modulus, etc., which are important in understanding the thermal stability, thermal history, compatibility, purity, polymorphism and many other characteristics of materials.

Thermal characterization of the samples was initially performed using differential scanning calorimetry (DSC), dynamic mechanical analysis (DMA) and thermogravimetric analysis (TGA). DSC provides information of different thermal events that occur to the samples throughout the heating, cooling and reheating process. DMA allows the investigation of both the thermal and mechanical changes of the samples within the monitored temperature and time ranges. TGA produces the thermogravimetric curves of the samples in a specific atmosphere and temperature range. Modulated temperature differential scanning calorimetry (MTDSC) has been applied for further thermal characterization of the samples. This section will give a brief description on each technique and experimental parameters that have been used for this work.

### 2.3.2 Differential Scanning Calorimetry

Differential scanning calorimetry (DSC) is one of the most widely used thermal techniques and has a variety of pharmaceutical applications, including physical changes and chemical reactions. DSC determines the glass transition temperature ( $T_g$ ). This approach works by applying a linear heating or cooling signal to a sample and the subsequent measurements of the temperature or energy associated with the relative events, such as melting,

crystallization, glass transition and decomposition reactions of the materials (Craig and Reading, 2007).

There are two types of DSC instruments: power compensation and heat flux. Power compensation DSC involves two separated furnaces for the reference and the sample, respectively. Both of these go through the same programmed temperature profile while the difference in electronic power supplied will be measured. Unlike the two furnaces for the power compensation, heat flux DSC requires only one furnace but two crucibles for the reference and the sample. Both of them are heated from the same source with symmetrical heat paths and the temperature difference between the sample and the reference is measured. This signal is then converted into the power difference – heat flow by this equation

$$\frac{dQ}{dt} = \frac{\Delta T}{R} \quad \text{Eq 2-1}$$

where  $Q$  is the heat,  $t$  is the time,  $\Delta T$  is the temperature difference between the sample and the reference and  $R$  is the thermal resistance of the heat paths between the furnace and the crucible. From Eq 2-1, we can deduce that if the heat paths are identical, the temperature difference between the reference and the sample is a measure of the difference in the heat flow signals of DSC.

The total heat content of a body is proportional to heat capacity  $C_p$ , which is the amount of heat that is required to change the temperature of the sample by 1 K and the temperature ( $T$ ) of the body, i.e.  $Q = C_p \cdot T$ . From the definition of heat capacity  $C_p$  comes the relation

$$C_p = \frac{dQ}{dT} \quad \text{Eq 2-2}$$

differentiating this equation with respect to the time

---

$$\frac{dQ}{dt} = C_p \cdot \frac{dT}{dt} \quad \text{Eq 2-3}$$

where  $\frac{dQ}{dt}$  is the heat flow and  $\frac{dT}{dt}$  is the heating rate. Therefore, the differential heat flow can be a measure of the sample heat capacity. DSC data is typically expressed in terms of the heat flow as a function of the temperature. Occasionally, the heat capacity or derivative heat capacity signals can be applied to analyze the data.

### 2.3.2.1 Calibration

DSC is defined as a differential method, where the thermal behaviour of the reference is compared with that of the sample. Therefore all the other factors apart from the sample itself should be eliminated by calibration, such as the heat adsorption by the crucibles, the heat loss through convection and the minor differences between the two crucibles and the pans, etc. Therefore, in order to produce accurate and reproducible results, it is necessary to calibrate the DSC using the exact same parameters as it is to run the samples. DSC Q1000 and Q2000 with Refrigerated Cooling System (RCS, TA Instruments, UK) were applied in this work. For the DSC Q series, three types of calibrations are required: Tzero<sup>TM</sup> baseline, cell constant and temperature. TA Instruments suggest that for accurate assessments, DSC should be recalibrated every month as well as when the experimental temperature range or heating rate is changed.

We can simplify Tzero<sup>TM</sup> baseline calibrations into two stages. The first being without any samples or pans: empty cells are run under the condition (-80°C to 400°C at 20°C/min) using nitrogen as the purge gas. The second stage is performed with two sapphire discs (approximately 95 mg, without pans) on both the sample and reference positions using the

---

same parameters as in the first stage. The slope and offset values will be calculated and subtracted from the experimental results.

Cell constant calibration (enthalpy calibration) was performed by heating indium through its melting transition. The corresponding heat flow with the transition was compared with the literature values. The ratio between the calculated heat of fusion and the theoretical value determines the cell constant that is required to be added to the software of DSC. The assumption of single cell constant calibrations is acceptable in the entire temperature range.

Temperature calibrations are designed to correct the thermocouple readings under the experimental conditions and to eliminate the systematic effects, since the heat transfer from the furnace to the pan, from the bottom of the pan to the sample and throughout the sample cannot be instantaneous. High purity metals exhibit sharp melting peaks by DSC that makes them ideal for calibrating the instrument response against the theoretical values. Therefore, three high purity calibrants: n-octadecane ( $T_m = 28.24^\circ\text{C}$ ), indium ( $T_m = 156.6^\circ\text{C}$ ) and tin ( $T_m = 231.93^\circ\text{C}$ ) were chosen as the three calibration points within the experimental temperature range. The practical melting temperatures under the conditions that will be applied to the samples may be compared with the literature values.

#### *2.3.2.2 Experimental Parameters*

Generally, a dry inert atmosphere and constant purge of gas in the furnace is required to run the DSC experiments to prevent any moisture or oxygen and to create a stable environment around the sample area. Dry nitrogen (50 mL/min) was used throughout the study as the purge gas for DSC cell and RCS. Although helium has a higher thermal conductivity, nitrogen is still normally sufficient for most DSC experiments which do not

---

involve rapid heating or cooling processes. It also takes a considerably shorter time for the DSC system to equilibrate after the cell has been opened to the air.

A large sample mass would increase the sensitivity of DSC. In contrast, decreasing the sample mass can actually improve the resolution of the experiment due to less thermal gradient across the sample. When the DSC Q1000 was used, the sample mass for the material powder and the cast films were optimized in the range of 3 – 5 mg in crimp aluminium and hermetically sealed pans, 5 – 7 mg in pin-holed pans, whereas when the DSC Q2000 was used, the sample mass applied was 2 mg less than that for DSC Q1000. This is because the DSC Q2000 has better sensibility than the DSC Q1000.

Special care needs to be taken when selecting pans for specific samples and DSC experiments to meet all the different needs. The majority of the work was carried out in crimped aluminium pans, while some were performed in hermetically sealed or pin-holed pans. Crimped aluminium pans (TA Instruments, USA) are the most widely used since they can provide the best thermal contact between the DSC, the pans and the samples and minimize the spillage. Crimp aluminium pans are sealed by pressing the lid down on top of the sample and folding the sidewall of the pans over the lid. The sealing process ensures a flat bottom. Therefore, there will be good heat transfer between the DSC and the pan. When oxidative degradation was investigated, hermetically sealed pans were required because the hermetical pans are sealed by a sample encapsulation press without putting pressure on the sample. The sealed pans should be airtight so as not to allow any gas exchange. This specific property of hermetically sealed pans can be applied to volatile liquids, materials that sublime, aqueous solutions and materials in self-generating atmospheres. This will increase the thermal gradient within the sample. Pin-holed pans

---

were used during the study of residual solvent in films as well as when the removal of the residual solvent was necessary during the heating process. Both of the hermetically sealed pans and pin-holed pans were purchased from Perkin Elmer.

Regardless of which type of pan is used to prepare the samples, DSC should be calibrated by using the same type of pan, simply because different types of pans exhibit different heat resistance and pan masses. Lids are always required to ensure good heat flow from the bottom to the top of the sample.

After placing the reference and the sample pans in the cell, the furnace was equilibrated at the starting temperature for 2 minutes. Consequently, the samples were heated from 20°C to 220°C and cooled down to 20°C and then reheated again to 220°C at a rate of 10°C/min. All the experiments were run in triplicate to verify the reproducibility of the data. Universal Analysis software (TA Instruments, USA) was used to analyze all DSC results.

### 2.3.3 Modulated Temperature Differential Scanning Calorimetry (MTDSC)

Conventional DSC, as described in section 2.3.2, is a very powerful tool for the characterisation of pharmaceutical materials. However, it cannot separate overlapping processes. In addition, heat capacity measurements generally require a rather high accuracy that simple DSC scans will not offer.

Modulated temperature differential scanning calorimetry (MTDSC) is based on conventional DSC with an extension of a ‘modulated’ sinusoidal heating and a mathematical procedure aiming to separate the different types of thermal behaviour (Reading et al., 1994). This separation procedure is explained by

$$\frac{dQ}{dt} = C_p \cdot \frac{dT}{dt} + f(t, T) \quad \text{Eq 2-4}$$

where  $\frac{dQ}{dt}$  is the heat flow,  $C_p$  is the heat capacity,  $T$  is the absolute temperature,  $t$  is time and  $f(t, T)$  is a function of the time and the temperature. In Eq 2-4,  $C_p \cdot \frac{dT}{dt}$  describes the heat flow associated with the sample's heat capacity. The heat capacity in Eq 2-4 describes the energy required for molecular motions, given a specific size of the sample. The energy required to raise the temperature of a material by a single unit will be released when decreasing the temperature by the same amount. Therefore, the heat flow contributed by the heat capacity change through the thermal events is reversible. The function  $f(t, T)$  in Eq 2-4 is the underlying kinetic response which is irreversible in most cases. The sample's response to the sinusoidal modulation is different from the linear heating of the conventional DSC. Under the modulated mode, the heat flow signal, which is equivalent to the conventional DSC, is calculated by an averaging process. The cyclic response of the heat flow signal gives the heat capacity directly by

$$C_p = \frac{A_{HF}}{A_{HR}} \quad \text{Eq 2-5}$$

where  $A_{HF}$  is the amplitude of the modulated heat flow and  $A_{HR}$  is the modulated heating rate. The reversing heat flow signal is obtained by multiplying the heat capacity by the heating rate. This is then subtracted from the heat flow signal to obtain the non-reversing heat flow signal.

Conventional DSC only presents one heat flow signal which may involve two or more overlapping processes. MTDSC has the capability to separate the reversing response from the non-reversing responses. The main component of the reversing signal is the heat capacity and thus the glass transition can be detected from this signal. Irreversible processes which are kinetically hindered, such as degradation, is seen in the non-reversing

---

signals. MTDSC has been applied to several aspects of polymer science (Hourston et al., 1996; 1997; Song et al., 1995; 1996; Song et al., 1997). It not only can measure the heat capacity to an accurate level (Coleman and Craig, 1996), but also improve the sensitivity and resolution due to the combination of large modulations and low heating rates (Hill et al., 1999). In addition, MTDSC is able to separate the glass transition process from the endothermic relaxation.

### *2.3.3.1 Calibration*

MTDSC calibration involves the same calibrations as in conventional DSC. In addition, a heat capacity calibration is required to accomplish accurate heat capacity data. The calibration uses a standard material with a well-known heat capacity at a specific temperature of interest. A sapphire (aluminium oxide) disc, provided by TA Instruments, was used as the calibrant in this work. Before performing the calibration, the total and reversing heat capacity constants need to be manually set at 1.0. In modulated mode, the sapphire disc was then run under the same conditions (pan type, heating rate, amplitude, modulation period) as those that will be used for the subsequent samples. At the end, the total and reversing heat capacity constants were manually calculated by dividing the theoretical value of the heat capacity, at a specific temperature of interest, by the measured value. This software is designed in the ways that these two calculated constants need to be entered manually and which are then to be applied in subsequent experiments.

### *2.3.3.2 Experimental Parameters*

To obtain reliable results, experimental parameters must be chosen carefully. There are three important factors that have significant effects on the measurements: the heating rate, the amplitude of modulation and the modulation period. All of these variables need to be

---

considered as a combination, because the sample needs to undergo at least six modulations through the transition process, which is of interest for reliable deconvolution to take place. Using a low heating rate can make the experiment time consuming and the signal-to-noise ratio may go out of the range. A relatively lower heating rate (1 – 5°C/min) is required in MTDSC than conventional DSC (5 – 20°C/min). 2°C/min is the typical rate employed with a nitrogen purge gas. The choice of the amplitude needs to be a compromise between a reasonable signal-to-noise ratio and a sound response to the modulation. In practice, the temperature amplitude of the modulation is usually selected from  $\pm 0.2^\circ\text{C}$  to  $\pm 0.5^\circ\text{C}$  with a typical modulation period between 30 to 60 seconds. Sample mass, pan type, purge gas and DSC cell cooling capacity all play a role in choosing the optimized modulation parameters (Hill et al, 1999).

Since MTDSC is an extension of DSC, the modulated mode was performed on the DSC Q1000 and Q2000 with RCS unit and dry nitrogen (50 mL/min) as the purge gas. The samples were heated from 20°C to 220°C, cooled down to 20°C and reheated to 220°C at 2°C/min with amplitude of  $\pm 0.5^\circ\text{C}$  over 40 seconds in the crimped aluminium pans. All these experiments were repeated three times and the Universal Analysis software was used to analyze the data.

#### 2.3.4 Dynamic Mechanical Analysis

Dynamic mechanical analysis (DMA) is an alternative method for the detection of small changes in the state of a material. This technique has a sinusoidal force (stress  $\sigma$ ) with a given frequency applied to a sample under a programmed temperature profile. The resultant displacement (strain  $\epsilon$ ) is measured. When the force is applied, some solids may deform elastically, returning to their former shape and size after withdrawing the force,

whereas liquids will flow, depending on their viscosity. The stress and strain can be expressed as

$$\sigma = \sigma_0 \sin(t\omega + \delta) \quad \text{Eq 2-6}$$

$$\epsilon = \epsilon_0 \sin(t\omega) \quad \text{Eq 2-7}$$

where  $\omega$  is the period of strain oscillation,  $t$  is the time and  $\delta$  is the phase lag between stress and strain. The resulting strain and stress of a perfectly elastic solid will be in phase i.e  $\delta = 0$ . For a purely viscous fluid, there will be a 90 degree phase lag between the strain and the stress i.e  $\delta = 90$ . Most polymers have viscoelastic behaviour with  $\delta$  between  $0^\circ$  and  $90^\circ$ .

For purely elastic materials, modulus ( $E$ ) is the ratio of the stress and the strain. The storage modulus ( $E'$ ) measures the energy stored within the material, representing the elastic behaviour. The loss modulus ( $E''$ ) measures the energy which is lost as heat during the process, representing the viscous behaviour of the material. The phase angle ( $\tan \delta$ ) is the ratio of the loss modulus and the storage modulus which are defined below by

$$E' = \frac{\sigma_0}{\epsilon_0} \cos \delta \quad \text{Eq 2-8}$$

$$E'' = \frac{\sigma_0}{\epsilon_0} \sin \delta \quad \text{Eq 2-9}$$

$$\tan \delta = \frac{E''}{E'} \quad \text{Eq 2-10}$$

One of the most important applications of DMA is to measure the glass transition temperature of polymers (Fadda et al., 2008). As a polymer passes through its  $T_g$ , the storage modulus usually decreases by two or three orders of magnitude, and the  $\tan \delta$  goes

---

through a maximum. The decrease in the moduli occurs when there is a main chain molecular motion and the maximum in  $\tan \delta$  occurs when the frequency of the forced vibration coincides with the frequency of the diffusional motion of the main chain. DMA is also often used to examine the degree of phase separation when the two components are mixed together (Craig and Johnson, 1995). Where two distinct  $T_g$  transitions are found that have the same values as the pure materials, then complete phase separation can be inferred. If a glass transition peak is observed at a temperature intermediate between the values for two pure materials, then the two materials are generally said to be miscible. The storage modulus usually represents the stiffness of a sample. Therefore, DMA can be used to investigate the mechanical properties of a sample (Podczeck and Almeida, 2002).

#### 2.3.4.1 Calibration

The aim of the calibration is to standardize each part of the instrument to endow a meaning to the collected data. Three categories of calibration are available for DMA 2980: instrument calibration, clamp calibration and temperature calibration. These calibrations procedures are described in detail below.

Since no instruments are perfectly rigid, the accuracy in the amount of deformation in the instrument becomes important. The deformation of rather stiff samples in the analyser could become greater than the sample's deformation, yielding inaccuracy in the data. Similarly, the deformation of very soft samples may not even be detected. Instrument calibration was carried out to relate the instrument's signal to a standard performance of the shaft. Instrument calibration includes: position, electronics, force (balance and weight) and dynamic calibration. After these calibrations, clamp mass, clamp zero and compliance calibration are required using the specific clamp which would be used for the following

---

experiment. Like any other thermal instrument, the accuracy of the temperature measurement relies heavily on the temperature calibration, which must be performed routinely to ensure reproducible results. The thermocouple in the furnace was calibrated by comparing to the ambient temperature, by using a reliable external thermometer, to the reading temperature of DMA 2980. The correct information was then added to the software. Further dynamic temperature calibration was conducted by running a standard calibrant (Indium) and comparing the practical melting value with the theoretical one.

DMA calibration was carried out once a month, and the clamp calibration was conducted every time the clamp was changed.

#### 2.3.4.2 Experimental Parameters

The shape and the modulus of most samples determine which clamp is going to be used for the experiment. There are six types of clamps. They are designed to meet the different needs of the samples. A 3-point bending clamp is used on stiff samples such as: metals, ceramics, highly filled thermosetting polymers and highly filled crystalline thermoplastic polymers. A cantilever clamp is suited for weak to moderately stiff samples whereas a shear clamp is for viscous liquids and elastomers above its glass transition. Gels and weak elastomers are usually investigated by using compression clamps whereas penetration theoretically can be used on any materials. In this project, a film tension clamp (tensile film mode, *Figure 2-2*) was mainly used to characterize the film properties on DMA 2980 (TA instruments, USA). This is because tension clamps are typically applied on thin films. A cantilever clamp was also used when the films were prepared on the stainless steel mesh (*Figure 2-3*). The stainless steel mesh produced a much stiffer sample than the thin film itself, which is suitable for the cantilever clamp.



*Figure 2-2 Tension film mode of DMA*



*Figure 2-3 Cantilever clamp of DMA*

Once the appropriate clamp is chosen, the DMA must be programmed to reflect the chosen clamp, so that the instrument can properly control the experiment and yield accurate data. The clamp calibration must be performed at this step. The thermocouples inside the furnace can be adjusted to ensure they are close to, but not touching the sample.

---

All of the samples were heated from 30°C to 180°C at a heating rate of 3°C/min under a frequency of 1 Hz with data sampling interval of 1 sec/pt. The amplitude for the tension clamp was 20 µm, since the samples (cut into 30.0 × 5.3 mm square pieces) were thin films with weak moduli. When a single cantilever clamp was used, the films were prepared on a stainless steel mesh (0.140 mm wire diameter). All of the mesh samples were cut into pieces with dimensions of 23.0 × 12.7 mm. 100 µm was then chosen as the amplitude because the samples with the steel mesh were relatively stiffer. Dry filtered air were used as purge gas and cooling system.

### 2.3.5 Thermogravimetric Analysis

Thermogravimetric analysis (TGA) is a technique which determines the changes in weight of samples in relation to their change in temperature or isothermally as a function of time. TGA is commonly employed in the characterization of materials if a mass change is involved. TGA can be used to determine degradation temperatures (Wilkie, 1999), absorbed moisture content or water loss of the materials (McPhillips et al., 1999; Tamburic and Craig, 1997), chemical reactions (Wang and Li, 2008; Yang et al., 1996) and thermal stability of materials (Yang et al., 2004). In the area of film coating, TGA is a useful technique to determine the residual solvent within cast films, which way may be used to optimize the drying methods. The amount of residual solvent can be calculated from the total mass loss. The temperature at which the mass loss occurs may be related to the type of solvent and the interaction between that solvent and the substrate.

Such analysis relies on a high degree of precision in the measurements of the weight, the temperature and the temperature change during the heating process. A high precision balance was the weighing device that allows accurate measurements of the sample mass (in

---

mg). A pan loaded with a sample was placed in a small electronically heated oven with a thermocouple which should be close to, but not touching the sample. A purge gas with optimized flow rate was required to establish a stable environment around the sample in the furnace. An inert gas is commonly chosen such as nitrogen or dry air in cases when oxygen is required for the reactions. A purge gas was always used to remove the product gases or carry on the reaction but not to affect the balance. The samples for TGA should be spread out in the pan evenly with the mass being between 5 and 10 mg. The heating rate plays an important role in deciding the transition temperature. A method known as Hi-Resolution TGA can be employed, in which the temperature increase slows as the weight loss increases. Greater accuracy of transition temperature can be obtained in this way.

Weight and temperature calibration are the two calibration procedures that are required for TGA. This is because they are the two key issues of the samples addressed by TGA. Weight calibration should be performed once a month and uses 100 mg and 1 g standards to calibrate the weight signals. The temperature should be calibrated using the same conditions (heating rate, purge gas and flow rate, thermocouple position) that will be used for the sample runs to eliminate the effect of the thermal lag between the thermocouple and the sample itself. A commonly used high purity material is indium, which was used for temperature calibration in this project and the calibration was repeated monthly.

In this experiment, TGA (Hi-Res TGA 2950, TA Instrument) was performed to investigate the water content and the degradation of the raw materials. For the prepared films, the solvent residues as well as the degradation were characterized. Approximately 10 mg of a sample was placed in an open aluminium pan, and then heated from room temperature to 300 °C at a rate of 10 °C/min. The gas line is split before it enters the nodule and two flow

---

meters are used to set the flow rates. Nitrogen with a heat flow of 60cc/min through the purge inlet and 40cc/min through the balance inlet was used as the purge gas. The compressed air was used as the cooling system. The weight loss signal and the derivative weight loss signal plotted against temperature were used to analyse the data in the Universal Analysis software (TA Instruments, USA).

## **2.4 Atomic Force Microscopy-Thermal Analysis**

### **2.4.1 Atomic Force Microscopy**

A scanning probe microscopy (SPM) is comprised of a sensing probe, piezoelectric ceramics for positioning the probe, an electronic control unit and a computer for controlling the operation of the experiment and generating images. SPM can be divided into scanning tunnelling microscopy (STM) and atomic force microscopy (AFM), due to different types of sensors (tunnelling sensor for STM and force sensor for AFM). Using a force sensor, AFM consists of a microscale cantilever (100  $\mu\text{m}$  long, silicon) with a sharp tip at its end that is used to scan the surface of the specimen. It works by moving the sharp tip on the surface of the sample, and the forces between them lead to a deflection of the cantilever. The deflection is measured by a laser spot reflected from the top of the cantilever into an array of photodiodes (*seen Figure 2-4*).

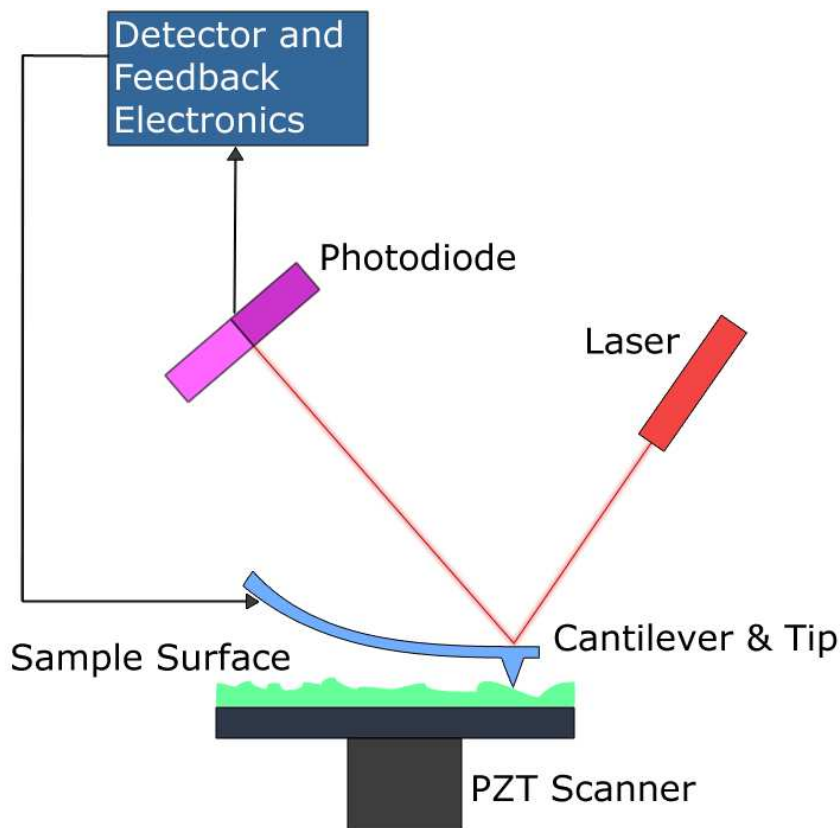


*Figure 2-4 Basic principle of AFM*

AFM has different scanning modes, mainly contact and non-contact, which simply refers to whether or not the scanning probe comes into physical contact with the surface of the sample. The probe tip may damage the fragile samples, such as biological specimens or polymers, when the cantilever moves across the surface of the sample during contact scanning. Pulsed force mode is an intermediate contact mode. It was used in this project because it minimized the shear forces to avoid the damaged surface that can result from utilizing contact mode on soft samples. The pulsed force mode introduces a sinusoidal modulation to the probe cantilever with amplitude of 10 – 500 nm and at a frequency between 100 Hz and 2 kHz. This extends the capabilities of the microscope beyond simply

---

measuring topography to many other properties, such as adhesion, viscosity and many more which can be analysed and imaged simultaneously along with topography. AFM enables the visualization of the sample's surface. The adhesion properties recorded during scanning may provide phase images when utilizing pulsed force mode AFM.

In this project, all topography and adhesion images of the sample films were recorded using Thermomicroscopes Explorer scanning probe microscope (pulsed force mode, Anasys Instruments, USA). Small pieces of these films (approximately 10×10mm) were cut and mounted on magnetic studs by double-sided tape. The frequency and amplitude for modulation and subtract baselines were 500 Hz and 50 nm, respectively.

#### 2.4.2 Hot Stage AFM

For some systems, AFM adhesion phase images at room temperature may have a low contrast due to the paucity of the differential thermo-mechanical properties of the phase domains. These render it difficult to interpret the AFM images properly and accurately. The development of the heating stages for AFM has further enhanced the capabilities of AFM (Fasolka et al., 2001). Simply connecting a heating apparatus to a traditional AFM allows the morphology developments of polymers through the phase transition, crystallization and melting, etc. This technique can also enhance the phase contrast if the stage is set at the temperature that is between the  $T_g$ s of the two phase domains. One needs to be careful to make sure that the heating process is magnifying, but not causing phase separation.

A Linkam TP93 controller (Linkam Scientific Instruments, UK) was equipped with the traditional AFM to control the temperature of the stage on which the samples were placed.

---

Topography and adhesion images of the prepared films were scanned at different temperatures using PFM.

### 2.4.3 Micro and Nano-Thermal Analysis

Micro and nano-thermal Analysis ( $\mu$ TA and nTA) have become increasingly popular in the pharmaceutical field over recent years (Grandy et al., 2000; Price et al., 1999; Royall et al., 1999). The traditional AFM is equipped with a thermal control unit. The scanning probe is then replaced by a micro or nano thermal probe. It is not difficult to tell by the names that the difference between  $\mu$ TA and nTA is the scale of the thermal probes that will be introduced in more detail in this section.

$\mu$ TA and nTA can be utilized mainly in two ways. When the thermal probe's tip is heated to a given temperature, the images obtained after scanning are based on the topography and the thermal properties of the materials. In other words, the response of the sample to the heating signal is recorded. Difficulties exist in differentiating between materials with similar thermal conductivities where adhesion properties can be applied. Localized thermal analysis (LTA) can be carried out using  $\mu$ TA and nTA that provide detailed information on the distribution of the constituents of the samples. After scanning at room temperature, the micro or nano scale probes can be located on the specific areas of interest, and then heated up following the temperature programme. When the samples go through a thermal transition that results in the softening of the material, such as glass transition or melting, the probe cantilever will undergo a downward deflection. The LTA profile is the probe's cantilever position plotted against the temperature. The onset temperature of the downward deflection is usually regarded as the softening point, i.e  $T_g$  or  $T_m$  in most cases.

The micro-thermal probe is made of a Wollaston wire (*Figure 2-5*) with a sensing element of 5  $\mu\text{m}$  diameter platinum/rhodium wire of length approximately 200  $\mu\text{m}$ . The spring constant is 10 N/m (Veeco Probes, USA). The nano-thermal probe (*Figure 2-6*) was purchased from Anasys Instruments, USA. It has Silicon as the cantilever material and doped Silicon as the resistor. The length of the probe's tip is approximately 200  $\mu\text{m}$  and the spring constant is 0.5 – 3 N/m.



*Figure 2-5 Scanning electron micrograph of the  $\mu\text{TA}$  probe (Craig et al., 2002)*

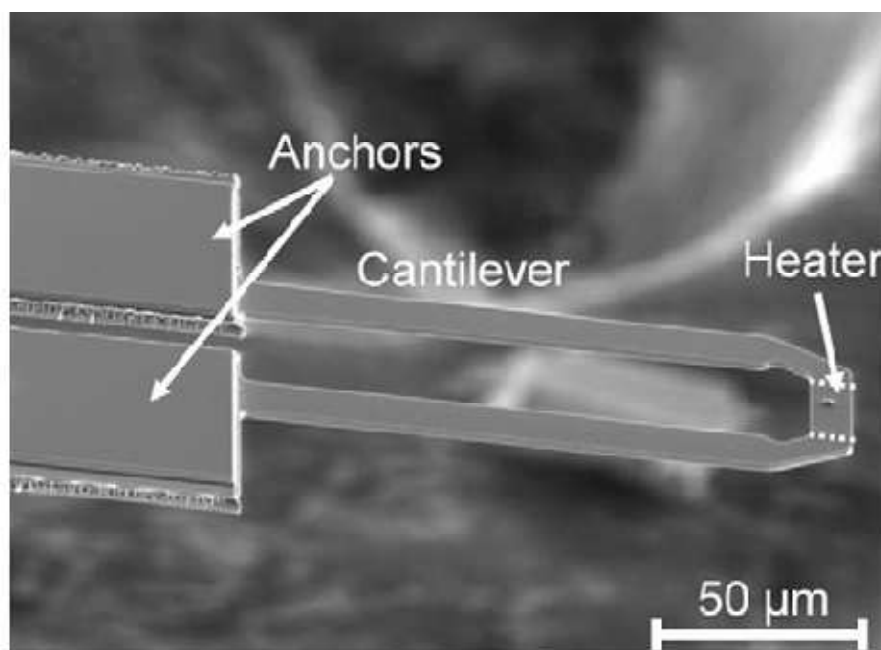


*Figure 2-6 Scanning electron micrograph of the nTA probe (Kim et al., 2007)*

When temperature is concerned, calibration of the system before the experiments is necessary to relate the thermal events to the accurate temperatures. The thermal system was calibrated by using the standard calibrants, PE, PET and PCL, which were provided with the instrument. The practical melting temperatures of the calibrants were correlated to the voltages applied on the thermal probe. These were then compared with the theoretical values. The instrument was calibrated every time before it was used to ensure the accuracy of the resulted softening temperature.

In the project,  $\mu$ TA and nTA were carried out using the same apparatus as in the traditional AFM, i.e Thermomicroscopes Explorer scanning probe microscope, combined with a nano-thermal unit (pulsed force mode, Anasys Instruments, USA). The micro-thermal probe can be cleaned by heating it up to 800°C between each experiment. However, the

nano-thermal probe can only be heated up to 400°C. Therefore, special care is needed to be taken when handling the nano-thermal probe due to its scale and relatively small thermal resistance.

## **2.5 Scanning Electron Microscopy**

Scanning electron microscopy (SEM) is a type of electron microscope capable of producing high-resolution images of a sample's surface. SEM images have a characteristic three-dimensional appearance and are useful to assess the surface structure of the sample. In this work, the surface morphology of coated pellets, EC films and those with different additives before and after dissolution was observed by SEM. The films were taken out from the dissolution medium at time intervals of 0, 2, 8 and 24 hours, then dried in desiccators with silica gel for 24 hours before testing.

The samples were gold coated by a Polaron SC7640 sputter gold coater manufactured by Quorum Technologies. The thickness of the gold coating is about 15 nm. The imaging process was performed in a high vacuum environment. Imaging process was performed with a JEOL JSM5900 LV SEM (Japan), mounted with a tungsten filament with an acceleration voltage of 5 – 20 kV.

## **2.6 Dissolution Studies**

### **2.6.1 Simulated Dissolution Studies on the Cast Films**

Morphology and thermal properties of free films before and after they were immersed into the release medium were examined. The aim of these studies is to compensate the dissolution profiles on model drugs in terms of understanding the drug release mechanism. However, after the dissolution, the model drugs or other excipients may not be fully

dissolved and removed from the coatings. Even if they are fully dissolved by the release medium, when the coated films were dried, these components would precipitate from the medium remaining in the films and appear on the surface. The properties of the films coated on the dosage forms may be affected by these excipients and yield inaccurate data. Therefore, imaging and thermal studies were conducted on free films with the same formulation as the ones applied on model drugs.

The preparation methods of cast films have been described in section 2.2. The films were then cut into 50×50 mm square pieces and immersed into 200 mL release medium. Three release mediums were used in this work: DI water, pH 1.2 and pH 6.8 buffer. The pH 1.2 buffer was prepared by placing 250 mL of 0.2 M sodium chloride into a 1000 mL volumetric flask, adding 425 mL of 0.2 M hydrochloric acid, then diluting to 1000 mL with DI water. 0.2 M sodium chloride solution was made by dissolving 11.69 g sodium chloride (Fisher Scientific Ltd. UK) into 1 L of DI water in a volumetric flask. 0.2 M hydrochloric acid solution was prepared by diluting 37% hydrochloric acid (M=36.46g/mol, 1.19 kg) purchased from Sigma Aldrich Co. (UK). Phosphate buffer pH 6.8 was made by placing 250 mL of 0.2 M sodium dihydrogen phosphate in a 1000 mL volumetric flask, adding 112 mL of 0.2 M sodium hydroxide, then diluting to 1000 mL with DI water. 0.2 M sodium dihydrogen phosphate solution was prepared by dissolving 31.2 g sodium dihydrogen phosphate (Sigma Aldrich Co., UK) into 1 L DI water in a volumetric flask. 0.2 M sodium hydroxide solution was prepared by dissolving 8 g sodium hydroxide (Fisher Scientific Ltd., UK) into 1 L DI water. The films were taken out at the time intervals of 0, 2, 8 and 24 hours and dried in a silica gel desiccator for 24 hours. MTDSC and SEM were then performed on these films.

---

### 2.6.2 Pellets Coating Process

Multiparticulate drug delivery systems have been of interest recently due to their benefits over single unit dosage forms, such as reduced risk of dose dumping and local irritative effect (Nikowitz et al., 2011). A drug layering technique was used for pellet production. In this technique, drug powder, drug suspension or drug solution is applied on the sugar based cores using a fluid bed or other coating systems. This method can dose multiple, even incompatible active pharmaceutical ingredients (API) together and produce pellets with desired processability. This process leads to the formation of multiple layers of drug particles around the inert cores. These drug layered pellets can be further coated by different polymers. Crystalline drug can be embedded in the film coating, and appear on the surface of the coatings, which may be fragments of the core that arose during the coating process during production (Ringqvist et al., 2003). Therefore, it is necessary to have a layer of seal coating outside the drug layer. As the name suggests, seal coating seals the drug inside and prevents drug appearing in film coats as well as drug loss during next procedure: film coating.

Paracetamol (14 mg/mL in water, 4-Acetamidophenol, Alfa Aesar, UK) and metoprolol succinate (100 mg/mL in water, Toprol XL<sup>®</sup>, AstraZeneca LP, UK) were used as the APIs in this project. The formulations of drug layering and seal coating process are shown in *Table 2-4* and *Table 2-5*. The binding liquids were prepared initially by adding appropriate amount of API into 20 g DI water, cooperated with HPMC (6 cP, Colorcon Ltd., USA) as a binding agent, magnetically stirred. The seal coating suspensions were prepared by adding 0.01 g talc (Fisher Scientific Ltd., UK) and 0.05 g HPMC (6 cP) to 10 g DI water, magnetically stirred. The binding liquids with API were sprayed onto the sugar beads SureSpheres<sup>™</sup> (1000 – 850  $\mu$ m, Colorcon Ltd., USA) as the substrate using a bench-top

fluid-bed tablet and spheroid (pellet) Coater/Drier (Caleva Process Solutions, UK). The seal coat suspensions were then sprayed onto the pellets as well. The drug coated pellets were consequently dried in the Mini Coater/Drier for 30 minutes. The film coating solutions (formulations shown in *Table 2-6*) were prepared in the same way as the solutions for the cast films, using ethanol/water (90:10 v/v) as the solvent system, described in section 2.2. The pellets were weighed before the film coating process and 8% weight gain was controlled. The coating parameters for drug layering, seal coating and film coating are shown in *Table 2-7*. After coating, the pellets were dried in the Drier for another 30 mins to allow the solvent to evaporate. The pellets were placed in the desiccator for 24 hours to equilibrate before further testing.



*Figure 2-7 A bench-top fluid-bed tablet and spheroid (Pellet) coater/drier for small scale  
(Caleva Process Solutions, UK)*

<b>Drug Layer</b>		
Component	Grams (g)	Total Formula (%)
Hypromellose 6 cP	0.167	1.6
Paracetamol	0.33	3.1
DI Water	20	
<b>Seal Coat</b>		
Component	Grams (g)	
Talc	0.01	0.1
Hypromellose 6 cP	0.05	0.5
DI Water	10	
SureSpheres (18/20, g)	10	94.7

*Table 2-4 Paracetamol drug layering formulation*

<b>Drug Layer</b>		
Component	Grams (g)	Total Formula (%)
Hypromellose 6cP	0.088	0.8
Metoprolol succinate	0.33	3.1
DI Water	20	
<b>Seal Coat</b>		
Component	Grams (g)	
Talc	0.01	0.1
Hypromellose 6cP	0.05	0.5
DI Water	10	
SureSpheres (18/20, g)	10	95.5

*Table 2-5 Metoprolol succinate drug layering formulation*

Film Former	Pore Former	Plasticizers		
EC (% w/w)	HPMC (% w/w)	OA (%w/w)	MCT (% w/w)	DBS (%w/w)
90	0	10	10	10
80	20	10	10	10

*Table 2-6 Formulation of the film coatings applied on APIS*

Parameters	Drug Layering	Seal Coating	Film Coating
Inlet Air Temperature (°C)	42	44	32
Air Flow (rpm)	1	1	1
Atomizing Air Pressure (Bar)	0.7	0.7	0.7
Agitator (Hz)	13	13	13
Fan (m/s)	10	10	11
Anti-static	on	on	on

*Table 2-7 Parameters used for drug laying, seal coating and film coating process using a Mini Coater/Drier instrument*

Drug content of the coated pellets were investigated by grinding 3 portions of 1 g coated pellets respectively. Each portion was dissolved in DI water in a 100 mL flask. After filtering, 5 mL solution was moved to a 50 mL flask and diluted with DI water. The absorbance of the solutions was then determined by an S-22 UV/VIS Spectrophotometer (Boeco, Germany) at 243 nm for paracetamol and 274 nm for metoprolol succinate respectively. The drug contents were calculated and these values were used in the calculation of the drug release, subsequently.

---

### 2.6.3 Dissolution of Coated Pellets

Dissolution testing was performed in a BP apparatus 1 (DIS 8000, Copley Scientific Ltd., UK). Sink conditions should be maintained in terms of the volume of the dissolution medium and temperature, etc. 900 mL DI water, which provided sufficient release medium, was used for all studies. The bath temperature was controlled at  $37\pm 0.5^{\circ}\text{C}$  and the baskets with 2 g pellets were rotated at 100 rpm in the dissolution medium. 10 mL of the sample volume was withdrawn at 0, 0.5, 1, 2, 4, 6, 8, 10, 12 and 24 hours, and replaced with 10 mL fresh medium maintain at the same temperature. After filtration through a  $0.2\ \mu\text{m}$  Springe filter (Sartorius Stedim Biotech S.A., UK), the absorbance of the samples were determined by UV spectrometer at the wavelength of the APIs. All dissolution experiments were carried out in triplicate and the average values of the absorbance were used to plot the dissolution curves.

Calibration curves were established before the dissolution study of model drugs. For paracetamol, a stock solution of 0.02% (w/v) was initially prepared by dissolving 100 mg of the model drug into DI water in a 500 mL flask. 1, 2, 3, 4 and 5 mL stock solution were taken out respectively and diluted by DI water in the 50 mL volumetric flasks. The set of absorbance values of each concentration was determined by UV spectrometer at 243 nm and the calibration curve is shown in *Figure 2-8*.

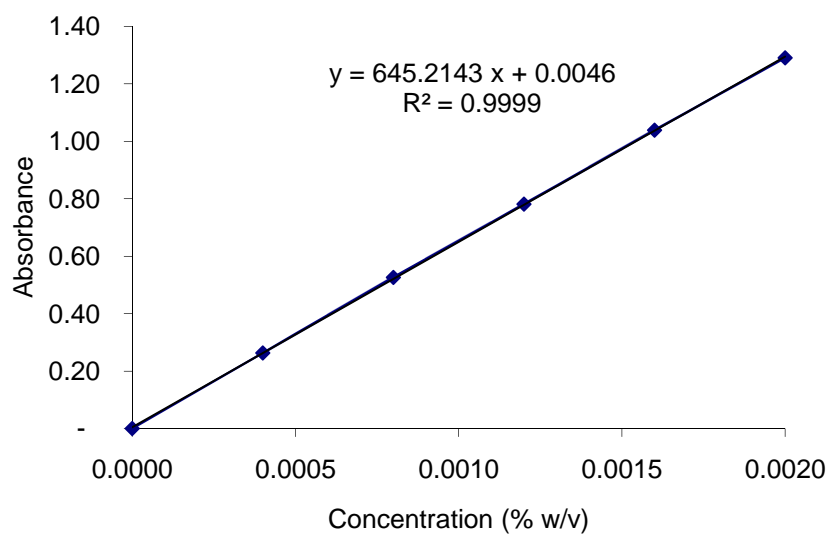


*Figure 2-8 Calibration curve for paracetamol*

Similarly, a stock solution of 0.1% (w/v) of metoprolol succinate was prepared by dissolving 100 mg of the model drug into DI water in a 100 mL flask. 1, 2, 3, 4 and 5 mL stock solution were taken out respectively and diluted by DI water in the 50 mL volumetric flasks. The set of absorbance values of each concentration was determined by an UV spectrometer at 274 nm and the calibration curve is shown in *Figure 2-9*.

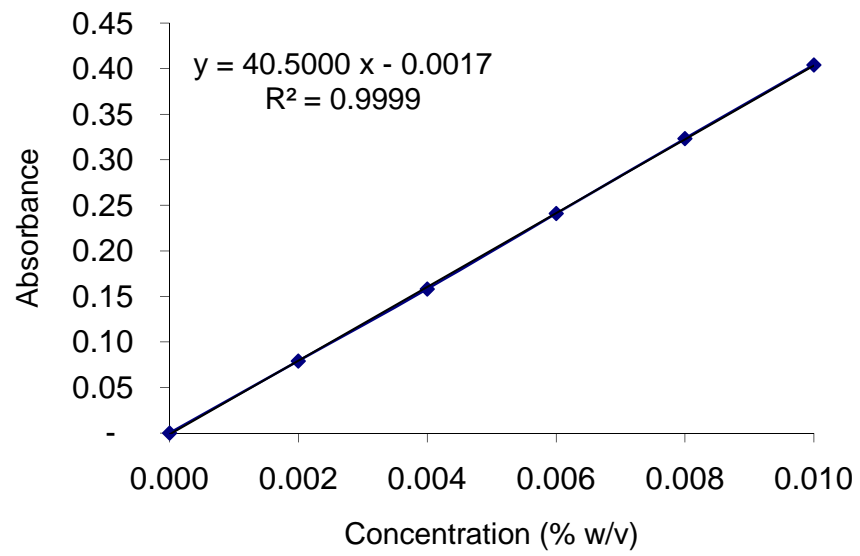


*Figure 2-9 Calibration curve for metoprolol succinate*

---

## CHAPTER 3 THERMAL CHARACTERIZATION OF ETHYL CELLULOSE AND ETHYL CELLULOSE FILMS

### 3.1 Introduction to Ethyl Cellulose Powder and Films

Due to its viscoelastic properties, ethyl cellulose (EC) has been used extensively as a film former in controlled-release systems (Dias et al., 2008; Missaghi et al., 2008; Muschert et al., 2009a). Before complex film systems are examined, a knowledge of the thermal and thermo-mechanical properties of the film former and its simple film formulations is essential since their characteristics determine the behaviour in the more complex film coating formulations both under ambient conditions and at elevated temperatures during the coating process and subsequent storage.

The issues of water content and residual solvents are crucial for film formers and the resulting films (Lindholm et al., 1984). Water or other solvents may act as a plasticizer, thus increasing the chain mobility of the polymer, lowering the  $T_g$ , causing phase separation if the excipients from the films and resulting in poor stability upon storage. Therefore, it is necessary to characterize the hygroscopicity of EC and the residual solvents in the prepared films. In this case, TGA is a highly applicable technique to investigate weight loss upon heating. Another application of TGA is to determine the degradation kinetics of materials, which provides valuable information since EC may be tested and processed under elevated temperatures.

---

The glass transition, that was introduced in *Chapter 1*, is a fundamental property of an amorphous material that affects its end-use properties such as the permeability, the thermal and mechanical properties (Brostow et al., 2008; Forrest and Dalnoki-Veress, 2001; Lafferty et al., 2002).  $T_g$  is very important in polymer characterization, as the properties of the material are highly dependent on its glass transition. The  $T_g$  of EC determines its behaviour in film coating formulations during the film coating process and the subsequent storage.  $T_g$  can also be a specific measurement of the effect of plasticizers on a polymer since it is a function of the molecular chain mobility. The purpose of a plasticizer is to increase the molecular chain mobility (Sakellariou et al., 1986a). It can also be applied to assess the miscibility between two or more polymers in a system. A polymer blend could be considered compatible if only one  $T_g$  is observed, and if the polymer consists of an immiscible binary blend, two  $T_g$ s will be observed.

In this chapter, the basic thermal properties of EC have been studied using TGA and DSC. The residual solvents, glass transitions and other thermal events of pure EC films with different concentrations of EC are discussed. A variety of thermal and thermo-mechanical techniques, including TGA, DSC, MTDSC and DMA are compared in terms of their thermal characterization.

## **3.2 Methodology**

### **3.2.1 Sample Preparation**

The study on the raw materials was carried out using the ETHOCEL<sup>TM</sup> 7 (EC 7) and ETHOCEL<sup>TM</sup> 20 (EC 20) powders, provided by Colorcon Ltd., USA. They were used as received without further purification or any drying processes.

2.5%, 5%, 7.5% and 10% w/v EC solutions were prepared by dissolving EC 7 and EC 20 with a relative weight mass into 20 ml of ethanol/acetone (40:60), respectively. The EC solutions were heated to 45°C on a hot plate and magnetically stirred until EC was fully dissolved. Parafilm was used to limit the evaporation of the solvents during the stirring process. After stirring, the solution was rested on a hot plate for another 5 minutes, which allowed the escape of air bubbles. The EC solutions were cast onto glass Petri dishes (9 cm diameter). Films from organic solutions were obtained by drying the polymeric solutions under room conditions for 24 hours. The dry films were then equilibrated under room conditions for another 24 hours before being tested.

### 3.2.2 TGA

The degradation profiles of EC powders were studied using TGA. These samples were heated from room temperature to 350°C at 2°C, 5°C and 10°C/min, respectively. Both the weight loss and derivative weight loss signals were used to analyse the onset of degradation. TGA was also used to determine the amount of residual solvents of the EC organic solution films. The samples were heated from room temperature to 150°C at 10°C/min. Approximately 5 – 10 mg samples were placed in the aluminium sample pans. Anhydrous nitrogen was used as the purge gas, whereas compressed air was used as the cooling system.

### 3.2.3 DSC and MTDSC

Conventional DSC experiments were conducted by running the samples from room temperature to 220°C, then cooling down to 80°C and reheating to 220°C at 2, 5 and 10°C/min in the hermetically sealed pans on a DSC Q1000 (TA Instruments, USA) with a sample mass of 3 – 5 mg. When the modulated mode was used, the sample went through

the same temperature program with  $\pm 0.5^{\circ}\text{C}$  modulation amplitude every 40 seconds at a heating rate of  $2^{\circ}\text{C}/\text{min}$ , using hermetically sealed pans. DSC was calibrated before the experiment by using standard calibrants (Indium, Tin and n-Octadecane). Dry  $\text{Al}_2\text{O}_3$  was used to perform the heat capacity calibration for the modulated mode. All experiments were completed in triplicate.

### 3.2.4 DMA

DMA in film tension mode (tensile clamp) was used to investigate the storage modulus, loss modulus and  $\tan \delta$  of film samples during the program used. The dry films were cut into  $30 \times 5.27 \text{ mm}^2$  square pieces and then mounted on fix clamps. Two clamp screws were tightened by using a torque wrench to the appropriate clamping torque (3 – 5 in-lbs). The thermocouple was positioned halfway between the two clamps and close to, but not touching, the sample. Samples were heated from  $30^{\circ}\text{C}$  to  $150^{\circ}\text{C}$  at a heating rate of  $3^{\circ}\text{C}/\text{min}$ . Dry filtered air was used as both the purge gas and the cooling system. Each run was conducted in triplicate. The instrument parameters were as follows: Data sampling interval: 1.0 sec/pt; Amplitude:  $20.00 \mu\text{m}$ ; Auto-strain: 120.0%; Static force: 0.050 N; Frequency: 1 Hz.

## 3.3 Results

### 3.3.1 General Properties of EC Powders

Ethyl cellulose has been used extensively as a film forming material for the controlled release of drugs (Desai et al., 2006; Frohoff-Hülsmann et al., 1999b). The thermal and mechanical properties of film coatings are consequently related to the basic physical properties of EC. Therefore, the general thermal properties of ETHOCEL<sup>TM</sup> 7 and

ETHOCEL™ 20 powders were studied initially in order to understand the basic physical properties of EC.

### 3.3.1.1 TGA Studies

The weight loss (TGA) and derivative weight loss signals (D-TGA) of EC 20, obtained at three heating rates (2°C, 5°C and 10°C/min) under dry nitrogen, are shown in *Figure 3-1*. Hardly any weight loss was observed before 100°C (data not shown), indicating the water content (free water) within the EC powder was low and could be ignored. EC 20 presented a degradation peak with the onset temperature of 250°C, reaching a maximum rate of weight loss at approximately 340°C. At 350°C, a total weight loss of 80% was observed. The weight loss of EC after 250°C is attributed to the anhydroglucose polymeric chain decomposition (Singh et al., 1996). Moreover, the weight loss between 100°C and 250°C of EC may be due to the dehydration of the hydrogen bonded water. In this case, EC powder has a very limited amount of water existing as either free water or bound moisture. After the experiments, the white EC powder became brown solid tar with a smell of burning hydrocarbon, strongly suggesting the degradation of EC occurred after 250°C. EC 7 showed a very similar degradation profile (data not shown), which was consistent with the literature that the molecular weight may have no effect on the thermal decomposition temperatures (Li et al., 1999). The heating rates used (2, 5 and 10°C/min) did not have a significant effect on the degradation onset, but did have an impact on the degradation profiles. Slow heating rate renders a faster degradation and a lower degradation peak temperature.

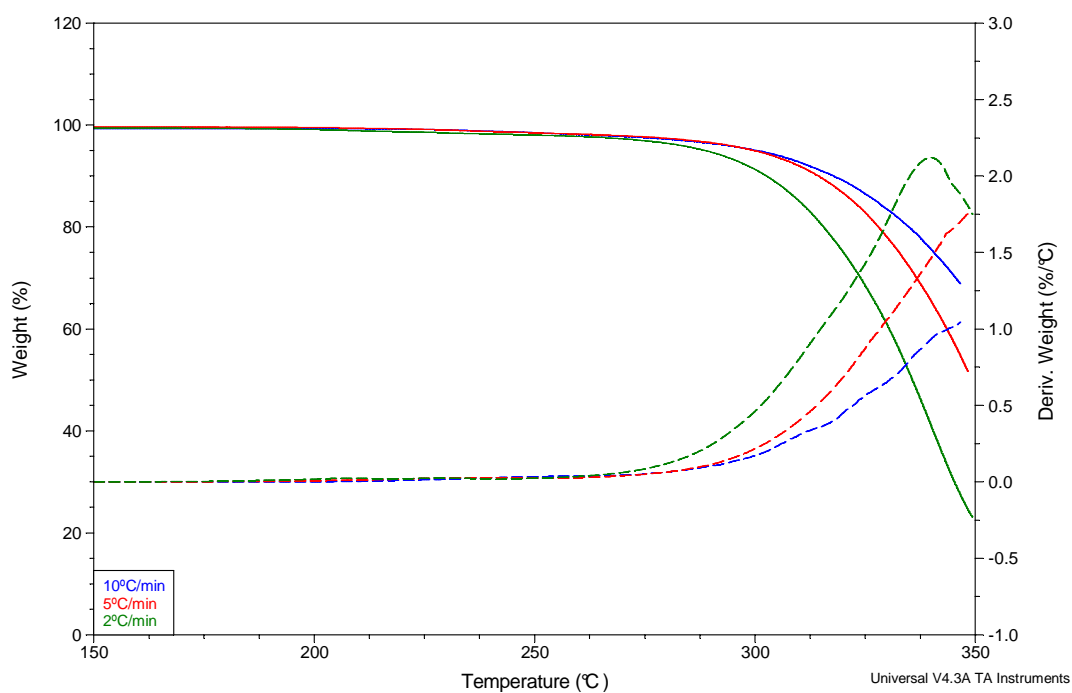


*Figure 3-1 Degradation of EC 20 in TGA and D-TGA at heating rates of 2°C, 5°C and 10°C/min under nitrogen conditions (solid line-weight loss signals, dash line-derivative weight loss signals)*

### 3.3.1.2 General Thermal Properties

From the TGA and D-TGA results above, it is shown that EC 7 and EC 20 start to degrade from 250°C, therefore, the DSC and MTDSC experiments were carried out with the maximum temperature of 220°C. The glass transition temperature and the other thermal events were investigated. *Figure 3-2* presents the heat flow signal of EC 20 at 10°C/min to 200°C during heating, cooling and reheating in a hermetically sealed pan.

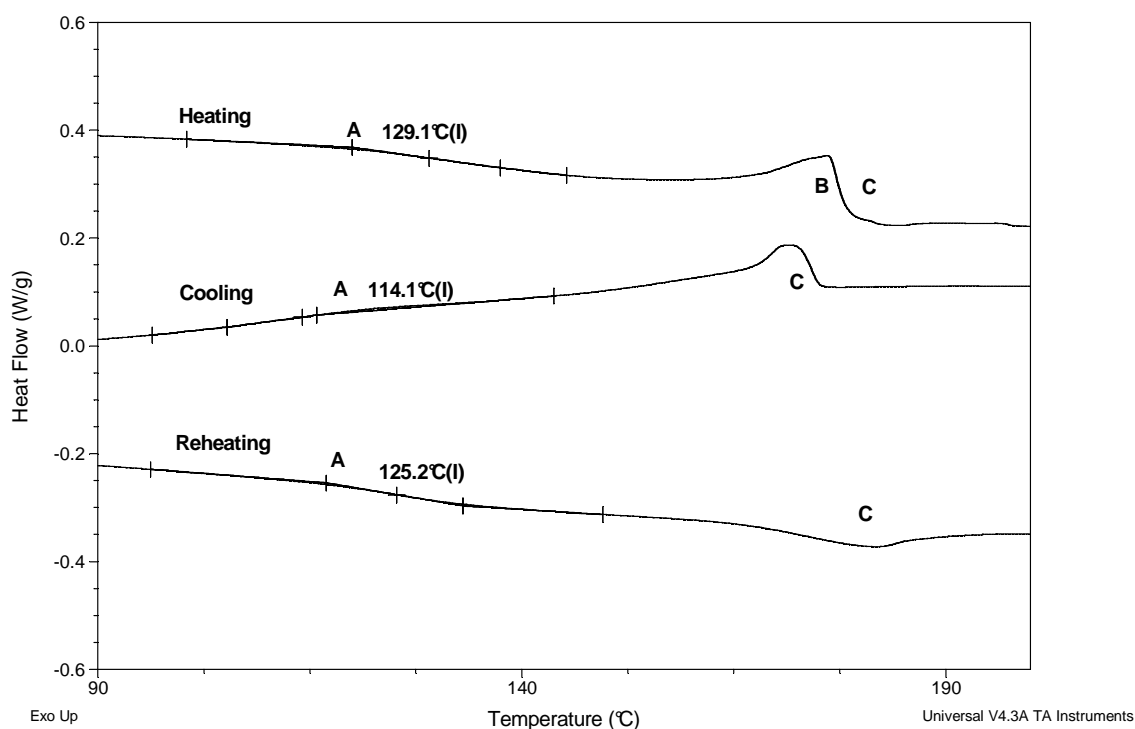


*Figure 3-2 DSC heat flow curve showing the heating, cooling and reheating signals of EC 20 powder in hermetically sealed pans at 10 °C/min to 200 °C*

The basic DSC curve (from 100°C to 200°C) revealed several thermal events, including a glass transition (process A), endo- and exothermic (process B and C) events. Process B was only observed in the initial heating signal. This process was ascribed to an oxidative degradation (Lai, 2005), even though the samples were placed in a hermetically sealed pan. This indicates that the oxidative degradation can be caused even by very small amounts of oxygen in the pans. Process C appeared on all three signals and thought to be associated with the melting and crystallization of the micro-crystallites within EC (Lai, 2005). This is an inherent property of EC, which needs to be borne in mind when interpreting the data of EC films. The glass transition temperature ( $T_g$ ) is a crucial property of polymeric films. Numerous effects by other components on EC film are based on the  $T_g$ s. Therefore, this issue will be discussed in more detail in a later section of this project.

### 3.3.1.3 Glass Transition Temperatures

The significance of the glass transition has been described in *Chapter 1*. In order to measure the  $T_g$  values accurately, a variety of methodologies are considered. First, heating rates have a pronounced effect on the  $T_g$  measurements. To find a better way to measure the  $T_g$ , 2°C, 5°C and 10°C/min were applied as heating rates. EC 7 and EC 20 were initially analyzed by Q1000 in the standard mode setting. *Figure 3-3* and *3-4* shows the heating of EC 7 and EC 20 powder at 2°C, 5°C and 10°C/min from room temperature to 220°C and cooling back to 80°C and subsequently reheating to 220°C.

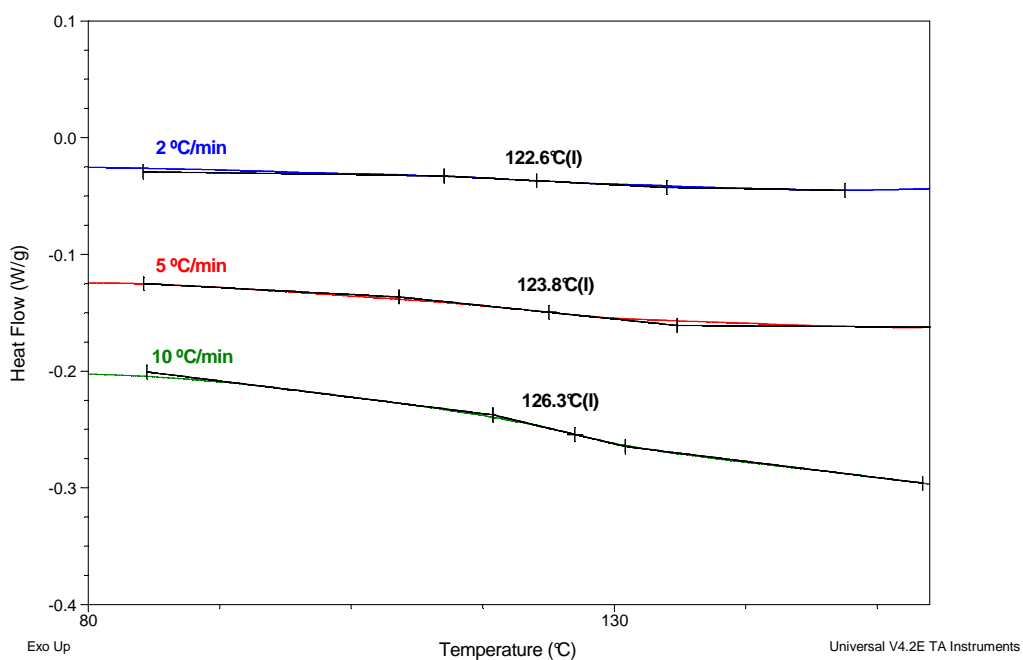


*Figure 3-3 Glass transition of EC 7 at 2°C, 5°C and 10°C/min during heating analyzed by conventional DSC*

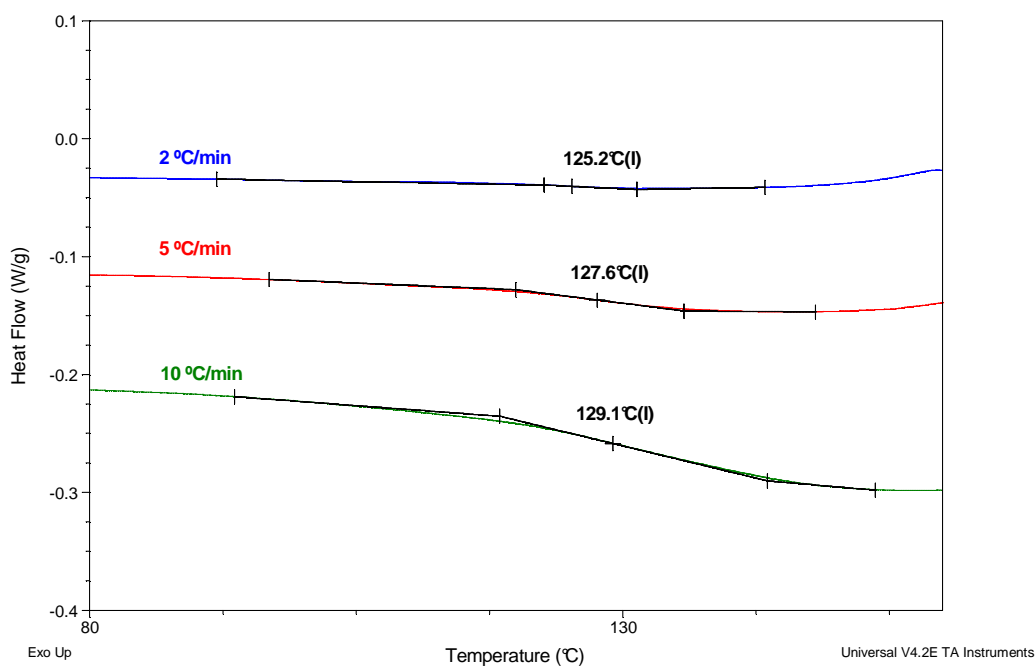


Figure 3-4 Glass transition of EC 20 powder at 2°C, 5°C and 10°C/min during heating analyzed by conventional DSC

Heating rate (°C/min)	$T_g$ heating (°C)	$T_g$ cooling (°C)	$T_g$ reheating (°C)
2	123.4 ± 1.2	112.2 ± 1.5	116.3 ± 1.1
5	126.0 ± 1.0	108.3 ± 1.3	117.1 ± 1.3
10	128.6 ± 1.1	111.2 ± 1.1	116.0 ± 0.8

Table 3-1 Glass transition temperatures of EC 7 powder on heating, cooling and reheating at 2°C, 5°C and 10°C/min (n=3)

Heating rate (°C./min)	$T_g$ heating (°C)	$T_g$ cooling (°C)	$T_g$ reheating (°C)
2	125.3 ± 0.1	113.4 ± 1.2	120.1 ± 1.0
5	126.9 ± 0.8	112.6 ± 1.2	120.0 ± 1.3
10	127.8 ± 2.2	113.5 ± 1.1	119.9 ± 1.5

*Table 3-2 Glass transition temperatures of EC 20 powder on heating, cooling and reheating at 2°C, 5°C and 10°C/min (n=3)*

Table 3-1 and Table 3-2 shows the effect of heating rates on the  $T_g$ s from heating, cooling and reheating signals. The  $T_g$ s on the heating signals varies considerably within the range of 122°C – 129°C in terms of the heating rates. The heating rate dependency of  $T_g$  values is probably possibly due to the thermal gradients developed across the sample, which may broaden the  $T_g$  and shift the  $T_g$  value to a higher temperature when the heating rate is increased. However, the  $T_g$ s on the cooling and reheating signals did not change dramatically on increasing the heating rates. The glass transition on heating depends on the thermal history and the preparation process of EC, whereas for the cooling and reheating signals, the thermal history of the materials has been eliminated. Therefore, the heating rates have less effect on the  $T_g$  values from the cooling and reheating than those from the heating signals. Another reasonable explanation is that after the initial heating process, the EC powder softened and became a molten layer which is thinner than the original powder samples. Therefore, the heat can be transferred more quickly across the whole sample. It is hard to conclude which transition (heating, cooling or reheating) is the best indication of the actual glass transition temperature in conventional DSC, in which, the measured heat flow is actually the total heat flow which is a combination of ‘kinetic’ and ‘heat capacity’

---

responses, hence the technique is not able to separate overlapping transitions that occur in the same temperature range. For instance, structural relaxation, that releases the molecular stress during its glass transition, could affect the accuracy of the  $T_g$  measurements (Schawe, 1995). The energy arising from the heat capacity event is reversible, but irreversible from the structural relaxation. MTDSC can separate the structural relaxation from the change in the heat capacity by applying a sine wave modulated heating rate.

From the MTDSC results,  $T_g$ s were observed in the reversing heat flow signal since they are associated with heat capacity change. The reversing signal showed an obvious glass transition of EC 20 at circa 120°C (*Figure 3-5*). *Table 3-3* shows the glass transition temperatures of EC 7 and EC 20 during heating, cooling and reheating at 2°C/min in MTDSC. The difference between the  $T_g$ s on heating, cooling and reheating was smaller than those observed in conventional DSC. It is probably because that at the same heating rate, MTDSC imposes a sinusoidal heating or cooling to the samples rather than a linear heating or cooling of conventional DSC. The difference in the heating or cooling process may have a different effect on the elimination of the thermal history of the samples.

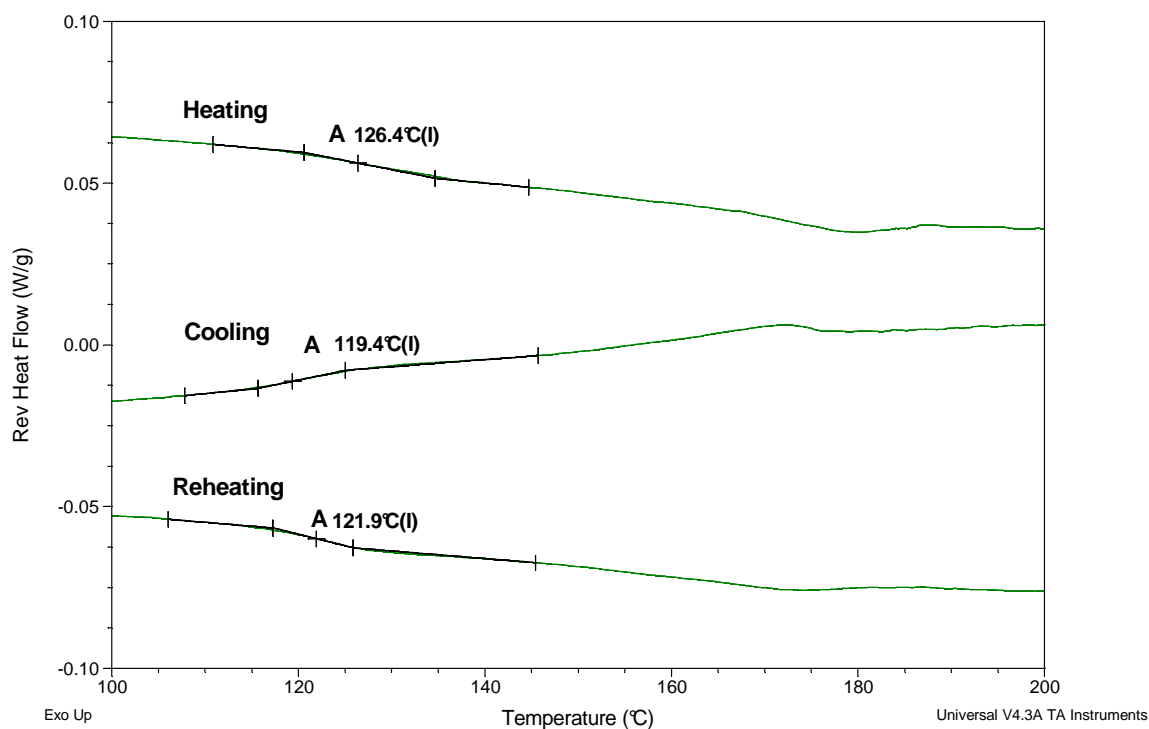


Figure 3-5 MTDSC reversing signal showing the heating, cooling and reheating of EC 20 in hermetically sealed pans at 2°C/min with a modulated amplitude of  $\pm 0.5^\circ\text{C}/40\text{s}$

Material	$T_g$ heating ( $^\circ\text{C}$ )	$T_g$ cooling ( $^\circ\text{C}$ )	$T_g$ reheating ( $^\circ\text{C}$ )
EC 7	$123.1 \pm 1.5$	$115.2 \pm 0.3$	$116.0 \pm 2.4$
EC 20	$124.6 \pm 1.5$	$120.4 \pm 1.3$	$123.5 \pm 1.5$

Table 3-3 Glass transition temperatures of EC 7 and 20 powder during heating, cooling and reheating at 2°C/min in MTDSC ( $n=3$ )

### 3.3.2 Thermal Properties of EC Films

#### 3.3.2.1 Visual Observation

Transparent EC organic solution films were prepared as the method stated in 3.1.1. Figure 3-6 is the 10% w/w EC 20 organic solvent film (ethanol/acetone 40:60). All the films

prepared were transparent. Therefore, the preparation and drying methods were considered to be efficient for EC films in terms of the appearances.



*Figure 3-6 10% (w/w) EC film prepared from 20 mL ethanol/acetone (40:60 v/v) organic solvent using 9 cm diameter petri dishes*

#### *3.3.2.2 Residual Solvents*

According to the TGA results, as shown in *Figure 3-7*, the weights of all dry films with 2.5%, 5%, 7.5% and 10% (w/v) EC 20 solution concentrations decreased when they were heated from room temperature to 150°C at a rate of 10°C/min. The weight loss was about 0.3% – 0.7%, which was regarded as the amount of the residual solvents in the dry films. The amount of residual solvents increased when increasing the concentrations of EC 20 solutions. These results are probably related to the hydrogen bonding property of acetone. Higher concentration of EC may be associated with more acetone through hydrogen bonding, hence resisting its evaporation from the EC films.

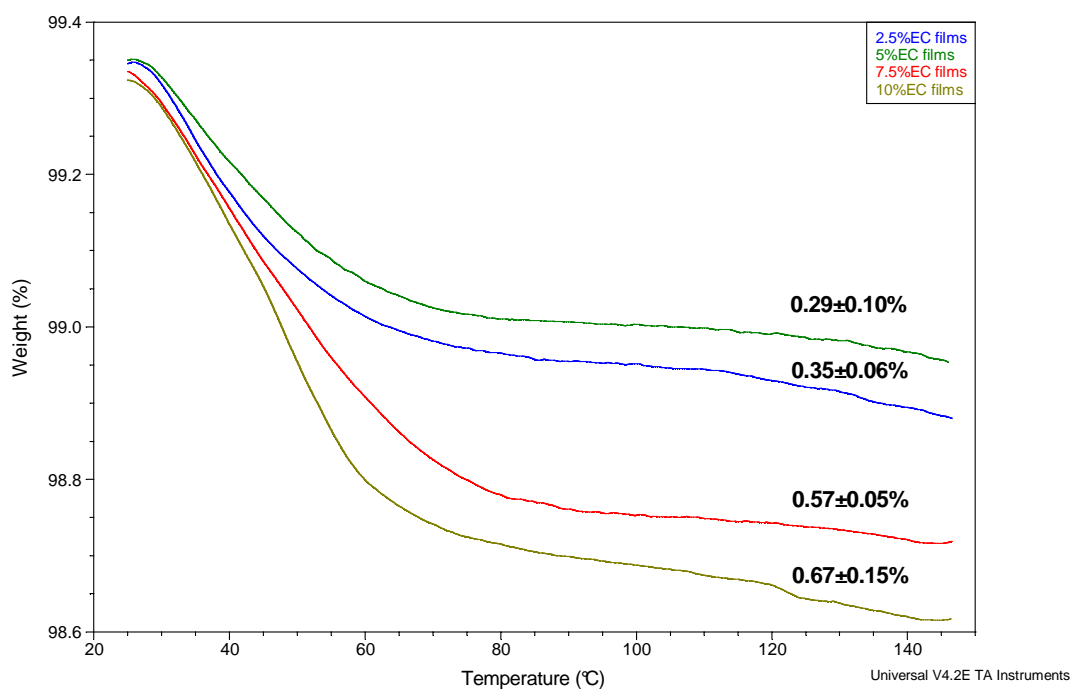


Figure 3-7 TGA curve of EC 20 organic solvent films on heating from room temperature to 150°C

### 3.3.2.3 DSC

Figure 3-8 shows the conventional DSC curve of EC organic solvent films on heating, cooling and reheating. It is reasonable to see that the heat flow signals of EC films were similar to those of the pure material. However, the oxidative degradation B appeared after the microcrystallites melting, which was the opposite order in the case of pure EC powder (Figure 3-2). This could be due to the small amount of organic solvents evaporating from the films when the hermetically sealed pans were heated up, therefore inhibiting the oxidative degradation of the films.

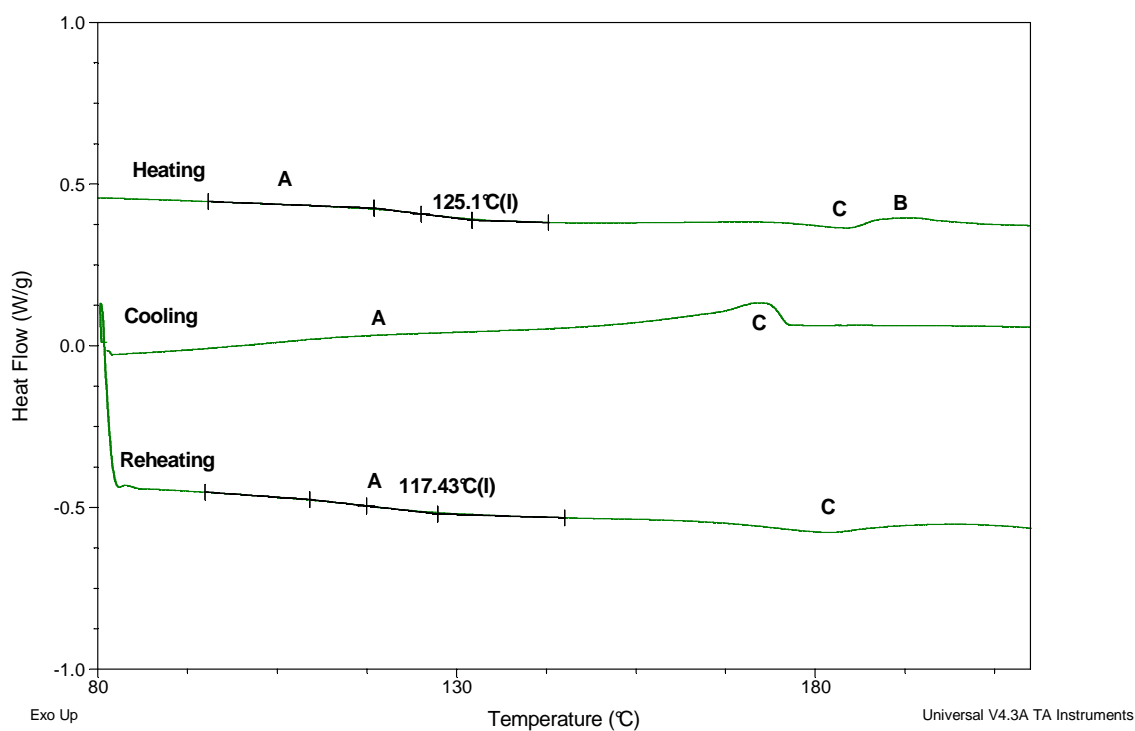


Figure 3-8 DSC curve of EC 20 organic solvent films on heating, cooling and reheating signals

EC 7	$T_g$ heating	$T_g$ cooling	$T_g$ reheating
2.5%	$120.2 \pm 0.3$	$109.4 \pm 1.7$	$108.0 \pm 1.7$
5.0%	$123.8 \pm 2.7$	$112.2 \pm 5.5$	$113.0 \pm 5.0$
7.5%	$122.6 \pm 2.0$	$110.7 \pm 1.7$	$110.8 \pm 0.2$
10.0%	$122.6 \pm 2.5$	$111.6 \pm 6.0$	$111.3 \pm 6.3$

Table 3-4 Glass transition temperatures of films prepared by EC 7 with different concentrations in ethanol/acetone (40:60) organic solvent system, obtained from MTDSC

( $n=3$ )

EC 20	$T_g$ heating	$T_g$ cooling	$T_g$ reheating
2.5%	122.6 ± 1.3	112.2 ± 3.6	114.3 ± 2.5
5.0%	125.6 ± 1.1	112.6 ± 0.6	113.9 ± 0.5
7.5%	126.0 ± 3.5	114.0 ± 0.5	117.6 ± 0.3
10.0%	129.1 ± 3.6	118.2 ± 4.5	121.1 ± 3.3

*Table 3-5 Glass transition temperatures of films prepared by EC 20 with different concentrations in ethanol/acetone (40:60) organic solvent system, obtained from MTDSC (n=3)*

MTDSC was also used to investigate the glass transition of EC organic solvent films. *Table 3-4* and *3-5* show the  $T_g$  values of films prepared by EC with different concentrations in the organic solvent of ethanol/acetone with a ratio of 40:60 (v/v). From these results, we can see that, the  $T_g$  is slightly higher when the concentration of EC is increased. This was possibly due to the effect of the organic solvent ethanol/acetone system on the  $T_g$  of the EC films, providing there was a small amount of organic solvent remaining in the film systems. The organic solvents can act as plasticizers, which may lower the  $T_g$  of the EC films. When the concentration of EC is high, the ratio of EC to solvent within the films may be relatively high, comparing to the films with lower levels of EC. Therefore, the films with more EC are less plasticized, rendering a higher  $T_g$ . Based on these results, during the DSC/MTDSC design of the experiment on the polymer films, further evaporation of organic solvent should be considered. Therefore, for the following MTDSC experiment, the crimped aluminium pans with a pin holed lid were utilized to prepare the film samples, in order to allow further evaporation of the solvent.

---

#### 3.3.2.4 DMA Studies

The principles of DMA have been introduced in *Chapter 2*. Ethyl cellulose films that are viscoelastic, exhibit behaviour somewhere in between purely elastic materials and purely viscous materials, i.e. some phase lag in strain. Film tension mode was used to investigate the storage modulus, loss modulus and  $\tan \delta$  of the EC films. When a polymer passes through its  $T_g$ , the storage modulus usually decreases by two or three orders of magnitude, and the  $\tan \delta$  goes through a maximum. The decrease in the moduli occurs when there is a main chain molecular motion and the maximum in  $\tan \delta$  occurs when the frequency of the forced vibration coincides with the frequency of the diffusional motion of the main chain. Typically, the glass transition is defined as the temperature at which either a maximum in the mechanical damping parameter  $\tan \delta$  or loss modulus occurs (David, 1999). The primary transition ( $\alpha$ , glass transition) can be attributed to an increased mobility of main polymeric chains, whereas, the  $\beta$  and  $\gamma$  transitions may be accredited to either side group mobility and/or end group motions of the main polymeric chains. In this Chapter, the peak temperatures of  $\tan \delta$  are used to analyze the glass transition temperatures of all the films.

*Figure 3-9, 3-10, 3-11 and 3-12* shows the DMA scans of 2.5%, 5%, 7.5% and 10% EC 20 films, respectively. The DMA curves for all the EC films with the four concentrations were similar. The storage modulus decreased dramatically when the films passed through the glass transitions, because of the main chain molecular motion. After that, it decreased to zero, since the films were still being heated at 3°C/min. The loss modulus of EC 20 films revealed a  $\beta$  transition at about 70°C, which did not change when increasing the EC levels. The maximum in  $\tan \delta$  occurs when the frequency of the forced vibration coincides with the frequency of the diffusional motion of the main chain of polymers, which indicates the glass transition temperature. However, the  $\tan \delta$  did not have an ideal glass transition peak,

because when a tensile clamp was used, the dry films were aligned vertically on the clamp, two ends of the films were fixed on the fixed clamp and movable clamp, respectively. When the samples were heated to a relatively high temperature and stretched at two ends, they became soft, and the storage modulus became zero at the end of the experiment, the instrument then stopped the run automatically. Despite the obstacle of the tensile clamp, it was clear that the frozen-in molecules began to move more freely at 60-70°C with maximum energy dissipation at circa 130°C. The glass transitions of EC films completed at 150°C.

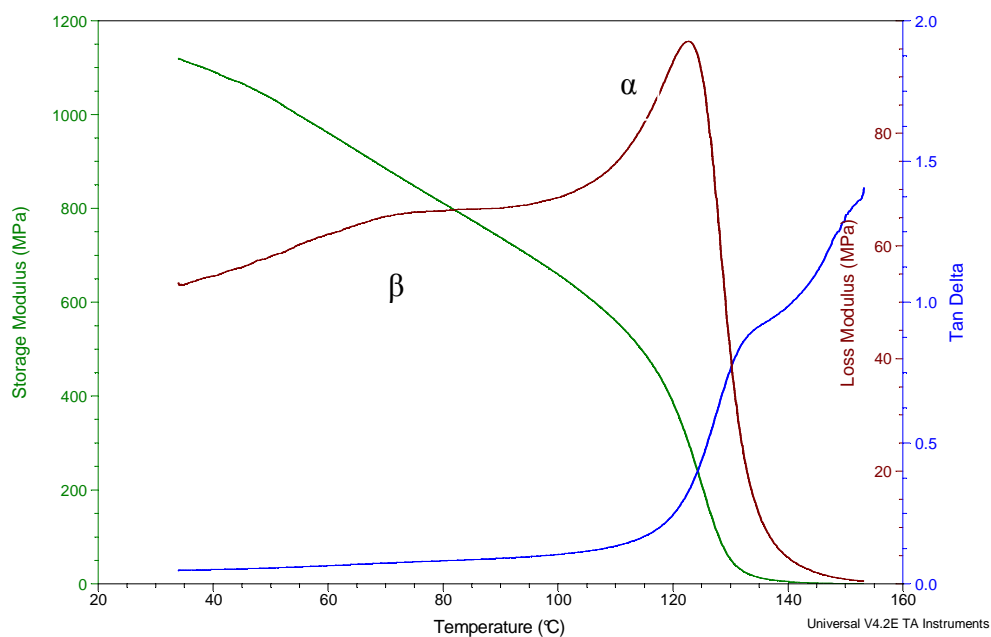


Figure 3-9 Storage modulus, loss modulus and  $\tan \delta$  of 2.5% EC 20 films with a heating rate of 3°C/min and a frequency of 1 Hz

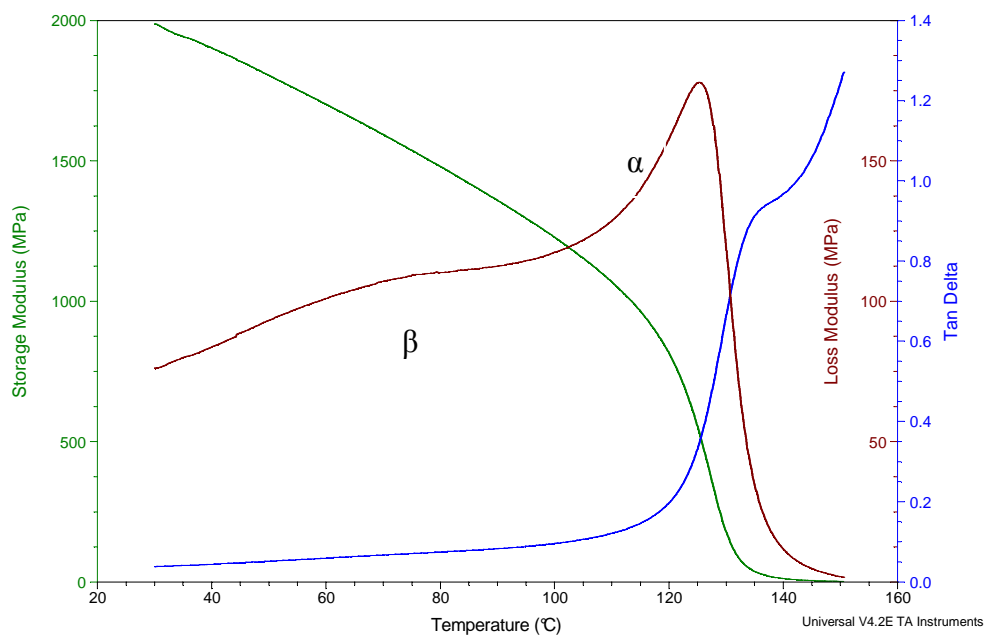


Figure 3-10 Storage modulus, loss modulus and  $\tan \delta$  of 5% EC 20 films with a heating rate of 3°C/min and a frequency of 1 Hz

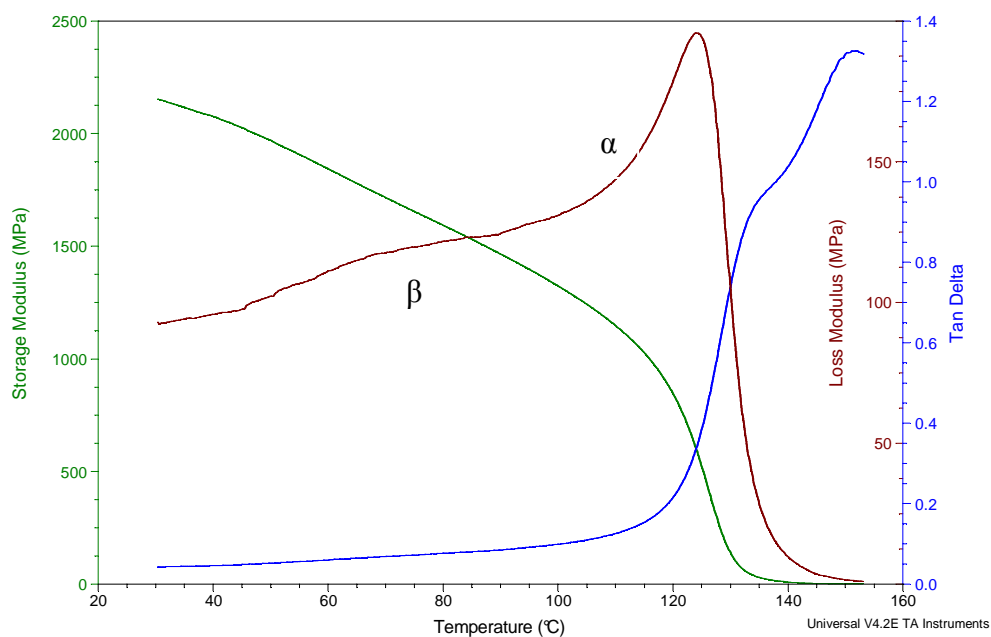


Figure 3-11 Storage modulus, loss modulus and  $\tan \delta$  of 7.5% EC 20 films with a heating rate of 3°C/min and a frequency of 1 Hz

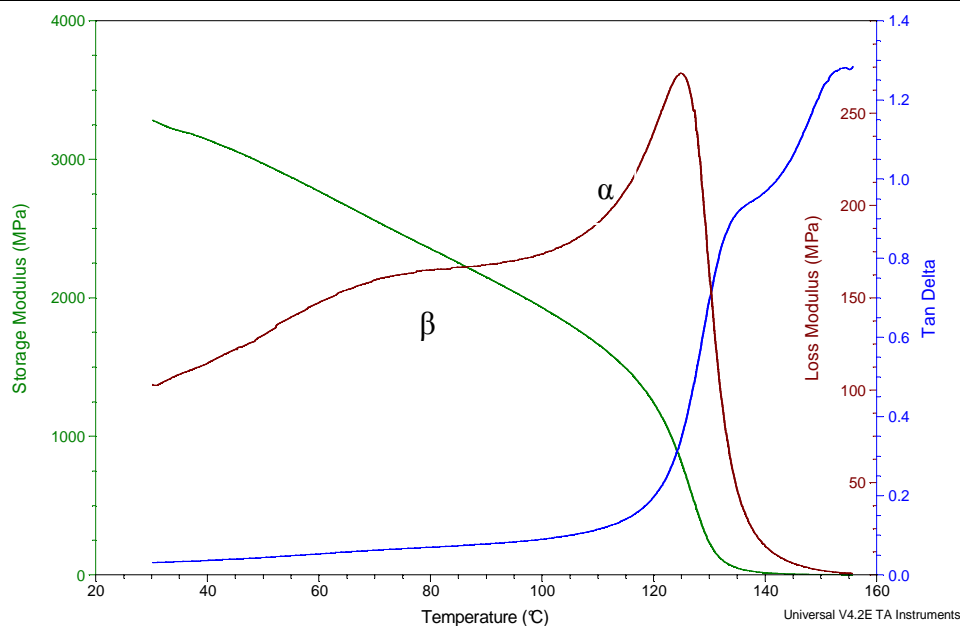


Figure 3-12 Storage modulus, loss modulus and  $\tan \delta$  of 10% EC 20 films with a heating rate of  $3^{\circ}\text{C}/\text{min}$  and a frequency of 1 Hz

EC 20	$T_g$ (MTDSC)	$T_g$ (DMA)
2.5%	$122.6 \pm 1.3$	$130.9 \pm 0.5$
5.0%	$125.6 \pm 1.1$	$132.9 \pm 0.7$
7.5%	$126.3 \pm 3.5$	$132.4 \pm 0.2$
10.0%	$129.1 \pm 3.6$	$133.2 \pm 0.4$

Table 3-6 Comparison of  $T_g$  values of EC 20 films produced from MTDSC and DMA ( $n=3$ )

As shown above in Table 3-6, the  $T_g$  values from DMA increased slightly when increasing the concentrations of EC in films, which were about  $8^{\circ}\text{C}$ ,  $7^{\circ}\text{C}$ ,  $6^{\circ}\text{C}$  and  $4^{\circ}\text{C}$  higher than those produced from MTDSC for the EC solution concentrations of 2.5%, 5%, 7.5% and 10%, respectively. The trend is consistent with the results of MTDSC, which may be due

to the plasticization of the small amount of solvent residue, as discussed in 3.3.2.3. Apparently, ethanol/acetone had a less significant effect on the  $T_g$  values from DMA than those from MTDSC. This is probably because DMA has a relatively open environment for the tested films, where ethanol/acetone was more likely to evaporate completely prior to the glass transition to occur. This explanation is actually reasonably consistent with the effect of organic solvents on the pure EC films with different concentrations from previous results. Therefore, care needs to be taken when preparing EC film formulations and interpreting the data.

EC 20	Storage Modulus	Loss Modulus
2.5%	759	705
5%	1954	646
7.5%	2240	1260
10%	3110	1310

*Table 3-7 The storage modulus and loss modulus of EC 20 films at room temperature*

The storage modulus and loss modulus of EC 20 films with different EC levels are listed in *Table 3-7*. The storage modulus of EC 20 films increased when increasing the EC levels. And the loss modulus of 7.5% and 10% EC 20 films were larger than those of the 2.5% and 5% EC 20 films. Solid bodies store applied energy and use this to recover from the deformation induced by the applied stress, and liquids dissipate applied energy as heat and hence are unable to recover their structure (David, 1999). The storage modulus represents the energy stored within the samples, i.e. the ‘solid’ response, whereas the loss modulus represents the energy dissipated within the sample, i.e. the ‘liquid’ response. Clearly, EC films with higher solid levels had more obvious viscoelastic characteristics.

### 3.4 Discussion

#### 3.4.1 Thermal Properties of EC

TGA experiments revealed the weight loss profiles of EC upon heating. The weight loss of EC below 100°C is due to the physical desorption of water (inter-molecular dehydration) in the samples (Li et al., 1999; Singh et al., 1996). The weight loss between 100°C and 250°C of EC may be due to the dehydration of the hydrogen bonding water. In this case, EC raw material did not show a great content of either free water or hydrogen-bonded moisture. EC, as a film coating polymer, may encounter elevated temperatures in processing. Thermo-stability and thermal degradation of EC is important from both practical and academic points of view. The experimental tests and the processing methodology should avoid increasing temperatures above its degradation temperature. Different heating rates may have an effect on the degradation kinetics of EC. However, the degradation onset was always at 250°C. The weight loss of EC after 250°C is attributed to the anhydroglucose polymeric chain decomposition (Singh et al., 1996).

Experimentally,  $T_g$  showed a dependency upon the heating rates. Higher values of  $T_g$  was observed for faster heating rates. The reason for this has been explained in the literature (Moynihan et al., 1974). If we take the isobaric heating at a constant rate is the limit at  $\Delta T \rightarrow 0$  of a series of instantaneous, small temperature changes  $\Delta T$ , each of which is followed by an isothermal hold of time duration

$$\Delta t = \Delta T/q \quad \text{Eq 3-1}$$

where  $q$  is the heating rate

$$q = dT/dt = \Delta T/\Delta t \quad \text{Eq 3-2}$$

We may define at any stage of this process a relaxation time  $\tau$  by the equation

---

$$(\partial H/\partial t)_T = -(H-H_e)/\tau \quad \text{Eq 3-3}$$

where  $(H-H_e)$  is the departure of the enthalpy  $H$  from the equilibrium liquid value,  $H_e$ , at the temperature of interest.  $\tau$  decreased with increasing the temperature. From Eq 3-1 it is evident that if the heating  $q$  is increased in magnitude, then the relaxation time  $\tau$  must be correspondingly smaller to hold, and the transition region is shifted to a higher temperature (Moynihan et al., 1974).

For the standard DSC experiments on EC, the heating rates had a less significant effect on the  $T_g$  values obtained from cooling and reheating signals than the heating signals. This is probably because the heating and cooling processes would cancel the effect of the thermal history and preparation of EC. Therefore, the reheating signals may be a better indication for the  $T_g$  values in this case. By superimposing a sinusoidal temperature change on the linear scanning program, MTDSC is capable of separating the irreversible kinetically controlled process, such as volume relaxation, from the reversible heat capacity change. To summarize, the  $T_g$  values analyzed from the reheating signals of MTDSC at 2°C/min may be the best indication of the glass transition of EC powders.

#### 3.4.2 Thermal Properties of EC Films

EC films were prepared in the solvent mixture system of ethanol/acetone 40:60, which has been proved to be a desirable solvent system for EC (Lai, 2005). Residual solvents were investigated to see if a more sophisticated drying method was needed. All prepared films appeared clear and the content residual solvents were lower than 0.7%. Therefore, it is reasonable to conclude that drying under room conditions is efficient for EC organic solvent films. However, the residual solvents increased when increasing the ratio of EC and the organic solvent, indicating that there is a certain interaction between the solvent

and the EC polymer chain, possibly hydrogen bonding. The EC polymer chain may, to some extent, restrain the solvents from evaporation.

In previous research (Lai, 2005), the thermal events B and C were attributed to the oxygen degradation and melting of microcrystallites, respectively. These two events were both observed from the DSC signals of EC powder and the EC films. However, in these films, the oxygen degradation B did not always happen before the melting C as the raw material did (seen *Figure 3-2* and *3-8*). It is possible that the oxydative degradation of the dissolved polymer chain of EC (in the solvent) was prohibited slightly by the presence of solvents.

From the results, we can see that the  $T_g$  values of EC films increased slightly when increasing the concentration of the EC. This is possibly due to the effect of the organic solvent ethanol/acetone system on the  $T_g$  of the EC films. According to the Fox equation and its extension for multi-component systems (Fox, 1956):

$$\frac{1}{T_g} = \frac{w_1}{T_{g1}} + \frac{w_2}{T_{g2}} \dots + \frac{w_n}{T_{gn}} \quad \text{Eq 3-4}$$

$T_g$  pertains to the blend,  $T_{gn}$  to pure component  $n$ , and  $w_n$  is the mass (weight) fraction of component  $n$ .

Ethanol or acetone can act as the plasticizers with low  $T_g$ s, hence when increasing the levels of EC, the  $T_g$  of films are closer to the  $T_g$  of EC, which is higher. Therefore, under the same evaporation level, organic solvents are expected to have a significant effect on the  $T_g$  values of EC 20 films with a lower level of EC, despite the films with high

concentrations of EC had more residual solvents. Therefore, in the next chapter, 10% w/w EC was used to prepare EC/plasticizer films in order to minimize the effect of the organic solvents. The effect was not obvious for EC 7, this might be because EC 7 has a lower viscosity than EC 20, and ethanol/acetone may evaporate more from EC 7 films than EC 20 films.

DMA is a method based on the thermo-mechanical property of materials. The changes of the mechanical properties upon heating will decide the  $T_g$  values. DMA results showed a less significant effect of the concentrations of EC on the  $T_g$  values of the EC films. In addition, DMA has a relatively open environment around the films compared with the hermetically-sealed pans used for DSC experiments, which allows the evaporation of the organic solvents during the heating process. The storage modulus and loss modulus of EC films revealed the viscoelastic properties of EC films. High level EC films tend to have higher storage modulus and loss modulus, i.e. more viscous and elastic responses when confronting mechanical forces.

### 3.5 Conclusion

Basic information on the thermal events associate with EC was provided. In particular the degradation had been investigated and found to commence at around 250°C. The  $T_g$  value varies depending on the measurement mode, but is around 110 - 120°C. It is a subtle transition so care will be required in identifying it with. EC 7 and EC 20 were found to have similar values of  $T_g$ . Further events were noted at around 180°C, which may be related to degradation and microcrystalline (Lai, 2005). These studies have shown that EC films may be prepared using ethanol/acetone mixes and that these films are satisfactory in appearance. The solvent residue could affect the  $T_g$  of dry films; if so, DMA may provide

---

more accurate values of the  $T_g$  in this case. The mechanical properties of EC films can also be affected by the concentrations of EC within the films.

---

## CHAPTER 4 THE EFFECTS OF PLASTICIZERS ON ETHYL CELLULOSE FILMS

### 4.1 Introduction

Pure EC films without plasticizers are normally brittle, which may result in cracks in the film coats (Rowe, 1986). This may in turn lead to uncontrolled drug release profiles. Hydrophilic plasticizers and/or pore formers are usually added to the EC films in order to adjust the mechanical properties as well as the drug release rates (Bonacucina et al., 2006; Pongjanyakul and Puttipipatkachorn, 2007). During the plasticization process, the plasticizer will partition into and soften the colloidal polymeric particles, thus promoting particle deformation and coalescence into a homogeneous film. The effectiveness of a plasticizer for a given polymer will depend on the plasticizer-polymer compatibility and the permanence of the plasticizer in the film during coating, storage and during contact with the drug release media. They can leak out from the polymeric coating after contact with the dissolution media, and drug transport may occur through the channels formed by the dissolved additives. The leaking of the hydrophilic plasticizers will alter the ratio of polymer to plasticizer in the film coating, hence they may cause changes in the film composition during dissolution (Frohoff-Hülsmann et al., 1999b), hence the glass transition temperature ( $T_g$ ) and the mechanical properties of the resulting films could be difficult to control. This may lead to completely different drug release mechanisms from the films produced by hydrophobic plasticizers.

Hydrophobic plasticizers may not have a significant effect on the release rates, but the film properties can be affected dramatically by the plasticizer's level, as indicated by a study on

---

the mechanism of release from pellets coated with an EC film incorporating a lipophilic plasticizer, dibutyl sebacate (Ozturk et al., 1990). The choice of polymer/plasticizer combination and the plasticizer level utilized in the film coating are crucial when deciding controlled release formulations. The polymer/plasticizer interaction and miscibility are therefore extremely important in understanding their transport mechanisms from the dosage form.

The objectives of this chapter is to develop a multiple discipline approach in order to evaluate the plasticizing efficiencies of selected plasticizers, characterize their interactions with EC 20 and distribution within the EC films, and optimize the controlled release formulations. EC 20 was used throughout the project because EC with higher viscosity may result in cracks and flaws in films (Rowe, 1986). Based on the previous results, 10% EC w/w was used to minimize the effect of the organic solvent. Oleic acid (OA), dibutyl sebacate (DBS) and medium-chain triglycerides (MCT) were chosen as lipophilic plasticizers in this project. OA and MCT have not yet been studied thoroughly as the plasticizers for EC films, whereas DBS has been used more often (Bodmeier and Paeratakul, 1994; Frohoff-Hülsmann et al., 1999b; Kangarlou et al., 2008; Lippold et al., 1999). EC/plasticizer films were produced to study the effect of these plasticizers on the thermal and mechanical properties of the EC films. The miscibility and interaction between the polymer and plasticizers within the film coats were investigated.

## **4.2 Methodology**

### **4.2.1 Preparation of EC/Plasticizers Films**

EC/plasticizers films were prepared by using the same method as for the pure EC films (introduced in *Chapter 3*). 5%, 10%, 15%, 20%, 25% and 30% (w/w) of oleic acid (OA),

dibutyl sebacate (DBS) and medium chain triglycerides (MCT) were added into the EC solutions, respectively. The solutions were stirred on a 45°C hot plate until the polymer was fully dissolved. A layer of PET Melinex sheet was laid over a toughened glass plate and was secured in place with sellotape. Wet films were then obtained by casting the organic solutions on the toughened glass plate using the film applicator with a wet film thickness of 2000 $\mu\text{m}$  in order to obtain a dry film thickness of 150 $\mu\text{m}\pm 10\mu\text{m}$ .

Plasticizer mixtures were used to investigate the effects of multiple component plasticizers on EC films. These films were prepared in a similar way to the EC/plasticizers films, i.e. by mixing the plasticizer mixtures with the EC solutions. 1.5 g of EC was applied in the formulations, and the other components were applied as shown in *Table 4-1*.

All of the films were dried under room conditions in a cupboard for 24 hours, and equilibrated at room temperature for another 24 hours before being tested. EC/MCT films were prepared again by drying them at 45°C in the oven for 3 hours, and then going through the same equilibration.

Formulation	Component (%)			
	EC	OA	DBS	MCT
EC/OA-DBS	75.2	8.8	16.0	-
EC/OA-FCO	75.2	8.8	-	16.0

*Table 4-1 Components of EC/plasticizer films*

---

#### 4.2.2 Thermogravimetric Analysis

TGA was used to determine the solvent residue and degradation of the produced films. All of the samples were heated from room temperature to 350°C at 10°C/min. Both the weight loss and the derivate weight loss signals were used to analyze the onset of degradation. The sample mass was approximately 5 – 10 mg. Dry nitrogen was used as the purge gas and compressed air was used as the cooling system.

#### 4.2.3 DSC Studies

MTDSC experiments were initially conducted by running samples from room temperature to 220°C with  $\pm 0.5^\circ\text{C}$  modulation amplitude every 40 seconds at a heating rate of 2°C/min. The sample mass was 2 – 5 mg. Initially MTDSC experiments were conducted using pin-holed pans, aiming to allow the evaporation of organic solvents. The repeatability was not satisfactory, possibly due to the films moving inside the pans. Pin-holed pans have a relatively larger space than the other pans, such as crimped and hermetically sealed pans, hence the signals were not stable. Therefore, crimped pans were considered, since the samples could be pressed tightly inside the pans, i.e. no movement. A hole was made on the lid of the crimped pans to allow the evaporation of organic solvents. The repeatability of the data was improved significantly.

Further MTDSC experiment was conducted on a Q2000 (TA Instruments, USA) using standard pans by heating the samples from room temperature to 100°C, cooling to room temperature and then heating to 180°C again with  $\pm 0.5^\circ\text{C}$  modulation amplitude every 40 seconds at a rate of 2°C/min. The glass transition temperatures ( $T_g$ s) were determined as the inflection points in the reversing heat capacity signals and the peaks of the derivative reversing heat capacity signals in some cases.

---

#### 4.2.4 DMA Studies

For the tension mode of DMA, approximately  $30 \times 5.27$  mm square pieces of the films were mounted on a tensile clamp of DMA. Samples were heated from  $30^{\circ}\text{C}$  to  $150^{\circ}\text{C}$  at a rate of  $3^{\circ}\text{C}/\text{min}$  with a frequency of 1 Hz and an amplitude of  $20\ \mu\text{m}$ . For the single cantilever mode of DMA, the film samples were prepared on the stainless steel mesh (0.140 mm wire diameter) first. They were then cut into pieces with dimensions of  $23.0 \times 12.7$  mm, and mounted on a single cantilever clamp. These samples were heated from  $30^{\circ}\text{C}$  to  $180^{\circ}\text{C}$ , then cooled down to  $30^{\circ}\text{C}$ , and then reheated to  $180^{\circ}\text{C}$  at a rate of  $3^{\circ}\text{C}/\text{min}$  with a frequency of 1 Hz and an amplitude of  $100\ \mu\text{m}$ . The storage modulus, loss modulus and  $\tan \delta$  of samples during the program were recorded to analyze the mechanical properties and the peak temperatures of the  $\tan \delta$  were taken as the glass transition temperatures of the films.

#### 4.2.5 AFM Studies

The theory of AFM, as well as heated stage AFM, micro- and nano-thermal analysis was described in *Chapter 2*. Small pieces of films (approximately  $10 \times 10$  mm) were cut and mounted on the magnetic stub by double-sided tape. The surfaces of the dry films were scanned initially to obtain topography and adhesion images simultaneously by using a pulsed force mode. The frequency and amplitude for modulation and subtract baseline were 500 Hz and 50 nm respectively. The scan area was between  $50 - 100\ \mu\text{m}^2$  and the scan speed was  $100\ \mu\text{m}/\text{s}$  with 200 lines of resolution.

After the images of the film surfaces were obtained at room temperature, the stage was heated to a relatively higher temperature of  $45^{\circ}\text{C}$  for the EC/plasticizers films and  $110^{\circ}\text{C}$  for the pure EC films. The surfaces of these films were scanned again using the same

---

parameters as those at room temperature. Images were recorded to compare with those taken at room temperature.

Micro- and nano-thermal analysis was applied to the areas of interest. Thermal analysis data was obtained at 5°C/s between room temperature and 150°C. Probe cantilever deflection was plotted against probe tip temperature to obtain the  $T_g$ s of specified locations on the film surfaces.

### 4.3 Results

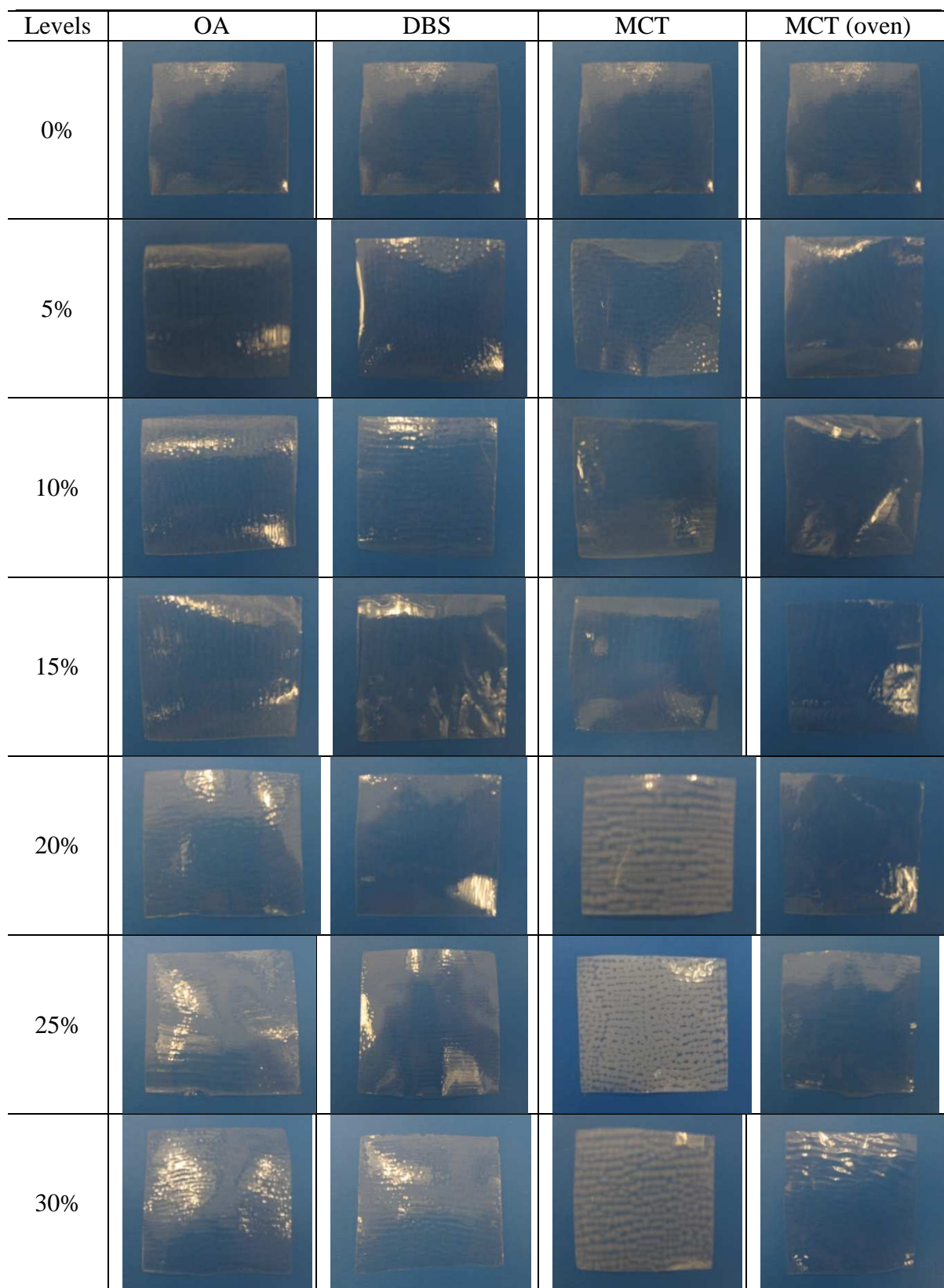
#### 4.3.1 Visual Observations

In general, film formation from organic solvents takes place via the evaporation of the solvent(s), which increases the polymer concentration until an intermediate gel-like stage is reached. Upon further evaporation, a solvent-free polymeric film is obtained. In order to compare their properties, all films were prepared using the same organic solvent system, i.e. ethanol/acetone (40:60 v/v), which has been shown to give optimal films (Lai, 2005). After drying at room temperature for 24 hours, all films were equilibrated under the same condition for a further 24 hours. *Figure 4-1* shows the appearance of pure EC films and those containing plasticizers at various concentrations. Even though the pure EC films were inflexible and easy to break, their transparency was satisfactory as expected. EC films with different concentrations of OA and DBS were as clear as the pure EC films. This implies that the added plasticizers at the levels used did not have any effect on the appearance of the resulting films. However, EC films with 20%, 25% and 30% MCT contained numerous white spots. The cloudiness of EC films with high concentrations of MCT might be due to the precipitation of EC caused by water sorption, which can subsequently lead to poor product performance. Therefore, EC/MCT films were dried at

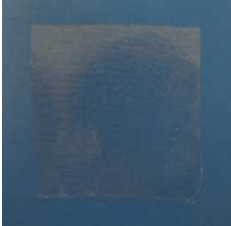
---

45°C for 3 hours in the oven, and they appeared clear when taken out. The drying conditions including two possible variables, temperature and humidity, may have an impact on the film appearance. Evidence has been presented that films prepared in desiccators with silica gel and in the oven at 45°C gave the best film appearance (Lai, 2005). However films prepared in desiccators with silica gel at various temperatures did not affect its transparency. Therefore the presence of moisture in the environment is the main contributing factor on the cloudiness of films. Comparing the appearance of EC/plasticizer films, only EC/MCT films were affected by the moisture at room conditions. This suggests MCT has more significant affinity to moisture than OA and DBS.

EC films that contained 8.8% OA and 16% DBS were shown to be clear, as shown in *Figure 4-2*. Interestingly, when plasticizer mixtures OA-MCT were applied, the films (dried under room temperature) presented as transparent again, even though the concentration of the overall plasticizer was over 24%, which was higher than 20% when EC/MCT films appeared cloudiness. Based on these results and the fact that EC films with 20% MCT and beyond had cloudiness phenomenon at room temperature, we can conclude that EC films with less than 20% MCT can obtain a clear appearance at room temperature.



*Figure 4-1 Visual observation of EC cast films incorporated various types of plasticizers with different concentrations dried at room temperature or 45°C in the oven*

	8.8% OA-16% DBS	8.8% OA-16% MCT
Appearance		

*Figure 4-2 EC cast films with 8.8% OA-16% DBS and 8.8% OA-16% MCT as the plasticizers, dried under room condition*

#### 4.3.2 Thermogravimetric Analysis

Ethanol and acetone have relatively low boiling points (78.4°C and 56.5°C, respectively). The weight losses of all of the prepared films were analyzed at temperature up to 120°C, based on the assumption that all the residual solvents, including ethanol, acetone and moisture, would evaporate by then. *Table 4-2* presents the percentage weight loss calculated at 120°C of EC films with OA, DBS and MCT. The sample mass decreased less than 0.7% for all of the films when they were heated up to 120°C. Surprisingly, the plasticizer concentration had a negative effect on the residual solvents of these films, irrespective of the plasticizer types. This indicates that the participation of the plasticizer molecules into the polymeric matrix possibly reduced the number of solvent molecules adhering to the polymer chains.

Both weight loss and derivative weight loss signals were used to analyze the degradation of pure MCT and EC/MCT films (*Figure 4-3*). All dry films had a degradation onset temperature at about 160°C. The degradation of dry films with a higher level of MCT was

quicker. This is probably due to MCT having a much lower degradation onset temperature (120°C) than pure EC (250°C, data shown in *Chapter 3*).

Plasticizer Concentrations	EC/OA Films (%)	EC/DBS Films (%)	EC/MCT Films (%)
0%	0.67	0.67	0.67
5%	0.60	0.59	0.53
10%	0.51	0.49	0.42
15%	0.45	0.40	0.44
20%	0.38	0.35	0.27
25%	0.33	0.29	0.28
30%	0.26	0.24	0.24

*Table 4-2 Weight loss of EC films with various formulations at 120°C*

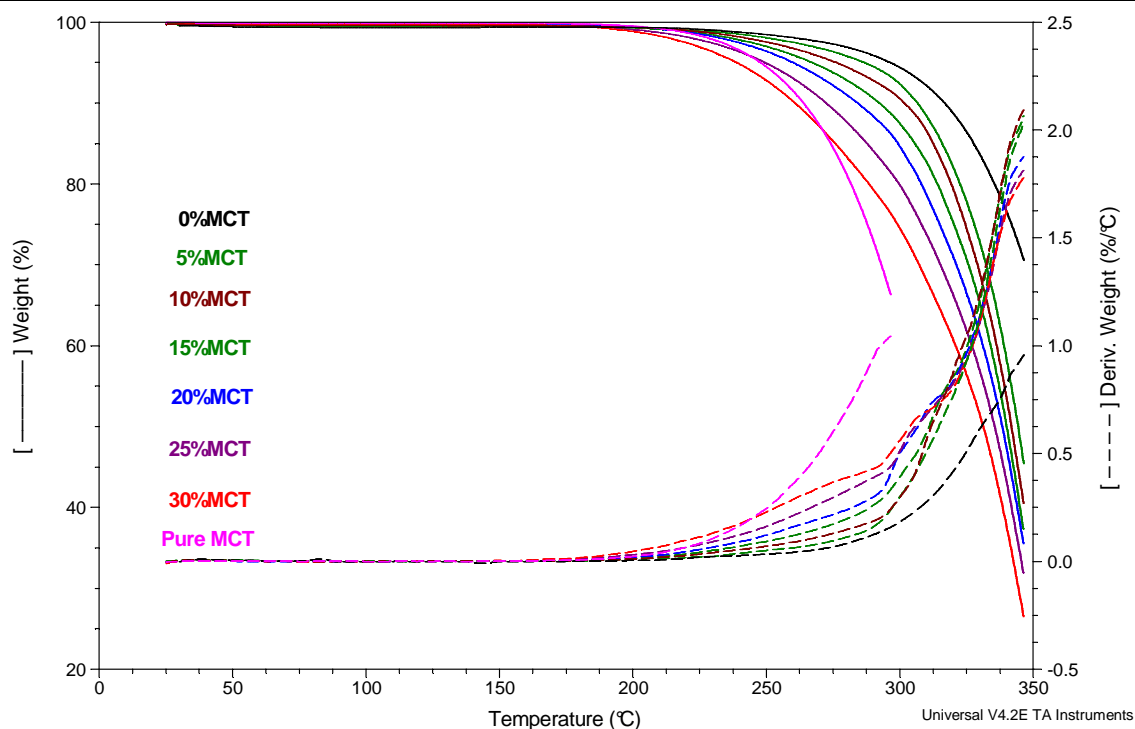


*Figure 4-3 Thermogram showing the degradation of EC/MCT dry films and pure MCT in weight loss and derivative weight loss signals at a heating rate of 10 °C/min under nitrogen conditions*

Figure 4-4 shows both of the weight loss and derivative weight loss signals of EC/OA-DBS films and EC/OA-MCT films. The weight loss of both films at 120°C is less than 0.5%, which means there was a rather small amount of residual solvent in the dry films. From the derivative weight loss signals, we can see that for the EC/OA-DBS films a degradation peak appeared at about 230°C with the onset temperature of 130°C. Nevertheless, the degradation acceleration rate was nearly constant after 285°C; it then increased at 320°C, which did not present a peak before the experiment finished (final temperature of 350°C). EC/OA-MCT films showed slightly different plots to EC/OA-DBS films. The derivative signal exhibited 3 degradation periods; first from 150°C (onset

temperature) to 300°C, second from 300°C to 320°C and, the third was from 320°C to 350°C. A total weight loss of 70% was observed for both films.

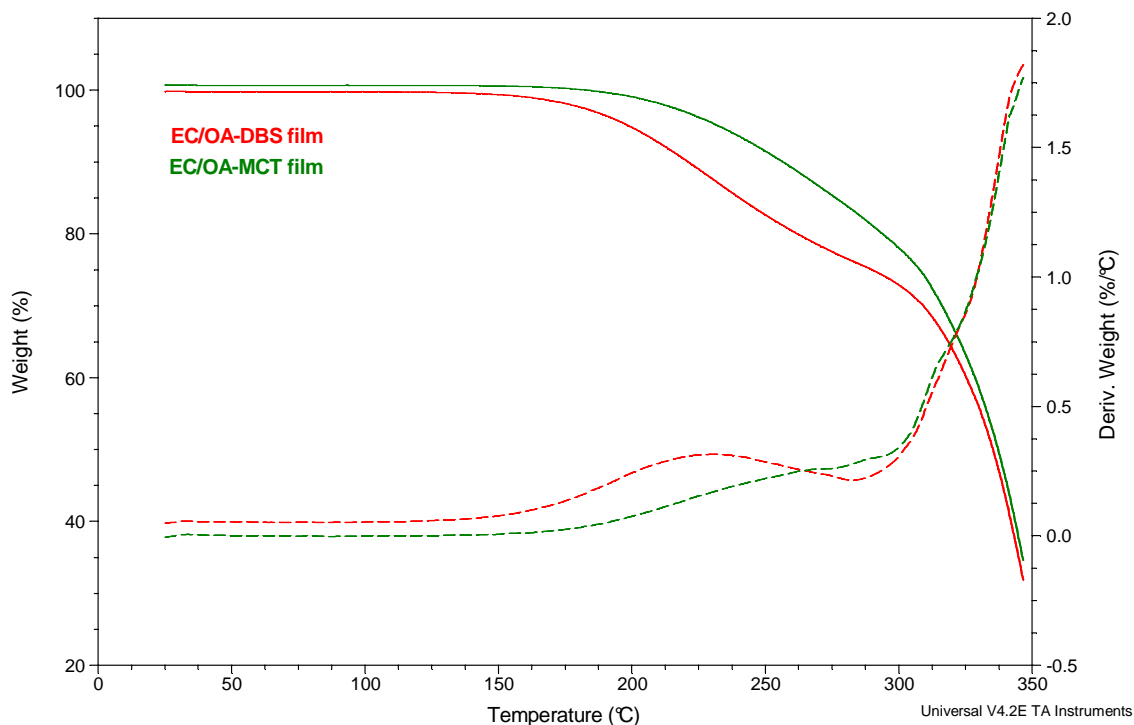


*Figure 4-4 Decomposition of EC/OA-DBS and EC/OA-MCT films in TGA and D-TGA at a heating rate of 10 °C/min*

#### 4.3.3 DSC Studies

The heat capacity change ( $\Delta C_p$ ) associated with the  $T_g$  of EC is known to be small (Lai et al., 2010). The heat flow baseline of EC films has been proven to be drifting due to the inherent property of EC (Lai, 2005) that was also observed in this study (data not shown). If two transitions are rather close to each other, the decision on the step range of transition is critical to obtain accurate data, which can be affected by the operator's choice. Therefore, the peaks of the derivative reversing heat capacity signals was utilized to analyze the  $T_g$ s of

EC/OA films, EC/DBS films and EC/MCT films. *Figure 4-5* shows the derivative reversing heat capacity signals of MTDSC scans of EC/OA films by heating from 20°C to 220°C with  $\pm 0.5^\circ\text{C}$  modulation amplitude every 40 seconds at a heating rate of 2°C/min. One single of  $T_g$  was observed from each film under the parameters used. The  $T_g$  values (shown in *Table 4-3*) decreased from  $129.2 \pm 0.1^\circ\text{C}$  to  $53.2 \pm 0.7^\circ\text{C}$  when the concentrations of OA (0% – 30% w/w) increased. This implies that EC could be plasticized by OA. The transition associated with the melting endotherm (described in *Chapter 3*) similarly decreased and became less pronounced.

Similarly to EC/OA films, DBS presents a plasticizing effect on EC films (*Figure 4-6*). The  $T_g$  values (shown in *Table 4-3*) decreased dramatically when the concentrations of DBS were increased up to 30% (w/w). However, from 20% onwards, the reduction of  $T_g$  values were rather small in comparison with those from 0% to 20%. This might be due to the plasticizing efficiency being reduced when the concentrations of DBS were increased. This will be further discussed in a later section.

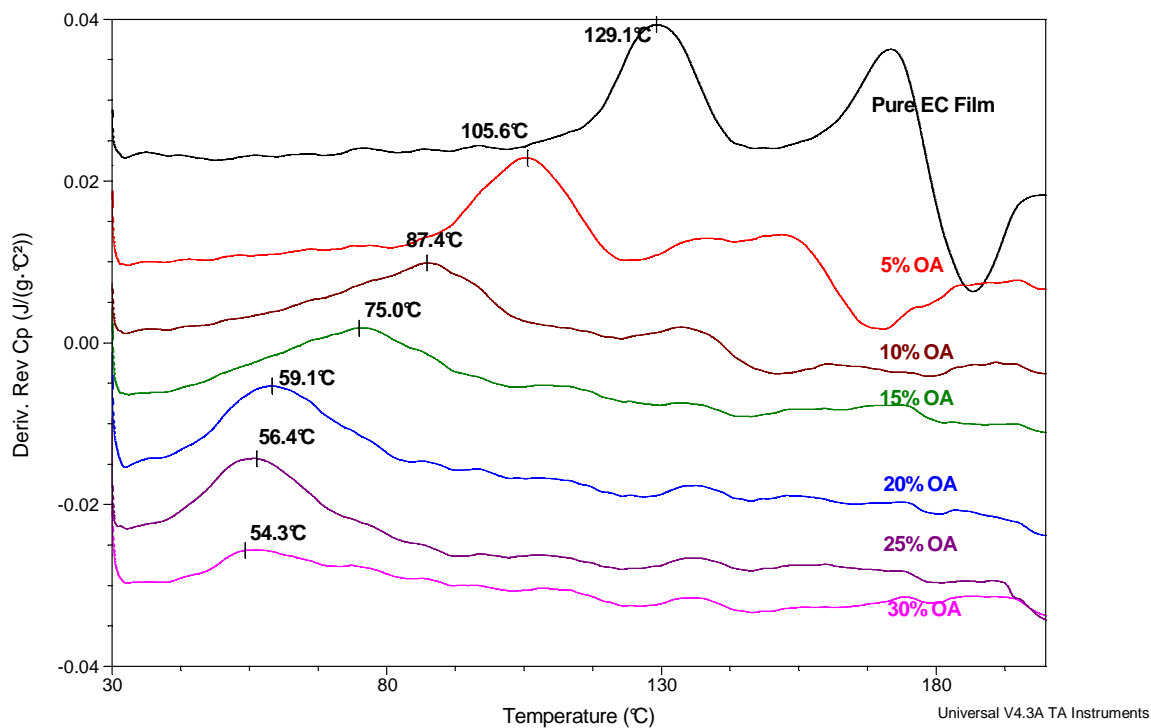


Figure 4-5 Derivative reversing heat capacity signals of MTDSC scans of EC/OA films by heating from 20  $^\circ C$  to 220  $^\circ C$  at a heating rate of 2  $^\circ C/min$

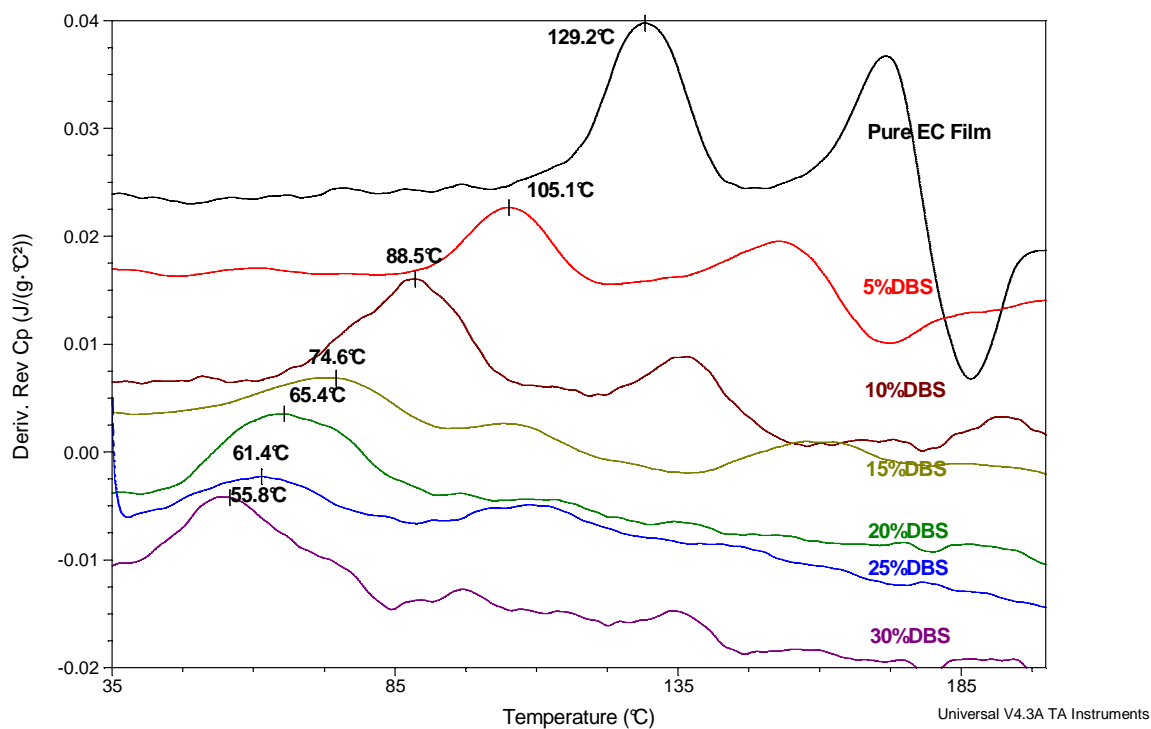
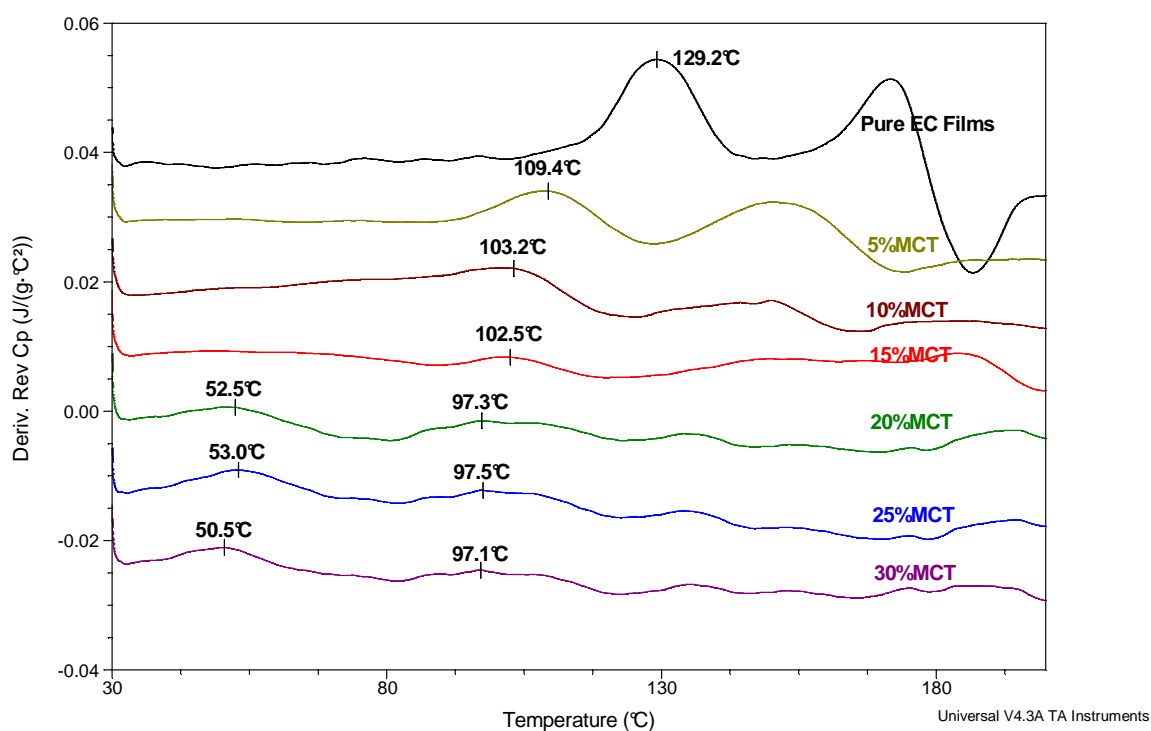


Figure 4-6 Derivative reversing heat capacity signals of MTDSC scans of EC/DBS films by heating from 20  $^\circ C$  to 220  $^\circ C$  at a heating rate of 2  $^\circ C/min$

The derivative reversing heat capacity signals from MTDSC scans of EC films and those with 5%, 10%, 15%, 20%, 25% and 30% MCT are shown in *Figure 4-7*. On adding 5% of MCT, the  $T_g$  value decreased from  $129.2 \pm 0.1^\circ\text{C}$  to  $110.5 \pm 0.3^\circ\text{C}$ . This decrease in  $T_g$  is consistent with behaviour associated with plasticizer miscibility and has been similarly observed for the 10% MCT system. However, the  $T_g$  of 15% MCT system was very similar to that of the 10% MCT system. On increasing the concentration of MCT to 20% and beyond, the  $T_g$  value remained reasonably constant at circa  $97^\circ\text{C}$  while a further lower temperature peak was observed at circa  $52^\circ\text{C}$ . Hence two transitions are seen that do not correspond to either individual component. We suggest that the phase separation may not comprise simply with the presence of individual components but may instead reflect mixed phases. This will be further discussed in a later section.



*Figure 4-7* Derivative reversing heat capacity signals of MTDSC scans of EC/MCT films by heating from  $20^\circ\text{C}$  to  $220^\circ\text{C}$  at a heating rate of  $2^\circ\text{C}/\text{min}$

Plasticizer concentration	OA Films $T_g$ (°C)	DBS Films $T_g$ (°C)	MCT Films $T_g$ (°C)
0%	129.2 ± 0.1	129.2 ± 0.1	129.2 ± 0.1
5%	104.9 ± 0.7	105.5 ± 0.8	110.5 ± 0.3
10%	88.4 ± 0.3	88.5 ± 0.4	103.8 ± 0.6
15%	74.3 ± 0.5	73.9 ± 0.5	103.9 ± 1.2
20%	59.1 ± 0.3	64.3 ± 1.2	54.0 ± 0.3 99.8 ± 2.1
25%	56.3 ± 0.6	59.3 ± 0.7	53.8 ± 1.9 99.3 ± 3.9
30%	53.2 ± 0.7	53.7 ± 0.7	51.0 ± 0.9 97.2 ± 1.1

*Table 4-3 Glass transition temperatures of EC/plasticizer films with different concentrations from MTDSC (n=3)*

*Figure 4-8* shows the reversing heat flow signals of EC/OA-DBS films and EC/OA-MCT films. Interestingly, these two films exhibited broad glass transitions at  $50.0 \pm 1.3^\circ\text{C}$  (EC/OA-DBS films,  $n = 3$ ) and  $52.1 \pm 0.7^\circ\text{C}$  (EC/OA-MCT films,  $n = 3$ ) respectively. There was no second glass transitions observed.

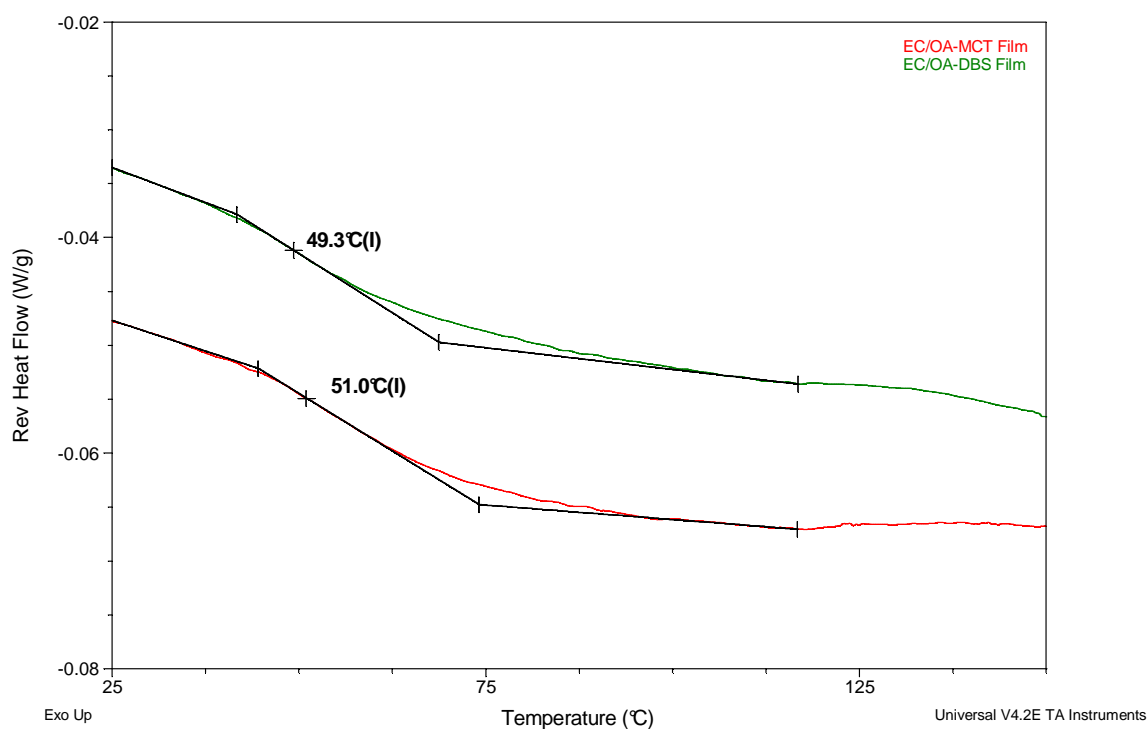


Figure 4-8 Reversing heat flow signals of EC/OA-DBS films and EC/OA-MCT films by heating from 20°C to 220°C at a heating rate of 2°C/min

#### 4.3.4 DMA Studies

##### 4.3.4.1 Thermal Properties

As described in *Chapter 2*, in viscoelastic materials, throughout the glass transition, the storage modulus decreases, and  $\tan \delta$  goes through a peak max, which indicated the glass transition temperatures. *Figure 4-9*, *Figure 4-10* and *Figure 4-11* shows the  $\tan \delta$  of DMA scans of EC films incorporated with a range of concentrations of plasticizers. Since the position of the maximum  $\tan \delta$  was shifted to lower temperatures with increasing plasticizer concentration, this was assigned to the plasticization of the polymer.

As shown in *Table 4-4*,  $T_g$  for EC/OA films went down from  $133.6 \pm 0.3^\circ\text{C}$  to  $65.6 \pm 0.5^\circ\text{C}$  when the OA concentration was increased from 0% to 30% (w/w). Only one  $\tan \delta$

maximum was observed in each DMA scan.  $T_g$  for EC/DBS films went down from  $133.6 \pm 0.3^\circ\text{C}$  to  $71.2 \pm 0.3^\circ\text{C}$  when the DBS concentration was increased from 0% to 30% (w/w), which was a similar trend to that seen for EC/OA films. These results indicate an appreciable interaction between the polymer and the plasticizers.

For EC/MCT films, the  $T_g$  decreased from  $133.6 \pm 0.3^\circ\text{C}$  to  $121.2 \pm 0.3^\circ\text{C}$  when its concentration was increased from 0% to 5% (w/w), and following the decreasing trend from 5% to 15%. At 20% MCT level, the  $T_g$  of films showed two tan delta peaks ( $69.8 \pm 1.3^\circ\text{C}$  and  $107.7 \pm 0.7^\circ\text{C}$ , *Figure 4-11*), that indicates a phase separation that occurred at this concentration level. Nevertheless, at both 25% and 30% (w/w) MCT levels, the storage modulus decreased dramatically when the temperature increased, in consequence the instrument stopped running the experiments automatically. Therefore, no further high temperature transitions could be detected.  $\tan \delta$  is a measure of the damping and therefore the degree of segmental motion taking place within a polymer. Damping at temperatures above and below the  $T_g$  is small but ideally rises to a maximum at the  $T_g$  itself. A sharp peak of  $\tan \delta$  denotes good polymer/plasticizer compatibility, whereas a broad peak denotes poor compatibility.

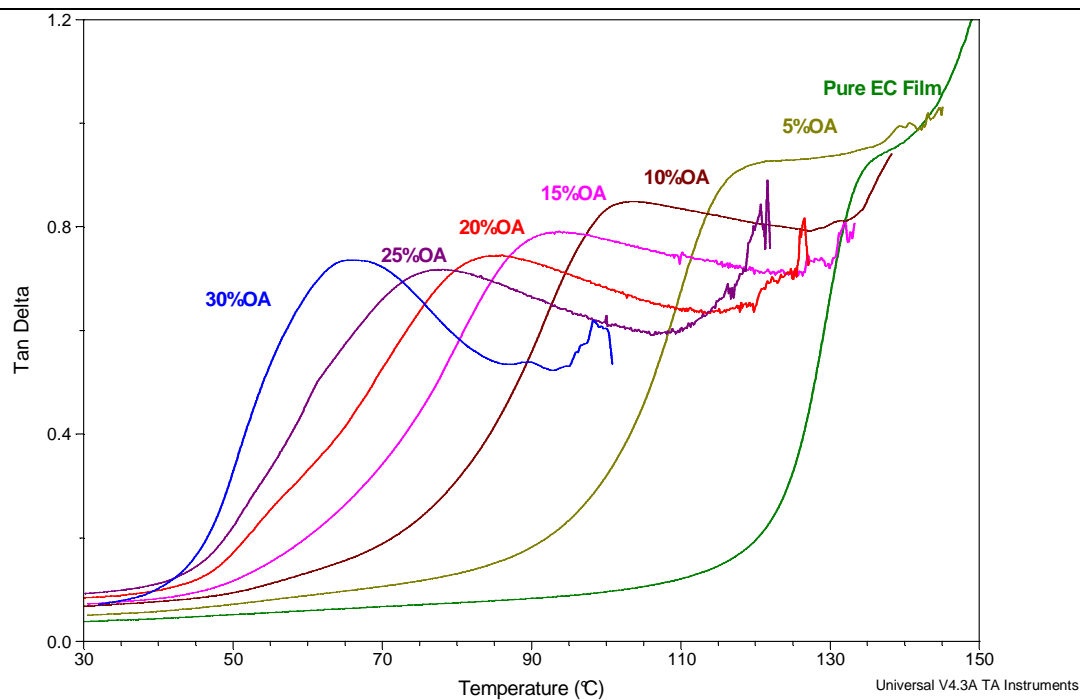


Figure 4-9  $Tan \delta$  of DMA scans of EC/OA films by heating from 30°C to 160°C at a heating rate of 3°C/min

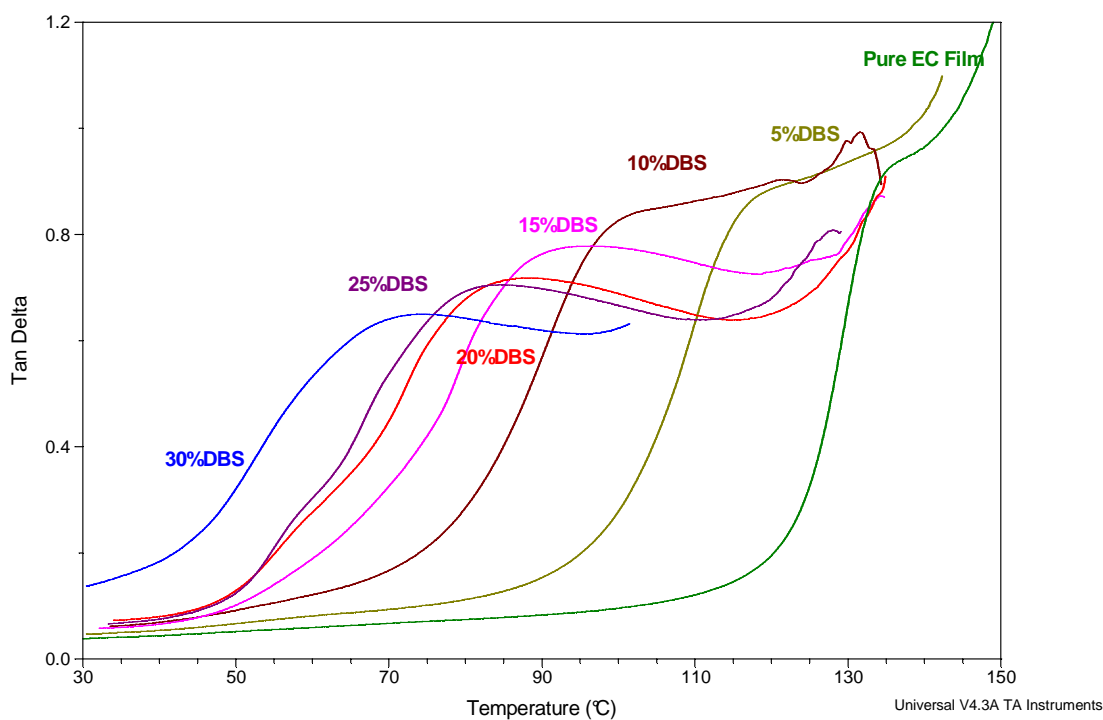


Figure 4-10  $Tan \delta$  of DMA scans of EC/DBS films by heating from 30°C to 160°C at a heating rate of 3°C/min

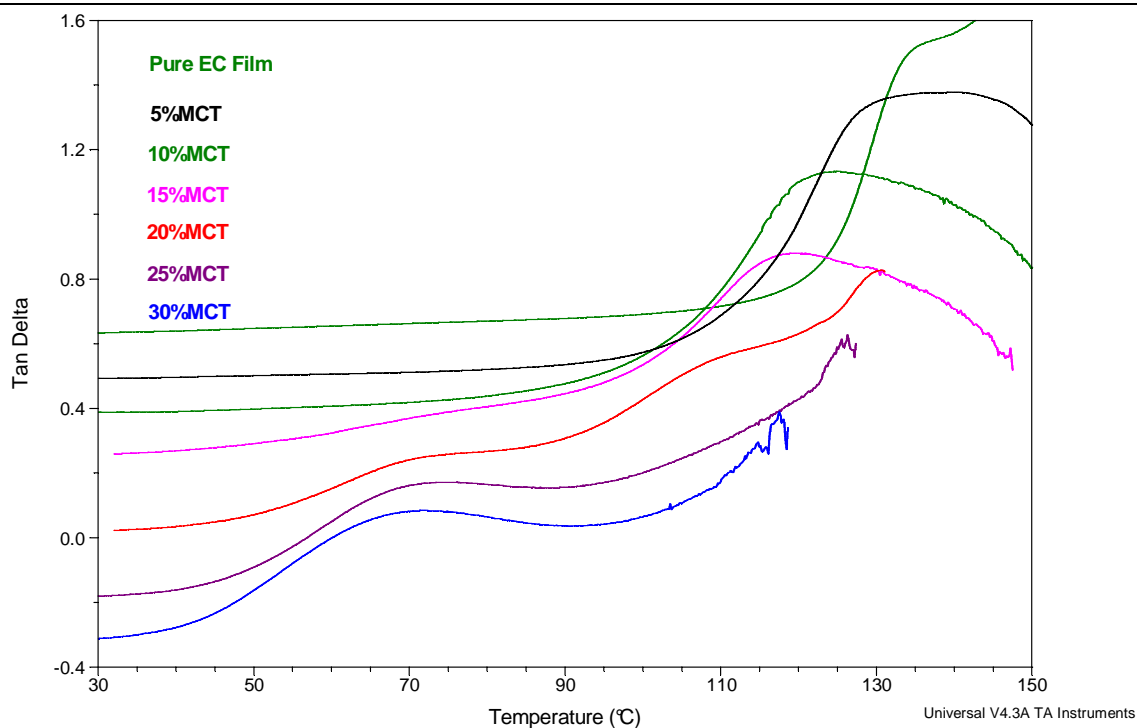
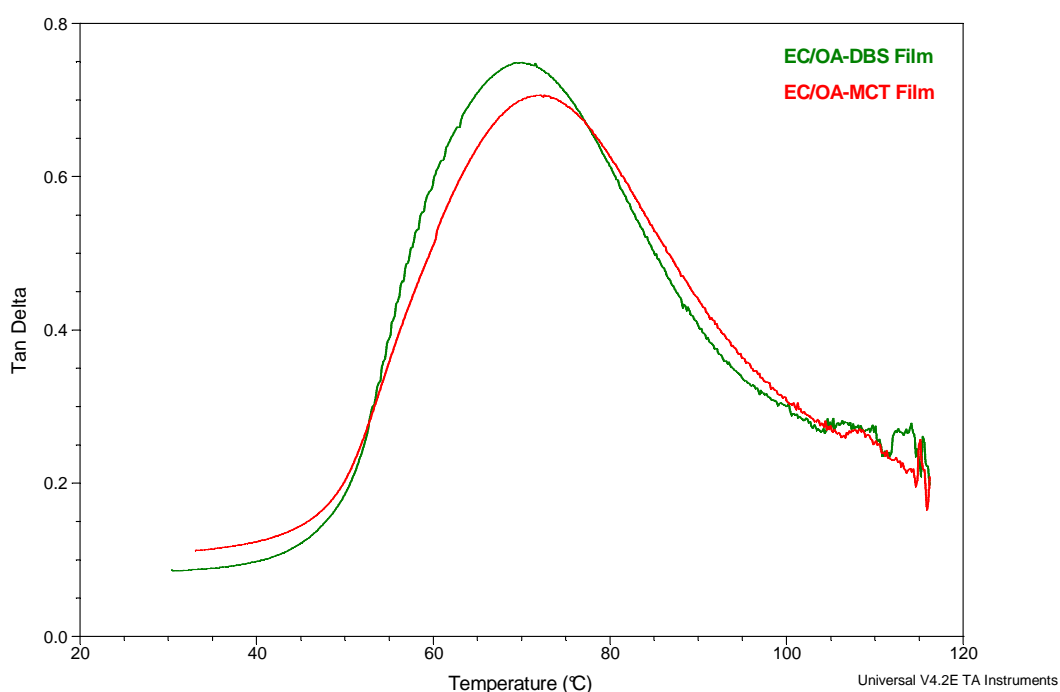


Figure 4-11  $Tan \delta$  of DMA scans of EC/MCT films by heating from 30 °C to 160 °C at a heating rate of 3 °C/min

Plasticizer concentrations	OA Films $T_g$ (°C)	DBS Films $T_g$ (°C)	MCT Films $T_g$ (°C)
0%	133.6 ± 0.3	133.6 ± 0.3	133.6 ± 0.3
5%	116.3 ± 0.7	117.1 ± 0.5	121.2 ± 0.3
10%	98.6 ± 0.7	97.6 ± 0.5	109.5 ± 0.4
15%	90.4 ± 0.4	89.9 ± 0.3	108.4 ± 0.4
20%	83.3 ± 0.5	83.9 ± 0.5	69.8 ± 1.3 107.7 ± 0.7
25%	76.3 ± 0.1	82.0 ± 0.5	69.4 ± 0.3
30%	65.6 ± 0.5	71.2 ± 0.3	68.2 ± 0.4

Table 4-4 Glass transition temperatures of EC/plasticizer films with different concentrations from DMA (n=3)

The DMA (tensile clamp) results indicated that the EC/OA-DBS films and EC/OA-MCT films presented the  $T_g$ s at  $70.9 \pm 0.1^\circ\text{C}$  and  $73.1 \pm 1.2^\circ\text{C}$  respectively (indicated by the  $\tan \delta$  peaks, as seen in *Figure 4-12*). Good reproducibility of data using the single cantilever clamp can be seen in *Figure 4-13*. These results are in good agreement with those from MTDSC studies. It is interesting to note that the  $\tan \delta$  peaks of EC films with plasticizer mixtures were sharper than those of EC films with a single plasticizer. This suggests a better compatibility between EC and the plasticizer mixture than that of EC and a single plasticizer.



*Figure 4-12 Tan  $\delta$  of EC/OA-DBS films and EC/OA-MCT films in tensile clamp*

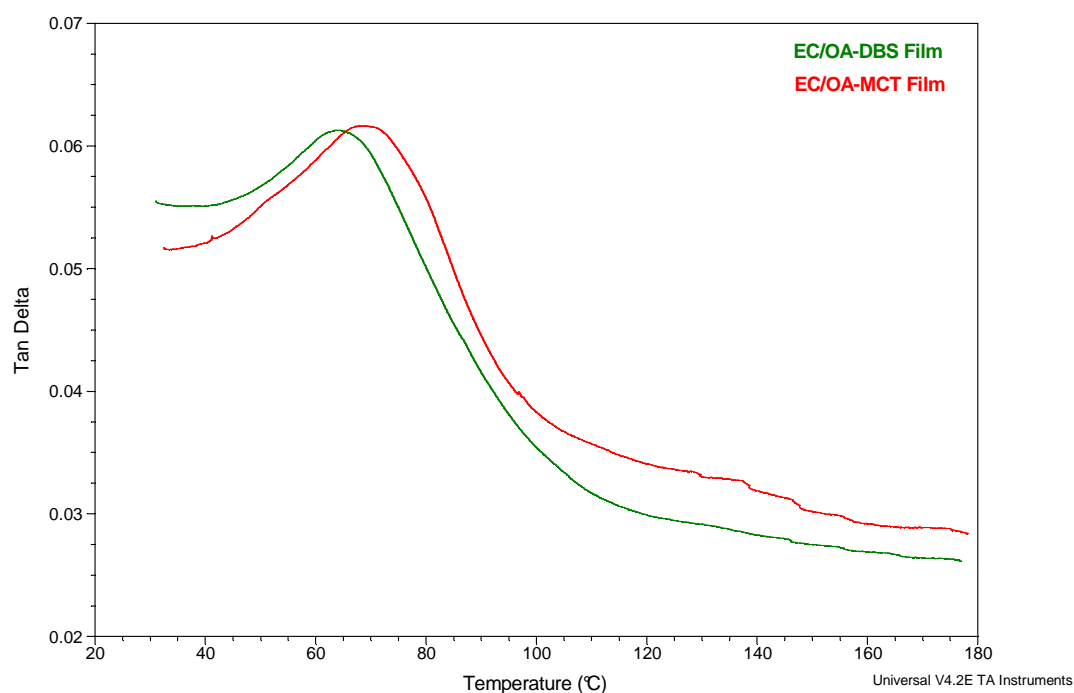


Figure 4-13  $\text{Tan } \delta$  of EC/OA-DBS films and EC/OA-MCT films in single cantilever clamp

#### 4.3.4.2 Mechanical Properties

The storage moduli of the films, determined by DMA (tensile clamp) at 50 mN dynamic force are showed in *Figure 4-14*. They measure the stored the energy, representing the elastic component of the sample behaviour. The storage moduli of all of the films were observed to decrease with increasing in plasticizer levels, regardless of the types of plasticizer. This could be attributed to the increase in the polymer chain mobility and the resulting flexibility of these EC films.

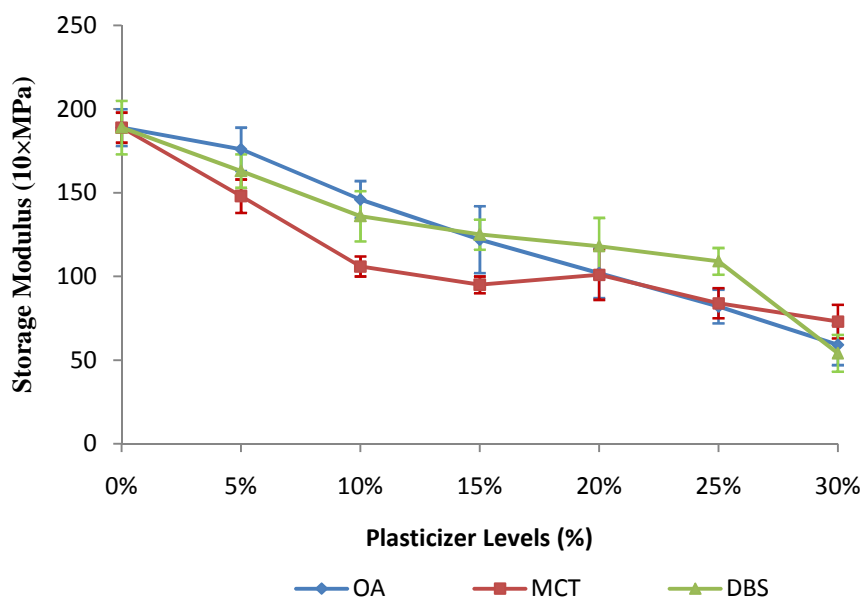


Figure 4-14 Storage moduli, determined at dynamic force of 50 mN and frequency of 1 Hz, of the films from different formulations

#### 4.3.5 AFM Studies

##### 4.3.5.1 AFM – Thermal Analysis

Figure 4-15 shows the topography, adhesion images and localized thermal analysis (LTA) of the pure EC, EC/30%OA, EC/30%DBS, EC/30%MCT, EC/OA-DBS and EC/OA-MCT films. The height range and the adhesion voltage range as well as the scales are presented along with the topography and adhesion images respectively. The numbers on the adhesion images present the locations where LTA was performed and the corresponding LTA data with their numbers were presented. Micro-thermal analysis ( $\mu$ TA) was initially carried out using a wollaston probe on all of the EC/additives films. For EC/30%MCT films alone, a nano-thermal probe was utilized to improve the resolution. The reason for this exception is explained later in this section.

Pure EC films appeared to have a relatively flat surface (174.57 nm height range, as indicated in *Figure 4-15*) with less features, when comparing the topography images, than those of EC/plasticizer films. LTA thermal data of selected areas revealed a constant expansion and had the repeatable downward deflection points at around 140°C. This softening temperature is regarded as the  $T_g$  in this case, which corresponds to the  $T_g$  of EC. As expected, these results implied only one single phase in this film. The topography image of EC/30%OA shows the height range (362.87 nm) was relatively high. More features on the adhesion images of EC/OA films were observed than those of the pure EC films, as seen in *Figure 4-15*; however, this may be due to the topographical features. When LTA was performed on the dark and bright areas on the adhesion image, it was found that the softening curves were rather similar and reproducible. The softening temperatures were observed at about 70°C. The topography and adhesion images of the EC/30%DBS films were similar to the EC/30%OA (*Figure 4-15*). The corresponding topographical features and thermal contrasts on the adhesion images were observed. LTA data showed similar softening temperatures at 70°C when the probe was located on the selected areas.

A wollaston probe was initially used to carry out the  $\mu$ TA experiment on the EC/30%MCT films. During the experimental program, the melting range on the surface would cover both dark and bright areas that resulted in unrepeatable softening profiles. Therefore, the Wollaston probe was replaced by a nano probe.  $5 \times 5 \mu\text{m}$  topography and adhesion images were scanned. Due to the smaller scan area applied for EC/30%MCT films, the peak height of the topography was about 138.38 nm, which was lower than those of EC/30%OA and EC/30%DBS films. When LTA was conducted on the selected dark and bright areas, a very different profile was revealed. The softening temperatures at the dark areas were

---

around 110°C whereas the bright areas started the downward deflection at about 63°C. These softening temperatures could be related to those obtained from MTDSC. This will be discussed in detail later in this Chapter.

The topography and adhesion images of EC/OA-DBS films and EC/OA-MCT films were very similar. Nearly no features or thermal contrasts were observed from the scanned images, which imply that uniform films were obtained. To be more rigorous, LTA was performed on the selected areas on both films. The expansion continued until about 55°C, which could be related to the MTDSC results of EC/OA-DBS films and EC/OA-MCT films. LTA results of EC films with plasticizer mixtures are supporting previous MTDSC and DMA studies. EC and the plasticizer mixtures had better miscibility than that between EC and a single plasticizer at the same level.

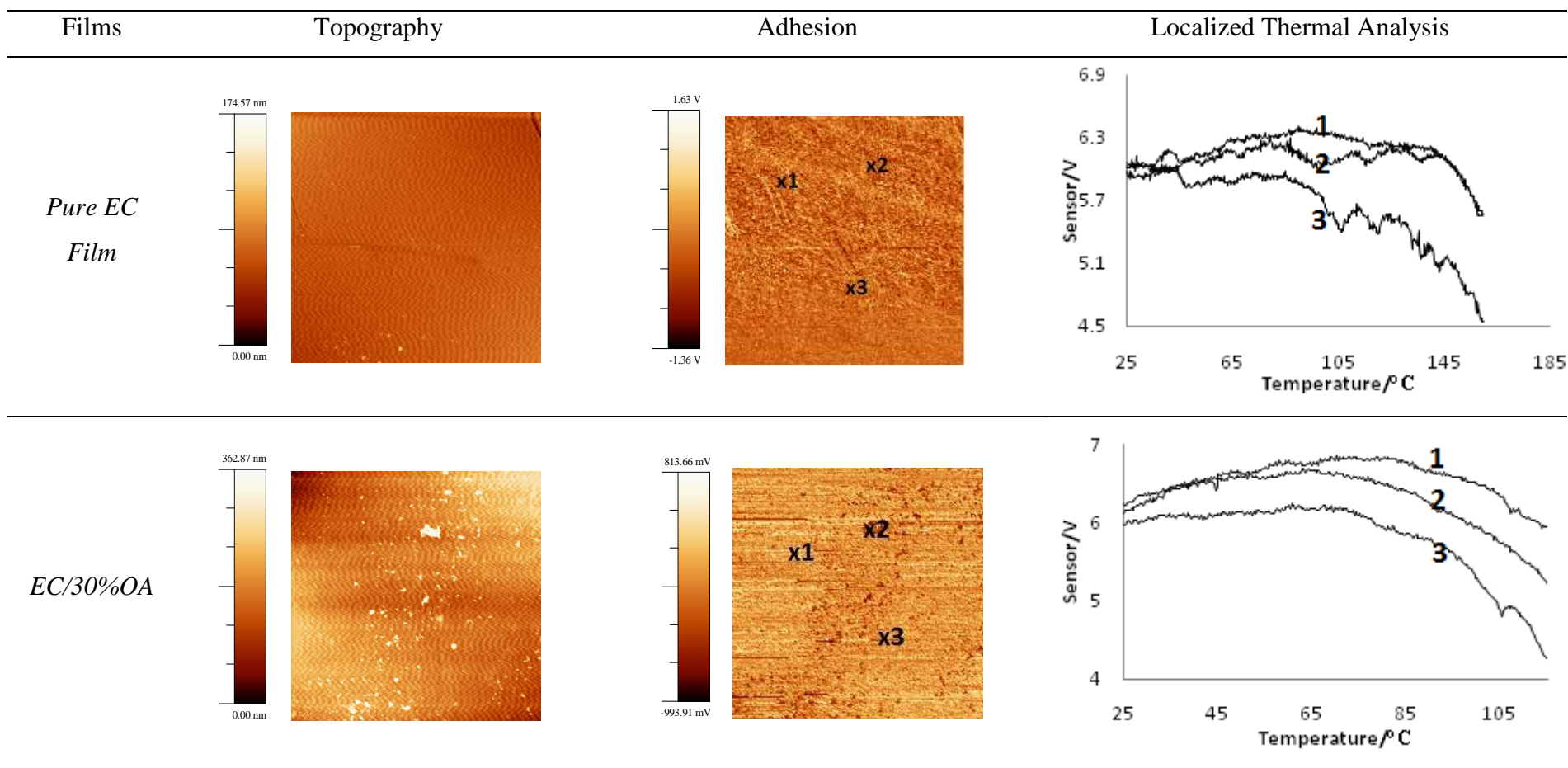


Figure 4-15 Topography, adhesion images and localized thermal analysis of pure EC, EC/30%OA, EC/30%DBS and EC/30%MCT films and their scales.

For adhesion images, × marks the site of thermal analysis for data shown in the LTA figures (to be continued)

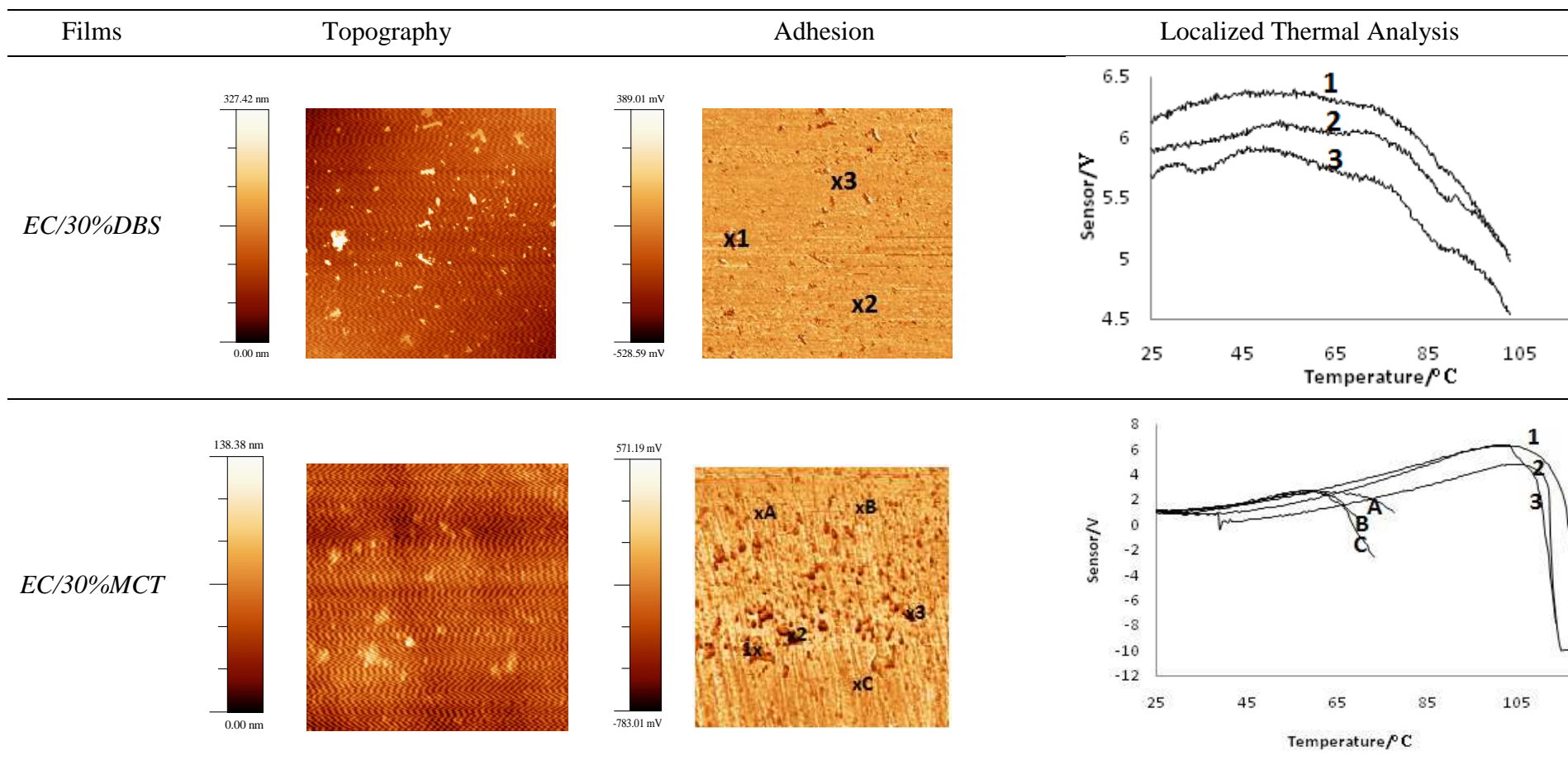


Figure 4-15 Topography, adhesion images and localized thermal analysis of pure EC, EC/30%OA, EC/30%DBS and EC/30%MCT films and their scales.

For adhesion images, × marks the site of thermal analysis for data shown in the LTA figures

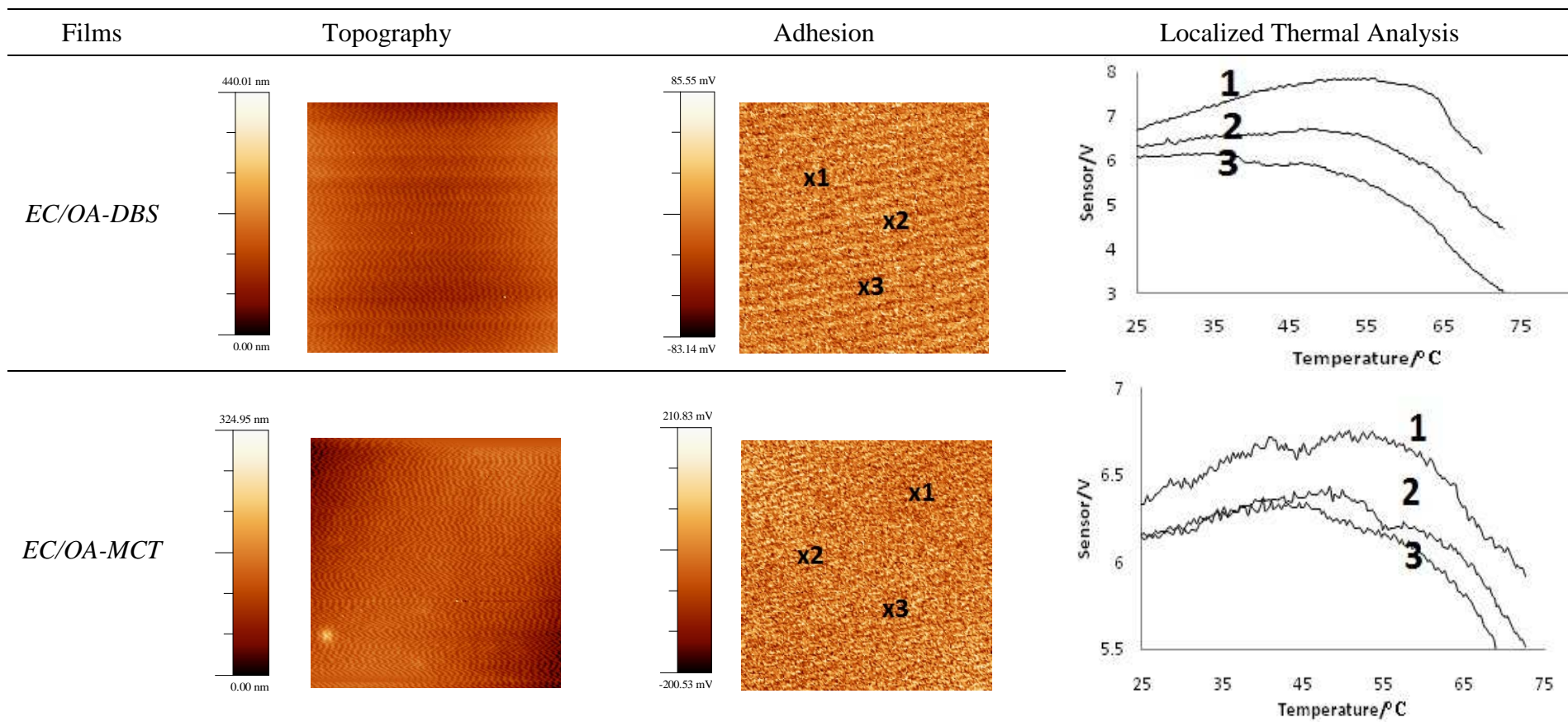


Figure 4-16 Topography, adhesion images and localized thermal analysis of EC/OA-DBS and EC/OA-MCT films and their scales. For adhesion images, × marks the site of thermal analysis for data shown in the LTA figures

---

#### 4.3.5.2 Hot Stage AFM Studies

*Figure 4-17* shows adhesion images and histograms of EC films incorporated with 0%, 5%, 10%, 15%, 20%, 25% and 30% of MCT, scanned at 25°C and 45°C respectively. The images were initially scanned at room temperature and then at several elevated temperatures, i.e. 35°C, 45°C, 65°C, 85°C and 110°C. It was decided that 45°C was the final temperature for the scanned images, because at a relatively high temperature, the samples presented flowing liquid at their surfaces. This could contaminate or even break the probe tip due to the liquid viscosity. Scanned at a rather low temperature, there was not a sufficient contrast to allow satisfactory images. The image histogram (*Figure 4-17*) represents the pixel intensity of the corresponding adhesion images, i.e. in theory the phases on the film surfaces. The pixel intensity may not necessarily reveal the phases of the whole sample, but only the surfaces.

Pure EC films did not show a significant difference between their adhesion images that were scanned at 25°C, 45°C and even at 110°C (data not shown). Similar results were obtained for EC films with a 5%, 10% and 15% of MCT. For EC films with 20% to 30% MCT, enhanced adhesion contrast of the images was observed. Two to three pixel intensity histogram peaks existed for the 25% and 30% MCT films. One can argue that the phase separation observed for EC/MCT films was caused by the temperature rising, rather than the film properties themselves under ambient conditions. However, LTA results obtained for EC/MCT films have suggested phase separation on the film surfaces. This indicates hot stage AFM is a complementary technique to detect the response of different phases to heat.

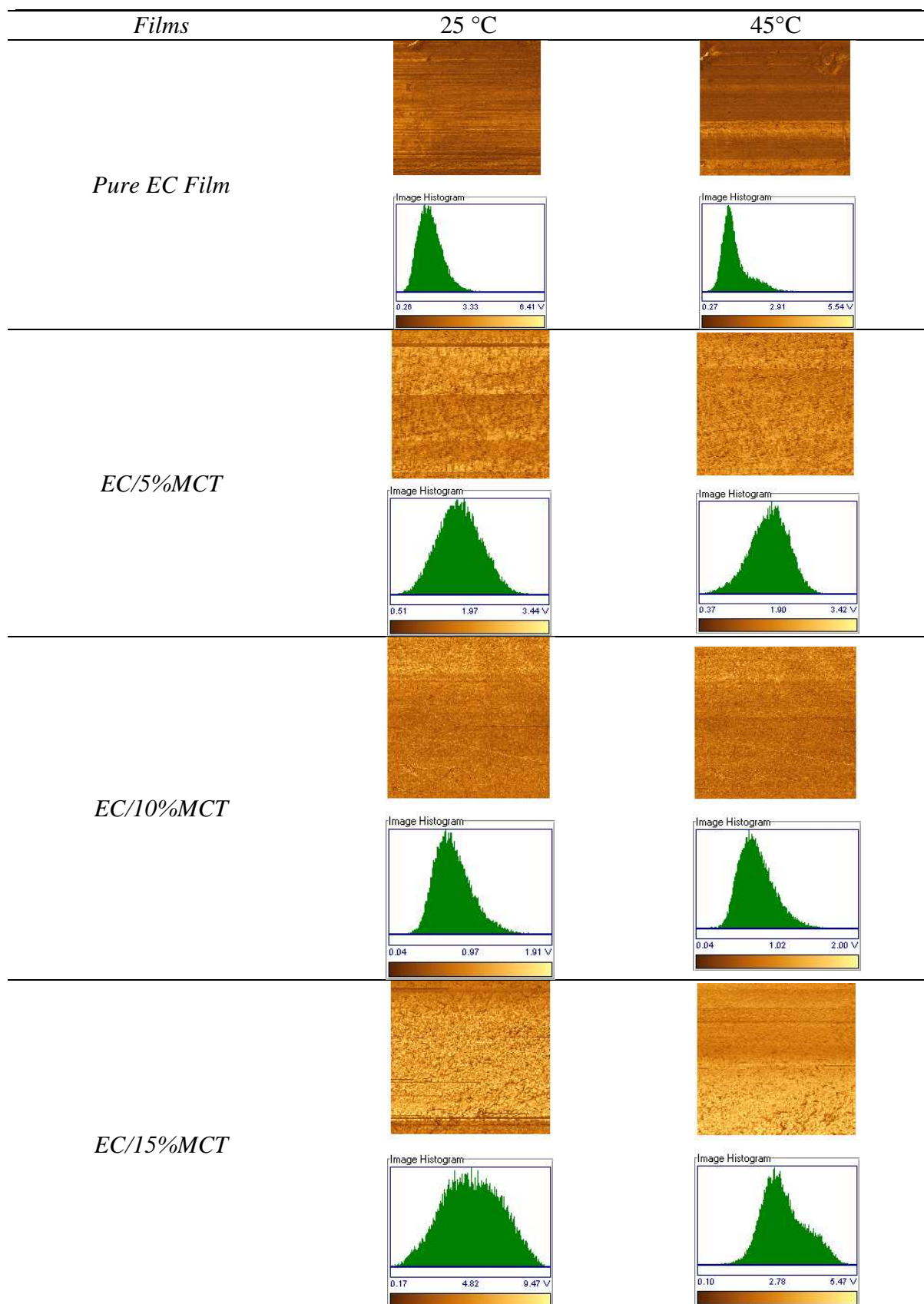
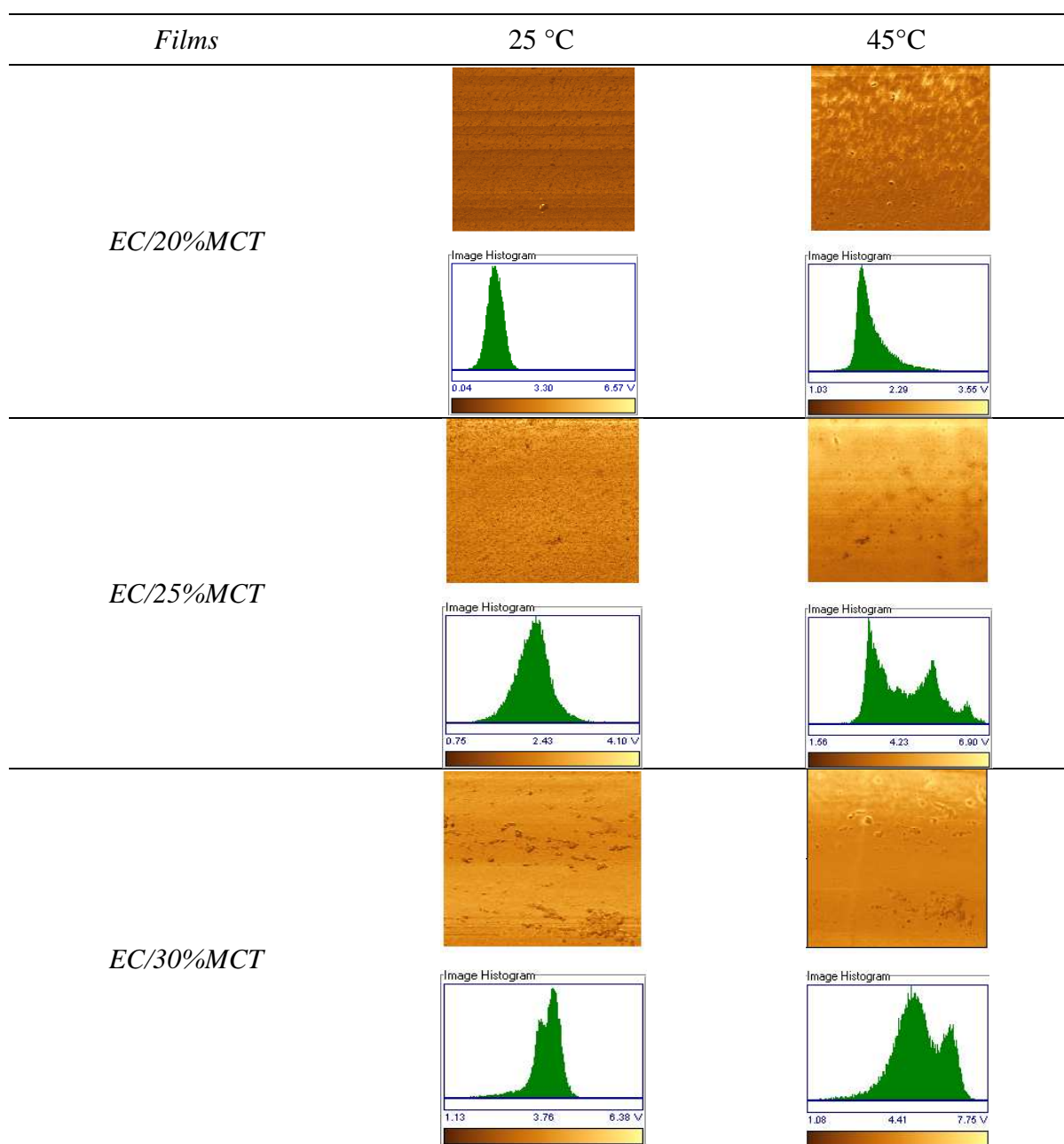


Figure 4-17 Adhesion images and histograms of EC films incorporated with 0%, 5%, 10%, 15%, 20%, 25% and 30% MCT, scanned at 25°C and 45°C, respectively ( to be continued)



*Figure 4-17 Adhesion images and histograms of EC films incorporated with 0%, 5%, 10%, 15%, 20%, 25% and 30% MCT, scanned at 25°C and 45°C, respectively*

## 4.4 Discussion

### 4.4.1 Visual observations

The solvent evaporation rate, that was mainly controlled by temperature and relative humidity (RH), may affect the appearance of the produced films (Lai, 2005). Slow solvent

evaporation will lead to less cloudy films, while fast evaporation rate makes the films cloudier with a crease appearance. Therefore, in this project, wet films on glass plates were placed in a fume cupboard to facilitate the solvent evaporation process. This drying method produced a satisfactory appearance for the EC, EC/OA, EC/DBS and EC/plasticizer mixture films.

Cloudiness was observed when MCT was applied alone as the plasticizer. The humidity of the casting environment and the water present in the solvent system can cause phase separation and polymer precipitation due to moisture condensation, which renders the film opaque (Arwidsson and Johansson, 1991; Lai, 2005). At a critical water concentration, EC precipitated out from the solution, which caused the formation of cloudy domains. From the visual observation of all of the films, MCT seemed to have a greater affinity for water than OA or DBS. Increased levels of MCT would be expected to attract more moisture into the solvent system. Even at the same plasticizer level, EC films with plasticizer mixture of OA and MCT did not show cloudiness whereas films with 20% and beyond MCT alone were cloudy. Therefore, an elevated temperature was needed to dry EC/MCT films, so that clear films will be obtained.

#### 4.4.2 The Study of Residual Solvents and Degradation

Residual solvent is an important issue when producing films. Small amounts of residual solvents could affect the properties of the resulting films, such as the  $T_g$ . The weight loss profiles obtained from TGA experiments can be caused by residual solvents and/or volatile plasticizers. EC/plasticizer films show very low weight loss at 120°C. There was no significant difference in the weight loss between these plasticizers or plasticizer mixtures, because the lipophilic plasticizers are expected to have very low volatility; the weight loss

---

is probably due to the residual solvents. Increased plasticizer concentrations actually decreased the amount of the residual solvents. This is probably because when no plasticizers are added, the solvent molecules would adhere to the polymer molecules to a certain extent. After the plasticizers are incorporated, their molecules would interact with the polymer molecules, rendering fewer molecules available for solvent molecules to interact with. Therefore, less organic solvent would adhere to the EC molecules strongly.

The speed of thermally-induced degradation of EC/MCT films, comparing with it of pure MCT as seen in *Figure 4-5*, increased when the concentrations of MCT were increased. MCT plays an important role in the degradation profile of EC/MCT films, since its degradation is faster. The hydroxyl group with a carbon chain of MCT may significantly decrease the degradation temperature, accelerate carbonization of polymer. The degradation profile of EC/plasticizer mixture films revealed three degradation rates. These results indicated that possibly the two types of plasticizer molecular chains decomposed first, where after the polymer chains were disassembled.

In conclusion, the weight loss of the EC films with lipophilic plasticizers is mainly due to the residual solvents. Increased level of plasticizers inhibited the adhesion of organic solvent molecules to the polymer molecules. Incorporation of plasticizers plays an important role in the degradation profiles of the resulted films. The applied drying method was sufficient for EC/plasticizer films.

#### 4.4.3 Plasticizing Efficiency

Plasticizers work by penetrating into the polymer and increasing the free volume between the polymer chains by reducing their intermolecular forces. The efficiency of a plasticizer

is determined by the compatibility with its paired polymer (Wang et al., 1997). In general, an effective and compatible plasticizer should have similar intermolecular forces as the polymer. Plasticization generally produces a decrease in the  $T_g$  of plasticized polymer films. The extent of decreasing  $T_g$ s ( $\Delta T_g = T_{gEC/plasticizer} - T_{gEC}$ ) is regarded as a good indicator for the plasticizing efficiency. The  $T_g$ s obtained from MTDSC, DMA showed a similar decreasing trend when increasing the concentrations of plasticizers. The  $T_g$  values obtained from DMA were 10 – 15°C higher than those from MTDSC, while the softening temperatures observed from localized thermal analysis were 10 – 20°C higher than those from MTDSC. This is because MTDSC is effectively a static technique whereas  $\tan \delta$  peak of DMA is obtained at a frequency of 1 Hz (Kalichevsky et al., 1992). LTA is not only a thermal technique but also a mechanical approach. At the high scan speed of LTA, the softening of the sample will be observed at an elevated temperature, comparing to those obtained from MTDSC and DMA results.

The Gordon Taylor/Simha Boyer equations are well known to predict glass transition temperatures of polymer blends (Gordon and Taylor, 1952; Simha and Boyer, 1962).

$$T_{gmix} = \frac{w_1 \cdot T_{g1} + K \cdot w_2 \cdot T_{g2}}{w_1 + K \cdot w_2} \quad Eq\ 4-1$$

$$K = \frac{T_{g1} \cdot \rho_1}{T_{g2} \cdot \rho_2} \quad Eq\ 4-2$$

where  $T_g$  is the glass transition temperature,  $w$  is the weight fraction of the components,  $K$  is a constant and  $\rho$  is the true density of the components.

The  $T_g$ s of the liquid plasticizers used in this project, i.e. OA, DBS and MTC could not be characterized using DSC, MTDSC or hyper DSC (data not shown). Therefore, in the Eq 4-1 and 4-2, at 5% plasticizer level,  $w_1 = 0.95$ ,  $w_2 = 0.05$ ,  $T_{g1} = 129.2^\circ\text{C}$  ( $T_g$  of EC),  $\rho_1 = 1.13$  g/mL,  $\rho_{OA} = 0.89$  g/mL,  $\rho_{DBS} = 0.94$  g/mL  $\rho_{MCT} = 0.92$  g/mL and  $T_{gmix}$  can be obtained from the MTDSC results for each plasticizer. The  $T_g$ s of each plasticizer can be estimated by using equations Eq 4-1 and 4-2 as  $T_g$  (OA) =  $-75^\circ\text{C}$ ,  $T_g$  (DBS) =  $-77^\circ\text{C}$  and  $T_g$  (MCT) =  $-50^\circ\text{C}$ . Using the same approach, the theoretical  $T_g$  values for 10% and onwards plasticizer system could be calculated. Therefore, the experimental  $T_g$ s from MTDSC were used to indicate the decreasing in  $T_g$  values, i.e. plasticizing efficiency ( $\Delta T_{gexp}$ ), whereas the calculated values using Gordon Taylor/Simha Boyer equations were compared in Table 4-5.

Plasticizer Levels	OA Films		DBS Films		MCT Films	
	$\Delta T_{gexp}$ ( $^\circ\text{C}$ )	$\Delta T_{gcal}$ ( $^\circ\text{C}$ )	$\Delta T_{gexp}$ ( $^\circ\text{C}$ )	$\Delta T_{gcal}$ ( $^\circ\text{C}$ )	$\Delta T_{gexp}$ ( $^\circ\text{C}$ )	$\Delta T_{gcal}$ ( $^\circ\text{C}$ )
0%	0	–	0	–	0	–
5%	-24.3	–	-23.7	–	-18.7	–
10%	-40.8	-45.4	-40.7	-44.4	-25.4	-35.4
15%	-54.9	-63.7	-55.3	-62.5	-25.3	-50.4
20%	-70.1	-79.9	-64.9	-78.6	-75.2/- 29.4	-63.9
25%	-72.9	-94.2	-69.9	-93.0	-75.4/- 29.9	-76.1
30%	-76.0	-107.0	-75.5	-105.9	-78.2/- 32.0	-87.3

Table 4-5 Comparison of measured ( $\Delta T_{gexp}$ ) and calculated plasticizing efficiencies ( $\Delta T_{gcal}$ ) of EC films with different levels of plasticizers

As can be seen, OA and DBS are more effective plasticizers than MCT. However, the two distinct  $T_g$ s of some EC/MCT films indicated a phase separation, which will be discussed in section 4.4.4. The plasticizing efficiencies of OA and DBS seem rather similar, compared to that of MCT. This is probably due to the similarity of OA and DBS on their molecular structures that are both long hydrocarbon chains, whereas MCT has three carboxyl groups with carbon chains. A positive deviation from ideal behaviour was observed for all of the EC/plasticizer films (decrease of the experimental  $T_g$ s was smaller than the theoretical values). The reasons for the deviations between the theory and practice are probably due to the assumption made for Eq 4-1, i.e. the mixture is an ideally compatible system. Therefore the plasticization process is simply a dilution effect on the polymer matrix through which the free volume is increased. This is not necessarily applicable to the tested system if phase separation occurs. At relatively low plasticizer concentrations, the deviation of the experimental and the theoretical values indicates that the assumption is reasonably valid in this case, i.e. there is good polymer/plasticizer compatibility. However, at high plasticizer concentrations, rather large differences between the experimental and the theoretical values suggest that the assumption is invalid due to poor compatibility. The plasticizers may aggregate into small domains dispersed in the polymer matrix. Consequently, the actual amount of the plasticizer dispersed in a molecular level is less than the nominal. In the case of EC/MCT films, the detected phase separation showed one separated  $T_g$ , this was rather close to the theoretical value. This is strongly supportive to the above explanation.

EC/OA-DBS films and EC/OA-MCT films have the reduced  $T_g$  values of  $-79.2^{\circ}\text{C}$  and  $-77.2^{\circ}\text{C}$ , respectively, whereas the theoretical reduced  $T_g$  values are  $-94^{\circ}\text{C}$  and  $-82^{\circ}\text{C}$ . The overall plasticizer concentration was 24.8%, which is close to the 25% plasticizer level that

was applied for a single plasticizer. The plasticizer mixtures were more efficient in reducing the  $T_g$  values of EC films than the same level of a single plasticizer. This indicates that when two types of plasticizers are applied, the free volume is increased more dramatically than when a single plasticizer is applied at the same level. It has been suggested that the molecular chain of a plasticizer can be encapsulated along its long dimension by the polymeric chains (Mauritz et al., 1990). Therefore, the increase of the free volume can be related to the length of the plasticizer molecules. When two plasticizers with different chemical structures are used, the encapsulation of the plasticizers may not necessarily be in the same direction, i.e. the plasticizer chains may not be parallel to each other. Hence it is possible that an increase in free volume is resulted from the encapsulation along different directions of the plasticizer chains.

#### 4.4.4 Miscibility Studies of EC/plasticizer Films

MTDSC and DMA allow the determination of the  $T_g$ s of the films, which can indicate the interactions and the degree of mixing between EC and the plasticizers applied. The mixture could be considered compatible if only one  $T_g$  is observed. Two  $T_g$ s are expected if phase separation occurs.  $\mu$ TA and nTA were chosen for the atomic force microscopy studies, because they can provide topographical, adhesion and thermal information simultaneously. This is based on the information provided by MTDSC and DMA on the thermal properties of the bulk samples, while LTA enables the characterization of specific regions of interest. Although, it is a semi-quantitative approach, LTA is sufficient to identify different phases on the sample surface. Besides, the topography images were presented and compared along with the adhesion images to prevent misinterpretation of the data. Observed adhesion contrast may be due to the topography features (convex and concave) or the different

---

phases. Hence, by considering the topography of film surfaces, the adhesion contrast due to more than one phase could be observed.

For EC/OA and EC/DBS films, no double  $T_g$ s were observed for all of the concentrations. However, there was a large difference between the theoretical and practical  $T_g$  values when plasticizers with relatively high concentrations were applied, indicating not ideal compatibility. When complete phase separation occurs, the  $T_g$  value should not be composition dependent, which is not the case for EC/OA and EC/DBS films. In other words, EC/OA films and EC/DBS films did not show a complete phase separation when the plasticizer concentration is relatively high.

The situation for EC/MCT films is more complicated than in EC/DBS films.  $T_g$  of EC/MCT films decreased when the concentration was increased from 0% to 10%, which was expected. However, it remained at about 103°C from 10% to 15% according to MTDSC results (109°C from DMA), which implies that another glass transition at a different temperature may occur. At 20% and beyond, the  $T_g$  remained at circa 97°C (MTDSC), 107°C (DMA) and 110°C (LTA), whereas a lower temperature transition was observed at circa 51°C (MTDSC), circa 69°C (DMA) and circa 63°C (LTA). Although, the values obtained from DMA and LTA were 10°C – 20°C higher than those from MTDSC results, there is a fine agreement between these techniques on these two glass transition events. Such phenomenon has been associated with phase separation. Two areas with different adhesion properties were imaged by using pulsed force mode AFM, which could be related to the low  $T_g$  and high  $T_g$  respectively from the LTA results. These two  $T_g$ s do not correspond with either the  $T_g$  of pure EC or that of MCT, therefore, two phases of EC/MCT mixture with different ratios were considered. These values for different levels of

---

MCT were rather similar, implying there might be a further glass transition occurring, possibly pure MCT.

Since the  $T_g$ s of plasticizers was estimated in the previous section 4-4-3, by using Gordon Taylor/Simha Boyer equations, one can estimate the constant  $K$  as  $K_{OA} = 2.57$ ,  $K_{DBS} = 2.47$  and  $K_{MCT} = 2.2$ . Similarly, at 20% MCT level and beyond, by using the values obtained from MTDSC as the  $T_{g_{mix}}$  of these two phases, the weight fraction of MCT in the high  $T_g$  phase can be estimated as approximately 8%, whereas about 24% in the low  $T_g$  phase. It is interesting to note that between 20% and 30% FCO the  $T_g$  values do not change, implying a further phase separation, possibly of pure MCT.

No more than one glass transition was observed for EC/OA-DBS films or EC/OA-MCT films from MTDSC or DMA (tensile clamp and single cantilever clamp). Results from the two types of clamps of DMA used on these samples further proved the great reproducibility of the technique. In terms of the  $T_g$ s, MTDSC and DMA results are in great agreement with each other. The topographical and adhesion images of EC/plasticizer mixture films showed more flat surfaces with less features than the EC/plasticizer films with the equivalent concentrations. It shows a great miscibility between the plasticizer mixtures and their polymers in terms of these techniques.

The plasticizer mixtures seem to have better compatibility with EC when they are on the same plasticizer level. Based on the free volume theory of the glass transition, the actual volume of a polymer can be expressed as a sum of the volume occupied ( $V_{occ}$ ) by the molecules and the free volume between the molecules ( $V_f$ ), which is used for molecules to undergo rotation and translational motion.

---

$$V(T) = V_{occ}(T) + V_f(T) \quad Eq\ 4-3$$

When plasticizers are introduced into polymer systems, they increase the occupied volume, but more dramatically increase the free volume, hence a lower of the  $T_g$ . However, different types of plasticizers may interact with different structural groups of EC. Therefore, at the same plasticizer level, the molecules of one type of plasticizer will compete with each other, whereas the molecules of two types of plasticizers will bond with different structural groups of EC or even bond with each other as well, rendering a much better compatibility and stability.

In summary, OA and DBS showed finer miscibility than MCT as a plasticizer for EC films. High concentration of MCT could lead to phase separation of EC films. Plasticizer mixtures of OA-DBS and OA-MCT provided better plasticizing efficiency with less risk of phase separation.

#### 4.4.5 Mechanical Properties

Generally, film coating systems suitable for tablets or pellets coating require certain mechanical strength and flexibility of the films. Otherwise, splitting or cracking may occur, which is not only unattractive but, more importantly, results in the protective advantages of the film coating being lost. These issues may be due to the stress that builds up within the film coating upon during drying, which exceed the mechanical strength of the coating (Gibson et al., 1988). This stress arises because when the sample is dried either under room conditions or in the oven, the wet films must shrink as the solvents evaporate. When the coated pellets are dried in an elevated temperature (in most cases), a thermal stress occurs as the coated pellets cool due to the higher thermal expansion of the polymeric films

---

compared with that of the pellet substrate. The mechanical properties of the film coatings determine their response to these stresses and hence its resistance to rupture. It has been demonstrated that when larger amounts of plasticizer are employed, tougher films (higher energy to break) are produced (Hutchings et al., 1994). Plasticizer, acting as a solvent for the polymer, can change the viscoelastic behaviour of polymer significantly. Essentially, a plasticizer transforms hard, brittle polymer into a soft, rubbery material. It provides greater resistance to the polymers when mechanical stresses are applied.

Storage modulus, representing the elastic portion of the sample, is a characteristic of the sample stiffness, i.e. higher storage modulus values are related to films having greater stiffness whereas lower modulus values are associated with softer films. As the plasticizer content increases in the polymer, the stiffness of the polymer will decrease as the polymer becomes simply a solute in the polymer-plasticizer solution. The decreasing trends of films when OA and DBS were employed are rather similar. This is probably due to the similarity of their chemical structures.

A critical plasticizer concentration, at which the tensile strength, and the modulus or elongation reach the original values of the unplasticized polymer has to surpass to yield the desired plasticization effect. Both the Young's modulus and tensile strength were not influenced by the hydrophilic or hydrophobic nature of the plasticizers. Plasticization of the polymer encourages stress relaxation because the plasticizer increases the free volume of the polymer, making it less rigid and more able to adapt to the applied stress.

---

## 4.5 Conclusion

This chapter indicates that a multi-disciplinary approach is necessary when characterizing the distribution of lipophilic plasticizers within the EC films and their interaction. While quantitative information on the polymeric systems can be provided by TGA and DSC, which however, only analyze the bulk sample. DMA gives not only thermal information, but also the mechanical properties of the bulk sample. Complementarily,  $\mu$ TA and nTA, as the semi-quantitative techniques, offer topographical as well as thermal properties of the film surfaces. Alternatively, HS-AFM allows assessing the effect of the temperature on the adhesion images of the surfaces of these films, which could be a temperature dependent interpretation of the data. All of these techniques indicate that

- (a) OA is miscible with EC and form a homogeneous film. It is an effective plasticizer and, therefore, be able to reduce the  $T_g$  of EC films.  $T_{gOA}$  was estimated as  $-75^\circ\text{C}$ ;
- (b) DBS is also an effective and miscible plasticizer for EC films. No phase separation was observed for up to 30% plasticizer level.  $T_{gDBS}$  was estimated as  $-77^\circ\text{C}$ ;
- (c)  $T_{gMCT}$  was estimated as  $-50^\circ\text{C}$ . Concentration-dependent phase separation occurs between EC and MCT. Two phases with corresponding  $T_g$ s were successfully imaged by using localized thermal analysis. We suggest that the separation may be detected and imaged using thermal and microscopic methods and that the composition profile may be more complex than a simple binary separation process.
- (d) Plasticizer mixtures seem to have more desirable miscibility with EC than a single plasticizer with equivalent concentrations.

The investigation of the miscibility and interactions between the polymer and the lipophilic plasticizers are extremely crucial in understanding their transport mechanisms when used

---

in the pharmaceutical dosage forms. The distribution of these components could affect the drug release mechanism, especially when these films are exposed to the drug release medium, in which case, the distribution of the additives may change.

## **CHAPTER 5 THE EFFECTS OF PORE FORMER INCLUSION ON ETHYL CELLULOSE FILMS**

### **5.1 Introduction**

The previous chapter focused on the thermal, thermo-mechanical properties and imaging studies of ethyl cellulose (EC) films with various added plasticizers. This chapter discusses EC films incorporating a pore former, hydroxypropyl methylcellulose (HPMC). A pore former is another important component that can be added into the EC films in order to adjust the drug release profiles of the coated controlled release formulations (Frohoff-Hülsmann et al., 1999b). The definition of a pore former is, as the name suggests, additives that generate pores on the film coats when in contact with the drug release media. Therefore, pore formers are generally water-soluble polymers. Even though some water-soluble plasticizers may perform similar functions during drug release, the effects of plasticizers and pore formers on the mechanical properties are significantly different (Heinämäki et al., 1994). This is because plasticizers (small molecules) increase the free volume of the polymer chain, hence lowering the stiffness and improving the flexibility of the films, whereas the HPMC is generally not compatible with the film forming polymers, hence it is difficult to evaluate its impact on the mechanical properties of the films.

The addition of HPMC to EC films can improve the water permeability of the resulting films, since HPMC will dissolve and dilute out from the EC films after contracting with release media. The water permeability of the polymeric membranes is of fundamental importance to the drug release profiles. However, attention must be paid to the effect of the concentration of the pore former, because the initially semipermeable EC/HPMC films

become also permeable for the drug at high HPMC content (Siepmann et al., 2006). Therefore, the interaction between the polymer blends at a molecular level becomes important (Siepmann et al., 2008), because this may affect the morphology and phase distribution of the polymers, hence affecting the drug release profiles. Polymer blends in general are immiscible, since the entropy of mixing is small and does not compensate for unfavourable endothermic heat of mixing (Siepmann et al., 2008). The significance of the phase morphology of polymer blends in controlling the drug release has been addressed in the literature (Menjoge and Kulkarni, 2007). HPMC has been reported to have no interactions with EC in the films (Lai, 2005). However, there is not much imaging evidence of the distribution of HPMC within the EC films and the relationship between that and the concentrations of HPMC added. Therefore, the thermal, thermo-mechanical properties of EC films with various levels of HPMC and their resulting phase distribution must be thoroughly understood.

In this chapter, the imaging and thermo-mechanical properties of EC/HPMC films are investigated, aiming to study the polymer-polymer interactions and the polymer distribution in the prepared free films. The weight loss profiles of EC films incorporated with different levels of HPMC and HPMC itself are compared by means of TGA. MTDSC and DMA are compared in terms of the characterization of the glass transition events of all films. Imaging and polymer distribution of these films are examined by using pulsed force AFM and LTA techniques.

## 5.2 Methodology

### 5.2.1 Preparation of EC/Pore Former Films

Pure EC and EC/HPMC films were prepared by the solvent solution casting method, which was introduced in *Chapter 2*. The formula of EC/HPMC films is seen in *Table 5-1*. After EC and HPMC were fully dissolved, the solutions were then cast onto a glass plate. The wet film thickness was controlled at 2000 $\mu\text{m}$  to achieve a dry film thickness of 150 $\pm$ 10 $\mu\text{m}$ . EC/HPMC films were dried in the oven at 45 $^{\circ}\text{C}$  for 3 hours. All the dry films were stored under ambient conditions for 24 hours to equilibrate before testing.

	EC (g)	HPMC (g)	Solvent System
EC/10%HPMC	1.8	0.2	20 mL ethanol/water (90:10)
EC/20%HPMC	1.6	0.4	20 mL ethanol/water (90:10)
EC/30%HPMC	1.4	0.6	20 mL ethanol/water (90:10)

*Table 5-1 Film formula of EC/HPMC films*

### 5.2.2 TGA Studies

For the raw materials of the pore former, TGA was used to detect the water content and also the degradation profile. HPMC powders were used as received. All the samples were heated from room temperature to 350 $^{\circ}\text{C}$  at 10 $^{\circ}\text{C}/\text{min}$ . For the EC/HPMC films, TGA was applied to determine the amount of residual solvents in the dry films. These samples were heated from room temperature, ramping 10 $^{\circ}\text{C}/\text{min}$  to 150 $^{\circ}\text{C}$ . 5 – 10mg samples were placed in the sample pans. Dry nitrogen was used as purge gas while compressed air was used as the cooling system.

---

### 5.2.3 DSC Studies

For the HPMC raw materials, MTDSC was performed by heating the samples from 25°C to 120°C, cooling to 25°C and then reheating the samples to 220°C with  $\pm 0.5^\circ\text{C}$  modulation amplitude every 40 seconds at a rate of  $2^\circ\text{C}/\text{min}$ . For the EC/HPMC films, MTDSC was conducted by running the samples from 25°C to 200°C with a modulation amplitude of  $\pm 0.5/40$  s at  $2^\circ\text{C}/\text{min}$ . The sample mass was 1 – 2 mg. Crimped pans were used.

### 5.2.4 DMA Studies

DMA tension film mode (tensile clamp) was used to investigate the storage modulus, loss modulus and  $\tan \delta$  values of samples during the program used. Approximately  $30 \times 5.27$  mm square pieces of samples were mounted onto the tensile clamp and then heated from 30°C to 180°C at a rate of  $3^\circ\text{C}/\text{min}$  under frequency of 1 Hz and amplitude of 20  $\mu\text{m}$ . Dry filtered air was used as the purge gas and the cooling system. The storage modulus, loss modulus and  $\tan \delta$  of samples during the program were recorded to analyze the mechanical properties and the peak temperatures of  $\tan \delta$  were taken as the glass transition temperatures of the films.

### 5.2.5 AFM Thermal Studies

Different locations of the dry film surfaces ( $10 \times 10$  mm) were initially scanned to obtain topography and adhesion images simultaneously by using the pulsed force mode AFM. The frequency and amplitude for modulation were 500 Hz and 50 nm respectively. The scan area was  $5 \mu\text{m}^2$  and the scan speed was  $5 \mu\text{m}/\text{s}$  with a resolution of 200 lines.

---

Nano-thermal analysis was applied to the areas of interest. Thermal analysis data was obtained at 5°C/s between room temperature and 150°C. Probe cantilever deflection was plotted against probe tip temperature to obtain the  $T_g$ s of specific areas on the film surface. The topography and adhesion images obtained of the samples were flattened and equalized by using a software named WSxM 5.0 (Horcas et al., 2007).

Heated tip AFM was also carried out on the prepared films by applying a heated (at 150°C) nano-thermal probe and scanning across the films surfaces under the pulsed force mode. However, no significant of enhancement of the phase separation was observed, therefore, the data is not shown in this chapter.

## 5.3 Results

### 5.3.1 Visual Observations

The prepared solutions of EC/HPMC films appeared to be relatively transparent, but slightly more opaque than pure EC solutions. These films were dried in the oven at 45°C for 3 hours in order to allow the complete evaporation of solvents. The visual observations of these dry films are shown in *Figure 5-1*, and they are relatively clear, irrespective of the concentrations of HPMC. All the films seem to have good mechanical strength, but very brittle and easy to break. This is probably due to the absence of plasticizers. EC films with 10% and 20% HPMC were relatively flat, whereas those with 30% HPMC were slightly creased. It can be assumed that high temperature promotes fast solvent evaporation rate and therefore give rise to wrinkled film. However, these films were dried under the same conditions. Therefore, it is reasonable to conclude that the solvent residue of these films, which can be related to the HPMC concentrations, may have an impact on the film appearance. This suggestion is supported by the TGA results.



*Figure 5-1 Visual observation of EC/HPMC films*

### 5.3.2 TGA Studies

TGA studies were initially carried out to investigate the weight loss profiles of the pure HPMC powder. The weight loss and derivative weight loss signals of pure HPMC powder are shown in *Figure 5-2*. More than 2% weight loss was observed at 150°C, which is higher than that of pure EC powder. This indicates that HPMC absorbed more moisture than pure EC. HPMC exhibited a degradation onset at about 180°C, showing a degradation peak at approximately 337°C. By the end of the experiment at 350°C, 80% weight loss was obtained.

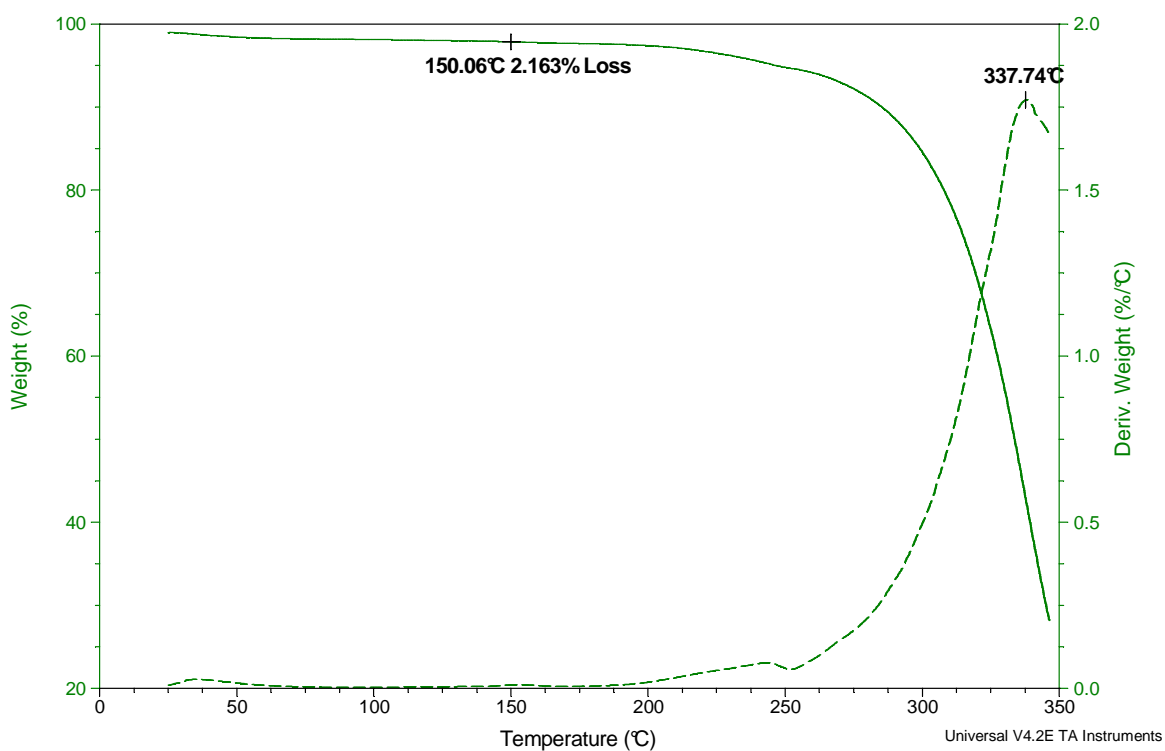


Figure 5-2 TGA scans of HPMC powder (weight loss and derivative weight loss signals)

Weight loss signals of EC films, EC/10%HPMC films, EC/20%HPMC films, EC/30%HPMC film and pure HPMC are compared in Figure 5-3. The total weight loss at 120°C was increased with increasing the concentration of HPMC (Table 5-2). The weight loss of the EC/HPMC films was proportional to the concentration of HPMC presented in the films. Pure HPMC had the greatest moisture content compared to the other samples.

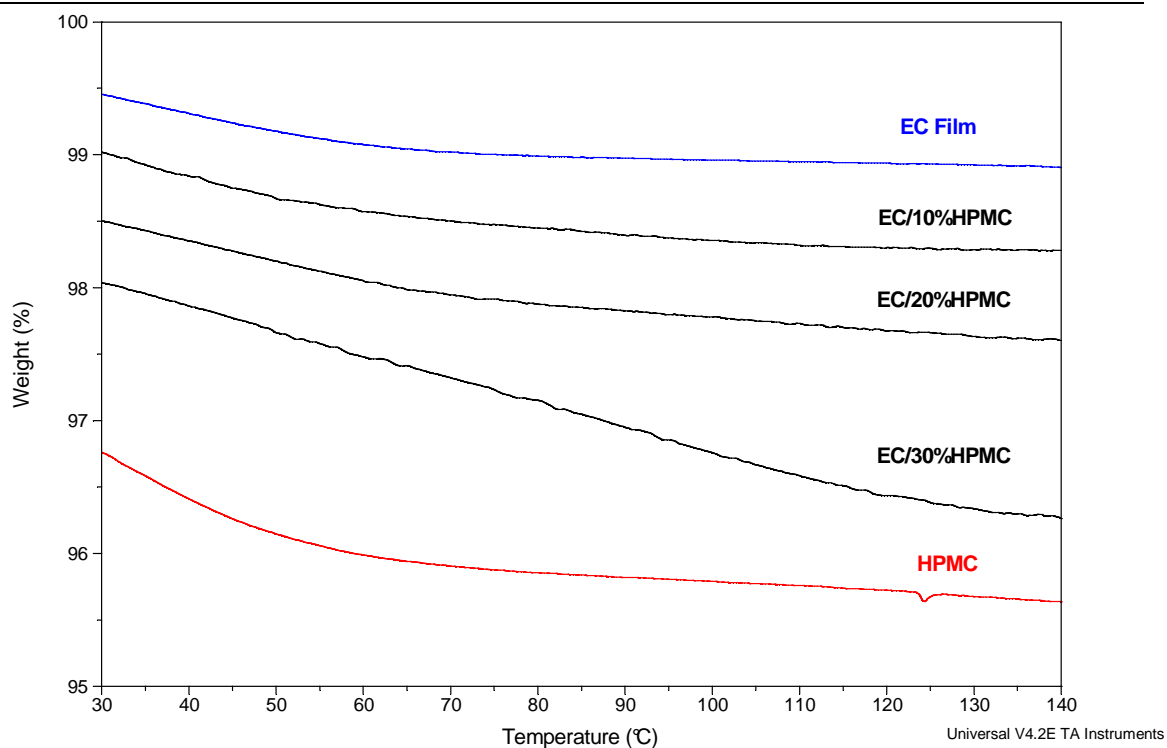


Figure 5-3 Comparison of the weight loss signals of EC film, EC/HPMC films and pure HPMC powder

Residual Solvents	EC Films (%)
EC film	$0.6 \pm 0.1$
EC/10%HPMC	$0.6 \pm 0.1$
EC/20%HPMC	$0.9 \pm 0.1$
EC/30%HPMC	$1.4 \pm 0.4$
HPMC	$1.6 \pm 0.2$

Table 5-2 Amounts of residual solvents of EC films incorporated with 0%, 10%, 20% and 30% HPMC and pure HPMC, data analyzed from TGA results at 120°C (n=3)

---

### 5.3.3 DSC Studies

The  $T_g$  of HPMC film is relatively weak and difficult to be detected by using MTDSC (Lai, 2005), even in the reversing signals. *Figure 5-4* shows the reversing heat flow signals of EC films added with 0%, 10%, 20% and 30% HPMC and HPMC powder in the standard aluminium pans. *Table 5-3* shows the comparison of the  $T_g$  values of EC/HPMC films, analyzed from the reversing heat flow signals of the MTDSC experiments. When increasing the levels of HPMC, the  $T_g$ s of EC films remained constant at circa 130°C, and the differences were as small as 1-2°C. It was concluded that this temperature corresponds with the  $T_g$  of EC 20 itself (Lai, 2005), whereas HPMC had a  $T_g$  at circa 150°C, indicating HPMC might not interact with EC dramatically in terms of the glass transition. Therefore, two  $T_g$  values of EC and HPMC respectively are expected from the MTDSC results. However, the heat flow change of HPMC might be too small to be revealed from the heat flow signals of EC/HPMC films. The melting of microcrystallites and oxidative decomposition events of EC film around 180°C became less significant and negligible when HPMC was introduced into the film systems.

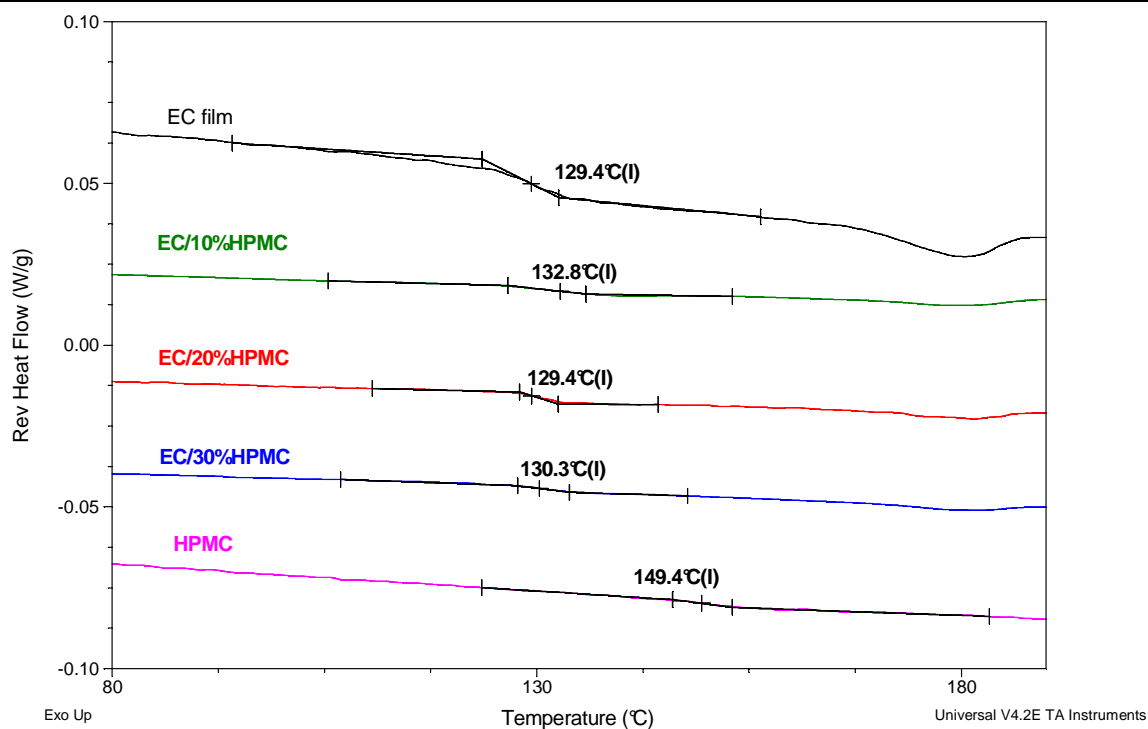


Figure 5-4 Comparison of the glass transitions of EC film, EC/HPMC films and pure HPMC powder by using the reversing heat flow signals

HPMC Concentration	$T_g$ (°C)
0%	$129.2 \pm 0.1$
10%	$131.7 \pm 0.9$
20%	$129.6 \pm 0.9$
30%	$130.7 \pm 1.2$
HPMC	$149.4 \pm 0.4$

Table 5-3 Glass transition temperatures of EC films with 0%, 10%, 20%, 30% HPMC and pure HPMC, obtained from the reversing heat flow signals of MTDSC ( $n=3$ )

## 5.3.4 Thermo-mechanical Properties

Typical examples of the thermo-mechanical behaviour of EC films added 0%, 10%, 20% and 30% HPMC are shown in *Figure 5-5* (Loss modulus against temperature) and *Figure 5-6* ( $\tan \delta$  against temperature), while the  $T_g$ s analyzed from the peaks of loss modulus and  $\tan \delta$  and storage modulus under room temperature of all the systems are listed in *Table 5-4*.

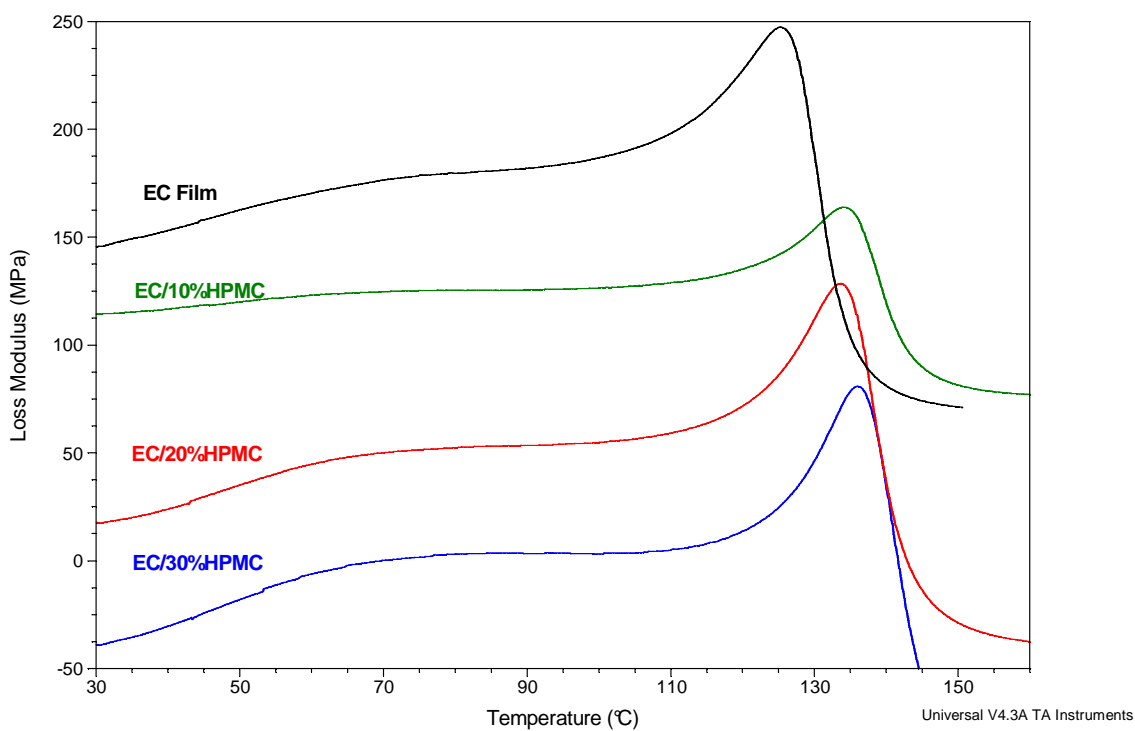


*Figure 5-5* DMA scans of EC films with different concentrations of HPMC using the tensile clamp at 3°C/min

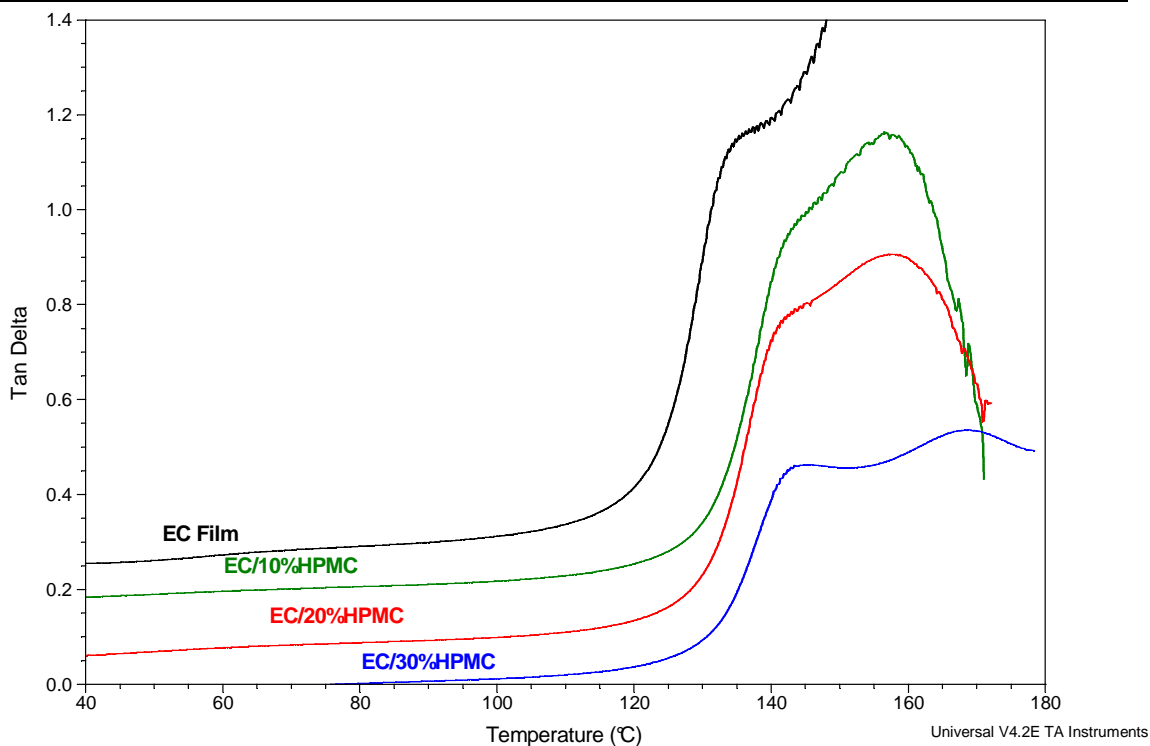


Figure 5-6  $Tan \delta$  of EC films with 0%, 10%, 20% and 30% HPMC

HPMC Concentration	$T_{peak}$ (°C, Loss Modulus)	$T_{peak}$ (°C, $tan \delta$ )		Storage Modulus (MPa)
0%	$125.8 \pm 0.7$	$133.6 \pm 0.3$		$982 \pm 269$
10%	$134.1 \pm 0.7$	$141.9 \pm 0.8$	$157.7 \pm 1.1$	$1178 \pm 312$
20%	$134.5 \pm 0.8$	$141.5 \pm 0.9$	$158.9 \pm 1.7$	$1948 \pm 193$
30%	$135.8 \pm 0.2$	$142.1 \pm 0.3$	$166.2 \pm 1.0$	$2050 \pm 478$

Table 5-4 Peak temperatures of loss modulus and  $tan \delta$  of EC films with 0%, 10%, 20% and 30% HPMC, obtained from DMA ( $n=3$ )

Generally, the onset temperature of storage modulus, the peak of loss modulus or the peak of  $tan \delta$  can be utilized to analyze the  $T_g$  of samples. However, for the EC/HPMC films,

one single peak was observed for each film from the loss modulus profile, but two slightly overlapping peaks from the  $\tan \delta$  plots. Therefore, both peak temperatures were analyzed for comparison and they are presented in *Table 5-4*. In previous chapters, peak temperatures of  $\tan \delta$  from DMA results were analyzed as the glass transition temperatures.  $\tan \delta$  may be a better indication of the glass transition than the loss modulus in this case, especially when it had a disagreement with the loss modulus. This is probably because the loss modulus represents the dissipated energy of the films. The difference between the glass transition temperatures of EC and HPMC is about 20°C. In other words, the softening of HPMC may follow that of the EC. The peak of  $\tan \delta$  could be more sensible than that of the loss modulus since it is the temperature that the frequency of the forced vibration coincides with the frequency of the diffusional motion of the polymer chain. Therefore, the  $\tan \delta$  data here would be selected in this chapter.

At 10%, 20% and 30% HPMC compositions, two transitions were recorded corresponding to the glass transition of the two polymers (circa 140°C for EC and circa 160°C for HPMC). These results are in agreement with a previous study (Sakellariou et al., 1986b), in which two glass transitions for EC and HPMC respectively were observed. Therefore, it is fair to conclude that an obvious phase separation occurred in the EC/HPMC films. The  $\tan \delta$  peaks of both transitions were overlapping, indicating an incomplete separation of the transitions of the components. It is interesting to note that the  $T_g$  value of the EC phase is higher than that of the pure EC film, and the  $T_g$  value of the HPMC phase is increasing slightly with increasing the weight fractions of HPMC. These phenomena may be a result of the increase in the film stiffness with increasing the HPMC levels as indicated by the storage moduli in *Table 5-4*, since DMA is not only a thermal but a mechanical technique. The  $T_g$  values obtained from the  $\tan \delta$  peaks were under specific mechanical stress applied

---

to the film samples. Another possibility is that a small amount of HPMC formed a phase with EC, resulting a slightly higher  $T_g$  values of EC phase. However, this cannot be concluded at this stage.

The storage modulus of EC/HPMC films was recorded as well. As introduced in previous sections, the storage modulus is the ratio of stress to strain under vibrating conditions (frequency of 1 Hz), which represents the in-phase (elastic) component of the oscillatory flow. In other words, storage modulus (tensile) is a measure of the stiffness of the samples. As seen in *Table 5-4*, the standard deviations of storage modulus were rather significant, which can be caused by the operator or instrument error. However, an increasing trend of storage modulus was observed when increasing the concentrations of HPMC. These results indicate that the addition of HPMC can enhance the stiffness of the resultant films. This is possibly due to the inherent property of HPMC since pure unplasticized HPMC films are regarded as brittle and hard (Heinämäki et al., 1994).

### 5.3.5 Localized Thermal Analysis (LTA)

Pulsed force AFM has been introduced and applied to assess the film samples in previous chapters. It was therefore applied again to investigate the phase distribution on the film surface and to further confirm the limited incompatibility of EC and HPMC, based on the phase separation between EC and HPMC within the films demonstrated from the MTDSC and DMA results. *Figure 5-7* shows the topography, adhesion and LTA nano data of located specific areas of EC/HPMC films. The numbers of the nano-thermal plots correspond to the numbers that highlighted in the adhesion images of EC/HPMC films.

The pure HPMC film presents a fairly flat surface with almost no features on the film surface. For the EC/HPMC films, with increasing the HPMC level, more features appeared on the surfaces. The adhesion images of those showed corresponding features in most cases. Care needs to be taken when interpreting this data, because of the colour differences, which represent different adhesion properties. Hence different phases on the adhesion images may be caused by the height differences on the topography images, rather than the separated phases. As seen in *Figure 5-7*, HPMC films provided repeatable nano-thermal downward deflections at approximately 170°C when the probe was located on selected areas. This temperature reasonably represents the  $T_g$  of HPMC. At 10% w/w HPMC level, it is difficult to differentiate EC or HPMC phases on the adhesion image, however, the nano thermal data is telling a different story. Some selected areas (1 and 2) provided softening temperatures at about 150°C while the other area (3) exhibited a  $T_g$  which was approximately 20°C higher than the lower one, and most selected areas (4-8) had both. For higher levels of HPMC (20% and 30%), the adhesion images revealed more features than that for the 10% w/w HPMC level. Reproducible separated glass transitions were observed for both levels of HPMC. The lower  $T_g$ , around 150°C, corresponds to the  $T_g$  of EC, while the higher one, around 170°C, corresponds to the  $T_g$  of HPMC. These temperatures are about 20°C higher than those observed from the MTDSC results. This is because LTA-AFM scanning is a mechanical method with a rapid heating rate, which was explained in detail in *Chapter 4*. This interesting phenomenon indicates the scale of the distribution of these two polymers is dependent on the level of HPMC. At a low HPMC level, the scale of the phase separation is smaller than the probe tip resolution.

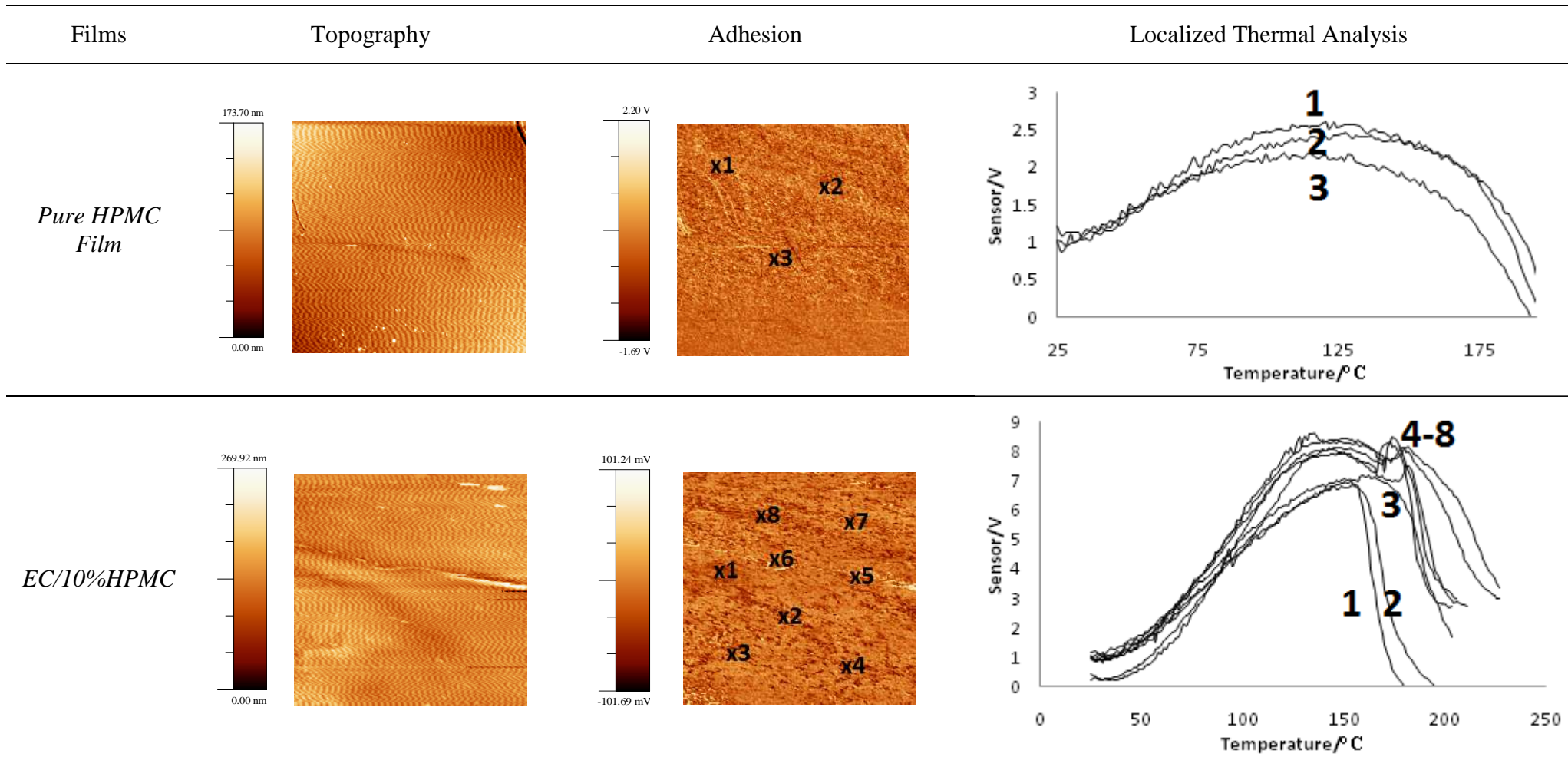


Figure 5-7 Topography, adhesion images and LTA nanothermal data of EC/HPMC films (5 $\mu\text{m}$  $\times$ 5 $\mu\text{m}$ , to be continued)

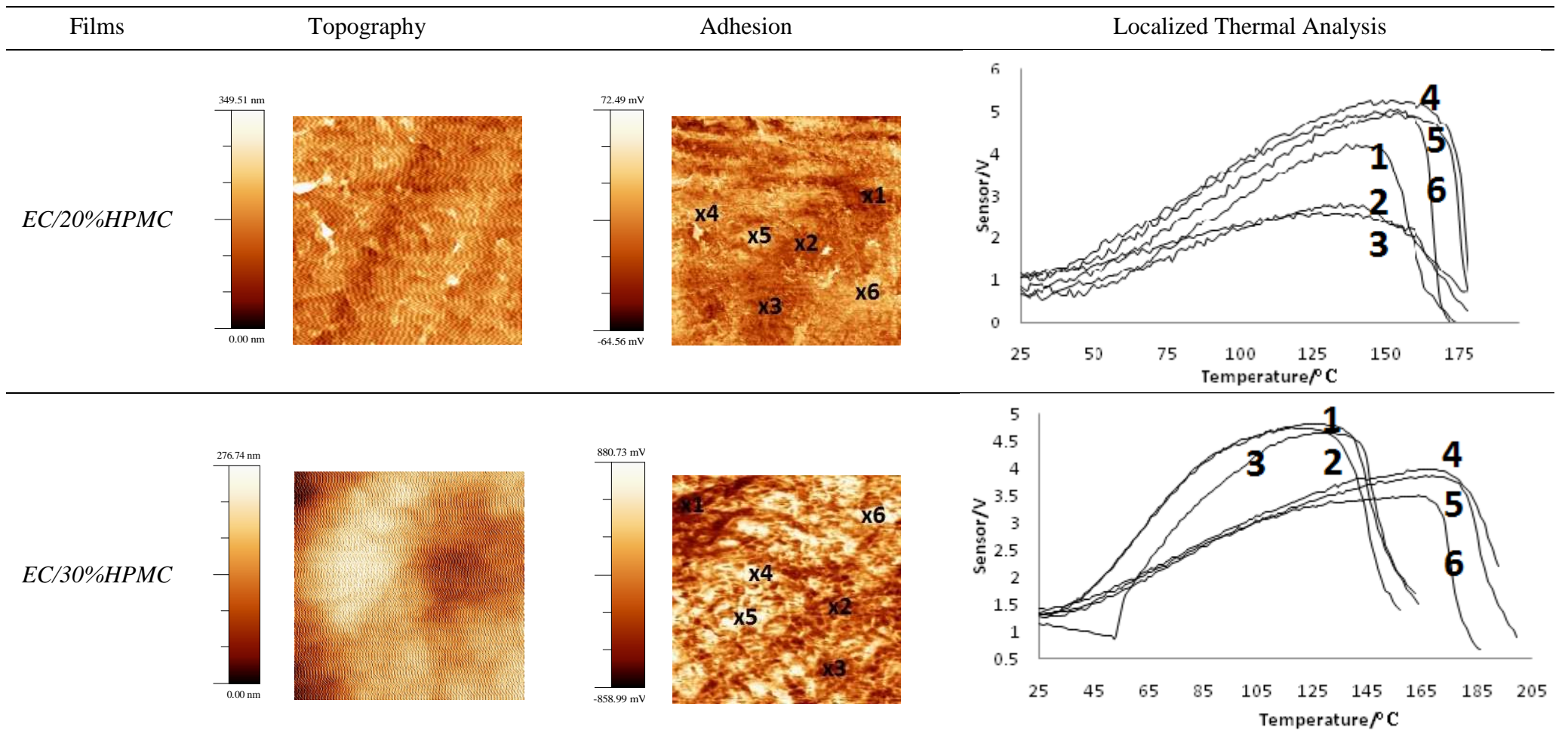


Figure 5-7 Topography, adhesion images and LTA nano-thermal data of EC/HPMC films ( $5\mu\text{m}\times 5\mu\text{m}$ )

---

## 5.4 Discussion

### 5.4.1 The Study of Residual Solvents

Residual solvent is one of the major concerns when producing the films, since even small amount of residual solvents can have a great impact on the thermal properties of the prepared films, such as  $T_g$  (Masilungan and Lordi, 1984). The extent of weight loss of prepared films can be summarized to comprise three key aspects: volatility of the excipients, hygroscopicity of the polymer and solvent content remained in the films. Unlike some volatile additives, such as triethyl citrate, HPMC will not evaporate from the films during heating. HPMC is a hygroscopic material and does not degrade until a much higher temperature (near 200°C). Therefore, it is reasonable to conclude that the weight loss for pure HPMC seen in *Figure 5-3* was due to water that HPMC absorbed. The weight loss of EC/HPMC films increased as the concentration of HPMC increased, implying two possibilities: the weight loss profiles of these films was due to the moisture content of HPMC (hygroscopicity of HPMC) or some extent of binding between HPMC and the solvents that hindered the evaporation of the solvents from the films.

In conclusion, the weight loss profiles of the EC films with added plasticizers and/or pore formers are mainly due to the nature of these additives. TGA is an easy and efficient technique in measuring the weight loss profiles of films. However, it cannot determine the nature of the weight loss. Trace amounts of water in a sample can be distinguished and determined by other analytical methods, such as Karl Fisher titration.

### 5.4.2 Miscibility between EC and HPMC

MTDSC is generally an effective tool to provide quantitative information on the degree of mixing and the compatibility of the polymer blends in the films. By determining the  $T_g$

values of the film systems, one should be able to conclude if there is any interaction between EC and the additives. For example, the plasticizers would shift the glass transition of EC to a lower temperature, as discussed in *Chapter 4*. HPMC has a  $T_g$  value at about 150°C. If these two polymers are compatible, there should be one  $T_g$  value observed between 130°C and 150°C from MTDSC results. However, a single  $T_g$  at circa 130°C was revealed for all EC films, irrespective of the concentrations of HPMC. The glass transition of HPMC was probably too weak to observe from MTDSC. These results are indicating that HPMC does not interact with EC dramatically within the film systems. However, the endo- and exo-thermal events of EC films around 180°C were much weaker after the incorporation of HPMC. This is probably because the oxidation event and the melting of micro-crystallites within EC were inhibited since they were sitting in a pool of molten EC and HPMC.

The dynamic thermal and thermo-mechanical properties of polymeric films are primarily dependent upon the compatibility of the components. If the two polymers are mutually compatible, a single glass transition is expected to be observed from both MTDSC and DMA, but if they are mutually incompatible, then providing the difference between the glass transition temperatures of the two polymers exceeds the resolution of the measuring technique, two glass transitions are expected to be recorded. Based on the MTDSC results, given the glass transition of HPMC was rather weak, phase separation between EC and HPMC was suspected. However, the results from DMA experiments are much more complicated than expected. Two  $T_g$ s of EC/HPMC films were recorded from the  $\tan \delta$  plots. The low  $T_g$  values remained relatively similar when increasing the levels of HPMC added, whereas the high  $T_g$  values had a more significant increase. From these results, we can tell

that DMA is a more sensitive technique comparing with DSC, in terms of the detection of the motion of the polymer chain.

If we apply the Gordon Taylor/Simha Boyer equations (Gordon and Taylor, 1952; Simha and Boyer, 1962) again to calculate the theoretical glass transition temperatures of EC/HPMC blends, providing that EC and HPMC are completely miscible, we can obtain the predicted values below (*Table 5-5*)

HPMC Concentration	Predicted $T_g$
10%	131.0°C
20%	132.8°C
30%	134.6°C

*Table 5-5 Predicted glass transition temperatures of EC films with 10%, 20% and 30% HPMC, using the Gordon Taylor/Simha Boyer equations, providing EC and HPMC are miscible*

The  $T_g$  of the pure EC films was determined to be 129.2°C from MTDSC results. The increase between each 10% HPMC is only 1-2°C, which would not be confirmed using MTDSC with confidence, even though the standard deviation values are less than 1°C. Therefore, based on the MTDSC results alone, we cannot conclude that EC and HPMC are not miscible at all. Based on the DMA results, it is possible that EC and HPMC are partially miscible. However, the miscibility of EC and HPMC could be rather low, in spite of the similarities in the chemical structures of these two polymers. Immiscibility between HPMC and another polymer hydroxypropyl cellulose (HPC), which has a similar chemical

structure as well, has been reported in the literature (Nyamweya and Hoag, 2000). However, polyvinylpyrrolidone (PVP), which has a very different structure than HPC, is miscible with HPMC (Nyamweya and Hoag, 2000).

The ability of polymers to form compatible blends requires that favourable intermolecular interactions occur between the polymer chains. From a thermodynamic point of view, two polymers are miscible if they form a single phase. For this to happen, the Gibbs free energy of mixing  $\Delta G_{mix}$  needs to be negative. This is given by

$$\Delta G_{mix} = \Delta H_{mix} - T\Delta S_{mix} \quad Eq\ 5-1$$

where  $\Delta H_{mix}$  and  $\Delta S_{mix}$  are the enthalpy and entropy of mixing, respectively, and  $T$  is the temperature. The right side of *Eq 5-1* needs to be negative to obtain a negative  $\Delta G_{mix}$ .

There are numerous ways of arranging the molecules of these two polymers in space; hence there is always an increase of entropy of mixing. However, the entropy of mixing EC and HPMC may be small, because the connectivity of the long polymer chains of EC and HPMC would normally restrict the ways of arranging the molecules. Therefore, a negative  $\Delta H_{mix}$  is required. Strong interactions, such as hydrogen bonding, between the polymeric chains are required to produce a negative of heat of mixing. HPMC is given the presence of unsubstituted hydroxyl group on the cellulose chain as well on the hydroxylpropyl substituent groups. These properties make it able to interact with PVP through hydrogen bonding (Nyamweya and Hoag, 2000), since PVP has the carboxyl and amido groups as the hydrogen acceptors. In EC however, a great portion of hydroxyls on the cellulose chain have been substituted by ethyl groups, leading to a relatively low hydrogen bonding potential, hence low interaction with HPMC. A concept called solubility parameter has been introduced to predict the polymer-polymer miscibility (Sakellariou et al., 1994; Sakellariou et al., 1986b). The solubility parameters of EC and HPMC are 20.6

and  $24.4 \text{ MPa}^{1/2}$  respectively, calculated by van Krevelen using the molecular structure of the polymer from the summation of the group molar attraction constants ( $F$ ) present in the molecule using the formula (Sakellariou et al., 1986c):

$$\Delta = \sum F / V \quad \text{Eq 5-2}$$

where  $V$  is the molar volume of the polymer. Even though a difference of less than  $7 \text{ MPa}^{1/2}$  in the solubility parameters is usually considered significant miscibility (Forster et al., 2001), EC and HPMC did not show great miscibility from the experiments. However, it may still be possible that EC and HPMC have a low miscibility, since the solubility parameters of these two polymers are relatively similar.

The AFM images of EC/HPMC films did provide a great amount of information on their distribution and phase behaviour. However, as a semi-quantitative technique, LTA would not be able to detect a softening temperature change as small as  $1\text{-}2^\circ\text{C}$ . Even so, increasing the levels of HPMC did have an impact on the distribution of EC and HPMC within the films. At low level (10%) of HPMC, the film surface is more homogeneous than those when more HPMC was added. The LTA nano-thermal data showed us that at 10% level, HPMC dispersed at a smaller scale than those at 20% and 30% level.

In summary, phase separation occurred in EC/HPMC films. However, the argument of HPMC is not miscible with EC may not be true in this case. A miscibility of less than 10% (HPMC) is possible. The distribution of HPMC within the EC films are affected by the concentrations of HPMC added. DMA is a more sensitive technique than DSC when detecting the motion of the polymer chains, hence the glass transition temperatures. AFM-LTA is of great use in distinguishing different phases and examining their softening temperatures.

---

## 5.5 Conclusion

The combination of TGA, DSC, DMA and AFM-LTA has allowed a better understanding of the phase behaviour of EC/HPMC films. It is inappropriate to conclude that EC does not interact with HPMC solely based on the DSC results, since the theoretical glass transition of 'miscible' EC/HPMC blends is only 1-2°C higher than that of the pure EC film. EC may be partially miscible with HPMC. However this miscibility between EC and HPMC was rather low. A clear phase separation between EC and HPMC phases occurred. AFM-LTA indicated that the concentrations of HPMC applied will definitely affect the phase distribution of EC and HPMC within the films.

The investigation of the miscibility and phase distribution between the polymer blends are of great significance in understanding the drug release mechanisms when used in the pharmaceutical dosage forms. The partially miscibility or immiscibility may play an important role in the controlled release formulations. Drug release profiles of partially miscible and immiscible formulations and their morphology before and after the dissolution process will be further discussed in the later chapters.

## **CHAPTER 6 THERMAL AND THERMO-MECHANICAL PROPERTIES OF ETHYL CELLULOSE FILMS INCORPORATING VARIOUS PLASTICIZERS AND HYDROXYPROPYL METHYLCELLULOSE**

### **6.1 Introduction**

Ethyl cellulose (EC) is a hydrophobic polymer, therefore formulations coated using pure EC films release the drug very slowly. Sometimes cracks may occur during processing or dissolution due to the brittleness of EC films. The incorporation of plasticizers primarily aims at: (a) reducing the brittleness of the polymeric films; (b) altering the permeability and (c) promoting film formation in the case of aqueous polymer dispersions (Lecomte et al., 2004). Hydrophilic pore formers can accelerate the drug release rate of the drug from the release controlling membranes (Gunder et al., 1995). Plasticizers and pore formers should therefore ideally be incorporated into the EC film system in order to achieve the desirable mechanical properties and drug release profiles. However, most studies have been only focused on plasticizers or pore formers (Hyppölä et al., 1996; Palmer et al., 2007). Even when both were incorporated, drug release profiles were more emphasized, rather than the interaction and distribution of the plasticizers and pore formers (Frohoff-Hülsmann et al., 1999a; Frohoff-Hülsmann et al., 1999b). Therefore, the aim of this chapter is to study the thermal and thermo-mechanical properties of EC/plasticizer films with various levels of HPMC and investigate their interactions, phase behaviour and distributions within the prepared films.

EC/plasticizers/pore former films were prepared to establish relatively complex film systems in order to investigate their interactions and behaviour within the films. 10% plasticizer level was used, since at this level, no phase separation was caused based on the previous findings. Hydroxypropyl methylcellulose (HPMC) was chosen to be the hydrophilic pore former. This chapter will discuss the preparation of EC/plasticizer/HPMC films and study the residual solvents, interactions, phase behaviour and distribution using TGA, MTDSC, DMA and AFM-LTA.

## 6.2 Methodology

### 6.2.1 Preparation of EC/Plasticizers/Pore Former Films

The solvent solution casting method (introduced in *Chapter 2*) was applied to prepare EC/plasticizers/pore former films. The formulations of all films are shown in *Table 6-1*. Oleic acid (OA), dibutyl sebacate (DBS) and medium chain triglycerides (MCT) were utilized as the plasticizers and their concentrations were controlled at 10% (w/w) in order to avoid phase separation caused by high plasticizer levels, based on the findings in *Chapter 4*. 10%, 20% and 30% HPMC were added to the film systems respectively. For the films with plasticizer mixtures, the ratios of EC and the plasticizers were 75.2:8.8:16.0 (EC: OA: DBS or MCT), the same as those used in *Chapter 4* for the films prepared without HPMC. After all ingredients were fully mixed and dissolved in ethanol/water (90:10 v/v), the solutions were then cast onto a glass plate. The wet film thickness was controlled using a film applicator at 2000 $\mu$ m. The resulting dry film thickness of all films was 150 $\pm$ 10 $\mu$ m. EC/plasticizer/HPMC films were dried in the oven at 45°C for 24 hours. All dry films were placed in a silica gel dessicator for 24 hours to equilibrate before being tested.

Films	EC (g)	OA (g)	DBS (g)	MCT (g)	HPMC (g)
EC/OA/10%HPMC	1.6	0.2	-	-	0.2
EC/OA/20%HPMC	1.4	0.2	-	-	0.4
EC/OA/30%HPMC	1.2	0.2	-	-	0.6
EC/DBS/10%HPMC	1.6	-	0.2	-	0.2
EC/DBS/20%HPMC	1.4	-	0.2	-	0.4
EC/DBS/30%HPMC	1.2	-	0.2	-	0.6
EC/MCT/10%HPMC	1.6	-	-	0.2	0.2
EC/MCT/20%HPMC	1.4	-	-	0.2	0.4
EC/MCT/30%HPMC	1.2	-	-	0.2	0.6
EC/OA-DBS/10%HPMC	1.354	0.158	0.288	-	0.2
EC/OA-DBS/20%HPMC	1.203	0.141	0.256	-	0.4
EC/OA-DBS/30%HPMC	1.053	0.123	0.224	-	0.6
EC/OA-MCT/10%HPMC	1.354	0.158	-	0.288	0.2
EC/OA-MCT/20%HPMC	1.203	0.141	-	0.256	0.4
EC/OA-MCT/30%HPMC	1.053	0.123	-	0.224	0.6

*Table 6-1 Film formulations of EC/plasticizers/HPMC films*

### 6.2.2 Residual Solvents

For the EC/HPMC films prepared, TGA (Hi-Res TGA 2950, TA Instrument) was used to determine the amount of residual solvents in the dry films. The samples were heated from room temperature, ramping at 10°C/min to 150°C. 5 – 10mg samples were placed in the sample pans. Dry nitrogen was used as purge gas while compressed air was used as the

---

cooling system. All experiments were carried out in triplicate. Weight loss of the dry films at 100°C was taken as the amount of residual solvent.

### 6.2.3 DSC Studies

MTDSC (Q2000, TA Instruments, USA) was conducted by running the samples from 0°C to 200°C with modulation amplitude of  $\pm 0.5^\circ\text{C}/40\text{s}$  at  $2^\circ\text{C}/\text{min}$ . Samples with a mass between 1 and 3 mg were prepared in the standard aluminium pans (TA Instruments, USA). Calibration was carried out before running the experiment. All experiments were carried out in triplicate. The  $T_g$  values of the films were taken from the midpoints of the reversing heat flow signals.

### 6.2.4 DMA Studies

DMA tension film mode (tensile clamp) was used to investigate the storage modulus, loss modulus and  $\tan \delta$  values of the prepared films during the program used. Samples were heated from 30°C to 180°C at a heating rate of  $3^\circ\text{C}/\text{min}$  under 1 Hz frequency and 20  $\mu\text{m}$  amplitude. Dry filtered air was used as purge gas and cooling system. Triplicate studies were performed to obtain an average value of the results.  $T_g$  of all films were analyzed using the  $\tan \delta$  peak values and the storage modulus values were taken at 30°C.

### 6.2.5 AFM Studies

AFM measurements were performed in a Thermomicroscopes Explorer scanning probe microscope (pulsed force mode, Anasys Instruments, USA). Small pieces of these films (approximately 10×10 mm) were cut and mounted on magnetic studs by double-sided tape. Different locations of the dry film surfaces were scanned initially to obtain topography and adhesion images simultaneously by using pulsed force mode AFM. The frequency and

amplitude for modulation and subtract baselines were 500 Hz and 50 nm respectively. The scan area was  $5 \times 5 \mu\text{m}^2$  and the scan speed was  $5 \mu\text{m/s}$  with a resolution of  $200 \times 200$  pixels. A WSxM 5.0 software was applied to analyzed the topography and adhesion images (Horcas et al., 2007). All resulting images were simply flattened and equalized. Nano-thermal analysis was applied to the areas of interest. Thermal analysis data was obtained at  $5^\circ\text{C/s}$  between room temperature and  $150^\circ\text{C}$ . Probe cantilever deflection was plotted against probe tip temperature to obtain the  $T_g$ s of specific area on the film surfaces.

### 6.3 Results

The residual solvent levels of all produced films were examined initially to ascertain that the drying method is adequate to allow the accurate investigation of the dry films. TGA results showed that the residual solvents were less than 0.6% (w/w) of all films (data not shown). Further investigations were then continued to characterize the thermo-mechanical properties of EC/plasticizers/HPMC films.

#### 6.3.1 MTDSC Studies

Interactions between HPMC and EC/plasticizer film systems with 10% plasticizer level were investigated. Therefore 10% plasticizers were used in the prepared films in order to avoid any phase separation by the plasticizers, and at the same time, allowing adequate plasticizing effect to be afforded. The reversing heat flow signals from MTDSC of EC/OA films and those with 10%, 20% and 30% (w/w) HPMC are compared in *Figure 6-1*. A single  $T_g$  was observed for all the systems, indicating a one phase system. However, the glass transition of HPMC powder was known to be small, based on the results in *Chapter 5*, and no  $T_g$  was observed from the pure HPMC films (data not shown). Therefore, even if HPMC was separated from the EC/OA films, it may not be revealed from the reversing

---

heat flow signals. It was noticed that the  $T_g$  values increased slightly when increasing the concentration of HPMC incorporated, especially from 0% to 10% HPMC levels. This result implies HPMC may have an interaction with the plasticizer. This is because if HPMC does not have any impact on the EC/OA phase in the films, the  $T_g$  values of the films should be lower than that of the EC/OA films without HPMC, since the ratio of EC to OA was decreased after adding 10% HPMC. However, the  $T_g$  values of EC/OA/HPMC films remained similar or even increasing slightly. It is possible that there were actually two phases existing, an EC domain and an HPMC domain. When more HPMC was added, some plasticizer formed a phase with HPMC, leaving less plasticizer with EC, resulting in a slightly higher  $T_g$  of the EC phase. Unfortunately, there was no trace of glass transition of the HPMC/plasticizer phase from the MTDSC signals due to the weak glass transition of HPMC. Very similar results were observed for EC/DBS/HPMC and EC/MCT/HPMC films, shown in *Figure 6-2* and *6-3* respectively.

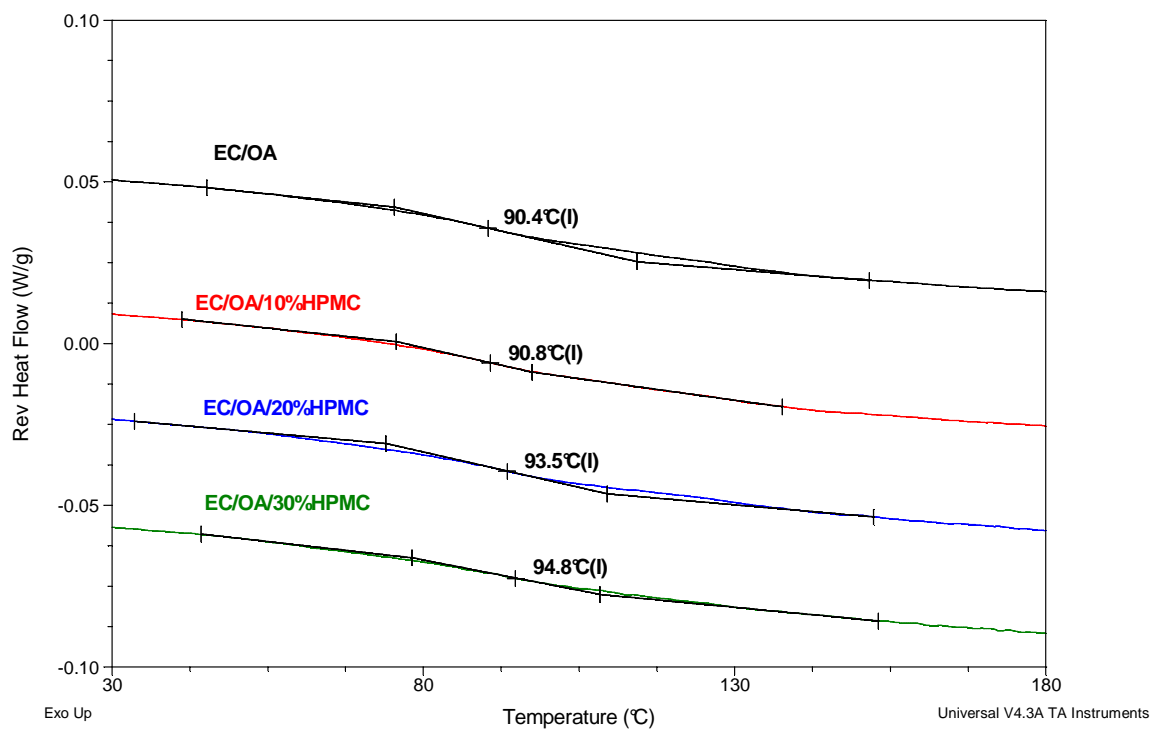


Figure 6-1 Reversing heat flow signals of EC/OA free films incorporated with 0%, 10%, 20% and 30% HPMC, obtained from MTDSC at 2°C/min in the standard aluminium pans

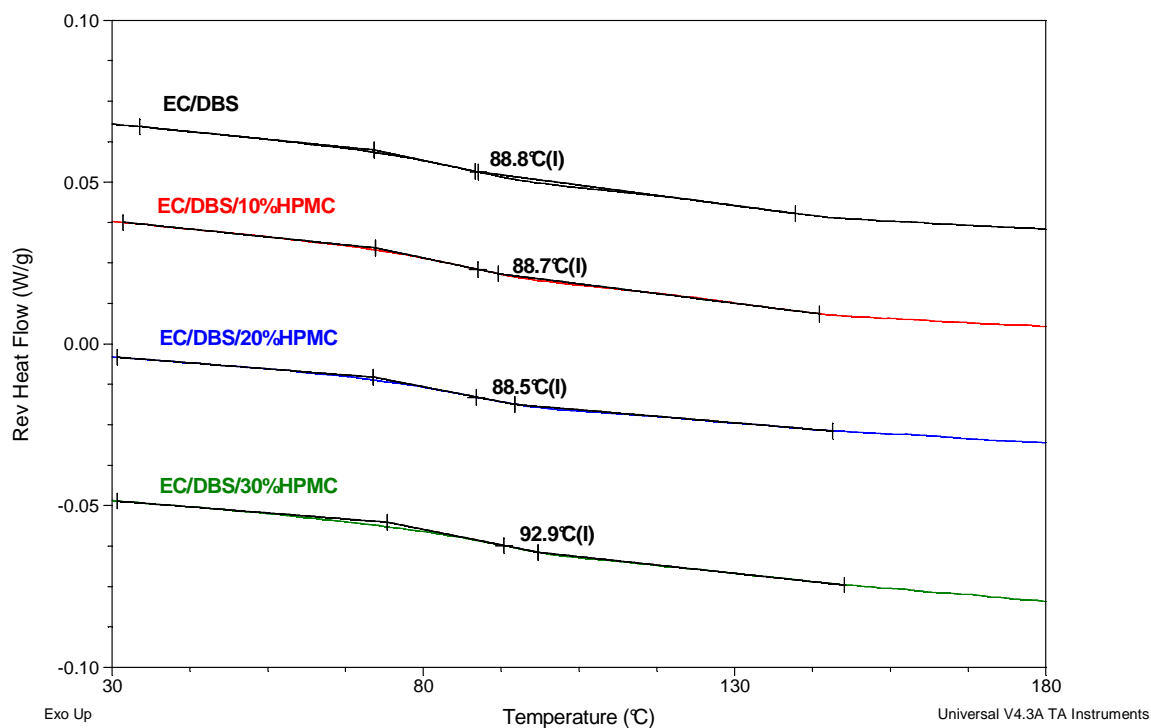


Figure 6-2 Reversing heat flow signals of EC/DBS free films incorporated with 0%, 10%, 20% and 30% HPMC, obtained from MTDSC at 2°C/min in the standard aluminium pans

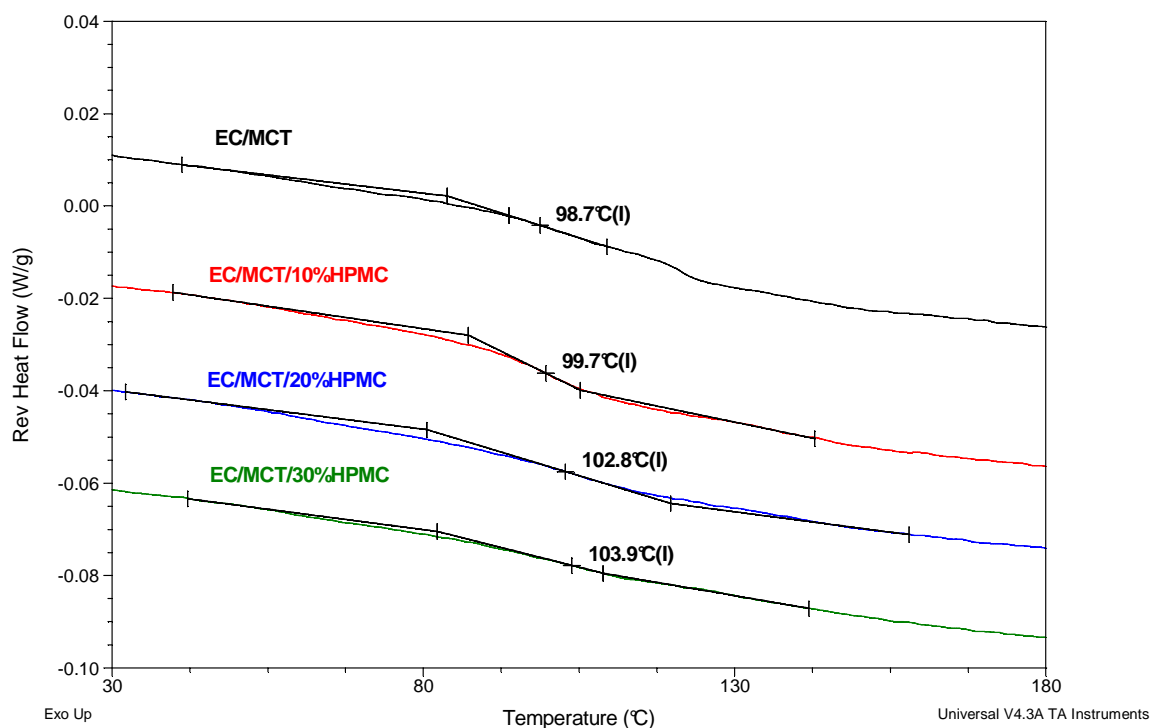


Figure 6-3 Reversing heat flow signals of EC/FCO free films incorporated with 0%, 10%, 20% and 30% HPMC, obtained from MTDSC at 2°C/min in the standard aluminium pans

Table 6-2 compares the  $T_g$ s of EC/plasticizer films with 0%, 10%, 20% and 30% HPMC. EC/MCT/HPMC films showed higher  $T_g$ s compared with the same levels of EC/OA/HPMC films and EC/DBS/HPMC films, suggesting lower plasticizing efficiency. This is consistent with previous EC/plasticizer films study, indicating the chemical structures of plasticizers may have an impact on the plasticizing efficiency.

	$T_g$ (°C) OA	$T_g$ (°C) DBS	$T_g$ (°C) MCT
0% HPMC	88.4±2.0	88.5±0.4	97.2±1.3
10% HPMC	92.3±1.4	88.7±1.7	100.7±2.7
20% HPMC	93.6±0.2	88.8±1.8	102.4±1.3
30% HPMC	94.2±0.6	91.6±1.4	104.2±1.1

*Table 6-2 Glass transition temperatures of EC/plasticizer films on adding different concentrations of HPMC, obtained from the reversing signals of MTDSC (n=3)*

EC/plasticizer mixture/HPMC showed  $T_g$ s at circa 50°C which is consistent with previous studies of EC/plasticizer mixture films, shown in *Figure 6-4*, *6-5* and *Table 6-3*. The incorporation of 10% HPMC resulted a 3-4°C higher  $T_g$  than those of the films without HPMC. However, when increasing the concentration of HPMC from 10% to 30%, no significant increasing of the  $T_g$  was observed. This may be because the plasticizer intake ability of HPMC is not significant. Therefore, extra HPMC did not have a dramatic impact on the  $T_g$  values of the EC/plasticizer films.

HPMC was reported to have a decreasing effect on minimum film forming temperature (MFT) of the EC/DBS films (Frohoff-Hülsmann et al., 1999b). The  $T_g$  of the polymer component is one of the factors which can influence the MFT of films (Leong et al., 2002). However, the relationship of  $T_g$  and MFT is rather complex since MFT is the property of entire formulation and not just the polymer. Nevertheless, these indicate HPMC may have limited interaction with plasticizers utilized in this project.

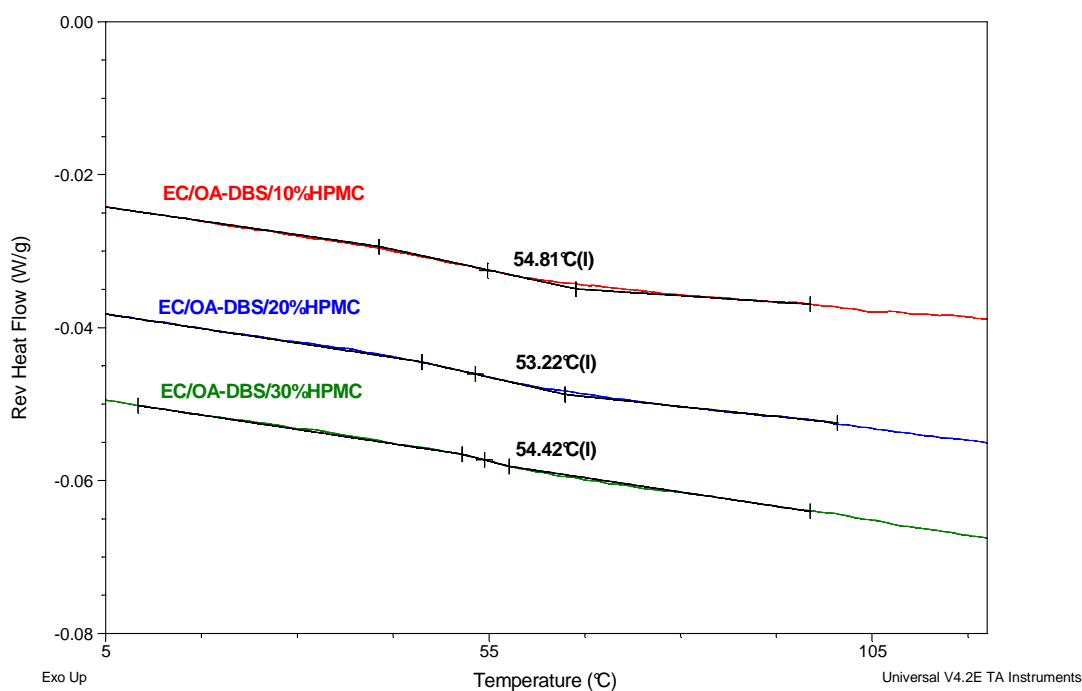


Figure 6-4 Reversing heat flow signals of EC/OA-DBS films with different concentrations of HPMC, obtained from MTDSC at 2°C/min in the standard aluminium pans

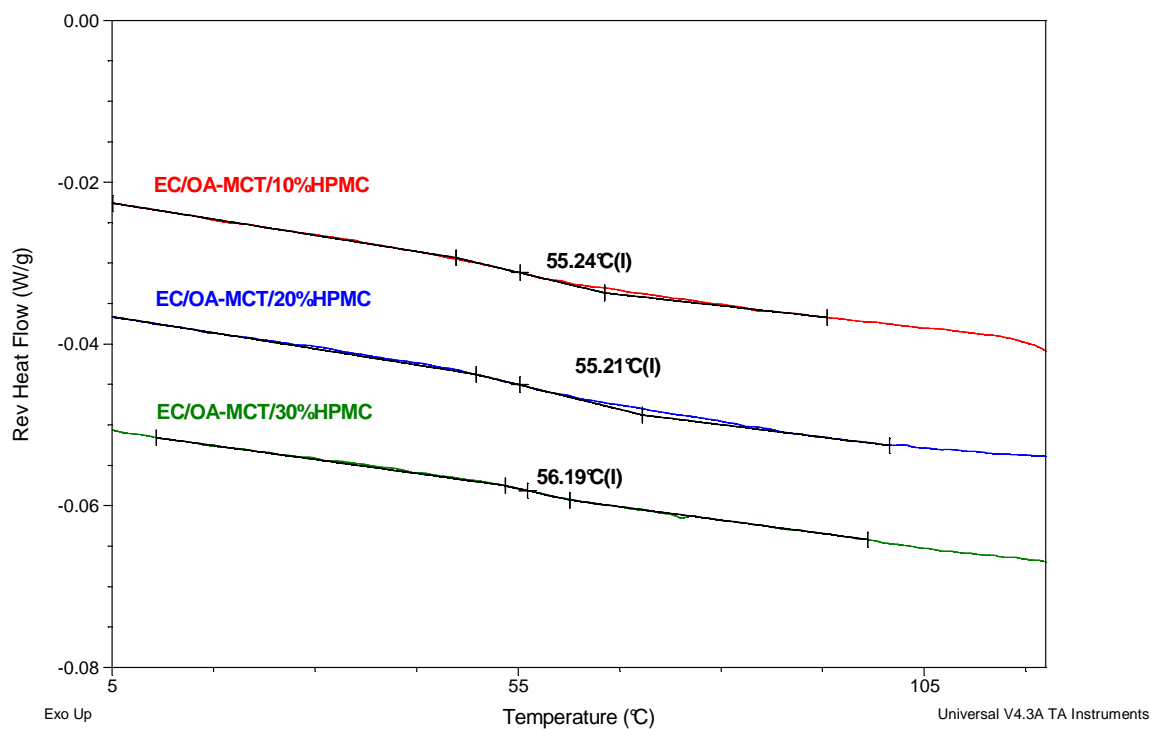


Figure 6-5 Reversing heat flow signals of EC/OA-MCT films with different concentrations of HPMC, obtained from MTDSC at 2°C/min in the standard aluminium pans

HPMC	$T_g$ (°C) EC/OA-DBS Films	$T_g$ (°C) EC/OA-MCT Films
0%	50.0 ± 1.3	52.1 ± 0.7
10%	53.1 ± 1.5	56.0 ± 2.7
20%	52.8 ± 1.7	55.4 ± 0.5
30%	54.4 ± 2.3	56.0 ± 0.8

*Table 6-3 Glass transition temperatures of EC/plasticizer mixture films on adding different concentrations of HPMC, obtained from the reversing signals of MTDSC (n=3)*

In summary, according to the MTDSC studies, one single  $T_g$  value can be observed for all film systems. The addition of 10%, 20% or 30% w/w HPMC to the EC/plasticizer films did not have a significant effect on the  $T_g$  values of these films. However, it is possible that two phases, i.e. EC and HPMC phases with plasticizers existed in the films.

### 6.3.2 DMA Studies

#### 6.3.2.1 Thermal Properties

Figure 6-6 shows the loss modulus and  $\tan \delta$  signals of EC/OA films with 0%, 10%, 20% and 30% HPMC. Without HPMC, EC/OA films showed one peak for the loss modulus and one peak for the  $\tan \delta$ . This is reasonable since 10% OA is able to plasticize the polymer but not cause phase separation. On adding 10% to 30% HPMC, another transition appeared in the range of 50-70°C on the loss modulus signals, at a temperature lower than the glass transitions. These may be  $\beta$  transitions, which are associated with the motion of small groups of either EC or HPMC. EC/OA films had a  $\tan \delta$  peak at 98.6, 107.2, 105.8 and 105.9°C, when adding 0%, 10%, 20% and 30% HPMC respectively. These values are

ascribed to the  $T_g$  values of EC/OA/HPMC films. The increasing of the  $T_g$  values of EC/OA films with 0% to 10% HPMC is consistent with the previous observations from MTDSC results. Similar behaviours were observed for EC/DBS/HPMC systems and EC/MCT/HPMC systems, as seen in *Figure 6-7* and *6-8*, further confirming that it is possible that HPMC interacted with the plasticizers.

In summary, the addition of 10% HPMC to the EC/plasticizer films increased the  $T_g$  values of these films slightly, however higher level (20% and 30%) of HPMC had no significant effect on these  $T_g$  values, indicating HPMC was plasticized by only a small amount of plasticizers.

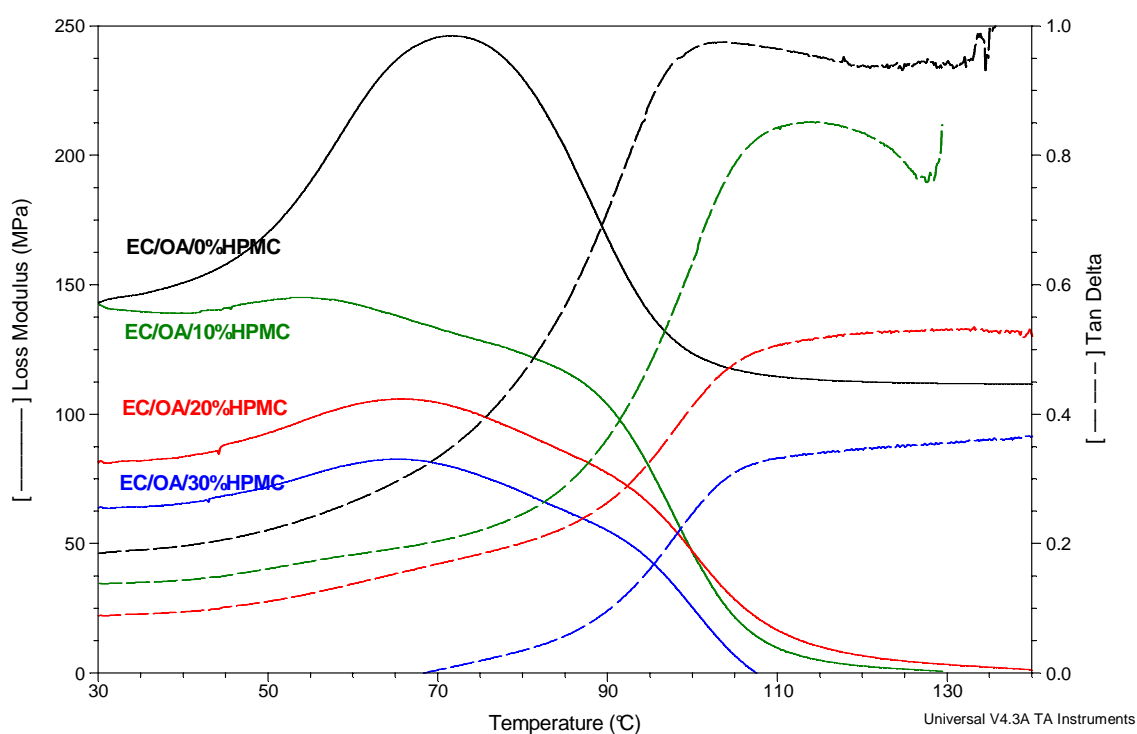


*Figure 6-6 Loss modulus and  $\tan \delta$  signals of EC/OA films with 0%, 10%, 20% and 30% HPMC, obtained from DMA*

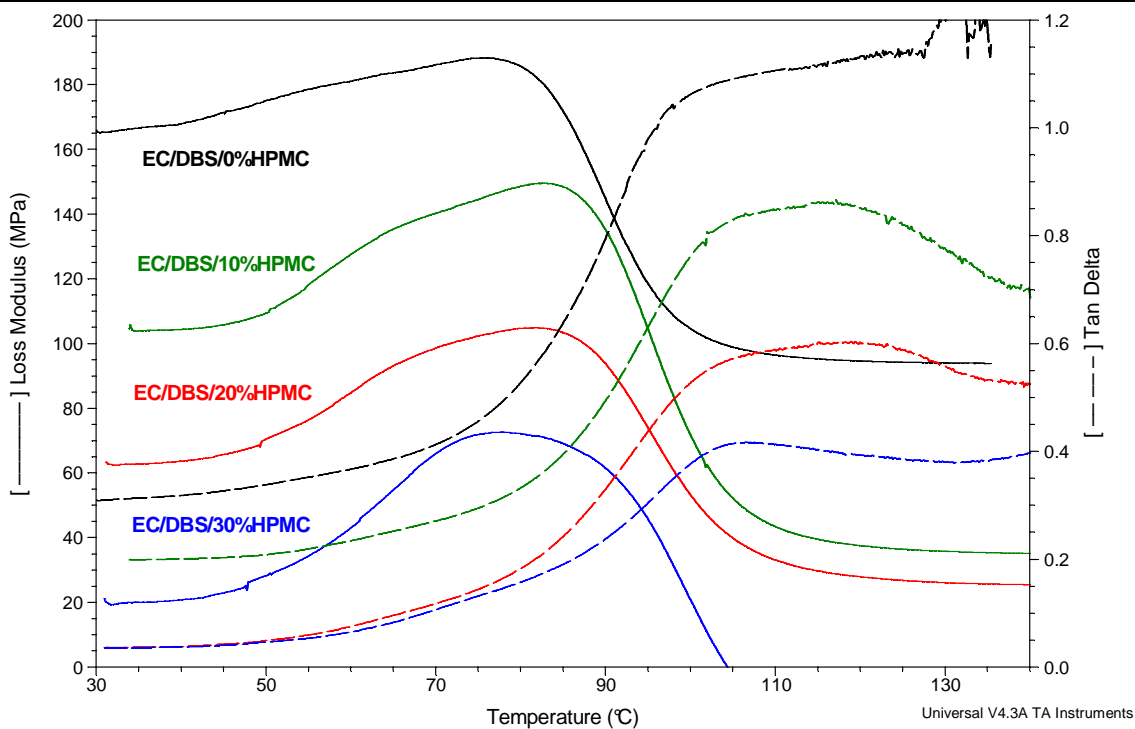


Figure 6-7 Loss modulus and  $\tan \delta$  signals of EC/OA films with 0%, 10%, 20% and 30% HPMC, obtained from DMA

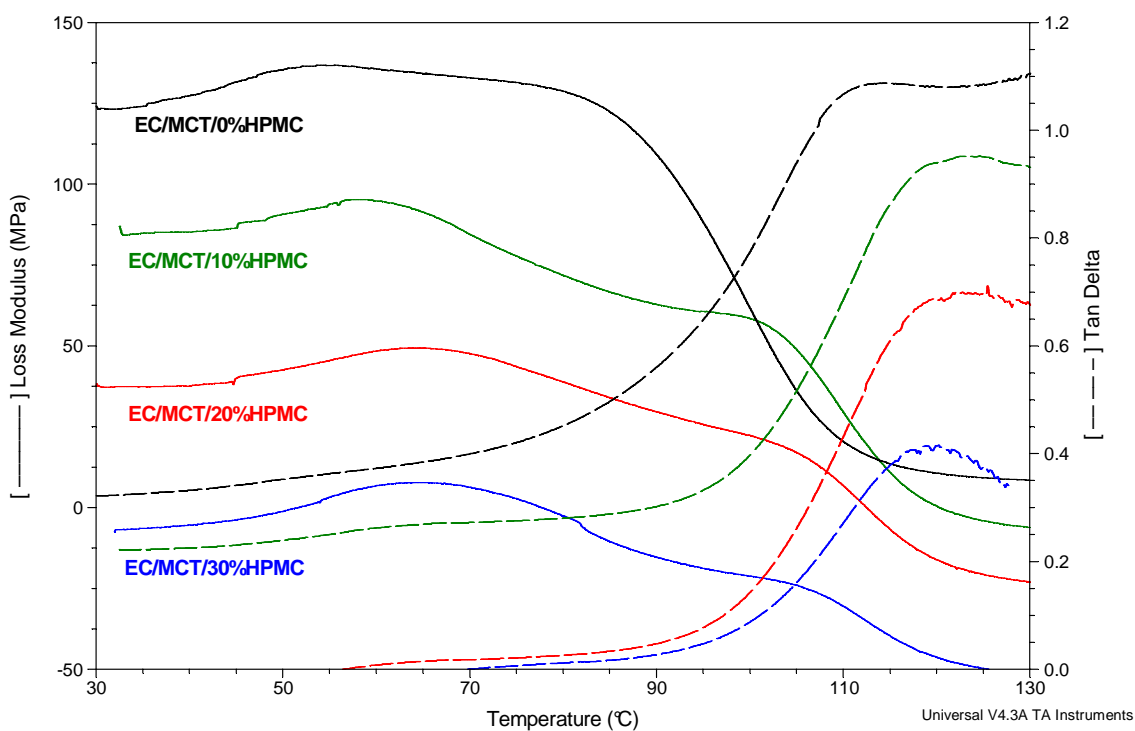


Figure 6-8 Loss modulus and  $\tan \delta$  signals of EC/MCT films with 0%, 10%, 20% and 30% HPMC from DMA

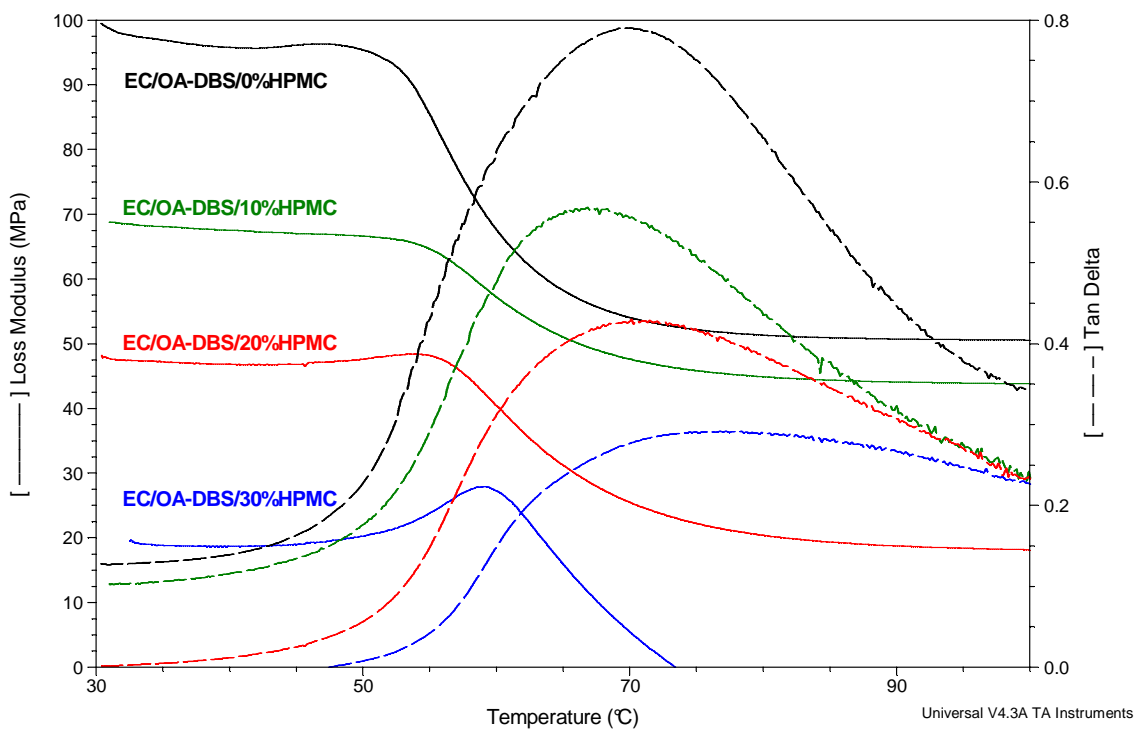


Figure 6-9 Loss modulus and  $\tan \delta$  signals of EC/OA-DBS films with 0%, 10%, 20% and 30% HPMC from DMA

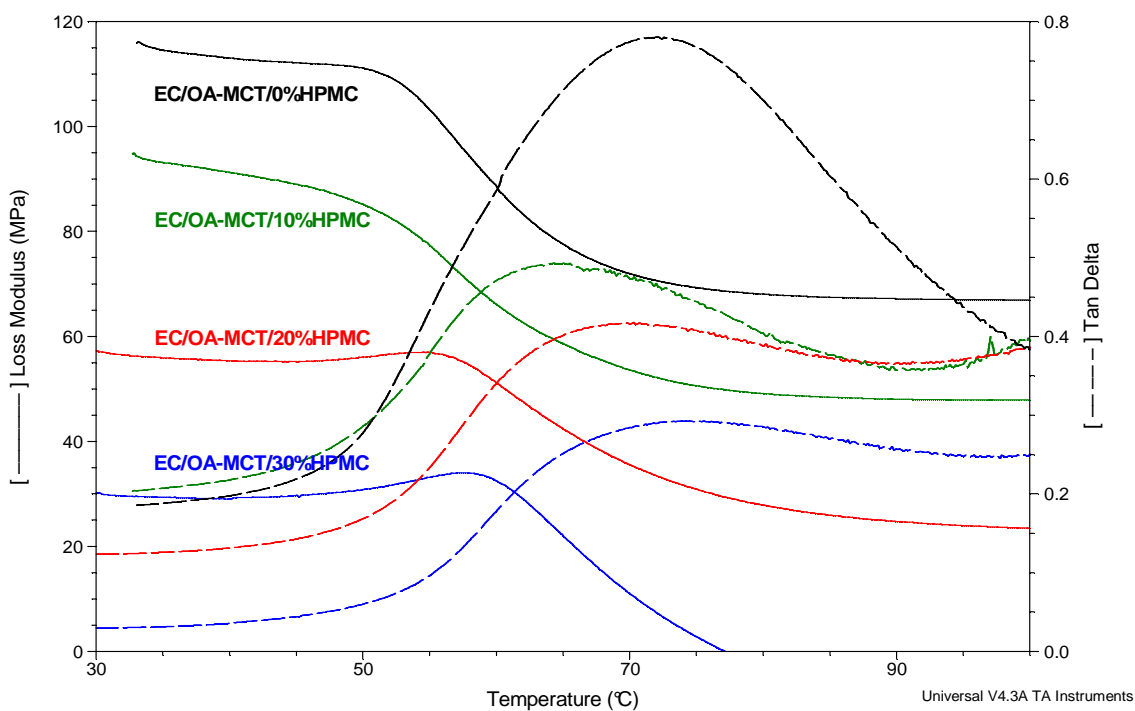


Figure 6-10 Loss modulus and  $\tan \delta$  signals of EC/OA-MCT films with 0%, 10%, 20% and 30% HPMC from DMA

The loss modulus and  $\tan \delta$  signals of EC/OA-DBS and EC/OA-MCT films with 0%, 10%, 20% and 30% HPMC are shown in *Figure 6-9* and *6-10*, respectively. A single peak was observed from the loss modulus and  $\tan \delta$  signals respectively for all systems. In contrast to from the EC/plasticizer films, the  $\beta$  transition in the temperature range 50-70°C disappeared. A possible explanation is that the plasticizer mixtures can crosslink with the polymers via different structure sites, hence limiting the motion of the side groups of the polymers. *Table 6-4* summaries the  $T_g$  values of EC/plasticizer/HPMC and EC/plasticizer mixture/HPMC films, obtained from the  $\tan \delta$  peaks of DMA.

HPMC Concentration	OA (°C)	DBS (°C)	MCT (°C)	OA-DBS (°C)	OA-MCT (°C)
0%	98.6±0.7	97.6±0.5	109.5±0.4	70.9±0.1	73.1±1.2
10%	107.2±0.4	106.2±1.9	116.9±0.8	65.4±0.4	66.6±1.2
20%	105.8±1.8	107.9±0.5	117.0±0.2	67.3±0.7	66.4±0.5
30%	105.9±0.9	106.3±1.5	119.4±0.8	71.2±0.3	68.6±1.1

*Table 6-4 Glass transition temperatures of EC/plasticizer films on adding different concentrations of HPMC, obtained from  $\tan \delta$  peaks of DMA (n=3)*

### 6.3.2.2 Mechanical Properties

*Figure 6-11* compares the storage modulus of EC films with a variety of plasticizer types and different concentrations of HPMC at 30°C. When increasing the concentration of HPMC, no constant increasing of the storage moduli was observed. This is probably because when the concentration of HPMC was increased, the concentration of EC was actually decreased, i.e. the overall solid concentration was constant. EC and HPMC both

can enhance the stiffness of the films. When the plasticizer mixtures were used, the involvement of HPMC and different plasticizer levels make it difficult to compare their storage modulus. However, higher plasticizer levels resulted in lower storage modulus of EC films, irrespective of the concentrations of HPMC. Therefore, we can conclude that in the EC/plasticizer/HPMC films, the plasticizer level is the main factor that is responsible for the change of the storage modulus.

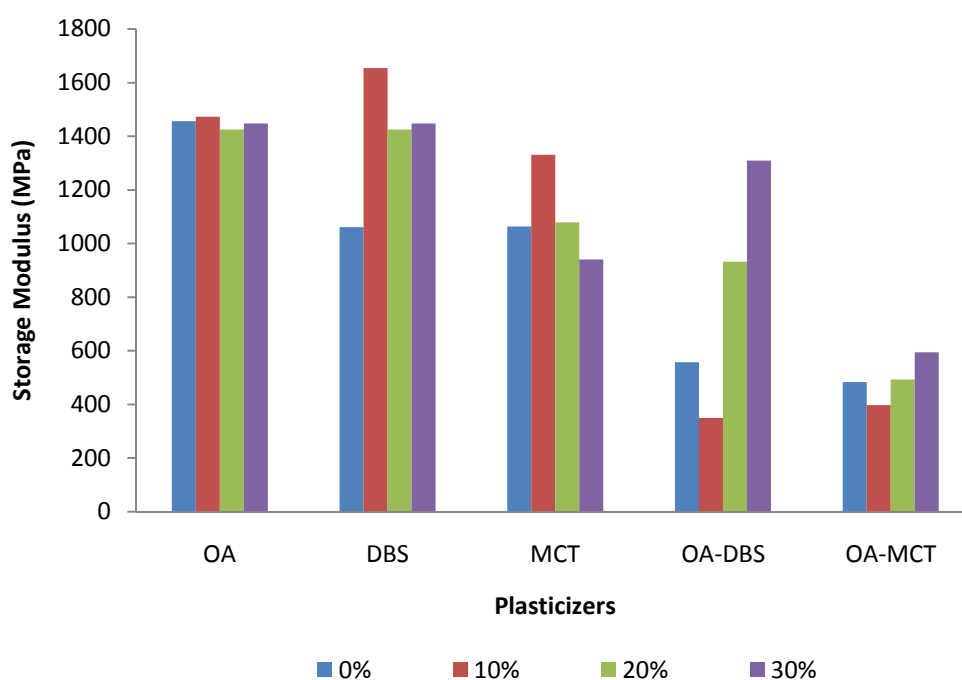


*Figure 6-11 Storage moduli of EC/plasticizer films with 0%, 10%, 20% and 30% HPMC at 30°C, obtained from DMA*

### 6.3.3 Localized Thermal Analysis (LTA) Studies

*Figure 6-12* shows the topography, adhesion (5 $\mu\text{m}$ ×5 $\mu\text{m}$ ) and the corresponding LTA nano-thermal data of EC/plasticizer/30% HPMC films. A few features were observed on the topography images for all systems, and the adhesion images showed corresponding

phases in bright and dark colour respectively. Therefore, the nano-thermal probe was located on selected bright or dark areas, presented as numbers on the adhesion images. The probe went up first due to the thermal expansion of the films. For the EC/OA/30%HPMC films, two softening temperatures at approximately 120°C and 165°C were observed, which are associated with the  $T_g$  values of the EC phase and HPMC phase respectively. Some selected areas went through a thermal expansion, a softening, another thermal expansion and another softening at the above temperatures, indicating a two layer structure at some areas. The probe would hit the EC/plasticizer phase first and then the HPMC/plasticizer phase, which was at a higher temperature.

For the EC/DBS/30%HPMC films, similar behaviour was revealed. The LTA nano data exhibited a high  $T_g$  and a low  $T_g$ , that were ascribed to the HPMC/plasticizer phase and EC/plasticizer phase respectively. However, a broad softening occurred, which covered both the softening temperatures of EC and HPMC phases. There was no second thermal expansion as the EC/OA/30%HPMC films. Two  $T_g$  values were again obtained for the EC/MCT/30%HPMC films. All these results are indicating that two phase systems were formed in the EC/plasticizer/30%HPMC films, even though MTDSC or DMA could not detect the  $T_g$  of HPMC phase.

The topography and adhesion images of EC/plasticizer mixture/30%HPMC films, as seen in *Figure 6-13*, showed no distinguishing features. Therefore the nano probe was located randomly on the images. EC/OA-DBS/30%HPMC films showed two probe downward deflections as well, whereas EC/OA-MCT/30%HPMC films only showed one, which was the  $T_g$  of the EC phase.

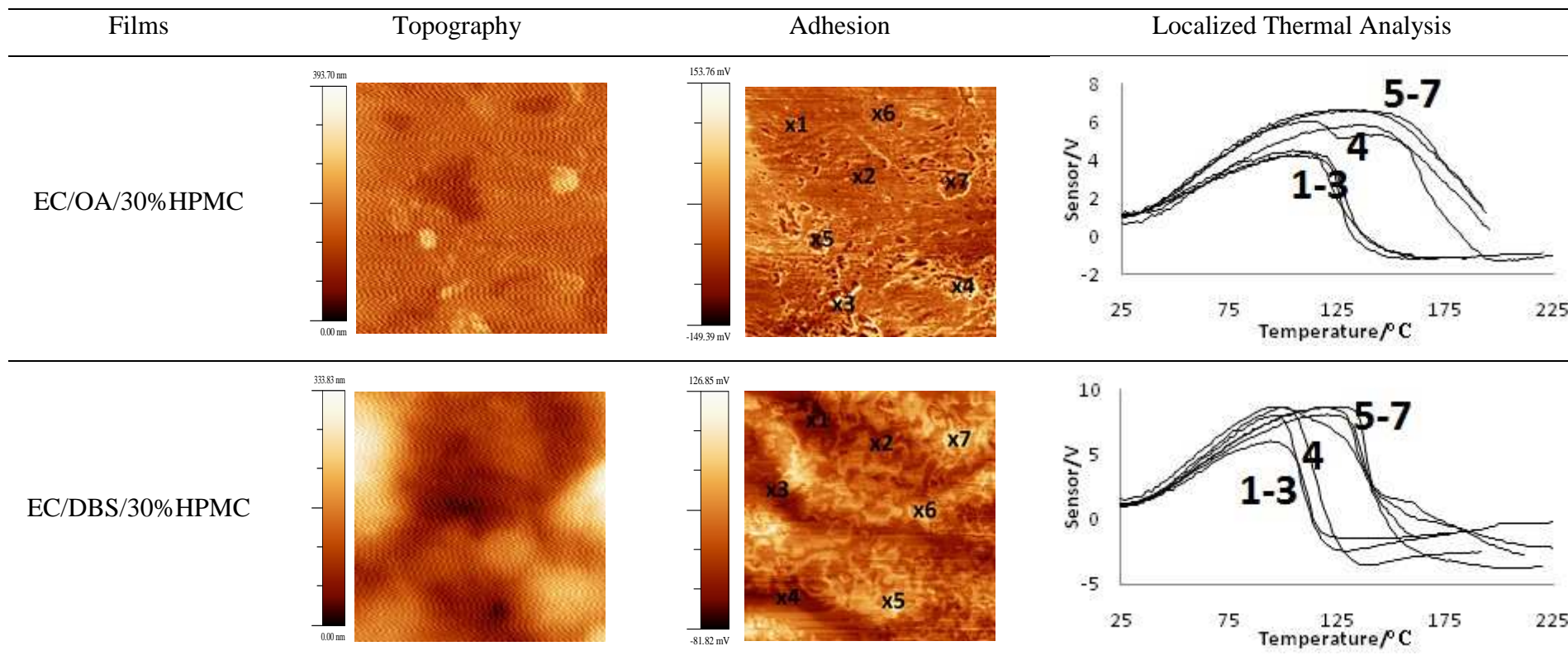
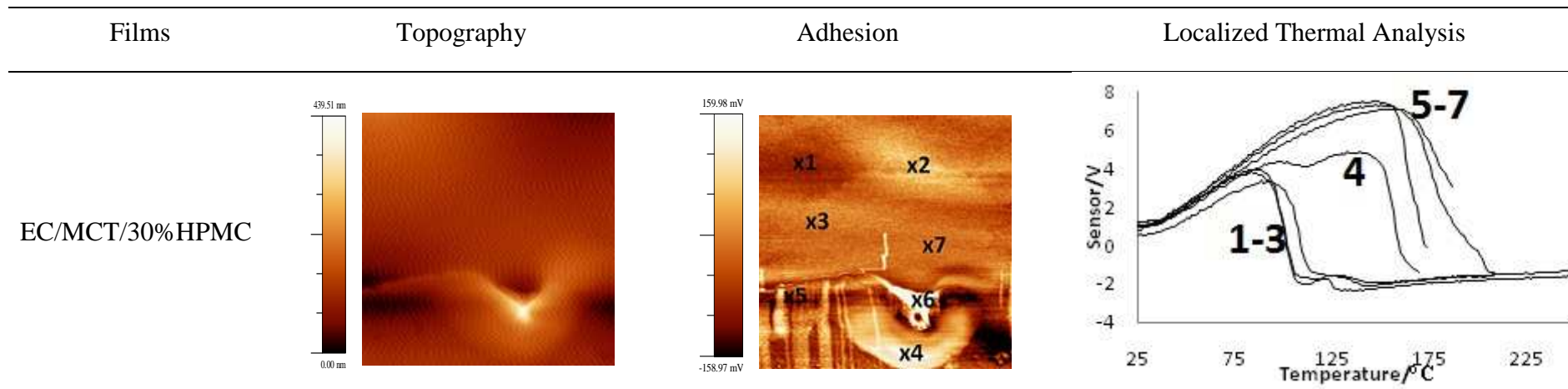


Figure 6-12 Topography, adhesion images ( $5\mu\text{m}\times 5\mu\text{m}$ ) and corresponding LTA data of EC/OA/30%HPMC, EC/DBS/30%HPMC and EC/MCT/30%HPMC films observed by using pulsed force mode AFM and LTA technique (to be continued)



*Figure 6-12 Topography, adhesion images ( $5\mu\text{m}\times 5\mu\text{m}$ ) and corresponding LTA data of EC/OA/30%HPMC, EC/DBS/30%HPMC and EC/MCT/30%HPMC films observed by using pulsed force mode AFM and LTA technique*

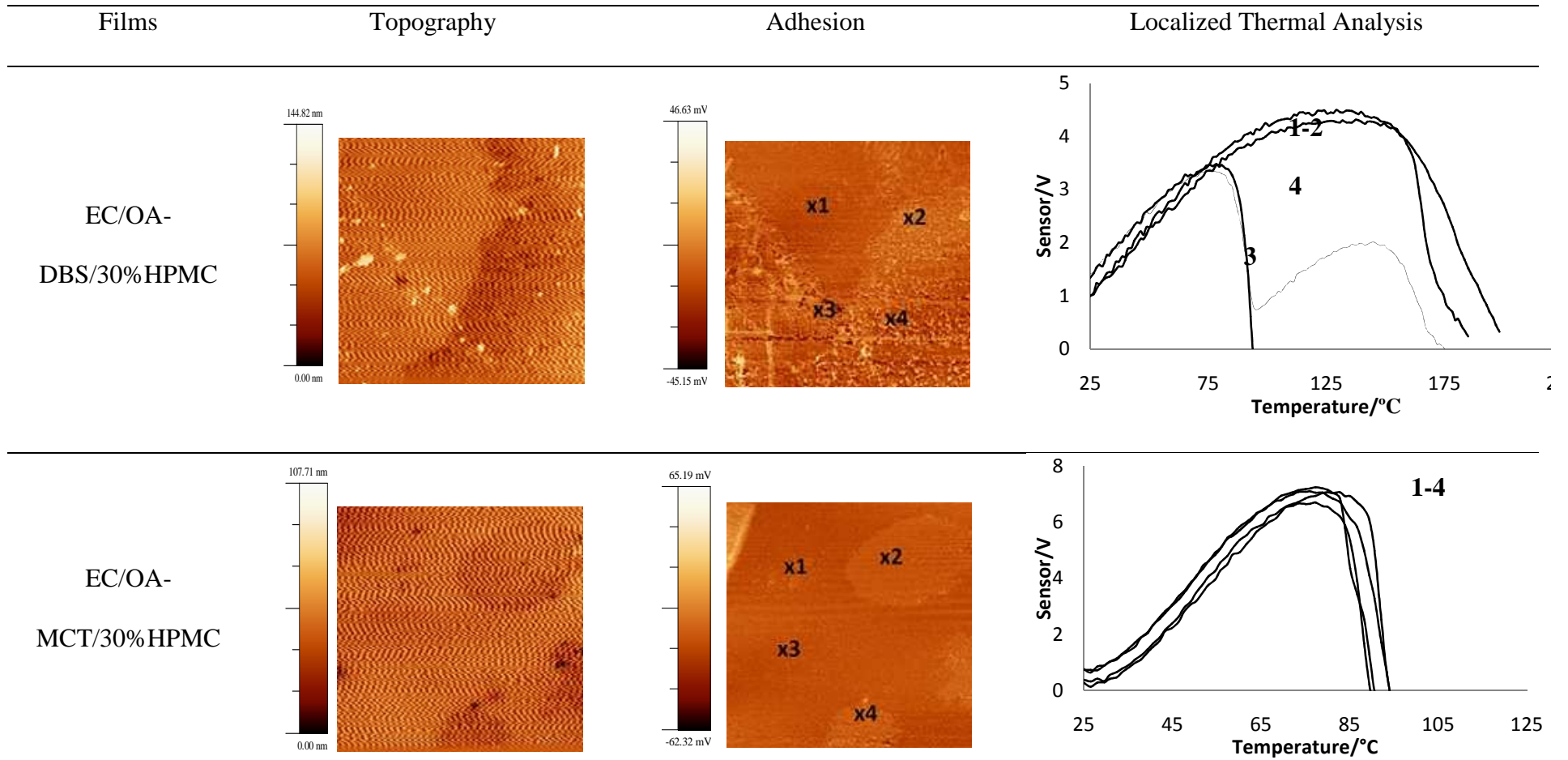


Figure 6-13 Topography, adhesion and corresponding LTA data of EC/OA-DBS/30%HPMC and EC/OA-MCT/30%HPMC films observed by using pulsed force mode AFM and LTA technique

---

## 6.4 Discussion

### 6.4.1 Miscibility Studies-MTDSC

MTDSC provides quantitative information on plasticizing efficiency of selected plasticizers and miscibility of the plasticizers with the polymer blends. By assessing the  $T_g$  of the films, one should be able to predict the miscibility of the film components and their interactions.

Comparing the  $T_g$  values of EC/plasticizer/HPMC films, DBS had the most significant plasticizing efficiency. However, DBS and OA revealed similar plasticizing efficiency for EC/plasticizer films (without HPMC), showed in *Chapter 4*. The chain length of plasticizers were reported to have an effect on the resulting film properties (Sánchez et al., 1998). However, DBS (18 C) and OA (17 C) have similar chain length. This indicates that DBS may interact with HPMC, possibly through hydrogen bonding, since it has two carbonyl groups that OA does not have. MCT had the lowest plasticizing efficiency that is consistent with previous study in *Chapter 4*. Plasticizers that have low molecular volumes can diffuse and interact with the active groups in the polymers more efficiently (Gutiérrez-Rocca and McGinity, 1994). Even it has only 6-12 C, MCT possesses three chains that may be a hindrance when it comes to embedding themselves in polymeric chains. Therefore, the chemical structures of plasticizers may play an important role in plasticizing the film coating polymers.

When HPMC was incorporated into the film systems, the  $T_g$  values increased slightly, but close to the  $T_g$  of EC. No trace of the glass transition of HPMC could be observed. When polymer blends are applied, plasticizers could migrate to the polymer domain that they have higher affinity to (Lecomte et al., 2004). Therefore, it is possible that the plasticizers

formed two phases with EC and HPMC, respectively. The  $T_g$  of the HPMC phase was too small to be observed using MTDSC, similarly observed for that of pure HPMC film. When more HPMC was incorporated, small amount of plasticizers joined the HPMC phase, leaving less plasticizer in the EC phase, hence resulting a slightly higher  $T_g$ .

#### 6.4.2 Miscibility Studies-DMA

DMA has been used to characterize the rheological properties and glass transition behaviours of materials of pharmaceutical interest (Craig and Johnson, 1995). Film coats are among those materials that can be assessed by DMA, due to their viscoelastic properties. The extensive theory of DMA has been introduced in *Chapter 2*. Several clamps can be used to detect the thermo-mechanical properties of films, such as single-cantilever, dual-cantilever, three-point bending and tension film (Craig and Johnson, 1995). The first three clamps were initially applied. However, the prepared films were too thin to obtain reproducible results, even when films were prepared on a metal mesh. These three clamps all involve the film coats lying flat with two or three points in contact with the clamps. Therefore, the film thickness may be crucial to obtain valuable and repeatable data. For the tension film clamp, the films were mounted vertically and placed in tension between a fix and movable clamp. In oscillation experiments, a small static force was applied in order to prevent buckling.

A number of output values can be obtained, among which, storage modulus, loss modulus and  $\tan \delta$  were analyzed. Amorphous polymers generally exhibit a major (glass) transition which is associated with the mobility of the main chain, while secondary ( $\beta$ ,  $\gamma$  and  $\delta$ ) transitions may also occur due to side chain motions (Craig and Johnson, 1995). A secondary transition was revealed from the loss modulus signals for EC/OA/HPMC and

EC/DBS/HPMC films, but could not be observed for those films without HPMC. This is indicating the observed  $\beta$  transition can be due to the side chains of HPMC, rather than EC or the plasticizers. For EC/MCT systems, the  $\beta$  transition was observed for films with and without HPMC. Unlike OA or DBS, MCT has three chains that may not all interact with EC or HPMC. Therefore, HPMC may be responsible for the side chain motion in this case. Apart from glass transition, no other transitions were observed at all for the EC/plasticizer mixture/HPMC films, indicating the plasticizer mixtures may work better in interaction with different polymeric chain groups, hence hindering side chain movements.

The  $T_g$  values obtained from DMA seemed to be in good agreement with those from MTDSC. However, the increase of the  $T_g$  values when increasing HPMC levels were not significant, probably due to system error. Even though the  $\tan \delta$  peaks, i.e. glass transition of these films were broad, no glass transition of HPMC was revealed. Therefore, the sensibility of DMA (2980) is not adequate for the detection of HPMC glass transition.

The mechanical strength of the film coats is one of the factors that can affect the drug release mechanisms, since polymeric films generally have hydration and swelling properties when contacting the drug release medium (Boateng et al., 2009). Cracks and other defects may occur if the films are brittle (Rowe, 1981). The mechanical strength can also determine the rate of hydration and eventual dissolution (Bashaiwoldu et al., 2004; Podczeczek and Almeida, 2002). In this chapter, when the plasticizer level was kept constant at 10% w/w, the changing of the storage modulus was not following any law, irrespective of the concentrations of HPMC. When the plasticizer mixtures were used, the ratio of the plasticizer mixtures was kept the same as in *Chapter 4*. From 10%, 20% to 30% HPMC film systems, the plasticizer mixture level decreased from 22.3%, 19.9% to 17.4%. The

---

resulting increasing stiffness of the films suggests in the polymer blend films, plasticizer level is a dominant factor which determines the mechanical strength of the prepared films.

#### 6.4.3 Miscibility Studies-LTA

Localized thermal analysis (LTA) was chosen to study the prepared EC/plasticizer/HPMC films as it provides simultaneous topographical and thermal information of the film surfaces. Rather than the bulk samples, it focuses on specific areas of interest on the films surfaces (Price et al., 1999) by using a nano-thermal probe. Unlike MTDSC or DMA, LTA is a semi-quantitative technique, since the heat transfer of the probes are affected by surrounding conditions. However, it is of wide usages in identifying phase separations and component distribution (Kim et al., 2007; Price et al., 1999). The adhesion images do not always present different phases since the observed adhesions may be a reflection of surface features due to differences in the contact area between the probe and the sample at the bumps and concaves of the film surfaces. Therefore the topography images are presented alongside with the adhesion images.

The topography features of the EC/plasticizer/HPMC films indicate that these films were relatively flat. The adhesion images had features which corresponded to the topography images, but did not represent different phases. When LTA was performed in the selected areas, two distinct softening temperatures were observed for all film systems, which are associated with EC and HPMC phases respectively. LTA provides a higher sensibility than MTDSC and DMA in this case since the glass transition of HPMC phase was too weak to be observed from either MTDSC or DMA. However, the deviation of the  $T_g$  values was not as satisfying as the results from MTDSC or DMA. This is because LTA is not only a thermal technique but can also be affected by the macroscopic viscosity of the samples

(Six et al., 2003). The macroscopic viscosity of located areas can vary if they are not molecularly dispersed, hence the resulting resistance to the probe tip penetration can be slightly different. Consequently, the observed softening temperatures can be several degrees different even if they are the same phase. Therefore, small increasing or decreasing observed by using MTDSC and DMA is not possible to be detected by using LTA. LTA is able to identify two phases that correspond to EC and HPMC phases respectively.

Before the probe tip experiences a downward deflection, a thermal expansion normally occurs. We can see from the nano-thermal data that some located areas had only one domain (either EC phase or HPMC phase), since one thermal expansion and a consequent downward deflection of the probe cantilever were observed. For some other areas, two thermal expansions and two softening were observed, indicating one phase domain was on top of the other phase domain. These unique phase separation patterns and scales may play a crucial part when deciding the drug release mechanisms.

## **6.5 Conclusion**

This chapter applied a variety of approaches to assess the miscibility, interaction and distribution of the film components. MTDSC provides quantitative information on the miscibility and interactions between EC, plasticizers and HPMC while DMA allows the determination of the thermo-mechanical properties of prepared films. Both of the techniques only allow the analysis of bulk samples. LTA focuses on the topography and adhesion images of the film surfaces and allow the observation of the thermal properties of different phases and their distribution on the film surfaces. All these techniques indicate that OA and DBS are more efficient plasticizers for EC and HPMC than MCT. The chemical structure of the plasticizers, including molecular volume and chain length, may

---

be an important factor that determines the plasticizing efficiency. HPMC does not interact with EC, however the plasticizers may form two phases with EC and HPMC respectively.

The study of miscibility, interaction and phase distribution of EC/plasticizer/HPMC films is extremely important in understanding the drug transport mechanisms and predict the drug release profiles. In next chapter, films after being immersed into drug release mediums are assessed to further understand the significance of phase distribution of these films.

## **CHAPTER 7 DRUG RELEASE MECHANISMS AND MORPHOLOGY OF EC/PLASTICIZER FILMS INCOPORATING A PORE FORMING AGENT**

### **7.1 Introduction**

Dissolution studies of film coated controlled-release formulations have drawn a significant amount of attention (Frohoff-Hülsmann et al., 1999b; Lippold et al., 1989; Ozturk et al., 1990; Schultz and Kleinebudde, 1997; Siepmann et al., 2006). This issue is of great importance since by understanding the underlying drug release mechanisms, one may be able to predict the resulting drug release kinetics and optimize the controlled drug delivery systems.

A drug layering technique was chosen to prepare EC coated pellets due to the various advantages of this approach (Nikowitz et al., 2011), including controlled processability and the ability to incorporate multiple components. The drug layering technique involves drug powder, suspension or solution being applied on to sugar based cores using a centrifugal fluid bed or another coating system. This process leads to the formation of multiple layers of drug particles around the inert cores. These drug layered pellets can be further coated by different polymers. Crystalline drug can be embedded in the film coating, and appear on the surface of the coatings, which may be fragments of the core that arose during the coating process during production (Ringqvist et al., 2003). Therefore, it is necessary to have a layer of seal coating the outside of the drug layer. As the name suggests, seal coating seals the drug inside and prevents drug appearing in film coats as well as drug loss during the next procedure, film coating.

Different types of release mechanism have been reported in the literature for polymer coated solid dosage forms (Ozturk et al., 1990; Schultz and Kleinebudde, 1997; Theeuwes, 1975; Zentner et al., 1985), including drug diffusion through the polymeric network, drug release through water-filled pores caused by cracks or water-soluble excipients, water penetration into the pellets, polymer hydration and swelling, drug dissolution, and osmotic effects generated by the pellet core. A number of mathematical models have also been developed in order to analyze the dissolution data. Ideal delivery of drugs would follow 'zero-order kinetics', wherein blood levels of drugs would remain constant throughout the delivery period. In its simplest form, zero order release can be represented as (Schultz and Kleinebudde, 1997)

$$Q_t = Q_0 + K_0 t \quad \text{Eq 7-1}$$

where  $Q_t$  is the amount of drug released or dissolved at time  $t$ ,  $Q_0$  is the initial amount of drug in solution, which is usually zero, and  $K_0$  is the zero order release constant.

Drug dissolution is also considered to be potentially governed by a first-order process (Ritger and Peppas, 1987)

$$\text{Log}Q_t = \text{Log}Q_0 + K_f t / 2.303 \quad \text{Eq 7-2}$$

where  $Q_t$  is the amount of drug released or dissolved at time  $t$ ,  $Q_0$  is the initial amount of drug in solution, which is usually zero, and  $K_f$  is the first order release constant. This equation in accordance with other rate law equations, predicts a first order dependence on the concentration gradient between the static liquid layer next to the solid surface and the bulk liquid.

The Hixson-Crowell cube root law describes the release from systems where there is a change in the surface area and diameter of particles or tablets. For a drug powder

consisting of uniformly sized particles, this equations is expressed as the rate of dissolution based on the cube root of the amount of drug released from the dosage form

$$Q_0^{1/3} - Q_t^{1/3} = K_{HC}t \quad \text{Eq 7-3}$$

where  $K_{HC}$  is the release rate constant for the Hixson-Crowell model.

Many controlled-release products are designed on the principle of embedding the drug in a porous matrix. Drug release medium penetrates the matrix and dissolves the drug, which then diffuses into the medium. Higuchi derived an equation to describe the release of a drug from an insoluble matrix as the square root of a time-dependent process based on Fickian diffusion (Higuchi, 1967), presented as

$$Q_t = K_H t^{1/2} \quad \text{Eq 7-4}$$

where  $K_H$  is the release rate constant for the Higuchi model. Ideally, we should be able to relate the drug release profiles to these existing mathematical models, in order to thoroughly understand the underlying drug release principles and optimize controlled-release formulations.

The aim of this chapter is to better understand the underlying drug release mechanisms from pellets prepared using drug layering technique. The drug release behaviour of EC cast films that incorporated with oleic acid (OA), dibutyl sebacate (DBS) or medium chain triglycerides (MCT) and/or the pore former, hydroxypropyl methylcellulose (HPMC), were studied by means of the standard BP II rotating basket dissolution method. The morphology of the prepared pellets before the drug release was examined by using SEM. In parallel, for the stimulated film dissolution studies, the prepared films were immersed into the drug release mediums with different pH values. After different time intervals, the

resulting films were then dried and tested using SEM and MTDSC in order to investigate the changing of the cast films during dissolution studies.

## 7.2 Methodology

### 7.2.1 Simulated Dissolution Studies on the Cast Films

Morphology and thermal properties of free films before and after they were immersed into the release medium were examined. The prepared films were then cut into 50×50 mm square pieces and immersed into 200 mL DI water, pH 1.2 and 6.8 buffers, respectively. The pH 1.2 buffer was prepared by placing 250 mL of 0.2 M sodium chloride into a 1000 mL volumetric flask, adding 425 mL of 0.2 M hydrochloric acid, then diluting to 1000 mL with DI water. 0.2 M sodium chloride solution was made by dissolving 11.69 g sodium chloride (Fisher Scientific Ltd. UK) into 1 L of DI water in a volumetric flask. 0.2 M hydrochloric acid solution was prepared by diluting 37% hydrochloric acid (M=36.46g/mol, 1.19 kg) purchased from Sigma Aldrich Co. (UK). Phosphate buffer pH 6.8 was made by placing 250 mL of 0.2 M sodium dihydrogen phosphate in a 1000 mL volumetric flask, adding 112 mL of 0.2 M sodium hydroxide, then diluting to 1000 mL with DI water. 0.2 M sodium dihydrogen phosphate solution was prepared by dissolving 31.2 g sodium dihydrogen phosphate (Sigma Aldrich Co., UK) into 1 L DI water in a volumetric flask. 0.2 M sodium hydroxide solution was prepared by dissolving 8 g sodium hydroxide (Fisher Scientific Ltd., UK) into 1 L DI water. The films were taken out at time intervals of 0, 2, 8 and 24 hours, dried in a silica gel desiccator for 24 hours. MTDSC and SEM were then performed on these films.

---

### 7.2.2 MTDSC Studies

MTDSC (Q2000, TA Instruments, USA) was carried out on the prepared samples from the simulated dissolution studies. After taken out from the medium at 2, 8 and 24 hours and then dried under appropriate conditions. All the samples were heated from room temperature to 220°C at 2°C/min with amplitude of  $\pm 0.5^\circ\text{C}/40\text{s}$  in the standard aluminium pans (TA Instruments, USA). MTDSC was calibrated before used. All the runs were completed in triplicate.

### 7.2.3 Morphology Studies

The samples prepared following 7.3.3 were gold coated by a Polaron SC7640 sputter gold coater manufactured by Quorum Technologies. The thickness of the gold coating is about 15 nm. The imaging process was performed in a high vacuum environment. Imaging process was performed with a JEOL JSM5900 LV SEM (Japan), mounted with a tungsten filament with an acceleration voltage of 5 – 20 kV.

### 7.2.4 Pellet Coating Process

The coated pellets for dissolution studies were prepared using a drug layering technique. The sugar beads SureSpheres<sup>TM</sup> (1000 – 850  $\mu\text{m}$ , Colorcon Ltd., USA) was coated as the substrate using a bench-top fluid-bed tablet and spheroid (pellet) Coater/Drier (Caleva Process Solutions, UK). The binding liquids of HPMC (6 cP, Colorcon Ltd., USA) solutions with selected model drugs and the seal coating suspensions of talc (Fisher Scientific Ltd., UK) and HPMC (6 cP) were applied onto the sugar beads. The drug coated pellets were consequently dried in the Mini Coater/Drier for 30 minutes. The film coating solutions were prepared in the same way as the solutions for the cast films, using ethanol/water (90:10 v/v) as the solvent system, described in *section 2.2*. 10% (w/w)

plasticizer and 20% (w/w) HPMC were added to EC films. The pellets were weighed before the film coating process and 8% weight gain was controlled. The detailed coating parameters for drug layering, seal coating and film coating have been introduced in *Chapter 2*. The pellets were placed in the desiccator for 24 hours to equilibrate before further testing.

### 7.2.5 Dissolution Studies

Dissolution testing was performed in a BP apparatus 1 (DIS 8000, Copley Scientific Ltd., UK). The bath temperature was controlled at  $37\pm 0.5^{\circ}\text{C}$  and the baskets with 2 g pellets were rotated at 100 rpm in 900 mL DI water. 10 mL of the sample volume was withdrawn at 0, 0.5, 1, 2, 4, 6, 8, 10, 12 and 24 hours, and replaced with 10 mL fresh medium maintain at the same temperature. After filtration through a 0.2  $\mu\text{m}$  Springe filter (Sartorius Stedim Biotech S.A., UK), the absorbance of the samples were determined by UV spectrometer at the wavelength of the APIs. All dissolution experiments were carried out in triplicate and the average values of the absorbance were used to plot the dissolution curves.

## 7.3 Results

### 7.3.1 Simulated Dissolution Studies on the Cast Films

The morphology and thermal properties of free films after they were immersed into the DI water, pH 1.2 and pH 6.8 buffers for 0, 2, 8 and 24 hours were examined. This would help understanding the drug release mechanisms of API pellets coated by prepared film formulations.

## 7.3.1.1 MTDSC Studies

Free cast films were immersed into DI water, pH 1.2 and pH 6.8 buffers, respectively. Samples were taken out at 0, 2, 8 and 24 hours intervals. After drying, MTDSC experiments were then conducted. *Figure 7-1* shows the reversing heat flow signals of EC films with 10%, 20% and 30% HPMC taken out from DI water at sampling interval 0 and 24 hours, and *Figure 7-2* shows those of films taken out from pH 1.2 and pH 6.8 buffers at 24 hours (2 and 8 hours sampling data not shown). The  $T_g$  values of EC films remained in the range of 127-130°C, irrespective of the HPMC concentration, pH values or immersion period. This is further confirming that HPMC does not interact with EC. Therefore the detected  $T_g$  values were only associated with the  $T_g$  of EC, which was not affected by HPMC concentrations, pH values or immersion period.

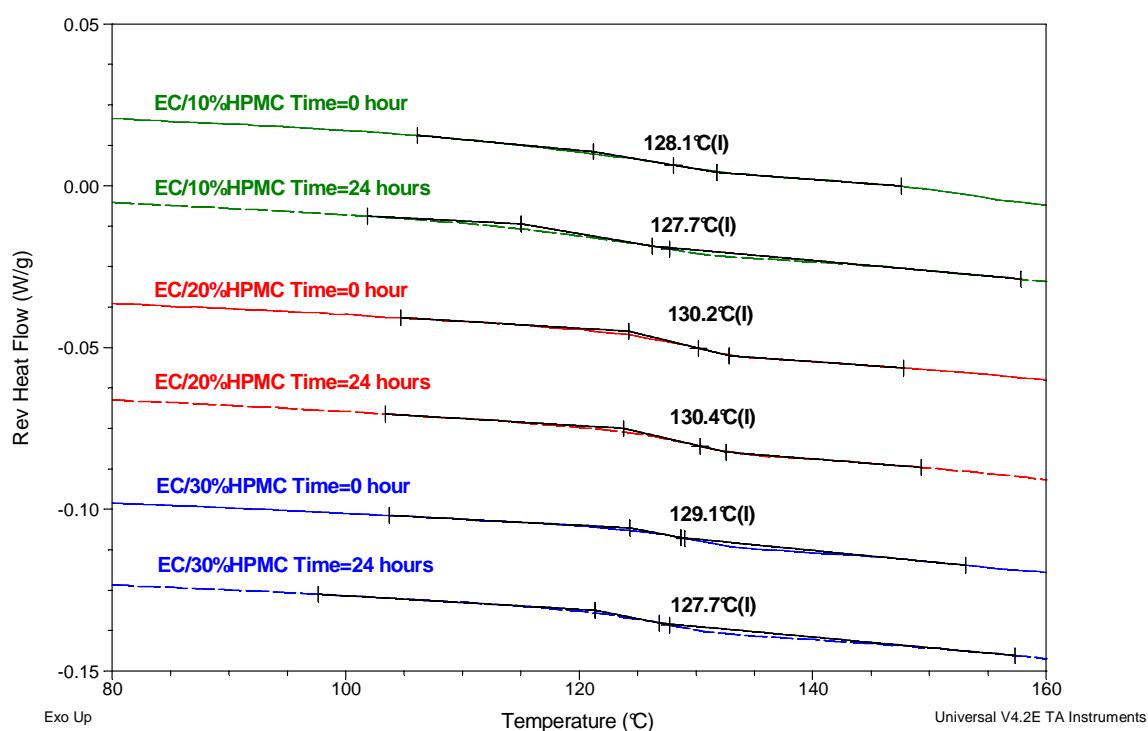


*Figure 7-1 Reversing heat flow signals of EC films with 10%, 20% and 30%HPMC before and after immersion into DI water for 24 hours*

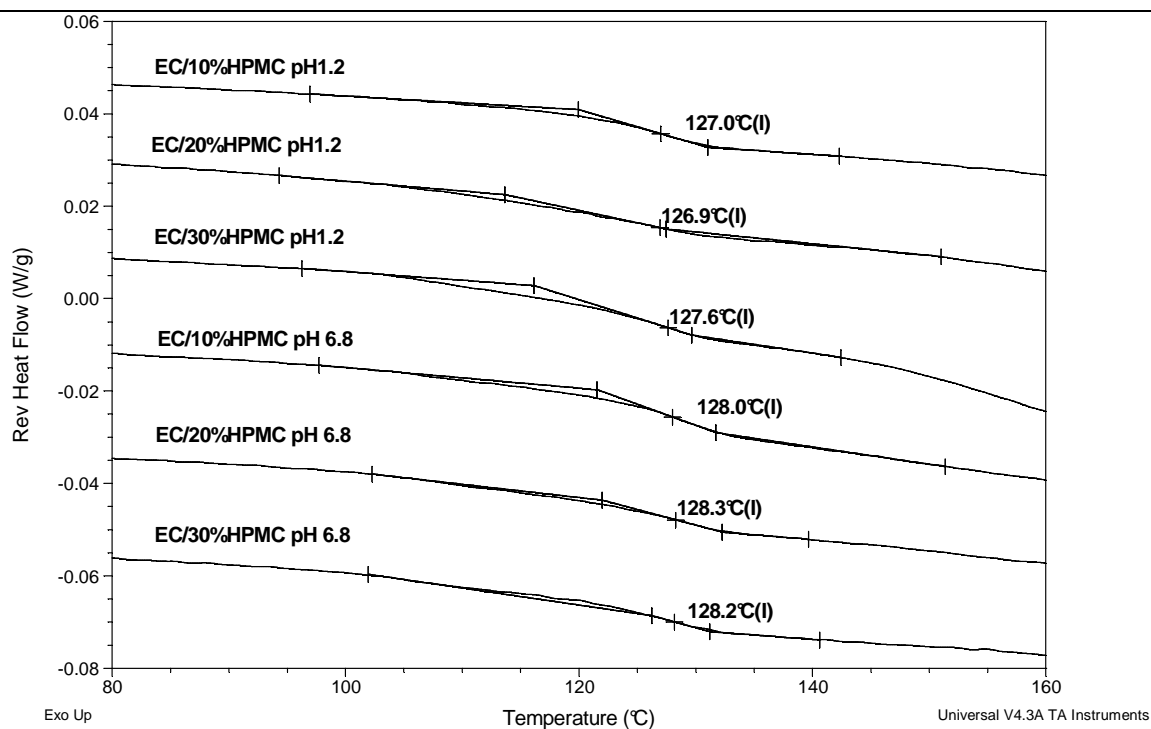
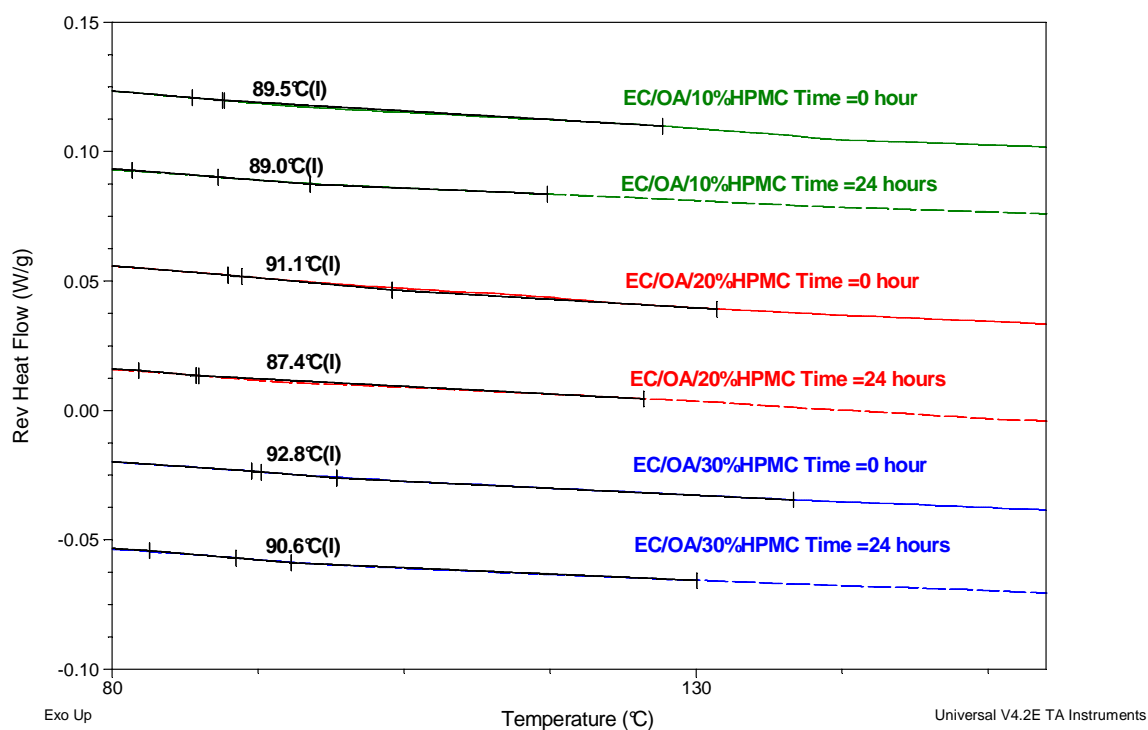


Figure 7-2 Reversing heat flow signals of EC films with 10%, 20% and 30%HPMC after immersion into pH1.2 and pH6.8 buffers for 24 hours

Figure 7-3 and Figure 7-4 shows the reversing heat flow signals of EC/10% OA films with 10%, 20% and 30% HPMC taken out from DI water, pH 1.2 and pH 6.8 buffers, respectively, at sampling interval 0 and 24 hours (2 and 8 hours sampling data not shown). The  $T_g$  values of EC/OA/HPMC films decreased up to 6°C after being placed in the release media, irrespective of the pH values. MTDSC could only detect one  $T_g$  value which has been ascribed to the  $T_g$  of EC/OA phase. The lowering of this  $T_g$  value suggests a change in terms of the phase components. It is possibly due to the moisture residue after drying of these films, hence water plasticization occurred. TGA was carried out on some randomly chosen samples. Less than 2% water residue was observed (data not shown). Therefore, it is possible that this slightly lowering in  $T_g$  values was a result of the water plasticization.

A similar decrease of the  $T_g$  values of EC/DBS/HPMC films after exposure to DI water, pH 1.2 and pH 6.8 buffer for 24 hours is presented in *Figure 7-5* and *7-6*. However, for EC/MCT/HPMC films, this decreasing trend was not consistent with all systems, shown in *Figure 7-7* and *7-8*. This is probably because MCT has a structure of 6-12 C. The variety of the chain length may result in slightly different  $T_g$  values, hence a more significant standard deviation.



*Figure 7-3* Reversing heat flow signals of EC/OA films with 10%, 20% and 30%HPMC before and after immersion into DI water for 24 hours

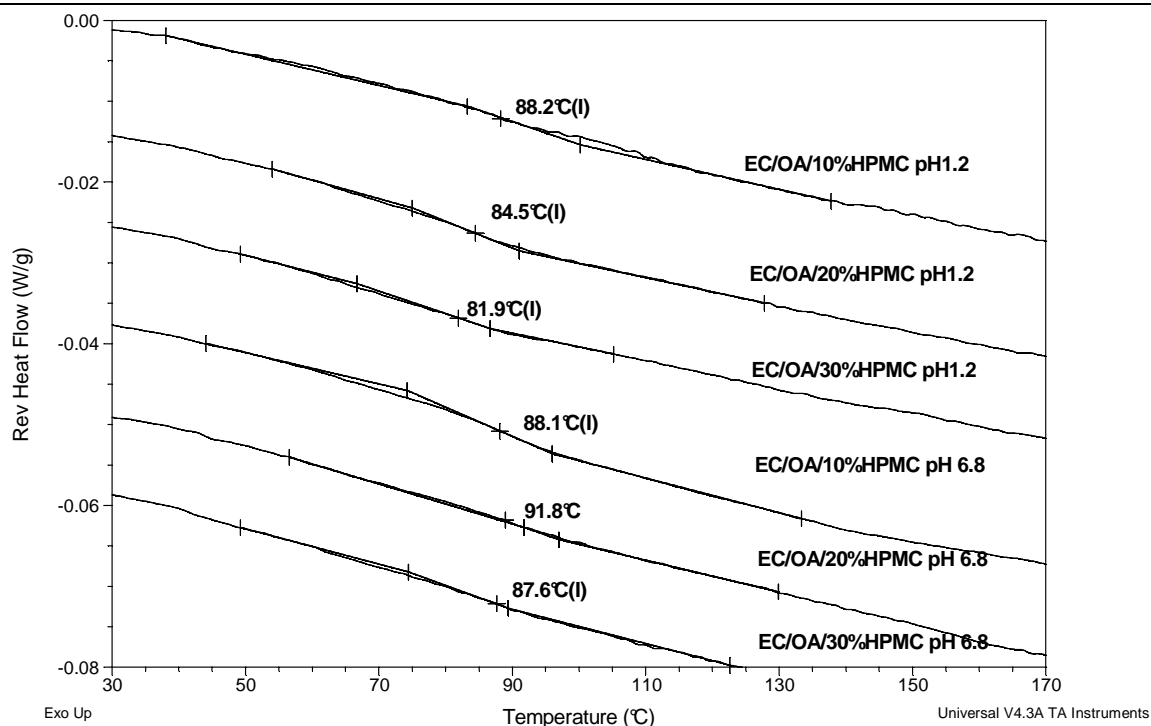


Figure 7-4 Reversing heat flow signals of EC/OA films with 10%, 20% and 30%HPMC after immersion into pH 1.2 and pH 6.8 buffers for 24 hours

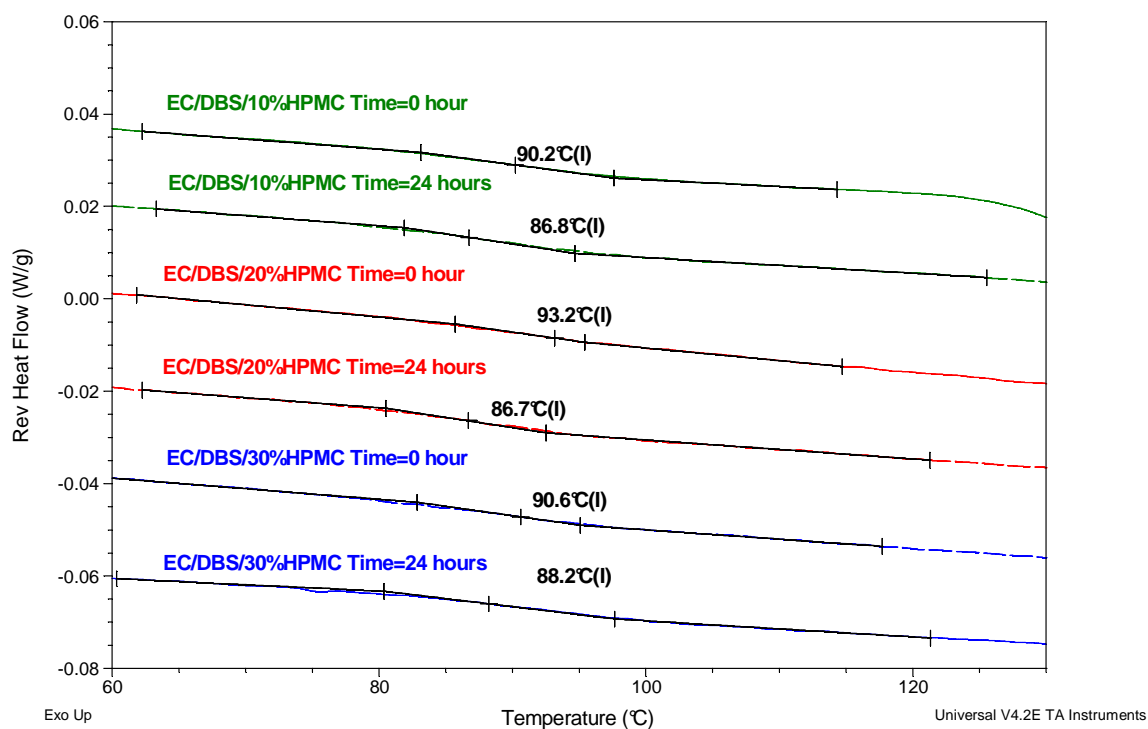


Figure 7-5 Reversing heat flow signals of EC/DBS films with 10%, 20% and 30%HPMC before and after immersion into DI water for 24 hours

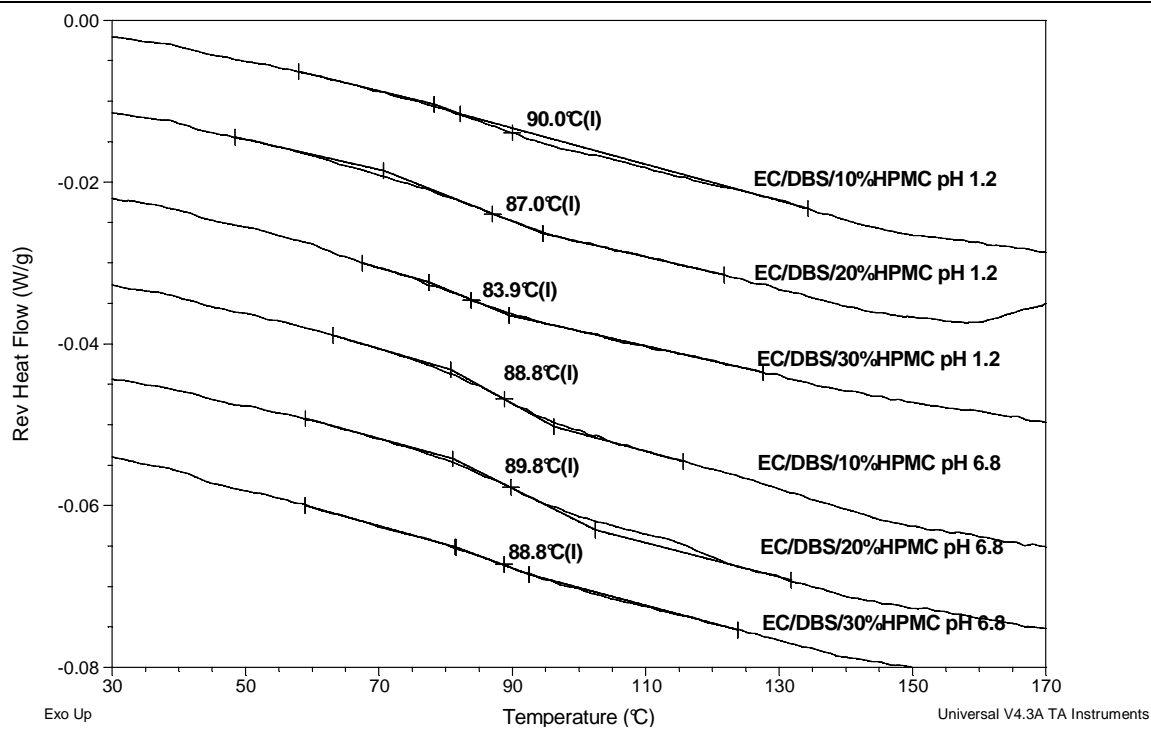


Figure 7-6 Reversing heat flow signals of EC/DBS films with 10%, 20% and 30%HPMC after immersion into pH 1.2 and pH 6.8 buffers for 24 hours

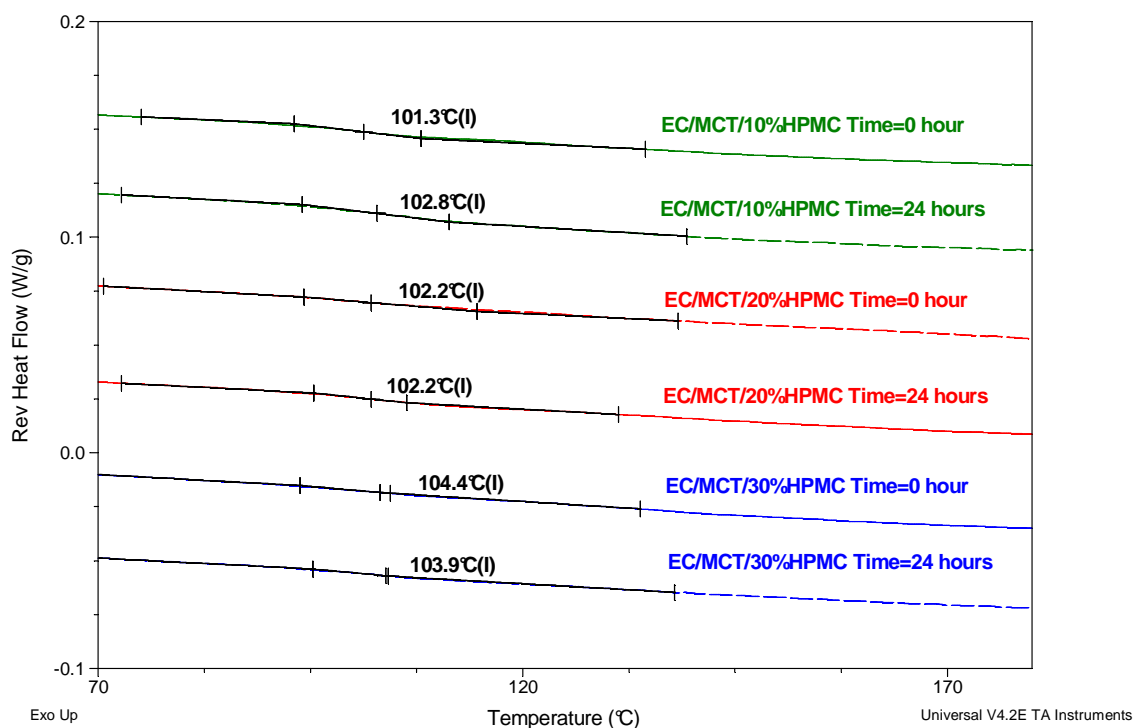


Figure 7-7 Reversing heat flow signals of EC/MCT films with 10%, 20% and 30%HPMC before and after immersion into DI water for 24 hours

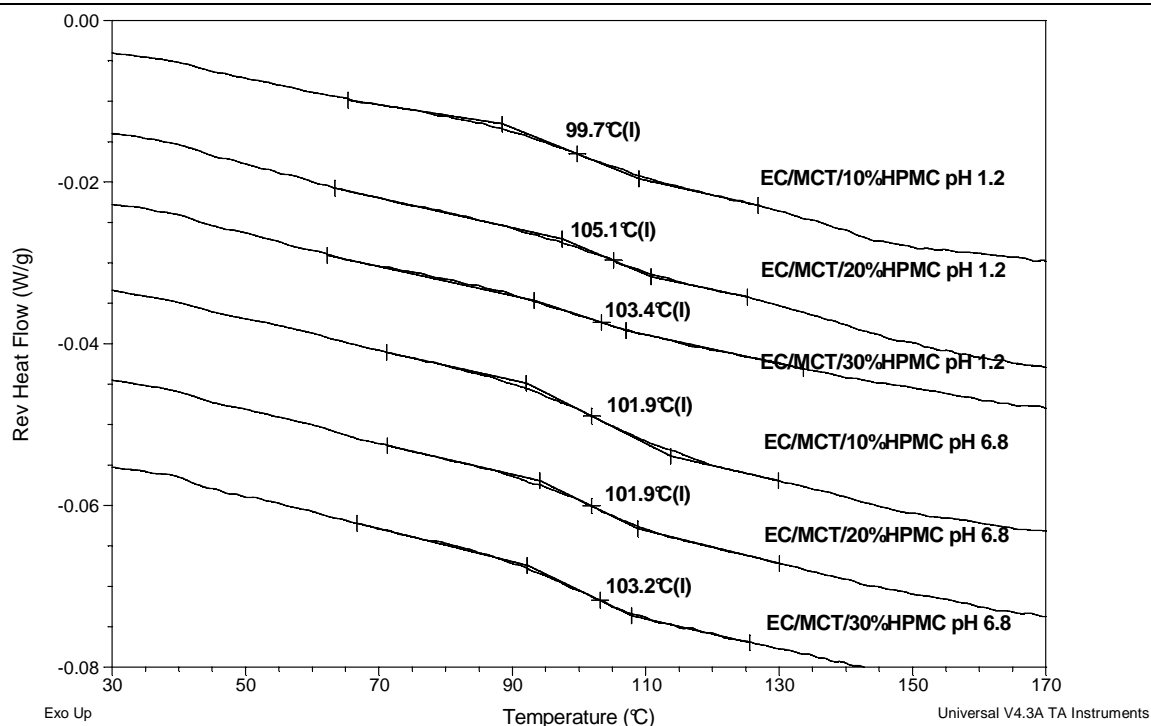


Figure 7-8 Reversing heat flow signals of EC/MCT films with 10%, 20% and 30%HPMC after immersion into pH 1.2 and pH 6.8 buffers for 24 hours

### 7.3.1.2 Morphology of Cast Films

Figure 7-9 compares the scanning electron micrographs of EC films with 10%, 20% and 30% HPMC after in contact with DI water for 0, 2, 8 and 24 hours. At time zero, i.e. before contacting with release medium, EC/HPMC films looked similar, in spite of the concentrations of HPMC. At  $t=2$  hours, small pores were generated on the films surfaces. After 8 hours in DI water, for the EC/10% HPMC films, some slightly larger pores remained, others looked like ‘dents’ on the film surfaces, indicating the HPMC on the surfaces dissolved completely. After 24 hours, the pores became slightly larger again, but not dramatically. For the higher concentration HPMC films, the dissolution of HPMC was obvious. Hence, significant hollows appeared on the film surfaces.

---

SEM images of EC/OA films with 0%, 10%, 20% and 30% HPMC removed from DI water at  $t=0$ , 2, 8 and 24 hours are presented in *Figure 7-10*. EC/OA films without HPMC exhibited no signs of pores and remained similar at all the time intervals. This indicates the OA may not migrate on the film surfaces or dissolve into water. Before dissolution, surfaces of EC/OA/HPMC films seemed smoother than those without OA, suggesting the plasticizing effect of OA. After dissolution, at 10% HPMC level, the pores that HPMC left were in the circle shapes and became outstanding. At 20% and 30% levels, those pores generated by HPMC were in irregular shapes. The difference between the morphology of 10% HPMC and higher level HPMC systems is indicating that the HPMC concentration has an effect on the distribution of EC and HPMC phases, which has been suggested in *Chapter 5*. From these images, we can see that HPMC dissolved quickly in the first two hours.

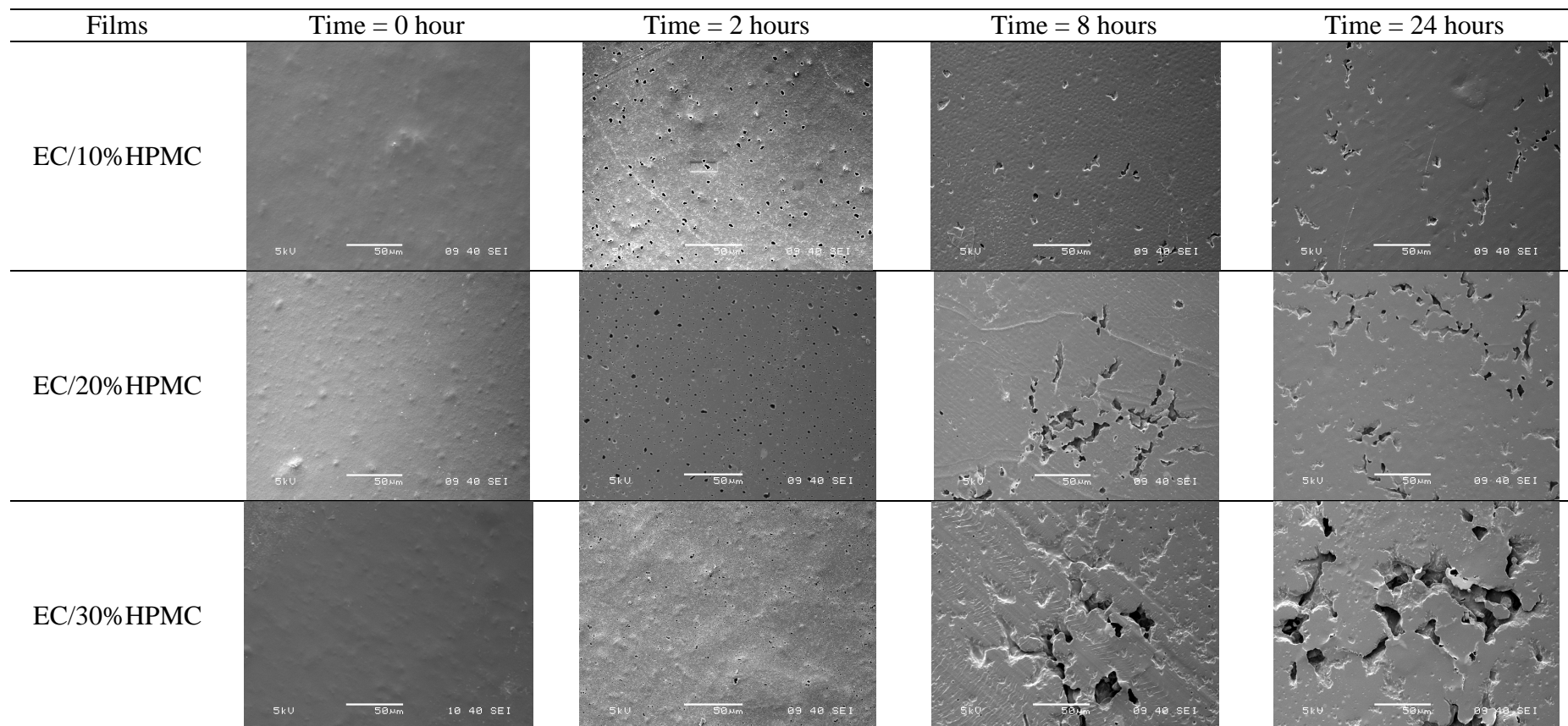


*Figure 7-9 SEM images of EC films with 10%, 20% and 30% HPMC removed from DI water at time=0, 2, 8 and 24 hours*

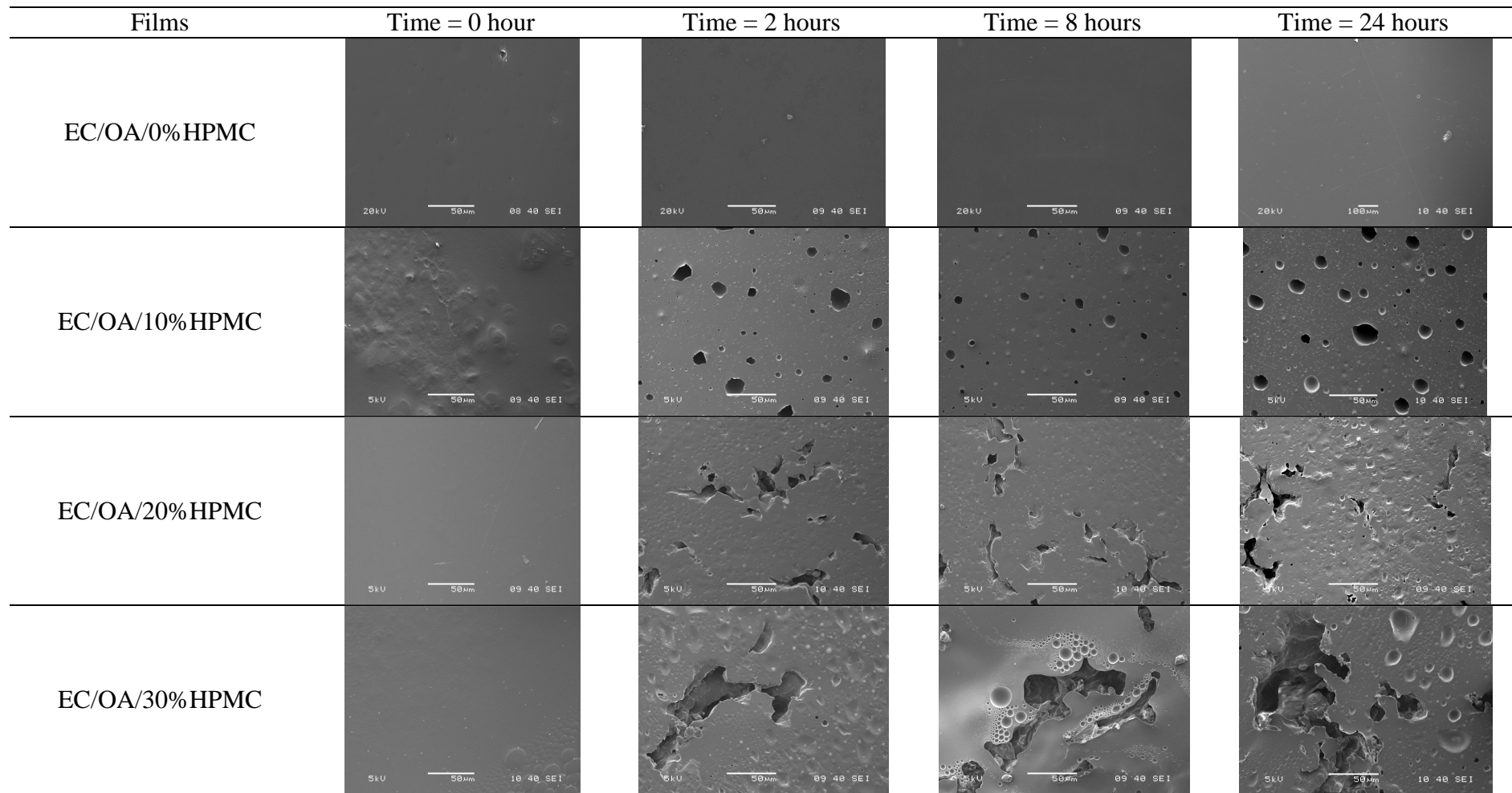


Figure 7-10 SEM images of EC/OA films with 10%, 20% and 30% HPMC removed from DI water at time=0, 2, 8 and 24 hours

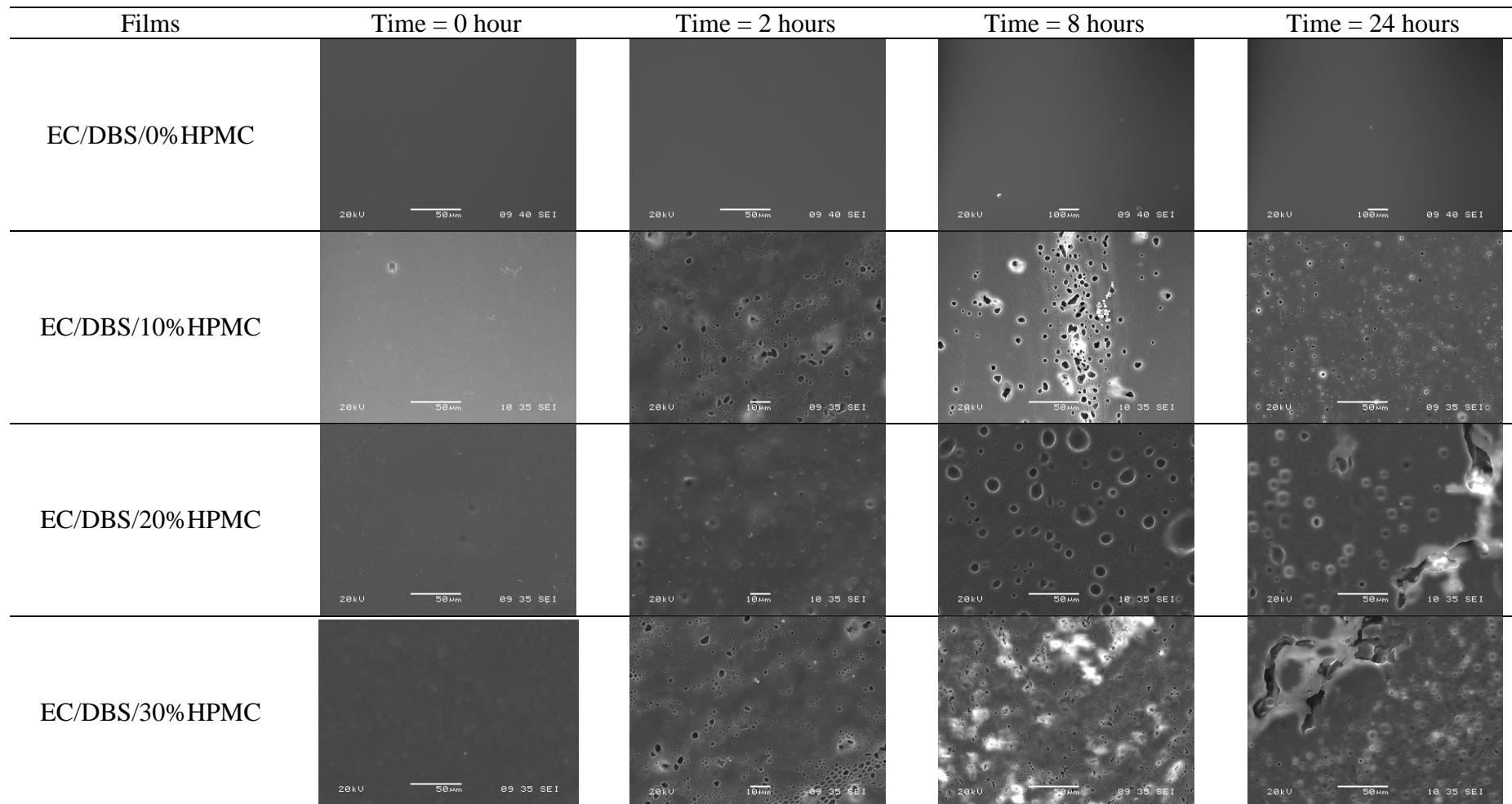


Figure 7-11 SEM images of EC/DBS films with 10%, 20% and 30% HPMC removed from DI water at time=0, 2, 8 and 24 hours

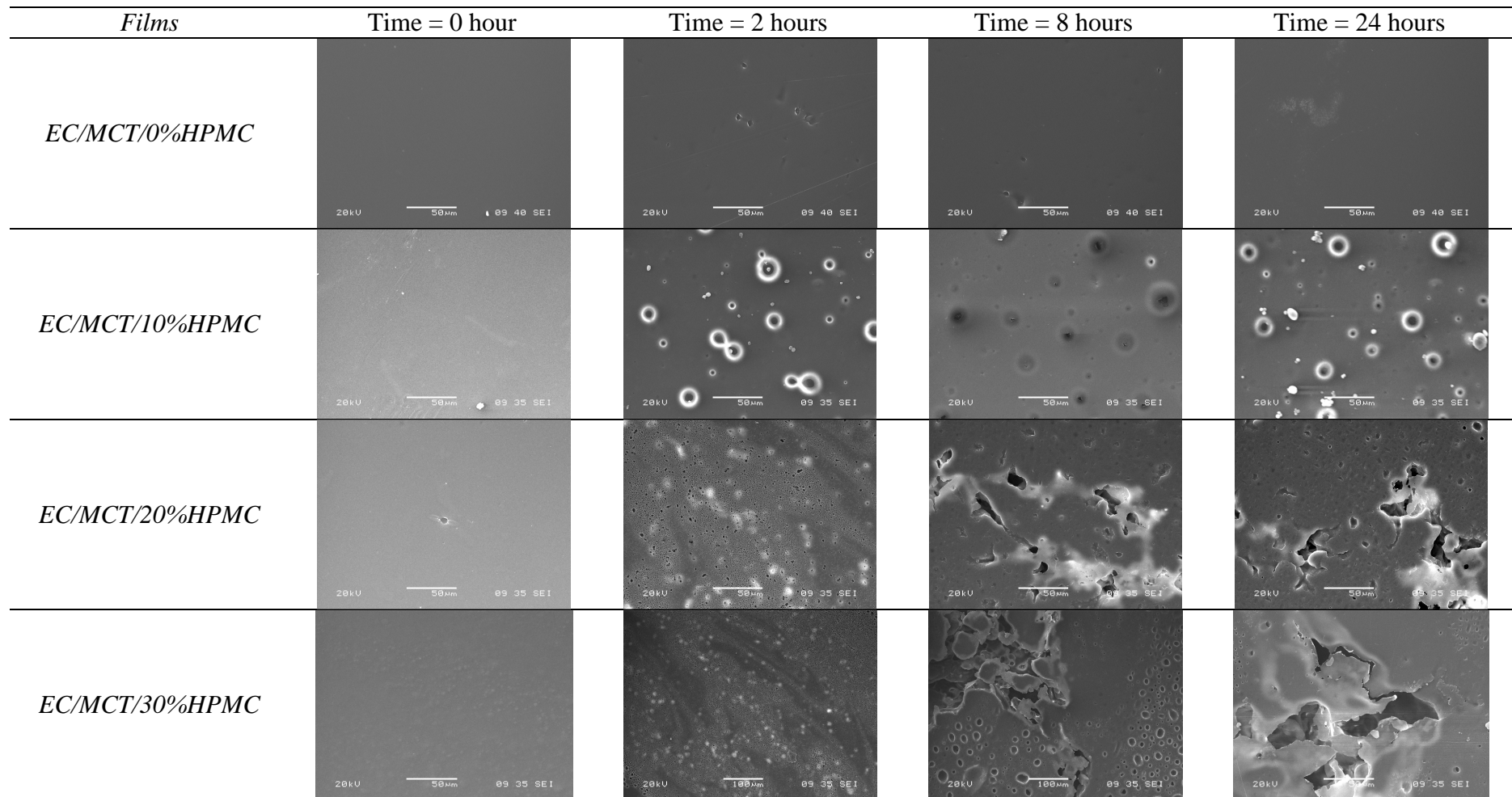


Figure 7-12 SEM images of EC/MCT films with 10%, 20% and 30% HPMC removed from DI water at time=0, 2, 8 and 24 hours

---

### 7.3.2 Morphology of Coated Pellets

The SureSpheres® sugar pellets were coated by the prepared API binding solutions and seal coat suspensions, following coated by the EC/plasticizer or EC/plasticizer/HPMC solutions as described in methodology. After drying, the coated pellets were examined using SEM. *Figure 7-13* shows the scanning electron micrographs of pellets coated by EC/OA, EC/DBS, EC/MCT, EC/OA/HPMC, EC/DBS/HPMC and EC/MCT/HPMC films. In general, the coated API pellets seemed undulating and rough as well as containing some surface debris, which is probably due to the pellet-pellet contact and the mutual rubbing. Those pellets coated by EC/plasticizer films seemed homogeneous and relatively smooth, compared with those coated by EC/plasticizer/HPMC films. This is probably due to the water content in the formulation of the EC/plasticizer/HPMC film coatings. It has been predicted that the water-based film coating formulations with a higher viscosity than organic solvent-based formulations would produce rougher films (Rowe, 1988). The shear stresses applied to the film coating formulation on drying may also have an impact on the roughness of the coated pellets. A thicker coating layer may facilitate better quality of surfaces of the coated pellets (Nikowitz et al., 2011). Study of the morphology of the coated pellets after dissolution was attempted. However, the pellets were difficult to handle and probably damaged by operation before SEM tests due to their softness.

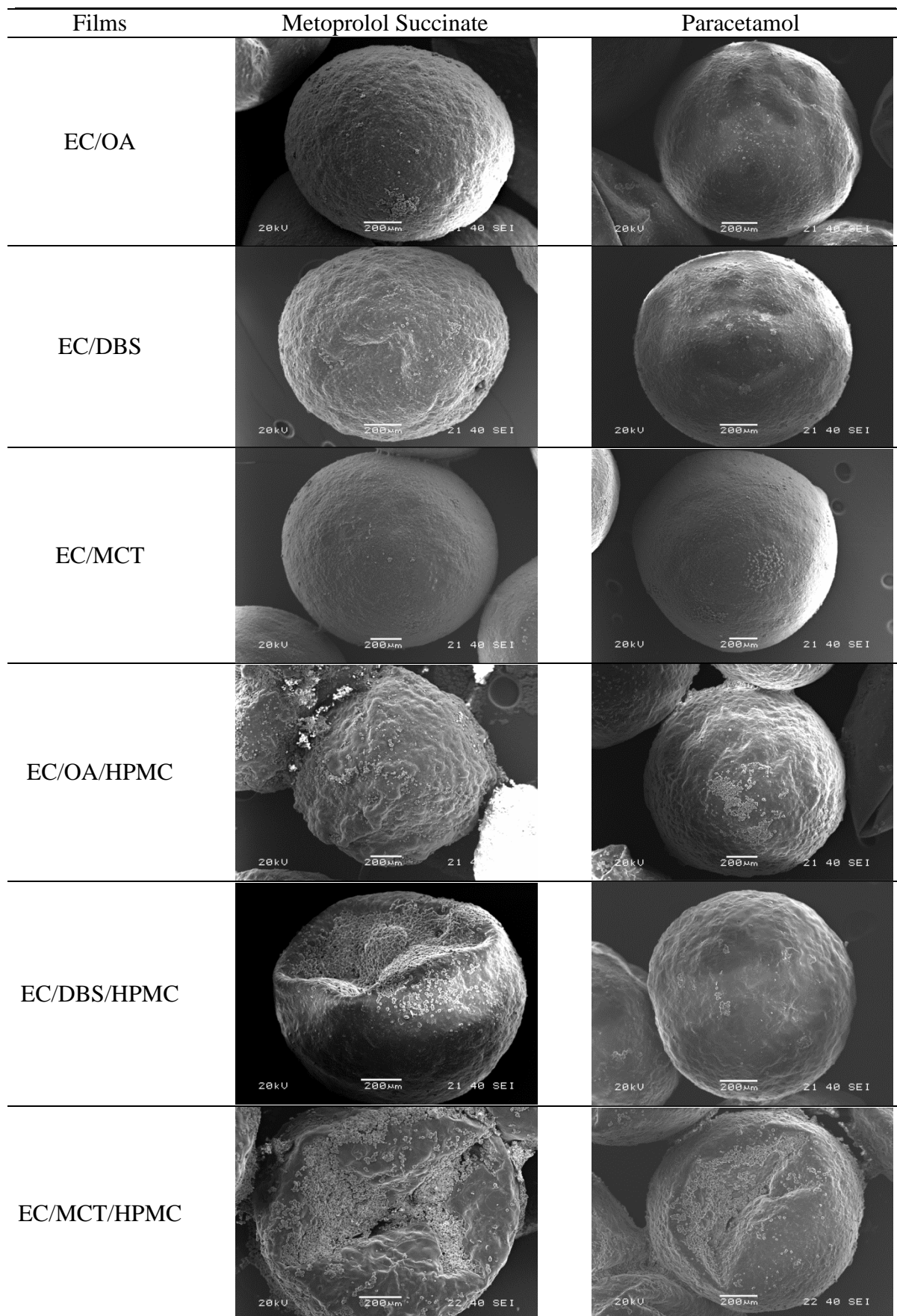


Figure 7-13 Morphology of API pellets coated by EC/10% plasticizer and EC/10% plasticizer/20% HPMC films

---

### 7.3.3 Drug Release from Coated Pellets

Metoprolol succinate and paracetamol were used as the model drugs to investigate the drug release profiles. The standard calibration curves of APIs in distilled water have been shown in *Chapter 2*.

#### 7.3.3.1 Metoprolol Succinate as the Model Drug

The percentage cumulative release profiles of metoprolol succinate from EC/10% plasticizer and EC/10% plasticizer/20% HPMC films are shown in *Figure 7-14*. Drug release from EC/10% plasticizer films was less than 30% after 24 hour releasing. Using OA or DBS as the plasticizer did not have a great impact on the drug release profiles, whereas the incorporation of MCT resulted in slightly slower drug release profile than those with OA and DBS. EC/OA/HPMC films produced the fastest drug release rate, releasing 100% of the initial amount of metoprolol succinate present by 8 hours. Drug release from EC/OA/HPMC films reached 100% after 10 hours releasing, however, EC/MCT/HPMC films did not produce 100% release at 24 hours.

The drug release profiles of metoprolol succinate from coated pellets in the first 12 hours were fitted into four different drug release models introduced in *Section 7.1*, including zero-order, first-order, Hixson-Crowell and Higuchi models, shown as *Eq 7-1, 7-2, 7-3 and 7-4*. *Table 7-1* shows the values of  $R^2$  and drug release constant  $K$  of the fitting results for each model respectively. By comparing the fitting results from different models, the one with  $R^2$  value closest to 1 would be the best fit. Metoprolol succinate is a water soluble drug with a solubility of 157 mg/mL (Ravishankar et al., 2006). When the pore former HPMC was not incorporated, approximately 30% metoprolol succinate was released according to a zero-order kinetic with  $R^2$  around 0.99. When HPMC was added to the EC/plasticizer films, the best model to fit the drug release data was the Higuchi model,

with  $R^2$  around 0.97. Therefore, zero-order and Higuchi model were the best fit for EC/plasticizer and EC/plasticizer/HPMC films.

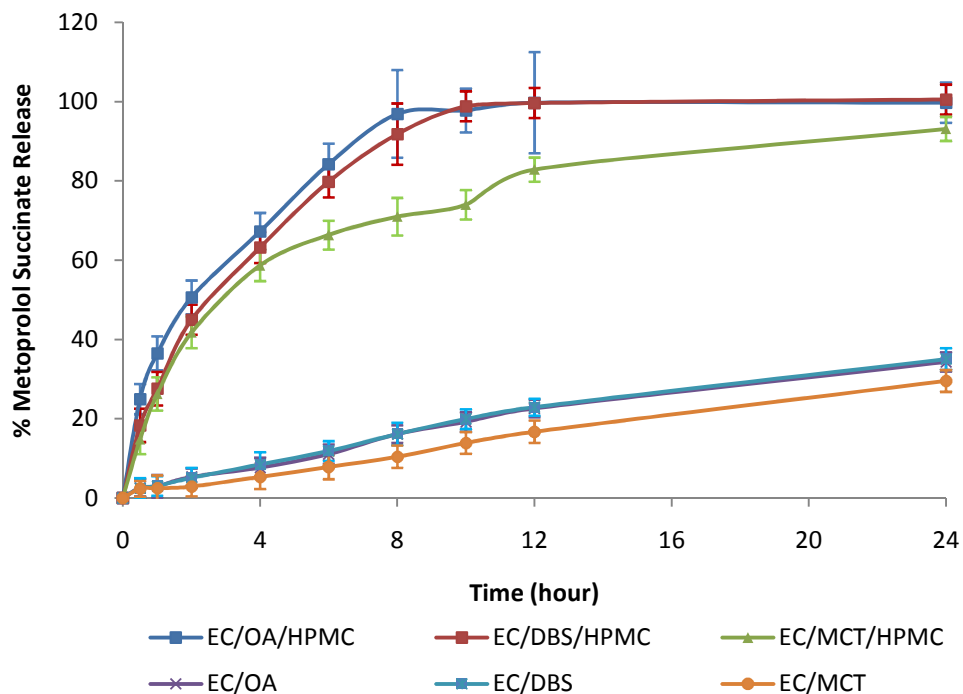


Figure 7-14 The percentage cumulative release profiles of metoprolol succinate from pellets coated with EC/OA, EC/DBS, EC/MCT, EC/OA/HPMC, EC/DBS/HPMC and EC/MCT/HPMC films up to 24 hours

Fitting Models	EC/OA		EC/DBS		EC/MCT		EC/OA/HPMC		EC/DBS/HPMC		EC/MCT/HPMC	
	R <sup>2</sup>	K										
Zero-order	0.994	1.774	0.998	1.813	0.987	1.274	0.897	6.525	0.918	7.197	0.873	5.305
First-order	0.940	0.187	0.931	0.189	0.977	0.180	0.802	0.108	0.799	0.132	0.723	0.119
Hixson-Crowell	0.975	0.128	0.970	0.129	0.983	0.112	0.839	0.139	0.846	0.164	0.779	0.138
Higuchi	0.953	7.309	0.966	7.506	0.921	5.180	0.972	28.59	0.983	31.34	0.961	23.42

*Table 7-1 The values of R<sup>2</sup> and K (drug release constant) of drug release profiles of metoprolol succinate from pellets coated by EC/OA, EC/DBS, EC/MCT, EC/OA/HPMC, EC/DBS/HPMC, and EC/MCT/HPMC films, obtained from dissolution model fitting, including zero-order, first-order, Hixson-Crowell and Higuchi models, according to Eq 7-1, 7-2, 7-3 and 7-4*

### 7.3.3.2 Paracetamol as the Model Drug

When paracetamol was used as a model drug, EC/OA/HPMC films produced the fastest drug release again, however, only up to 90% of the initial model drug present. The drug release from EC/DBS/HPMC and EC/MCT/HPMC films was slightly slower. Incomplete drug release is probably due to the solubility of paracetamol (14.9 mg/mL) (Granberg and Rasmuson, 2000) being lower than that of metoprolol succinate (157 mg/mL) (Ravishankar et al., 2006), since metoprolol succinate had 100% drug release using the same film coating formulations.

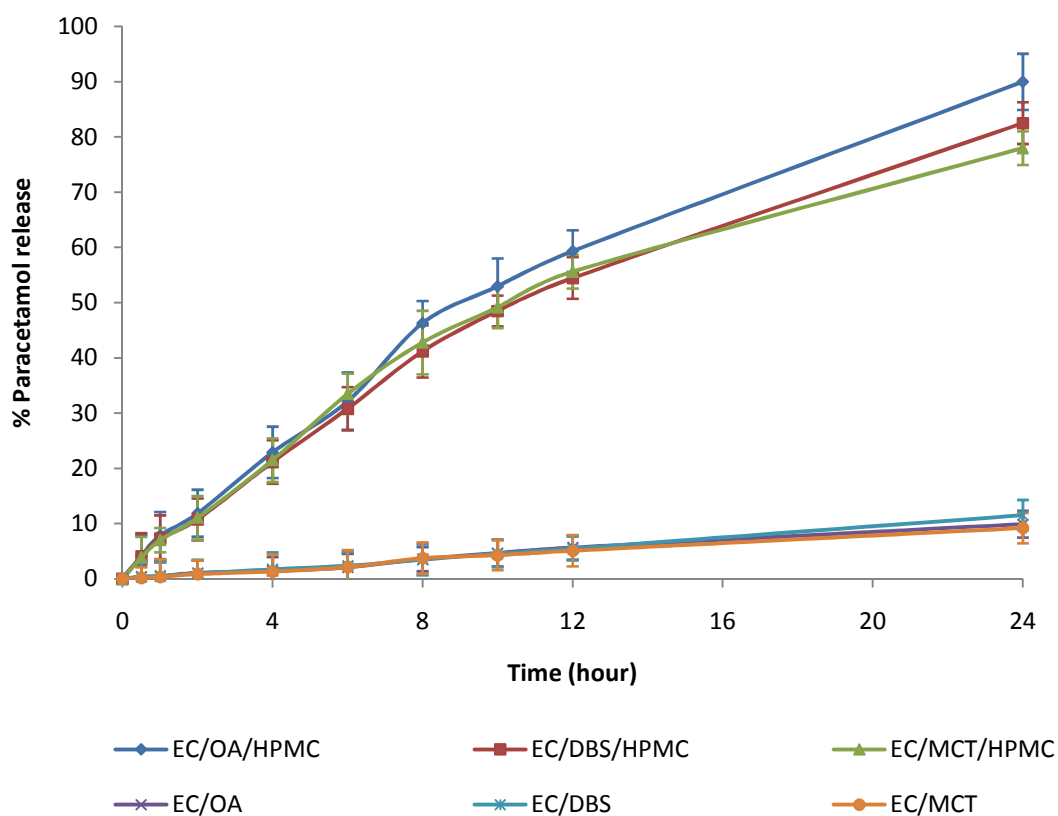


Figure 7-15 The percentage cumulative release profiles release profile of paracetamol from pellets coated with EC/OA, EC/DBS, EC/MCT, EC/OA/HPMC, EC/DBS/HPMC and EC/MCT/HPMC films up to 24 hours

Fitting Models	EC/OA		EC/DBS		EC/MCT		EC/OA/HPMC		EC/DBS/HPMC		EC/MCT/HPMC	
	R <sup>2</sup>	K										
Zero-order	0.976	0.458	0.992	0.445	0.984	0.441	0.991	4.958	0.994	4.522	0.990	4.647
First-order	0.935	0.225	0.927	0.222	0.871	0.268	0.882	0.213	0.885	0.210	0.873	0.215
Hixson-Crowell	0.976	0.090	0.976	0.089	0.950	0.098	0.941	0.194	0.942	0.187	0.932	0.191
Higuchi	0.909	1.861	0.939	1.823	0.940	1.817	0.977	20.71	0.980	18.90	0.984	19.50

*Table 7-2 The values of R<sup>2</sup> and K (drug release constant) of drug release profiles of paracetamol from pellets coated by EC/OA, EC/DBS, EC/MCT, EC/OA/HPMC, EC/DBS/HPMC, and EC/MCT/HPMC films, obtained from dissolution model fitting, including zero-order, first-order, Hixson-Crowell and Higuchi models, according to Eq 7-1, 7-2, 7-3 and 7-4*

Drug release fitting was subsequently carried out on the release data of paracetamol from pellets coated by EC/OA, EC/DBS, EC/MCT, EC/OA/HPMC, EC/DBS/HPMC and EC/MCT/HPMC films in the first 12 hours. As seen in *Table 7-2*, for the pellets coated by EC/plasticizer films, zero-order kinetic was the best fit with  $R^2$  around 0.99, whereas for the pellets coated by EC/plasticizer/HPMC films, the drug release data were also following the zero-order release pattern with  $R^2$  around 0.99. Even though when HPMC was incorporated the drug release rates were much higher than those from pellets coated with EC/plasticizer films, the release mechanism did not change. This is probably due to the relatively lower solubility of paracetamol (14.9 mg/mL) (Granberg and Rasmuson, 2000). This suggests the drug release mechanism was not only controlled by the properties of the film coatings, but also affected by the solubility of the model drugs.

#### **7.4 Discussion**

A type of commercial sugar spheres was chosen to be the pellet core since the type of starter core (sugar cores, MCC cores, sealed sugar cores) did not have a significant effect on the drug release kinetics, irrespective of the type of release medium (Muschert et al., 2009b). Drug release was predominantly controlled by the polymeric membrane barrier, and not by the starter core. Pellets containing drug layered sugar cores revealed smaller changes in the release rate when increasing the osmolality of the release medium than pellets containing MCC cores or sealed sugar cores, irrespective of the type of release medium (Muschert et al., 2009b). Therefore, SureSpheres® was the best choice to prepare the film coated pellets. The roughness of the coated pellets could be due to three aspects: coating formulation, method of application and the roughness of the substrate. Tablet-tablet contact and mutual rubbing have been suggested (Rowe, 1988).

The release data of metoprolol succinate and paracetamol from pellets coated by EC/plasticizer films followed a zero-order release, as shown by linear regression of the drug release data of metoprolol succinate and paracetamol coated pellets. SEM images of these films showed that the plasticizers did not migrate or leak out from the EC/plasticizer films after dissolution. Therefore, it is reasonable to conclude that the drug release from pellets coated by EC/plasticizer films was mainly controlled by the diffusion process of the drug through the continuous plasticized polymer matrix. However, the overall drug release was probably well affected by the solubility of the model drugs, since paracetamol coated pellets only released a third of the drug amount that metoprolol succinate coated pellets released.

The drug release mechanisms of pellets coated by EC/plasticizer/HPMC films were expected to follow first-order or Higuchi models, since these films with 20% HPMC were reasonably hydrophilic. SEM studies of free films after dissolution did show significant amount of pores generated by the dissolution of HPMC. From the data regression fitting results, we can see that the metoprolol succinate release from pellets coated by EC/plasticizer/HPMC films was a Higuchi model release, whereas the paracetamol release from pellets coated by EC/plasticizer/HPMC films was a zero-order release. In both cases, the rate of dissolution of HPMC into the dissolution medium was controlling the rate of drug release and not its rate of diffusion through the films. The thermal properties of polymer films containing plasticizers and pore forming agents give insight in the behaviour of the respective coatings of pellets. During dissolution, the incorporated water did not act as plasticizer, but was only mechanically fixed in pores and channels, and enabled the high permeability of the films. Water insoluble plasticizers mainly remained in the EC films during the exposure to the release medium, whereas HPMC dissolved and migrated from

---

the films. It has been suggested that during the migration of HPMC, the polymer chains of EC squeezed out water from pores and channels and reduced the free volume (Frohoff-Hülsmann et al., 1999a). These films, plasticized with the lipophilic plasticizer and water, have a good mechanical stability. Hence, no flaws or cracks were presented.

A two phase order release model with a fast release at the beginning and a slow release during the second phase has been suggested (Frohoff-Hülsmann et al., 1999b). In the first phase, the drug diffused through water-filled pores and channels after the migration of HPMC. In the second phase, the free volume between the polymer chains was reduced dramatically and therefore the permeability of the films decreases. The drug diffused through a swollen heterogeneous membrane containing EC and DBS. This phenomenon was also revealed for the metoprolol succinate release profile from pellets coated by EC/plasticizer/HPMC films. However, this theory may not be appropriate for all water-soluble drugs. As indicated, the paracetamol release profiles from pellets coated by EC/plasticizer/HPMC films were not a first-order or Higuchi, but a zero-order release. In addition, the drug release data of paracetamol did not show two phase release profiles. Therefore, it is reasonable to conclude that the solubility of paracetamol was hindering its drug release rate, since a limited amount of paracetamol can dissolve in the water influx through the pores and/or channels generated by HPMC. During the constant rate release period a saturated solution of the API is the present within the pellet giving a constant driving force for the release (Borgquist et al., 2002).

Mechanistic mathematical modelling of the drug release from controlled-release pharmaceuticals is an important tool in obtaining information on the mechanisms governing the release process. The use of modelling in the development of new

---

pharmaceuticals allows drug release rates and drug diffusion behaviour through polymers to be predicted (Borgquist et al., 2004; Borgquist et al., 2002). The main release process occurring during the lag phase in pellets coated with a semi-permeable membrane (Menjoge and Kulkarni, 2007).

## 7.6 Conclusion

In summary, the dissolution data of metoprolol succinate from pellets coated by EC/plasticizer films was best fitted into the zero-order release, while those from pellets coated by EC/plasticizer/HPMC films was best fitted into the Higuchi model. When paracetamol was the model drug, the release mechanism was following the zero-order drug release, irrespective of the types of the film coatings. This indicates that the release rate was governed by the dissolution of HPMC within the film and also affected by the drug solubility. It is reasonable to predict the drug release mechanism by correlating the regression of the drug release data and the morphology of the free films before and after exposure to the release mediums. Therefore, it can be concluded that

- a) The release of metoprolol succinate and paracetamol from pellets coated by EC/plasticizer films were probably via the drug diffusion through the continuous plasticized polymeric phase; the drug release rate was mainly governed by the hydration-erosion of the polymeric films;
- b) The release of metoprolol succinate and paracetamol from pellets coated by EC/plasticizer/HPMC films was via the aqueous filled pores generated by the dissolve HPMC; the drug release rate was mainly governed by the rate of HPMC dissolution;

- 
- c) In both the release mechanism, the drug release was also affected by the solubility of the model drugs;

---

## CHAPTER 8 CONCLUSIONS

Ethyl cellulose films are of great significance for controlled release formulations in pharmaceutical industry, due to the hydrophobic characteristics of ethyl cellulose. Even though EC films have been used for decades, the interactions between EC and other film components, such as plasticizers and pore forming agents and their phase distribution are still not fully understood. Consequently, the principal goal of this project was to investigate the thermal, thermo-mechanical and phase distribution properties of EC films with plasticizers and pore forming agents, and understand the release characteristics in relation to these properties.

### 8.1 Thermal Properties of EC and EC Organic Solvent Films

The thermal properties of EC powder were initially investigated. The degradation of EC powder was found to commence at around 250°C. EC 7 and EC 20 were found to have similar values of  $T_g$ . The glass transition of EC powder was subtle and in the range of 110 - 130°C, depending on the measurement mode. Further events were noted at around 180°C, which may be related to oxidative degradation and microcrystalline melting (Lai, 2005).

EC films prepared using ethanol/acetone mixes have shown satisfactory appearances, irrespective of the solid concentrations. MTDSC results showed that the  $T_g$  values for 2.5%, 5.0%, 7.5% and 10% w/w EC 20 films were 122.6°C, 125.6°C, 126.3°C and 129.1°C, respectively. DMA results presented  $T_g$  values between 130.9°C and 133.2°C for these films. Even though the residual solvents of all EC films were less than 0.7% w/w, they could still affect the  $T_g$  of dry films. Therefore, DMA may provide more accurate values of

the  $T_g$  in this case. High level EC films had higher storage modulus and loss modulus, i.e. more viscous and elastic responses when confronting mechanical forces. Therefore it is reasonable to conclude that the mechanical properties of EC films can also be affected by the concentrations of EC within the films.

## 8.2 Plasticizing Efficiency of OA, DBS and MCT

OA, DBS and MCT, as lipophilic plasticizers, are expected to reduce the  $T_g$  values of EC films. However, their original  $T_g$  values have not been published in the literature and could not be obtained by using DSC, MTDSC or hyper DSC. By using the Gordon Taylor/Simha Boyer equations, one could estimate the  $T_g$ s of OA, DBS and MCT as  $-75^\circ\text{C}$ ,  $-77^\circ\text{C}$  and  $-50^\circ\text{C}$  respectively. The plasticizing efficiency of plasticizers is one of the criteria that have been used to evaluate a plasticizer for a polymer. It has been presented in this thesis in the format of reduced the  $T_g$  values ( $\beta$ ), i.e.  $T_{gEC/plasticizer\ films} - T_{gEC\ films}$ . OA and DBS were more efficient than MCT in reducing the  $T_g$  values of EC films, probably because they have lower  $T_g$  values than MCT and MCT may have a space hindrance when it comes to embedding themselves in the polymeric chains comparing with OA and DBS due to their structural characteristics. By comparing the experimental and calculated (using Gordon Taylor equation) reduced  $T_g$  values of EC/plasticizer films, we can conclude that at lower plasticizer loading, the compatibility of EC and the plasticizers is better than that at higher plasticizer loading. However, no evidence of phase separation was observed from MTDSC or DMA for EC/OA and EC/DBS films, irrespective of the plasticizer concentrations.

The application of the plasticizer mixtures (OA-DBS and OA-MCT) seemed to be more efficient than using a single plasticizer at the same concentration. OA and DBS have a single chain with 17C and 18C respectively, whereas MCT possesses three shorter chains.

When the plasticizer mixtures were used, more activation sites of EC chains could interact with OA and DBS or MCT respectively. This work is of great practical significance since it is concluded that plasticizer mixtures are more efficient in plasticizing EC films and a stronger interaction between EC and the plasticizer mixtures may result in better real-time stability.

### 8.3 Miscibility of EC and Selected Plasticizers

The determination of the  $T_g$  values is one of the best approaches to detect the interactions and the degree of mixing between EC and the plasticizers. For EC/OA and EC/DBS films, a single  $T_g$  was observed for all concentrations, indicating no complete phase separation occurred. However at higher plasticizer loading, the compatibility of EC and the plasticizers is poorer than that at lower plasticizer loading. For EC/MCT films, clear phase separation was observed at and above 20% w/w plasticizer loading from MTDSC results. This finding has been further confirmed with the DMA and LTA results. By using Gordon Taylor/Simha Boyer equation, the weight fractions of MCT in the high  $T_g$  and low  $T_g$  phases were estimated as 8% and 24% w/w respectively. The EC/plasticizer mixture films did not show any sign of phase separation, indicating plasticizer mixtures can provide better plasticizing efficiency with less risk of phase separation, comparing with a single plasticizer.

### 8.4 Phase Distribution of EC/Plasticizer/HPMC Films

Before examining the more complex systems, EC/HPMC films were initially investigated. Only the glass transition of EC was observed from MTDSC, whereas DMA showed both glass transitions of EC and HPMC. It is unfair to conclude that EC does not interact with HPMC solely based on the these results, since the theoretical glass transition of ‘miscible’

EC/HPMC blends is only 1-2°C higher than that of the pure EC film. EC may be partially miscible with HPMC, and the miscibility will be less than 10% w/w. AFM-LTA indicated that the concentrations of HPMC applied will definitely affect the phase distribution of EC and HPMC within the films. LTA showed two softening temperatures which were approximately 20°C higher than the  $T_g$  values of EC and HPMC from MTDSC results. This is in good agreement with the DMA results. However, the distribution of HPMC may vary with different concentrations of HPMC. At 10% w/w, HPMC was agglomerating closely to EC domains, and the size of the HPMC domains was smaller than the range that a nano probe covered at each heating point. At 20% and 30% w/w levels, HPMC phase domain was much larger and the nano probe can only detect one phase at each located area. These special phase distribution of EC/HPMC films may lead to different drug release mechanisms, since the water channels and pores generated by dissolved HPMC may be in different physical states and sizes.

At 10% w/w plasticizer level, the  $T_g$  values of EC films increased slightly when increasing the concentrations of HPMC. However, this increasing in the  $T_g$  values of EC films was too subtle and was not confirmed with DMA results. Therefore, we would not be able to conclude that HPMC affect the  $T_g$  values of EC/plasticizer films. The superior sensibility of LTA was again reflected since two transition temperatures for EC phase and HPMC phase were observed respectively. The disadvantage of LTA is that the detected softening temperatures were not as accurate as those from MTDSC or DMA. Therefore, the subtle changes in the  $T_g$  values cannot be confirmed. The distribution of EC phase and HPMC phase was revealed by the AFM adhesion images and LTA data. Most areas were either EC domains or HPMC domains, while minority areas can be both, probably distributed in two layers.

---

### 8.5 Mechanical Properties of EC films with Additives

Generally, film coating systems suitable for tablets or pellets coating require high mechanical strength and desirable flexibility of the films. Various parameters used for the evaluation of the mechanical properties of free film coatings have been published in the literatures, such as tensile strength, Young's modulus, deformability, energy at break, storage modulus, loss modulus, etc. Storage modulus, loss modulus and  $\tan \delta$  of a series of EC films were examined in this project. The storage modulus of free films decreased during heating due to the softening of the polymeric chains. The loss modulus is related to a material to lose energy in tension.  $\tan \delta$  is a good indicator of how efficiently a material loses energy to molecular rearrangements and internal friction.

Pure EC films are brittle and easy to break. Plasticizers and the pore forming agent HPMC worked in different ways in the EC films. The selected plasticizers decreased the storage modulus of EC films at room conditions within the concentration range of plasticizers used in this project. However this decreasing trend was less significant when the plasticizer concentration was above 10% w/w, signifying the dilution effect of the plasticizers on the polymeric chains was less influential with increasing the plasticizer concentrations. Overall, plasticizers can reduce the stiffness and enhance the flexibility of EC films. On the other hand, the incorporation of HPMC to the EC films increased the storage modulus of the EC films, even though EC may not interact with HPMC. This was ascribed to the inherent property of HPMC, since unplasticized HPMC films were regarded as brittle and hard films.

When the plasticizers and HPMC were both incorporated into the EC film systems, the overall impact of the plasticizers and HPMC on EC films became more complex. The

addition of HPMC to the EC/plasticizer films did not have a significant effect on the storage modulus profiles of these films during heating. However, the concentration of plasticizers had a more significant impact on the initial storage modulus values of EC/plasticizer/HPMC films than the concentration of HPMC. Therefore, it is reasonable to conclude that the application of plasticizers may be an efficient method to modify the mechanical properties of the film coatings for controlled release formulations.

### 8.6 Dissolution Studies

The thermal and thermo-mechanical properties of freshly prepared EC/plasticizer films and those incorporated with HPMC have been characterized in previous chapters. The thermal and imaging properties of these films after being placed into drug release mediums were also investigated to understand the underlying changes of these films during drug dissolution. MTDSC results of EC/plasticizer films with or without HPMC did show a dramatic change after these films have been immersed into DI water, pH 1.2 or pH 6.8 buffer for 24 hours. After dissolution, the absence of HPMC in the EC/plasticizer films did not have a significant effect on the thermal properties of these films, which indicated a desirable stability of the coating films throughout the whole dissolution process. Comparing the SEM images of EC/plasticizer films with and without HPMC after dissolution, we can conclude that HPMC dissolved quickly in the first two hours and generated water filled pores and channels. As indicated in *Chapter 5*, the concentration of HPMC had an effect on the distribution and size of EC and HPMC phases. Consequently, the morphology and size of the pores generated by dissolved HPMC were also affected by the concentration of HPMC.

The dissolution data of metoprolol succinate from pellets coated by EC/plasticizer films was best fitted into the zero-order release, while those from pellets coated by EC/plasticizer/HPMC films was best fitted into the Higuchi model. The release of metoprolol succinate from pellets coated by EC/plasticizer films was probably via the drug diffusion through the continuous plasticized polymeric phase, since the thermal and imaging properties of these films did not change significantly after dissolution studies. The drug release rate of metoprolol succinate from pellets coated by EC/plasticizer films was mainly governed by the diffusion of the dissolved drug through the film coatings and the hydration-erosion of the polymeric films. The release of metoprolol succinate from pellets coated by EC/plasticizer/HPMC films followed the Higuchi model. In this model, the drug release rate is affected by the diffusion coefficient, solubility of drug in the dissolution medium, porosity and the drug content per cubic centimetre of the pellet. The release of metoprolol succinate probably involved the simultaneous penetration of the surrounding liquid, dissolution of the drug, and leaching out of the drug through the water filled pores or channels.

When paracetamol was the model drug, the release mechanism was following the zero-order drug release, irrespective of the types of the film coatings. This indicated that the release rates of paracetamol from pellets coated by EC/plasticizer films were governed by the diffusion process of dissolved paracetamol through the polymeric films. The film properties may have an effect on the drug release rate. From the pellets coated by EC/plasticizer/HPMC films, dissolved paracetamol was expected to release through the pores or channels generated by the dissolution of HPMC. However, the relatively low drug solubility of paracetamol limited the amount of drug dissolved and leaked out from the water filled pores or channels. It is reasonable to predict the drug release mechanism by

---

correlating the regression of the drug release data and the morphology of the free films before and after exposure to the release mediums.

### 8.7 Overall Conclusions

In this thesis, ethyl cellulose films incorporating oleic acid, dibutyl sebacate and medium chain triglycerides as plasticizers as well as HPMC as the pore forming agent were characterized in order to understand their miscibility, interaction and phase distribution as well as the resulting drug release profiles.

The  $T_g$  values of selected plasticizers were predicted by using the Gordon Taylor-Simha Boyer equations and the experimental results. We present a useful approach to evaluate the weight fraction of phase separated components. Oleic acid and dibutyl sebacate were more efficient in plasticizing EC films than the medium chain triglycerides. They also had a better compatibility than medium chain triglycerides with ethyl cellulose. In order to achieve adequate film flexibility and avoid phase separation, 10% w/w plasticizers were utilized to produce EC films. HPMC did not have significant effect on the resulting  $T_g$  values of the polymer blends. Clear phase separation was observed between EC and HPMC. After in contact with the drug release media, HPMC dissolved and generated water filled pores, the shape and size of which were HPMC concentration dependent. This can be related to the phase distribution of localized thermal analysis results. When HPMC was not added to the film coatings, the drug release rate was mainly controlled by the thermal and thermo-mechanical properties of the film coatings. When HPMC was incorporated, the drug release rate may be affected by the dissolution of HPMC, film properties and drug solubility.

---

## 8.8 Future Work

Future work can be done to further investigate the interactions between the film components, especially when plasticizer mixtures are used. For example, solid-state nuclear magnetic resonance (NMR) can assess the chemical bonds and other interactions between those components. The morphology, mechanical properties and deformation behaviour of free films do not necessarily reflect the properties of pellets containing polymeric binding layers. Therefore, it may be interesting to assess those properties of the coated formulations. The following lists the focuses of the future work:

- a) Interactions between EC, plasticizers and HPMC using solid state NMR;
- b) Drug release studies of EC films with plasticizers and pore formers at different levels;
- c) Stability studies of EC film formulations;
- d) Morphology of coated formulations using AFM-LTA;
- e) Mechanical properties of coated formulations, such as film coated pellets or tablets;
- f) Thermal and thermo-mechanical properties of aqueous solid dispersion films, such as Surelease® films;
- g) Dissolution study of controlled-release formulations coated by aqueous solid dispersions;

---

**References**

Abu Diak, O., Bani-Jaber, A., Amro, B., Jones, D., Andrews, G.P., 2007. The manufacture and characterization of casein films as novel tablet coatings. *Food and Bioproducts Processing* 85, 284-290.

Arwidsson, H., Johansson, B., 1991. Application of intrinsic viscosity and interaction constant as a formulation tool for film coating. III. Mechanical studies on free ethyl cellulose films, cast from organic solvents. *International Journal of Pharmaceutics* 76, 91-97.

Arwidsson, H., Nicklasson, M., 1989. Application of intrinsic viscosity and interaction constant as a formulation tool for film coating. I. Studies on ethyl cellulose 10 cps in organic solvents. *International Journal of Pharmaceutics* 56, 187-193.

Arwidsson, H., Nicklasson, M., 1990. Application of intrinsic viscosity and interaction constant as a formulation tool for film coating II. Studies on different grades of ethyl cellulose in organic solvent systems. *International Journal of Pharmaceutics* 58, 73-77.

Bashaiwoldu, A.B., Podczeck, F., Newton, J.M., 2004. Application of Dynamic Mechanical Analysis (DMA) to the determination of the mechanical properties of coated pellets. *International Journal of Pharmaceutics* 274, 53-63.

Boateng, J.S., Matthews, K.H., Auffret, A.D., Humphrey, M.J., Stevens, H.N., Eccleston, G.M., 2009. In vitro drug release studies of polymeric freeze-dried wafers and solvent-cast

---

films using paracetamol as a model soluble drug. *International Journal of Pharmaceutics* 378, 66-72.

Bodmeier, R., Paeratakul, O., 1994. The distribution of plasticizers between aqueous and polymer phases in aqueous colloidal polymer dispersions. *International Journal of Pharmaceutics* 103, 47-54.

Bodmeier, R., Paeratakul, O., 1997. Plasticizer uptake by aqueous colloidal polymer dispersions used for the coating of solid dosage forms. *International Journal of Pharmaceutics* 152, 17-26.

Bonacucina, G., Di Martino, P., Piombetti, M., Colombo, A., Roversi, F., Palmieri, G.F., 2006. Effect of plasticizers on properties of pregelatinised starch acetate (Amprac 01) free films. *International Journal of Pharmaceutics* 313, 72-77.

Borgquist, P., Nevsten, P., Nilsson, B., Wallenberg, L.R., Axelsson, A., 2004. Simulation of the release from a multiparticulate system validated by single pellet and dose release experiments. *Journal of Controlled Release* 97, 453-465.

Borgquist, P., Zackrisson, G., Nilsson, B., Axelsson, A., 2002. Simulation and parametric study of a film-coated controlled-release pharmaceutical. *Journal of Controlled Release* 80, 229-245.

Brostow, W., Chiu, R., Kalogeras, I.M., Vassilikou-Dova, A., 2008. Prediction of glass transition temperatures: Binary blends and copolymers. *Materials Letters* 62, 3152-3155.

---

Coleman, N.J., Craig, D.Q.M., 1996. Modulated temperature differential scanning calorimetry: A novel approach to pharmaceutical thermal analysis. *International Journal of Pharmaceutics* 135, 13-29.

Craig, D., Kett, V., Andrews, C., Royall, P., 2002. Pharmaceutical applications of micro-thermal analysis. *Journal of Pharmaceutical Sciences* 91, 1201-1213.

Craig, D., Reading, M., 2007. *Thermal Analysis of Pharmaceuticals*. CRC Press, Taylor&Francis Group, Boca Raton.

Craig, D.Q.M., Johnson, F.A., 1995. Pharmaceutical applications of dynamic mechanical thermal analysis. *Thermochimica Acta* 248, 97-115.

Dai, Q., Huang, Y., 1998. Formation of lyotropic liquid crystals and molecular interactions in maleyl ethyl cellulose/acetic acid system. *Polymer* 39, 3405-3409.

David, J., 1999. Dynamic mechanical analysis of polymeric systems of pharmaceutical and biomedical significance. *International Journal of Pharmaceutics* 179, 167-178.

Desai, J., Alexander, K., Riga, A., 2006. Characterization of polymeric dispersions of dimenhydrinate in ethyl cellulose for controlled release. *International Journal of Pharmaceutics* 308, 115-123.

---

Dias, V.D., Ambudkar, V., Fegely, K.A., Rajabi-Siahboomi, A.R., 2008. The influence of solvent type on extended release coating with ethylcellulose barrier membranes. Controlled Release Society Annual Meeting.

Fabra, M.J., Talens, P., Chiralt, A., 2008. Tensile properties and water vapor permeability of sodium caseinate films containing oleic acid-beeswax mixtures. *Journal of Food Engineering* 85, 393-400.

Fadda, H.M., Hernández, M.C., Margetson, D.N., McAllister, S.M., Basit, A.W., Brocchini, S., Suárez, N., 2008. The molecular interactions that influence the plasticizer dependent dissolution of acrylic polymer films. *Journal of Pharmaceutical Sciences* 97, 3957-3971.

Fasolka, M.J., Mayes, A.M., Magonov, S.N., 2001. Thermal enhancement of AFM phase contrast for imaging diblock copolymer thin film morphology. *Ultramicroscopy* 90, 21-31.

Felton, L.A., McGinity, J.W., 1997. Influence of plasticizers on the adhesive properties of an acrylic resin copolymer to hydrophilic and hydrophobic tablet compacts. *International Journal of Pharmaceutics* 154, 167-178.

Forrest, J.A., Dalnoki-Veress, K., 2001. The glass transition in thin polymer films. *Advances in Colloid and Interface Science* 94, 167-195.

Forster, A., Hemenstall, J., Tucker, I., Rades, T., 2001. Selection of excipients for melt extrusion with two poorly water-soluble drugs by solubility parameter calculation and thermal analysis. *International Journal of Pharmaceutics* 226, 147-161.

---

Fox, T.G., 1956. Influence of diluent and copolymer composition on the glass temperature of a polymer system. *Bull. Am. Phys.* 2 123.

Frohoff-Hülsmann, M.A., Lippold, B.C., McGinity, J.W., 1999a. Aqueous ethyl cellulose dispersion containing plasticizers of different water solubility and hydroxypropyl methylcellulose as coating material for diffusion pellets II: properties of sprayed films. *European Journal of Pharmaceutics and Biopharmaceutics* 48, 67-75.

Frohoff-Hülsmann, M.A., Schmitz, A., Lippold, B.C., 1999b. Aqueous ethyl cellulose dispersions containing plasticizers of different water solubility and hydroxypropyl methylcellulose as coating material for diffusion pellets: I. Drug release rates from coated pellets. *International Journal of Pharmaceutics* 177, 69-82.

Gibson, S.H.M., Rowe, R.C., White, E.F.T., 1988. Mechanical properties of pigmented tablet coating formulations and their resistance to cracking I. Static mechanical measurement. *International Journal of Pharmaceutics* 48, 63-77.

Gordon, M., Taylor, J.S., 1952. Ideal polymers and the second-order transitions of synthetic rubbers I :Non-crystalline copolymers. *Journal of Application Chemistry*, 493-500.

Granberg, R.A., Rasmuson, Å.C., 2000. Solubility of Paracetamol in Binary and Ternary Mixtures of Water + Acetone + Toluene. *Journal of Chemical & Engineering Data* 45, 478-483.

---

Grandy, D.B., Hourston, D.J., Price, D.M., Reading, M., Silva, G.G., Song, M., Sykes, P.A., 2000. Microthermal Characterization of Segmented Polyurethane Elastomers and a Polystyrene-Poly(methyl methacrylate) Polymer Blend Using Variable-Temperature Pulsed Force Mode Atomic Force Microscopy. *Macromolecules* 33, 9348-9359.

Gunder, W., Lippold, B.H., Lippold, B.C., 1995. Release of drugs from ethyl cellulose microcapsules (diffusion pellets) with pore formers and pore fusion. *European Journal of Pharmaceutical Sciences* 3, 203-214.

Gutiérrez-Rocca, J., McGinity, J.W., 1994. Influence of water soluble and insoluble plasticizers on the physical and mechanical properties of acrylic resin copolymers. *International Journal of Pharmaceutics* 103, 293-301.

Heinämäki, J.T., Lehtola, V.M., Nikupaavo, P., Yliruusi, J.K., 1994. The mechanical and moisture permeability properties of aqueous-based hydroxypropyl methylcellulose coating systems plasticized with polyethylene glycol. *International Journal of Pharmaceutics* 112, 191-196.

Higuchi, W.I., 1967. Diffusional models useful in biopharmaceutics. Drug release rate processes. *Journal of Pharmaceutical Sciences* 56, 315-324.

Hill, V.L., Craig, D.Q.M., Feely, L.C., 1999. The effects of experimental parameters and calibration on MTDSC data. *International Journal of Pharmaceutics* 192, 21-32.

- 
- Horcas, I., Fernández, R., Rodríguez, G., Colchero, J., Herrero, G., Baro, A.M., 2007. WSXM: A software for scanning probe microscopy and a tool for nanotechnology. *Review of Scientific Instruments* 78, 013705.
- Houde, A.Y., Stern, S.A., 1997. Solubility and diffusivity of light gases in ethyl cellulose at elevated pressures Effects of ethoxy content. *Journal of Membrane Science* 127, 171-183.
- Hourston, D.J., Song, M., Hammiche, A., Pollock, H.M., Reading, M., 1996. Modulated differential scanning calorimetry: 2. Studies of physical ageing in polystyrene. *Polymer* 37, 243-247.
- Hourston, D.J., Song, M., Hammiche, A., Pollock, H.M., Reading, M., 1997. Modulated differential scanning calorimetry: 6. Thermal characterization of multicomponent polymers and interfaces. *Polymer* 38, 1-7.
- Hutchings, D., Clarson, S., Sakr, A., 1994. Studies of the mechanical properties of free films prepared using an ethylcellulose pseudolatex coating system. *International Journal of Pharmaceutics* 104, 203-213.
- Hyppölä, R., Husson, I., Sundholm, F., 1996. Evaluation of physical properties of plasticized ethyl cellulose films cast from ethanol solution Part I. *International Journal of Pharmaceutics* 133, 161-170.

- 
- Kalichevsky, M.T., Jaroszkiewicz, E.M., Ablett, S., Blanshard, J.M.V., Lillford, P.J., 1992. The glass transition of amylopectin measured by DSC, DMTA and NMR. *Carbohydrate Polymers* 18, 77-88.
- Kangarlou, S., Haririan, I., Gholipour, Y., 2008. Physico-mechanical analysis of free ethyl cellulose films comprised with novel plasticizers of vitamin resources. *International Journal of Pharmaceutics* In Press, Corrected Proof.
- Kim, K.J., Park, K., Lee, J., Zhang, Z.M., King, W.P., 2007. Nanotopographical imaging using a heated atomic force microscope cantilever probe. *Sensors and Actuators A: Physical* 136, 95-103.
- Krögel, I., Bodmeier, R., 1999. Floating or pulsatile drug delivery systems based on coated effervescent cores. *International Journal of Pharmaceutics* 187, 175-184.
- Lafferty, S.V., Newton, J.M., Podczek, F., 2002. Dynamic mechanical thermal analysis studies of polymer films prepared from aqueous dispersion. *International Journal of Pharmaceutics* 235, 107-111.
- Lai, H.L., 2005. A thermal and microscopic investigation into the physical characteristics and drug release behaviour of ethylcellulose films. School of Chemical Sciences and Pharmacy. University of East Anglia, Norwich, p. 265.

---

Lai, H.L., Pitt, K., Craig, D.Q.M., 2010. Characterisation of the thermal properties of ethylcellulose using differential scanning and quasi-isothermal calorimetric approaches. *International Journal of Pharmaceutics* 386, 178-184.

Lecomte, F., Siepmann, J., Walther, M., MacRae, R.J., Bodmeier, R., 2004. Polymer blends used for the aqueous coating of solid dosage forms: importance of the type of plasticizer. *Journal of Controlled Release* 99, 1-13.

Leong, C.W., Newton, J.M., Basit, A.W., Podczek, F., Cummings, J.H., Ring, S.G., 2002. The formation of colonic digestible films of amylose and ethylcellulose from aqueous dispersions at temperatures below 37°C. *European Journal of Pharmaceutics and Biopharmaceutics* 54, 291-297.

Li, X.G., Huang, M.R., Bai, H., 1999. Thermal decomposition of cellulose ethers. *Journal of Applied Polymer Science* 73, 2927-2936.

Lindholm, T., Huhtikangas, A., Saarikivi, P., 1984. Organic solvent residues in free ethyl cellulose films. *International Journal of Pharmaceutics* 21, 119-121.

Lindstedt, B., Ragnarsson, G., Hjærtstam, J., 1989. Osmotic pumping as a release mechanism for membrane-coated drug formulations. *International Journal of Pharmaceutics* 56, 261-268.

Lippold, B.C., Gunder, W., Lippold, B.H., 1999. Drug release from diffusion pellets coated with the aqueous ethyl cellulose dispersion aquacoat® ECD-30 and 20% Dibutyl Sebacate

---

as plasticizer: partition mechanism and pore diffusion. *European Journal of Pharmaceutics and Biopharmaceutics* 47, 27-32.

Lippold, B.r.H., Sutter, B.K., Lippold, B.C., 1989. Parameters controlling drug release from pellets coated with aqueous ethyl cellulose dispersion. *International Journal of Pharmaceutics* 54, 15-25.

Masilungan, F.C., Lordi, N.G., 1984. Evaluation of film coating compositions by thermomechanical analysis. I. Penetration mode. *International Journal of Pharmaceutics* 20, 295-305.

Mauritz, K.A., Storey, R.F., George, S.E., 1990. A general free volume-based theory for the diffusion of large molecules in amorphous polymers above the glass temperature. I. Application to di-n-alkyl phthalates in PVC. *Macromolecules* 23, 441-450.

McConnell, E., Tutas, J., Mohamed, M., Banning, D., Basit, A., 2007. Colonic drug delivery using amylose films: the role of aqueous ethylcellulose dispersions in controlling drug release. *Cellulose* 14, 25-34.

McPhillips, H., Craig, D.Q.M., Royall, P.G., Hill, V.L., 1999. Characterisation of the glass transition of HPMC using modulated temperature differential scanning calorimetry. *International Journal of Pharmaceutics* 180, 83-90.

Menjoge, A.R., Kulkarni, M.G., 2007. Mechanistic investigations of phase behavior in Eudragit®E blends. *International Journal of Pharmaceutics* 343, 106-121.

---

Missaghi, S., Fegely, K.A., Rajabi-Siahboomi, A.R., 2008. Investigation of venlafaxine HCl release from extruded and spheronized beads coated with ethylcellulose using organic or aqueous coating systems. Controlled Release Society Annual Meeting.

Mitchell, K., Ford, J.L., Armstrong, D.J., Elliott, P.N.C., Rostron, C., Hogan, J.E., 1990. The influence of additives on the cloud point, disintegration and dissolution of hydroxypropylmethylcellulose gels and matrix tablets. *International Journal of Pharmaceutics* 66, 233-242.

Moynihan, C.T., Easteal, A.J., Wilder, J., Tucker, J., 1974. Dependence of the glass transition temperature on heating and cooling rate. *The Journal of Physical Chemistry* 78, 2673-2677.

Muschert, S., Siepmann, F., Leclercq, B., Carlin, B., Siepmann, J., 2009a. Drug release mechanisms from ethylcellulose: PVA-PEG graft copolymer-coated pellets. *European Journal of Pharmaceutics and Biopharmaceutics* 72, 130-137.

Muschert, S., Siepmann, F., Leclercq, B., Carlin, B., Siepmann, J., 2009b. Prediction of drug release from ethylcellulose coated pellets. *Journal of Controlled Release* 135, 71-79.

Nikowitz, K., Kása Jr, P., Pintye-Hódi, K., Regdon Jr, G., 2011. Study of the preparation of a multiparticulate drug delivery system with a layering technique. *Powder Technology* 205, 155-159.

---

Nyamweya, N., Hoag, S.W., 2000. Assessment of polymer-polymer interactions in blends of HPMC and film forming polymers by modulated temperature differential scanning Calorimetry. *Pharmaceutical Research* 17, 7.

Obara, S., McGinity, J.W., 1995. Influence of processing variables on the properties of free films prepared from aqueous polymeric dispersions by a spray technique. *International Journal of Pharmaceutics* 126, 1-10.

Oh, E., Luner, P.E., 1999. Surface free energy of ethylcellulose films and the influence of plasticizers. *International Journal of Pharmaceutics* 188, 203-219.

Ohara, T., Kitamura, S., Kitagawa, T., Terada, K., 2005. Dissolution mechanism of poorly water-soluble drug from extended release solid dispersion system with ethylcellulose and hydroxypropylmethylcellulose. *International Journal of Pharmaceutics* 302, 95-102.

Okhamafe, A.O., York, P., 1984. Effect of solids-polymer interactions on the properties of some aqueous-based tablet film coating formulations. II. Mechanical characteristics. *International Journal of Pharmaceutics* 22, 273-281.

Ong, K.T., Rege, P.R., Rajabi-Siahboomi, A.R., 2006. Effect of hypromellose as a pore-former in aqueous ethylcellulose dispersion: characterization of dispersion properties. *Controlled Release Society*.

---

Ozturk, A.G., Ozturk, S.S., Palsson, B.O., Wheatley, T.A., Dressman, J.B., 1990. Mechanism of release from pellets coated with an ethylcellulose-based film. *Journal of Controlled Release* 14, 203-213.

Palmer, D., Vuong, H., Levina, M., R.Rajabi-Siahboomi, A., 2007. The influence of hydrophilic pore formers on dipyridamole release from aqueous ethylcellulose film-coated pellets. *AAPS Annual Meeting*.

Pearce, E.M., 1997. *Thermal characterization of polymeric materials* (second edition), edited by Edith A. Turi, Academic Press, San Diego, CA, 1997, 2420 pp. Price: \$375.00. *Journal of Polymer Science Part A: Polymer Chemistry* 35, 2535-2537.

Podczec, F., Almeida, S.M., 2002. Determination of the mechanical properties of pellets and film coated pellets using Dynamic Mechanical Analysis (DMA). *European Journal of Pharmaceutical Sciences* 16, 209-214.

Pongjanyakul, T., Puttipipatkachorn, S., 2007. Alginate-magnesium aluminum silicate films: Effect of plasticizers on film properties, drug permeation and drug release from coated tablets. *International Journal of Pharmaceutics* 333, 34-44.

Price, D.M., Reading, M., Hammiche, A., Pollock, H.M., 1999. Micro-thermal analysis: scanning thermal microscopy and localised thermal analysis. *International Journal of Pharmaceutics* 192, 85-96.

- 
- Ravishankar, H., Patil, P., Samel, A., Petereit, H.-U., Lizio, R., Iyer-Chavan, J., 2006. Modulated release metoprolol succinate formulation based on ionic interactions: In vivo proof of concept. *Journal of Controlled Release* 111, 65-72.
- Reading, M., Luget, A., Wilson, R., 1994. Modulated differential scanning calorimetry. *Thermochimica Acta* 238, 295-307.
- Ringqvist, A., Taylor, L.S., Ekelund, K., Ragnarsson, G., Engström, S., Axelsson, A., 2003. Atomic force microscopy analysis and confocal Raman microimaging of coated pellets. *International Journal of Pharmaceutics* 267, 35-47.
- Ritger, P.L., Peppas, N.A., 1987. A simple equation for description of solute release II. Fickian and anomalous release from swellable devices. *Journal of Controlled Release* 5, 37-42.
- Roberts, R.J., Rowe, R.C., 1987. The Young's modulus of pharmaceutical materials. *International Journal of Pharmaceutics* 37, 15-18.
- Rowe, R.C., 1981. The cracking of film coatings on film-coated tablets—a theoretical approach with practical implications. *Journal of Pharmacy and Pharmacology* 33, 423-426.
- Rowe, R.C., 1982. The molecular weight of methyl cellulose used in pharmaceutical formulation. *International Journal of Pharmaceutics* 11, 175-179.

---

Rowe, R.C., 1986. The effect of the molecular weight of ethyl cellulose on the drug release properties of mixed films of ethyl cellulose and hydroxypropylmethylcellulose. *International Journal of Pharmaceutics* 29, 37-41.

Rowe, R.C., 1988. Tablet-tablet contact and mutual rubbing within a coating drum -- an important factor governing the properties and appearance of tablet film coatings. *International Journal of Pharmaceutics* 43, 155-159.

Rowe, R.C., 1992. Molecular weight dependence of the properties of ethyl cellulose and hydroxypropyl methylcellulose films. *International Journal of Pharmaceutics* 88, 405-408.

Rowe, R.C., Kotaras, A.D., White, E.F.T., 1984. An evaluation of the plasticizing efficiency of the dialkyl phthalates in ethyl cellulose films using the torsional braid pendulum. *International Journal of Pharmaceutics* 22, 57-62.

Royall, P.G., Craig, D.Q.M., Price, D.M., Reading, M., Lever, T.J., 1999. An investigation into the use of micro-thermal analysis for the solid state characterisation of an HPMC tablet formulation. *International Journal of Pharmaceutics* 192, 97-103.

Sakellariou, P., Rowe, R.C., 1995a. The morphology of blends of ethylcellulose with hydroxypropyl methylcellulose as used in film coating. *International Journal of Pharmaceutics* 125, 289-296.

Sakellariou, P., Rowe, R.C., White, E.F.T., 1986a. An evaluation of the interaction and plasticizing efficiency of the polyethylene glycols in ethyl cellulose and hydroxypropyl

---

methylcellulose films using the torsional braid pendulum. *International Journal of Pharmaceutics* 31, 55-64.

Sakellariou, P., Rowe, R.C., White, E.F.T., 1986b. Polymer/polymer interaction in blends of ethyl cellulose with both cellulose derivatives and polyethylene glycol 6000. *International Journal of Pharmaceutics* 34, 93-103.

Sakellariou, P., Rowe, R.C., White, E.F.T., 1986c. The solubility parameters of some cellulose derivatives and polyethylene glycols used in tablet film coating. *International Journal of Pharmaceutics* 31, 175-177.

Sánchez, A.C., Popineau, Y., Mangavel, C., Larré, C., Guéguen, J., 1998. Effect of Different Plasticizers on the Mechanical and Surface Properties of Wheat Gliadin Films. *Journal of Agricultural and Food Chemistry* 46, 4539-4544.

Schawe, J.E.K., 1995. Principles for the interpretation of modulated temperature DSC measurements. Part 1. Glass transition. *Thermochimica Acta* 261, 183-194.

Schultz, P., Kleinebudde, P., 1997. A new multiparticulate delayed release system.: Part I: Dissolution properties and release mechanism. *Journal of Controlled Release* 47, 181-189.

Shimamoto, S., Gray, D.G., 1998. A Method To Preserve the Chiral Nematic Order of Lyotropic Ethylcellulose and (Acetyl)(ethyl)cellulose Mesophases in Solid Films. *Chemistry of Materials* 10, 1720-1726.

---

Siepmann, F., Hoffmann, A., Leclercq, B., Carlin, B., Siepmann, J., 2007. How to adjust desired drug release patterns from ethylcellulose-coated dosage forms. *Journal of Controlled Release* 119, 182-189.

Siepmann, F., Siepmann, J., Walther, M., MacRae, R., Bodmeier, R., 2006. Aqueous HPMCAS coatings: Effects of formulation and processing parameters on drug release and mass transport mechanisms. *European Journal of Pharmaceutics and Biopharmaceutics* 63, 262-269.

Siepmann, F., Siepmann, J., Walther, M., MacRae, R.J., Bodmeier, R., 2008. Polymer blends for controlled release coatings. *Journal of Controlled Release* 125, 1-15.

Siepmann, J., Paeratakul, O., Bodmeier, R., 1998. Modeling plasticizer uptake in aqueous polymer dispersions. *International Journal of Pharmaceutics* 165, 191-200.

Simha, R., Boyer, R.F., 1962. On a general relation involving the glass temperature and coefficients of expansion of polymers. *Journal of Chemistry and Physics*, 1003-1007.

Singh, R., Arora, S., Lal, K., 1996. Thermal and spectral studies on cellulose modified with various cresyldichlorothiophosphates. *Thermochimica Acta* 289, 9-21.

Six, K., Berghmans, H., Leuner, C., Dressman, J., Van Werde, K., Mullens, J., Benoist, L., Thimon, M., Meublat, L., Verreck, G., Peeters, J., Brewster, M., Van den Mooter, G., 2003. Characterization of Solid Dispersions of Itraconazole and Hydroxypropylmethylcellulose Prepared by Melt Extrusion, Part II. *Pharmaceutical Research* 20, 1047-1054.

---

Song, M., Hammiche, A., Pollock, H.M., Hourston, D.J., Reading, M., 1995. Modulated differential scanning calorimetry: 1. A study of the glass transition behaviour of blends of poly (methyl methacrylate) and poly (styrene-co-acrylonitrile). *Polymer* 36, 3313-3316.

Song, M., Hammiche, A., Pollock, H.M., Hourston, D.J., Reading, M., 1996. Modulated differential scanning calorimetry: 4. Miscibility and glass transition behaviour in poly (methyl methacrylate) and poly (epichlorohydrin) blends. *Polymer* 37, 5661-5665.

Song, M., Pollock, H.M., Hammiche, A., Hourston, D.J., Reading, M., 1997. Modulated differential scanning calorimetry: 8. Interface development between films of polyepichlorohydrin and poly (vinyl acetate). *Polymer* 38, 503-507.

Sousa, J.J., Sousa, A., Moura, M.J., Podczek, F., Newton, J.M., 2002. The influence of core materials and film coating on the drug release from coated pellets. *International Journal of Pharmaceutics* 233, 111-122.

Strübing, S., Metz, H., Mäder, K., 2007. Mechanistic analysis of drug release from tablets with membrane controlled drug delivery. *European Journal of Pharmaceutics and Biopharmaceutics* 66, 113-119.

Sumit, N., Sarbani, G., Santinath, G., 2004. Production of medium chain glycerides and monolaurin from coconut acid oil by lipase-catalyzed reactions. *Journal of Oleo Science* 53, 497-501.

- 
- Tamburic, S., Craig, D.Q.M., 1997. Thermorheological and thermogravimetric analysis of bioadhesive polymer/mucin mixtures. *Thermochimica Acta* 294, 99-106.
- Tarvainen, M., Sutinen, R., Peltonen, S., Mikkonen, H., Maunus, J., Vähä-Heikkilä, K., Lehto, V.-P., Paronen, P., 2003. Enhanced film-forming properties for ethyl cellulose and starch acetate using n-alkenyl succinic anhydrides as novel plasticizers. *European Journal of Pharmaceutical Sciences* 19, 363-371.
- Theeuwes, F., 1975. Elementary osmotic pump. *Journal of Pharmaceutical Sciences* 64, 1987-1991.
- Vaithiyalingam, S., Khan, M.A., 2002. Optimization and characterization of controlled release multi-particulate beads formulated with a customized cellulose acetate butyrate dispersion. *International Journal of Pharmaceutics* 234, 179-193.
- Vargas, M., Albors, A., Chiralt, A., González-Martínez, C., 2008. Characterization of chitosan-oleic acid composite films. *Food Hydrocolloids* In Press, Corrected Proof.
- Vesey, C.F., Farrell, T., Rajabi-Siahboomi, A.R., 2005. Evaluation of alternative plasticizers for Surelease<sup>®</sup>, an aqueous ethylcellulose dispersion for modified release film-coating. *Controlled Release Society Annual Meeting*.
- Wang, C.-C., Zhang, G., H. Shah, N., Infeld, M.H., Waseem Malick, A., McGinity, J.W., 1997. Influence of plasticizers on the mechanical properties of pellets containing Eudragit<sup>®</sup> RS 30 D. *International Journal of Pharmaceutics* 152, 153-163.

---

Wang, G., Li, A., 2008. Thermal Decomposition and Kinetics of Mixtures of Polylactic Acid and Biomass during Coprolysis. *Chinese Journal of Chemical Engineering* 16, 929-933.

Wesseling, M., Bodmeier, R., 1999. Drug release from beads coated with an aqueous colloidal ethylcellulose dispersion, Aquacoat<sup>®</sup>, or an organic ethylcellulose solution. *European Journal of Pharmaceutics and Biopharmaceutics* 47, 33-38.

Wilkie, C.A., 1999. TGA/FTIR: an extremely useful technique for studying polymer degradation. *Polymer Degradation and Stability* 66, 301-306.

Wu, C., Huang, Y., Chen, S., 2002. The synthesis and thermotropic liquid crystalline behavior of mesogenic moiety-linked ethyl cellulose. *Polymer Bulletin* 48, 33-41.

Yang, J.M., Su, W.Y., Leu, T.L., Yang, M.C., 2004. Evaluation of chitosan/PVA blended hydrogel membranes. *Journal of Membrane Science* 236, 39-51.

Yang, W.P., Shyu, S.S., Lee, E.-S., Chao, A.-C., 1996. Effects of PVA content and calcination temperature on the properties of PVA/boehmite composite film. *Materials Chemistry and Physics* 45, 108-113.

Yie, W.C., Senshang, L., 2006. Drug Delivery: Controlled Release. *Encyclopedia of Pharmaceutical Technology*, Third Edition. Informa Healthcare, pp. 1082-1103.

---

Yu, N., Gray, G.R., 1998. Analysis of the positions of substitution of acetate and propionate groups in cellulose acetate-propionate by the reductive-cleavage method. *Carbohydrate Research* 313, 29-36.

Zentner, G.M., Rork, G.S., Himmelstein, K.J., 1985. Osmotic flow through controlled porosity films: An approach to delivery of water soluble compounds. *Journal of Controlled Release* 2, 217-229.

---

**Appendix****Conference Abstracts****36<sup>th</sup> Annual Meeting and Exposition of the Controlled Release Society 2009  
(Copenhagen Denmark)****A Thermal and Thermomechanical Investigation into the Effects of Plasticizer Incorporation on the Properties of Ethylcellulose (Ethocel<sup>TM</sup> 20) Films**

Jin Meng<sup>1</sup>, Ali Rajabi-siahboomi<sup>2</sup>, Marina Levina<sup>2</sup>, Mike Reading<sup>1</sup> and Duncan Q. M. Craig<sup>1</sup>

<sup>1</sup>School of Chemical Sciences and Pharmacy, University of East Anglia, Norwich NR4 7TJ, UK

<sup>2</sup>Colorcon Limited, Flagship House, Victory Way, Crossways, Dartford, Kent DA2 6QD, UK

**ABSTRACT SUMMARY**

A series of ethylcellulose (Ethocel<sup>TM</sup> 20) films containing varying amounts of fractionated coconut oil (FCO) as a plasticizer were prepared. The thermal and thermo-mechanical properties of the films were characterized using modulated temperature differential scanning calorimetry (MTDSC) and dynamic mechanical analysis (DMA) respectively. A clear evidence of phase separation was obtained using both techniques, although the composition and concentration dependence of the respective phases showed a complex profile. We suggest a model whereby the composition of the phases may be estimated. The thermo-rheological properties are also considered in relation to the glassy behaviour of the films.

**INTRODUCTION**

Ethylcellulose (EC) is a water-insoluble polymeric material which has a significant importance for developing controlled release systems such as matrix devices, barrier membrane application in multi-particulate systems and microspheres. The material is composed of cellulose chains substituted with ethoxyl groups. In pharmaceutical applications the degree of substitution is typically 48%-49.5%. EC can form strong films with good substrate adhesion, thus providing a diffusion barrier whose properties can be modified by film thickness, level of plasticizers and the type of solvent used<sup>1,2</sup>.

Unplasticized EC films are brittle and also confer very slow drug release; hence plasticizers are almost invariably incorporated. These are comparatively low molecular weight materials which increase the mobility of the constituent molecules, leading to an increased flexibility of the corresponding films. More specifically, the plasticizer increases the overall molecular free volume and so reduces the  $T_g$ . On this basis, molecular miscibility is a common and reasonable assumption associated with the plasticization process but there remains the possibility of phase separation as the plasticizer content is increased beyond a certain value.

While being a major concern in the polymer sciences, the issue of plasticizer miscibility and saturation is one which has received comparatively little attention in the pharmaceutical arena, hence here we explore the use of two complementary techniques for the detection and assessment of this phenomenon, namely MTDSC and DMA. More

specifically, we explore the relationship between the composition and the associated thermal events with a view to both comparing the applicability of the two techniques and also elucidating the structures formed on adding the plasticizer, fractionated coconut oil.

## EXPERIMENTAL METHODS

20ml of 10% (w/v) EC solutions were prepared by dissolving 2g Ethocel™ 20 (Colorcon, USA) powder in 20ml ethanol/acetone (60/40 v/v), with the specified level of plasticizer then added. Fractionated coconut oil (Colorcon, USA) was used as a plasticizer at concentrations of 5%, 10%, 15%, 20%, 25% and 30% (w/w of EC). Films were obtained by casting solutions on a glass plate by using REF 1117 film applicator (Sheen Instruments Ltd., England). The wet film thickness was controlled at 2500 $\mu$ m by adjusting the micrometers of the film applicator. The films were dried at 45°C in the oven for 3h. Clear dry films were obtained. 0.67% residual solvent was detected using thermogravimetric analysis (TGA).

MTDSC experiments were conducted from 20°C to 220°C with a modulation amplitude of  $\pm 0.5^\circ\text{C}$  and a period of 40 seconds at a heating rate of 2°C/min using DSC Q1000 (TA instruments, USA). The sample mass was 2-5mg and pinholed crimped pans were used. The DSC cell was purged with 50 cm<sup>3</sup>/min dry nitrogen and the RCS was purged with 150 cm<sup>3</sup>/min nitrogen. Baseline calibration was conducted by running two empty pans in the same temperature program used for running the samples. Temperature calibration was performed using high purity calibrants (indium, tin and n-octadecane). Heat capacity calibration was performed by using sapphire (aluminium oxide) run in the same temperature program used for running the samples and compared with the literature heat capacity value of a sapphire at the temperature of interest.

DMA was used in a tension mode (tensile clamp) (DMA 2980, TA instruments, USA) to investigate the storage modulus, loss modulus and  $\tan\delta$  of the samples as a function of temperature. The films were cut into 30 $\times$  5.27 mm square pieces and then mounted on the fixed clamps. Two clamp screws were tightened by using the torque wrench to the appropriate clamping torque (3-5 in-lbs). Samples were heated from 30°C to 180°C at a rate of 3°C/min. Dry filtered air was used as purge gas and cooling system.

## RESULTS AND DISCUSSION

The heat capacity change ( $\Delta C_p$ ) associated with EC is known to be small<sup>3</sup>, thus rendering detection and/or assessment of  $\Delta C_p$  difficult. On this basis, derivative reversing heat capacity signals from MTDSC scans of EC 20 films and those with 5%, 10%, 15%, 20%, 25% and 30% FCO are shown in Figure 1. This method of data presentation was utilized due to the clearer detection of baseline shifts associated with  $T_g$ . The value of  $T_g$  for the EC film was  $129.2 \pm 0.1^\circ\text{C}$ . An endothermic event was observed around 180°C which was consistent with previous observations by Lai<sup>3</sup> who ascribed this to melting of microcrystallites in the EC (this endotherm is expressed at an upward then downward peak in the derivative signal).

On adding 5% FCO, the  $T_g$  value decreased to 110.5°C, while the transition associated with the melting endotherm similarly decreased and became less pronounced. This decrease in  $T_g$  is consistent with behaviour associated with plasticizer miscibility and was similarly observed for the 10% FCO systems; again with a higher temperature event that we associate with the microcrystallite melting. However on increasing the concentration of FCO to 20% and beyond, the  $T_g$  value remained reasonably constant at circa 97°C while a further lower temperature peak was observed at circa 53°C. Such phenomena have been associated with phase separation. However it is also recognized that such separation may

not comprise simply the presence of individual components but may instead reflect mixed phases potentially occurring on a scale down to circa  $100\text{\AA}^{2-4}$ . Indeed it is possible to

estimate the composition of these phases by considering the Gordon Taylor/Simba Boyer equations in the context of the  $T_g$  of the 5% FCO films (thereby allowing K and the  $T_g$  of FCO to be estimated) and then to estimate the compositions of the two phases in the 20% systems as being 23.5% FCO and 8.3% FCO for the low and high  $T_g$  phases respectively. It is interesting to note that between 20 and 30% FCO the  $T_g$  values do not change, implying further phase separation, possibly of pure FCO.

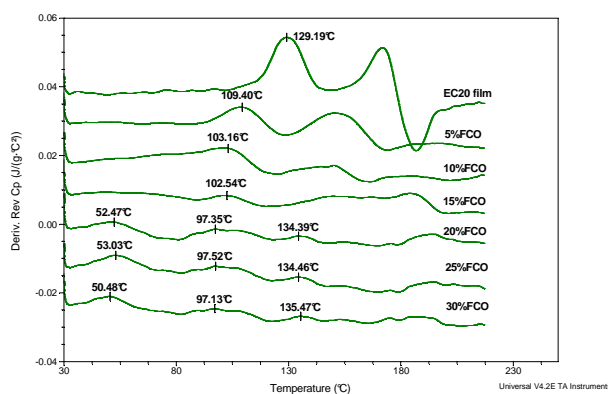


Figure 1. Derivative reversing heat capacity signals from MTDSC scans of EC 20 films with 5%, 10%, 15%, 20%, 25% and 30% FCO

Figure 2 shows the corresponding DMA data for the EC films. Two glass transitions are also observed in the  $\tan \delta$  plot for 20% FCO film, further supporting the conclusion that phase separation occurs. However, for the 25% and 30% systems the storage modulus decreased dramatically above  $T_g$  thus rendering it difficult to observe any higher temperature transitions. Nevertheless there was a broad agreement between the two techniques in terms of the discontinuous (with respect to concentration) appearance of the distinct  $T_g$  events. We also noted that the storage and loss moduli showed a fairly continuous decrease with increasing FCO, implying that both (or possibly all three if one includes separated FCO) phases contributed to the increased plasticity of the films.

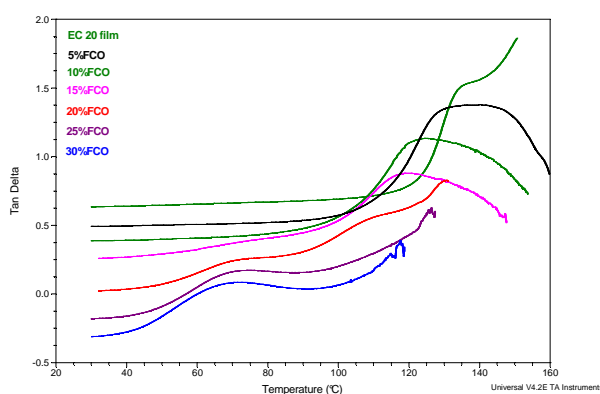


Figure 2.  $\tan \delta$  values from DMA of EC 20 films with 5%, 10%, 15%, 20%, 25% and 30% FCO (top to bottom)

---

**CONCLUSIONS**

Our results suggest that phase separation can occur in EC/FCO systems and that this event may be detected using MTDSC and DMA, although in this case both the measurement and interpretation were non-trivial. We suggest an approach whereby we can estimate the composition of the phases. Although indirect evidence is obtained for further

FCO separation at higher plasticizer concentrations we also suggest that these are effectively conjugate systems rather than pure components. It is believed that such studies are of considerable importance for understanding drug release, product stability and film integrity for barrier membrane controlled release dosage forms.

**REFERENCES**

1. Arwidsson, H.; Johansson, B. *Int. J. Pharm.* 1991, 76 (1-2), 91-97.
2. Wesseling, M.; Bodmeier, R. *Eu. J. Pharm. Biopharm.* 1999, 47 (1), 33-38.
3. Lai H. L. *PhD Thesis, University of East Anglia, Norwich UK.* 2005, p. 265
4. Bair H.E. and Warren P.C. *J.Macromol.Sci.Phys.* 1981, B20, 381-402

**ACKNOWLEDGEMENTS**

Financial support was provided by Colorcon Limited (UK).

---

**British Pharmaceutical Conference 2009 (Manchester UK)**

---

**A Study into the Miscibility of Ethylcellulose (Ethocel<sup>TM</sup>20) with Different Concentrations of Plasticizer in Cast Film Coats**

Jin Meng<sup>1</sup>, Ali Rajabi-siahboomi<sup>2</sup>, Marina Levina<sup>2</sup>, Mike Reading<sup>1</sup> and Duncan Q. M. Craig<sup>1</sup>

<sup>1</sup>School of Chemical Sciences and Pharmacy, University of East Anglia, Norwich NR4 7TJ, UK

<sup>2</sup>Colorcon Limited, Flagship House, Victory Way, Crossways, Dartford, Kent DA2 6QD, UK

**Objectives**

Polymer and plasticizer phase separation and saturation are critical in functionality performance and stability of pharmaceutical film coating systems. Here we explore the relationship between the composition and the associated thermal events of ethylcellulose (Ethocel<sup>TM</sup>20) films loaded with fractionated coconut oil. In particular we compare the applicability of two techniques, modulated temperature differential calorimetry (MTDSC) and dynamic mechanical analysis (DMA) to measure the glass transition temperature and detect potential phase separation processes.

**Methods**

Ethylcellulose (EC) solutions were prepared by dissolving 2g Ethocel<sup>TM</sup> 20 (Colorcon, USA) in 20ml ethanol/acetone (60/40 v/v) with 5%, 10%, 15%, 20%, 25% and 30% (w/w) fractionated coconut oil (FCO, Colorcon, USA) added respectively. Solutions were cast by using a REF 1117 film applicator (Sheen Instruments, England) and dried at 45°C for 3h. MTDSC experiments were conducted using a DSC Q1000 (TA instruments, USA) from 20°C to 220°C with a modulation amplitude of  $\pm 0.5^\circ\text{C}/40\text{s}$  at 2°C/min in pinholed crimped pans. A DMA 2980 (TA instruments, USA, tensile film mode) was used, ramping from 30°C to 180°C at 3°C/min.

**Results**

MTDSC gave a value of T<sub>g</sub> for the EC film of 129.2±<0.1°C. An endothermic event was observed around 180°C which was ascribed to melting of microcrystallites in the EC<sup>1</sup>. The T<sub>g</sub> decreased when adding FCO. However on adding FCO to 20% and beyond, the T<sub>g</sub> remained constant at circa 97°C while a lower temperature peak was observed at circa 53°C. Such phenomena have been associated with phase separation. This event may indicate multiple mixed phases. The composition of these phases was estimated by considering the Gordon Taylor/Simba Boyer equations in the context of the T<sub>g</sub> of the 5% FCO films (allowing K and the T<sub>g</sub> of FCO to be estimated) then estimating the compositions of the two phases in the 20% systems as being 23.5% and 8.3% FCO respectively. It is noted that between 20% and 30% FCO the T<sub>g</sub> values do not change, implying further phase separation.

DMA data shows a similar trend of decreasing T<sub>g</sub> with increasing FCO concentrations. Two glass transitions were observed in the tanδ plot for 20% FCO film, supporting the

---

suggestion of phase separation. However, the storage modulus decreased dramatically above  $T_g$  thus rendering it difficult to observe any higher temperature transitions.

### **Conclusions**

MTDSC and DMA results suggest that phase separation can occur in EC/FCO films. We suggest the formation of binary mixed systems rather than pure component separation and outline a novel method for estimating the associated composition.

### **References**

- 1 Lai H. L. (2005) *PhD Thesis, University of East Anglia, Norwich UK.*

**Annual Meeting and Exposition of American Association of Pharmaceutical Sciences  
2009 (Los Angeles, US)**

**An Investigation into Potential Phase Separation of Ethocel™ (EC) 20 Film Coatings with Incorporated Plasticizers**

Jin Meng<sup>1</sup>, Ali Rajabi-siahboomi<sup>2</sup>, Marina Levina<sup>2</sup>, Mike Reading<sup>1</sup> and Duncan Q. M. Craig<sup>1</sup>

<sup>1</sup>School of Chemical Sciences and Pharmacy, University of East Anglia, Norwich NR4 7TJ, UK

<sup>2</sup>Colorcon Limited, Flagship House, Victory Way, Crossways, Dartford, Kent DA2 6QD, UK

**PURPOSE**

The miscibility of polymer and plasticizer in pharmaceutical film coating systems is of major importance in polymer sciences. Here we explore the miscibility of EC20 films on adding plasticizer, fractionated coconut oil (FCO, medium chain triglycerides), and compare the applicability of two techniques, modulated temperature differential calorimetry (MTDSC) and dynamic mechanical analysis (DMA) to measure the glass transition temperature and detect potential phase separation processes.

**METHODS**

EC20 films were prepared using the solution casting method. 2g Ethocel™ 20 (Colorcon, USA) and 5%, 10%, 15%, 20%, 25% and 30% (w/w) FCO (Abitec Corporation, USA) were added respectively into 20ml ethanol/acetone (60/40). MTDSC experiments were performed using a DSC Q1000 (TA Instruments, USA) from 20°C to 220°C with a modulation amplitude of  $\pm 0.5^\circ\text{C}/40\text{s}$  at 2°C/min. A DMA 2980 (TA Instruments, USA) was used, ramping from 30°C to 180°C at 3°C/min.

**RESULTS**

From the MTDSC results, T<sub>g</sub> values decreased from 129.2 $\pm$ <0.1°C (EC20 film) when adding FCO to, for example, 109.79 $\pm$ 0.63°C on adding 5% FCO. However on increasing FCO to 20% and beyond, two derivative reversing heat capacity peaks (circa 97°C and 53°C) were observed. Such phenomena have been associated with phase separation which may indicate multiple mixed phases. The composition of these phases was estimated by considering the Gordon Taylor/Simba Boyer equations in the context of the T<sub>g</sub> of the 5% FCO films (allowing K and the T<sub>g</sub> of FCO to be estimated) then estimating the compositions of the two phases in the 20% systems as being 23.5% and 8.3% FCO respectively. It is noted that between 20% and 30% FCO the T<sub>g</sub> values do not change, implying further phase separation rather than continued plasticization.

DMA data showed a similar trend of decreasing T<sub>g</sub> with increasing FCO concentrations. Two glass transitions were observed in the tan $\delta$  plot for 20% FCO film, supporting the suggestion of phase separation.

**CONCLUSIONS**

We suggest the formation of binary mixed systems in EC/FCO films, which are polymer-plasticizer concentration dependent, rather than pure component separation and outline a novel method for estimating the associated composition.

We are grateful to Colorcon Limited (USA) for their financial support.

**Annual Meeting and Exposition of American Association of Pharmaceutical Sciences  
2011 (Washington D.C., US)**

**A Thermal and Nanothermal Imaging Study of Hydroxypropyl Methyl Cellulose Incorporation into Ethylcellulose Films**

Jin Meng<sup>1</sup>, Ali Rajabi-siahboomi<sup>2</sup>, Marina Levina<sup>2</sup> and Duncan Q. M. Craig<sup>1</sup>

<sup>1</sup>School of Pharmacy, University of East Anglia, Norwich NR4 7TJ, UK

<sup>2</sup>Colorcon Limited, Flagship House, Victory Way, Crossways, Dartford, Kent DA2 6QD, UK

**PURPOSE:** To characterize and map ethylcellulose (EC) films containing the pore former hydroxypropyl methylcellulose (HPMC) using a combination of thermal (modulated temperature DSC), and imaging (scanning electron microscopy, atomic force microscopy and nanothermal) analysis with a view to understanding the size and distribution of the pore former within the inert film.

**METHODS:** 10%, 20% and 30% HPMC was incorporated into films using a solvent evaporation method. MTDSC (Q2000, TA Instruments, US) was conducted from 0°C to 200°C with  $\pm 0.5/40s$  at 2°C/min. DMA in tension mode (DMA 2980, TA instruments, USA) was performed from 30°C to 180°C at 3°C/min. AFM and nanothermal analysis was conducted using a NanoTA Thermal Analyzer (Anasys Instruments, USA) combined with an Explorer scanning probe microscope (Thermomicroscopes). Localized thermal analysis (LTA) was performed on selected areas, heating from room temperature to 300°C at 25°C/s. The surface morphology of the EC films before and after immersion into DI water was observed using a JEOL JSM5900 LV (Japan) scanning electron microscope.

**RESULTS:** The T<sub>g</sub> values of EC films with 10%, 20% and 30% HPMC remained broadly constant at circa 130°C; it was not possible to reliably identify the HPMC T<sub>g</sub> using this method. DMA on these films revealed two tan  $\delta$  peaks at circa 140°C and 160°C. LTA showed that at 10% HPMC level, some sites had a softening temperature at circa 150°C, while many others had the first softening at circa 150°C following by another thermal expansion and softening at circa 180°C which we ascribe to the softening of the EC and HPMC respectively. For the films with 20% and 30% HPMC, two separated phases were observed using LTA with T<sub>g</sub>s corresponding to EC and HPMC respectively. The morphology of EC films after immersion observed using SEM revealed that time-dependent pore formation was noted which we ascribe to HPMC being washed out.

### **CONCLUSIONS**

The distribution of HPMC in the EC films was successfully identified using nanothermal analysis, with that distribution appearing to be composition dependent. SEM examination of films before and after immersion in dissolution medium showed time dependent pore formation which we ascribe to phase separated HPMC leaching out of the film. Financial support was provided by Colorcon Limited (UK).

---

**Published Papers****Pharmaceutical Research March 2012 Paper Accepted****The Development of Thermal Nanoprobe Methods as a Means of Characterizing and Mapping Plasticizer Incorporation into Ethylcellulose Films**

Jin Meng, Marina Levina<sup>1</sup>, Ali R. Rajabi-Siahboomi<sup>1</sup>, Andrew N. Round, Mike Reading, Duncan Q.M. Craig\*

School of Pharmacy, University of East Anglia, Norwich, UK, NR4 7TJ

<sup>1</sup>Colorcon Limited, Flagship House, Victory Way, Crossways, Dartford, Kent DA2 6QD, UK

Correspondence author: Duncan Craig

Email: d.craig@uea.ac.uk

**ABSTRACT**

The interaction between polymers and plasticizers is of major interest within the polymer and related sciences, yet to date little information is available with regard to the mapping of plasticizer phase separation. In this investigation, ethylcellulose (EC) films containing varying amounts of fractionated coconut oil (FCO; a mixture of medium-chain triglycerides) were prepared in order to develop novel methods of studying the phase relationship between these components. The thermal and thermo-mechanical properties of the films were characterized using modulated temperature differential scanning calorimetry (MTDSC) and dynamic mechanical analysis (DMA). Clear evidence of distinct conjugate phases was obtained for the 20%-30% FCO/EC film systems. We suggest a model whereby the composition of the distinct phases may be estimated via consideration of the glass transition temperatures observed using DSC and DMA. By combining pulsed force AFM and nano-thermal analysis we demonstrate that it is possible to map the two separated phases. In particular, the use of thermal probes allowed identification of the distinct regions via localized thermomechanical analysis, whereby nanoscale probe penetration is measured as a function of temperature. The study has therefore indicated that by using thermal and imaging techniques in conjunction it is possible to both identify and map distinct regions in binary films.

Key words: phase separation, film coating, ethylcellulose, plasticizers, thermal analysis, atomic force microscopy